National and Kapodistrian University of Athens

School of Health Sciences

Faculty of Medicine

Thesis for doctoral degree (Ph.D)

'Study of the transcriptional regulation of α-synuclein'

Georgia Dermentzaki, MSc

Biomedical Research Foundation

Academy of Athens

Center for Neuroscience

September 2015

'Transcriptional regulation of α-synuclein in primary neurons and *in vivo*; focus on the ZSCAN21 transcription factor'

<u>Supervisor</u>

Stefanis Leonidas, M.D., Ph.D

Professor of Neurology and Neurobiology

Faculty of Medicine, University of Athens

<u>Advisory Committee</u>

1. **Stefanis Leonidas, M.D., Ph.D**
Professor of Neurology and Neurobiology
Faculty of Medicine, University of Athens

2. **Thanos Dimitrios, Ph.D**
Professor, President of the Scientific Board
Biomedical Research Foundation of the Academy of Athens

3. **Stamboulis Elefterios, M.D., Ph.D**
Professor of Neurology
Faculty of Medicine, University of Athens

<u>Examination Committee</u>

1. **Stefanis Leonidas, M.D., Ph.D**
Professor of Neurology and Neurobiology
Faculty of Medicine, University of Athens

2. **Thanos Dimitrios, Ph.D**
Professor, President of the Scientific Board
Biomedical Research Foundation of the Academy of Athens

3. **Stamboulis Elefterios, M.D., Ph.D**
Professor of Neurology,
Faculty of Medicine, University of Athens

4. **Politis Panagiotis, Ph.D**
Assistant Professor - Level C
Biomedical Research Foundation of the Academy of Athens

5. **Poul Henning Jensen, M.D., Ph.D,**
Professor of Medical Biochemistry
Aarhus University, Denmark

6. **Efthimiopoulos Spyros, Ph.D**
Professor of Physiology and Neurobiology
Faculty of Biology, University of Athens

7. **Papazafiri Panagiota, Ph.D**
Associate Professor of Physiology
Faculty of Biology, University of Athens

THE HIPPOCRATIC OATH

"I swear by Apollo the physician, and Asclepius, and Hygieia and Panacea and all the gods and goddesses as my witnesses, that, according to my ability and judgement, I will keep this Oath and this contract:

To hold him who taught me this art equally dear to me as my parents, to be a partner in life with him, and to fulfill his needs when required; to look upon his offspring as equals to my own siblings, and to teach them this art, if they shall wish to learn it, without fee or contract; and that by the set rules, lectures, and every other mode of instruction, I will impart a knowledge of the art to my own sons, and those of my teachers, and to students bound by this contract and having sworn this Oath to the law of medicine, but to no others.

I will use those dietary regimens which will benefit my patients according to my greatest ability and judgement, and I will do no harm or injustice to them.

I will not give a lethal drug to anyone if I am asked, nor will I advise such a plan; and similarly I will not give a woman a pessary to cause an abortion.

In purity and according to divine law will I carry out my life and my art.

I will not use the knife, even upon those suffering from stones, but I will leave this to those who are trained in this craft.

Into whatever homes I go, I will enter them for the benefit of the sick, avoiding any voluntary act of impropriety or corruption, including the seduction of women or men, whether they are free men or slaves.

Whatever I see or hear in the lives of my patients, whether in connection with my professional practice or not, which ought not to be spoken of outside, I will keep secret, as considering all such things to be private.

So long as I maintain this Oath faithfully and without corruption, may it be granted to me to partake of life fully and the practice of my art, gaining the respect of all men for all time. However, should I transgress this Oath and violate it, may the opposite be my fate."

Translation by National Library of Medicine, USA, 2002

ACKNOWLEDGEMENTS

LIST OF ABBREVIATIONS

AAVs: Adeno-Associated-Virus

ANOVA: Analysis of Variance

AP: Anteroposterior

ASYN: α-Synuclein Protein

AVs: Adenovirus

BDNF: Brain-Derived Neurotrophic Factor

bFGF: Basic Fibroblast Growth Factor

BSA: Bovine Serum Albumin

CHIP: Chromatin Immunoprecipitation Assay

CNS: Central Nervous System

CRM: Cis-Regulatory Module

DAB: 3,3′-Diaminobenzene

DBS: Deep Brain Stimulation

DG: Dentate Gyrus

DIV: Days in Vitro

bp: Base Pairs

DV: Dorsoventral

EGFP: Enhanced Green Fluorescence Protein

ERK: Extracellular Signal Regulated Kinase

FACS: Fluorescence-Activated Cell Sorting

FI: Fluorescent Immunohisto- / Immunocyto-chemistry

GPi: Globus Pallidus Interna

GSP: Gene-Specific Primer

GWAS: Genome Wide Association Studies

hEGF: Human Epidermal Growth Factor

HEK 293A Cells: Human Embryonic Kidney 293 A Cells

HEK 293T Cells: Human Embryonic Kidney 293 Cells

LB: Lewy Body

LBV/AD: Lewy Body Variant of Alzheimer's Disease

LBD: Dementia with Lewy Bodies

L-DOPA: Levodopa

LN: Lewy Neurite

lncRNA: Long Non Coding RNA

mi-RNA/mir : Micro-RNA

ML: Mediolateral

MOI: Multiplicity of Infection

mRNA: Messanger RNA

ncRNA: Non Coding RNA

NeuN: Neuronal Nucler Antigen

NGF: Nerve Growth Factor

NGS: Normal Goat Serum

PBS: Phosphate-Buffered Saline

PC12 Cells: Pheochromocytoma Cells

PCR: Polymerase Chain Reaction

PD: Parkinson's Disease

PDD: Parkinson's Disease Dementia

PI: Protease Inhibitor

PI3K: Phosphatidyl-inositol 3 Kinase

PMSF: Phenylmethanesulfonyl Fluoride

PTMs: Post-translational Modifications

RT: Room Temperature

RT-PCR: Reverse Transcription PCR

shRNA: Small Hairpin RNA

si-RNA: Small Interfering RNA

SHSY5Y Cells: Human Neuroblastoma SHSY5Y Cell Line

SNCA: Human α-Synuclein Gene

Snca: Rat and Mouse α-Synuclein Gene

SNP: Single Nucleotide Polymorphism

SNpc: Substantia Nigra Pars Compacta

STN: Subthalamic Nucleus

TF: Transcription Factor

TFBS: Transcription Factor Binding Sites

Tg: Transgenic

TU: Transduction Units

TUJ1: Beta-III Tubulin

UAP: Universal Amplification Primer

WPRE: Woodchuck Hepatitis Post-Transcriptional Regulatory Element

WT: Wild-Type

ZSCAN21: Human Zinc Finger and SCAN Domain Containing 21 Transcription Factor Gene

Zscan21: Rat Zinc Finger and SCAN Domain Containing 21 Transcription Factor Gene

ZSCAN21: Zinc Finger and SCAN Domain Containing 21 Transcription Factor Protein

3C: Chromosome Conformation Capture

3' RACE: 3' Rapid Amplification of cDNA Ends

3'-UTR: 3' Untranslated Region

5'-UTR: 5' Untranslated Region

Contents

ABSTRACT

α-synuclein is a small presynaptic neuronal protein, encoded by the *SNCA* gene, that is implicated genetically and neuropathologically in Parkinson's disease (PD). A large body of evidence has established that PD pathogenesis is closely linked to increased levels of *SNCA*; however to date, the biochemical pathways and transcriptional elements that control *SNCA* expression are still obscure. Previous experiments in our laboratory in the PC12 cell line demonstrated that the transcription factor ZSCAN21 binds to the intron 1 region of the *Snca* gene and is strongly involved in its transcriptional regulation. Therefore, in the current experiments, we wished to characterize further the role of ZSCAN21 in *Snca* transcriptional regulation in primary cultures and *in vivo*. We find that *in vivo* ZSCAN21 is expressed in neurons and its levels are developmentally regulated in different brain regions where ASYN is also detected. Further, we confirmed through Chromatin Immunoprecipitation its presence in a binding complex in the intron 1 region of the *Snca* gene in rat cortical neuronal cultures. Importantly, lentiviral-mediated silencing of *Zscan21* increased significantly the promoter activity of *Snca* as well as its mRNA and protein levels in such cultures. In contrast, *Zscan21* mediated silencing in differentiated neurosphere cultures reduced *Snca* levels. Stereotaxic delivery of adeno-associated virus against *Zscan21* in the postnatal and adult hippocampus, an area linked with the non-motor symptoms of PD, revealed no significant alterations in *Snca* levels, despite efficient *Zscan21* knock-down. Interestingly, *Zscan21* overexpression in cortical neurons with adenoviruses led to robust mRNA but negligible protein expression, suggesting that ZSCAN21 protein levels are tightly regulated post-transcriptionally and / or post-translationally. Therefore, overall, our study demonstrates that ZSCAN21, a transcription factor whose levels are under strict posttranscriptional / posttranslational control in neurons, is diversely implicated in the transcriptional regulation of *Snca* in respect to the developmental stage, at least in *in vitro* primary neuronal settings. *In vivo,* however, the unaltered *Snca* levels observed following *Zscan21* downregulation, imply the presence of alternative or perhaps compensatory mechanisms that regulate *Snca* transcription in such settings. Furthermore, in a genetic case control study of the ZSCAN21 binding site in *SNCA* intron 1, we did not find polymorphisms between PD patients and controls, suggesting that genetic diversity within this region does not contribute to disease pathogenesis. Overall, given the diverse effects in cell culture, and the lack of discernible *in vivo* effects, and although further studies are needed, our work does not provide sufficient support for the idea of targeting ZSCAN21 in order to manipulate *SNCA* levels in synucleinopathy models.

ΠΕΡΙΛΗΨΗ

Η νόσος του Πάρκινσον (ΝΠ) αποτελεί μια χρόνια νευροεκφυλιστική νόσο με άγνωστη μέχρι σήμερα αιτιολογική θεραπεία. Ένα από τα σημαντικότερα γονίδια που εμπλέκονται στη παθολογία της ΝΠ είναι η α-συνουκλεΐνη (*SNCA*), η οποία κωδικοποιεί για μια μικρή, νευρωνική, προσυναπτική πρωτεΐνη. Πλήθος μελετών υποστηρίζουν ότι η υπερέκφραση της *SNCA* οδηγεί σε φαινότυπους που προσομοιάζουν με τη ΝΠ σε διάφορα κυτταρικά και ζωικά μοντέλα. Παρόλα αυτά τα βιοχημικά μονοπάτια καθώς και τα ρυθμιστικά στοιχεία που ελέγχουν τα επίπεδα έκφρασής της παραμένουν σε μεγάλο βαθμό αδιευκρίνιστα. Προηγούμενα πειράματα στο εργαστήριο μας, στην κυτταρική σειρά PC12, έχουν δείξει ότι ο μεταγραφικός παράγοντας ZSCAN21 προσδένεται στη ρυθμιστική περιοχή του πρώτου εσωνίου της *Snca* και συμμετέχει ενεργά στη μεταγραφική της ρύθμιση. Βασιζόμενοι σε αυτό το εύρημα, στη παρούσα μελέτη διερευνήσαμε περαιτέρω τη δράση του ZSCAN21 στη ρύθμιση των επιπέδων της *Snca* σε πρωτογενείς καλλιέργειες νευρώνων καθώς και σε εγκεφάλους από επίμυες *in vivo*. Διαπιστώσαμε τη νευρωνική έκφραση του ZSCAN21 καθώς και τη διαφορική του ρύθμιση σε διακριτά αναπτυξιακά στάδια σε περιοχές του εγκεφάλου (από επίμυ) όπου εντοπίζεται και η ASYN. Επιπλέον, μέσω πειραμάτων ανοσοκατακρήμνισης χρωματίνης (CHIP), επιβεβαιώσαμε τη συμμετοχή του ZSCAN21 στο ρυθμιστικό σύμπλοκο-πρόσδεσης στη περιοχή του πρώτου εσωνίου της *Snca* σε καλλιέργειες φλοιού από επίμυ. Στοχευμένη σίγαση της έκφρασης του *Zscan21* σε πρωτογενείς καλλιέργειες νευρώνων μέσω λεντι-ιών οδήγησε σε σημαντική αύξηση της *Snca* τόσο σε επίπεδο ενεργότητας του υποκινητή της όσο και σε επίπεδο mRNA και πρωτεΐνης. Αντίθετα, σίγαση του *Zscan21* σε καλλιέργειες νευρικών βλαστικών κυττάρων (νευροσφαιρών, neurosphere cultures) είχε σαν αποτέλεσμα τη μείωση των επιπέδων της *Snca*. Στερεοταξική έγχυση αδενοσχετιζόμενων ιών (AAVs) έναντι του *Zscan21* σε μετεμβρυϊκούς (postnatal) και ενήλικες επίμυες στην περιοχή του ιππόκαμπου, η οποία συνδέεται κύρια με τα μη κινητικά συμπτώματα της ΝΠ, δε μετέβαλε σημαντικά τα επίπεδα της *Snca*. Πειράματα υπερέκφρασης του *Zscan21* σε πρωτογενείς φλοιϊκές καλλιέργειες από επίμυ μέσω αδενο-ιών (AVs) δεν αύξησαν σημαντικά τα επίπεδα της πρωτεΐνης του ZSCAN21, παρά τη σημαντική αύξηση στο επίπεδο του mRNA του *Zscan21*, υποδηλώνοντας ότι τα επίπεδα του ZSCAN21 πρέπει να υπόκεινται σε αυστηρό μετα-μεταγραφικό ή / και μετα-μεταφραστικό έλεγχο. Λαμβάνοντας υπόψιν τα παραπάνω αποτελέσματα διαπιστώνεται ότι ο ZSCAN21, ένας μεταγραφικός παράγοντας του οποίου τα πρωτεϊνικά επίπεδα ρυθμίζονται αυστηρά, εμπλέκεται ποικιλοτρόπως στη μεταγραφική ρύθμιση της *Snca* ανάλογα με το αναπτυξιακό στάδιο, τουλάχιστον στα *in vitro* συστήματα πρωτογενών καλλιεργειών που μελετήσαμε. Παρόλα αυτά, το γεγονός ότι δε παρατηρήθηκαν σημαντικές αλλαγές στα επίπεδα της *Snca* έπειτα από σίγαση του *Zscan21* σε επίμυες *in vivo,* υποδηλώνει τη παρουσία αντιρροπιστικών μηχανισμών που συμμετέχουν στη ρύθμιση της. Επιπλέον, ανάλυση δειγμάτων ασθενών με ΝΠ και ατόμων ελέγχου, σχετικά με την εύρεση πιθανών πολυμορφισμών τόσο στη θέση πρόσδεσης του ZSCAN21 όσο και στο ευρύτερο τμήμα στη περιοχής του πρώτου εσωνίου της *SNCA* που περιέχει επιπλέον ρυθμιστικά στοιχεία δεν αποκάλυψε σημαντικές διαφορές μεταξύ των δύο ομάδων. Το εύρημα αυτό

υποδηλώνει ότι η γενετική πολυμορφία μέσα στη συγκεκριμένη περιοχή δε φαίνεται να συνεισφέρει στη παθογένεια της νόσου. Συνολικά, η πολυπλοκότητα της δράσης του ZSCAN21 στη ρύθμιση της *Snca* σε διαφορετικά συστήματα πρωτογενών καλλιεργειών νευρώνων, σε συνδυασμό με την απουσία επίδρασης του ZSCAN21 στα επίπεδα της *SNCA* στα in vivo πειράματα, συνηγορούν στο ότι η στόχευση του ZSCAN21 ως πιθανό θεραπευτικό μέσο δε φαίνεται να αποτελεί τη κατάλληλη επιλογή για τη ρύθμιση των επιπέδων της *SNCA*.

1. INTRODUCTION

1.1 Neurodegenerative diseases

Neurodegenerative diseases is an umbrella term for a range of conditions that primarily affect the neurons in the human brain. Examples of neurodegenerative diseases include Parkinson's, Alzheimer's, Huntington's, amyotrophic lateral sclerosis, spinal muscular atrophy, prion, and spinocerebellar ataxia. Neurodegenerative diseases are incurable and debilitating conditions that result in progressive degeneration and / or death of nerve cells. This broadly causes problems with movement or mental functioning or both. The discovery of causative genetic mutations in affected family members has historically dominated our understanding of neurodegenerative diseases. However, to date, it is becoming increasingly clear that most cases of neurodegenerative diseases cannot be explained only by Mendelian inheritance of known genetic variants, but instead have a complex etiology with numerous genetic and environmental factors contributing to susceptibility (Bertram and Tanzi 2005, McCarthy, Abecasis et al. 2008, Noorbakhsh, Overall et al. 2009, Gandhi and Wood 2010, Ku, Loy et al. 2010). However, despite their innate genetic variability, neurodegenerative diseases share common cellular and molecular mechanisms, with the most prominent being protein misfolding / aggregation and neuronal cell death (Bredesen, Rao et al. 2006, Rubinsztein 2006), which offers hope for therapeutic advances that could ameliorate many diseases simultaneously.
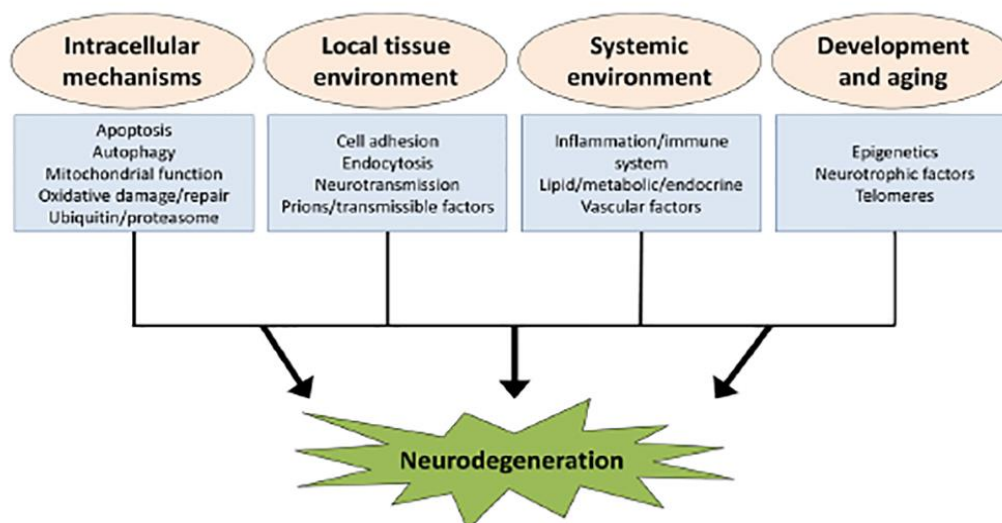
(Ramanan and Saykin 2013)

Figure 1. Conceptual model of candidate pathways contributing to neurodegeneration. Candidate pathways influencing the balance of neuronal survival and degeneration are displayed within broader functional groups based on their major site or mode of action (intracellular mechanisms, local tissue environment influences, systemic influences, and mechanisms related to neurodevelopment and aging). The pathways and overarching functional groups in this model are highly related and can have overlapping or interacting components that can collectively modulate neurodegenerative processes.

1.2 Parkinson's Disease (PD)

Parkinson's disease (PD) is the second most common age-related chronic neurodegenerative disorder after Alzheimer's disease (AD) that affects globally 2–3% of people aged 55 years and above (Trenkwalder, Schwarz et al. 1995, von Campenhausen, Bornschein et al. 2005). It was first described in 1817 by the British doctor James Parkinson in a monograph termed ''An Essay of the Shaking Palsy.'' Clinical diagnosis is based on the presence of the motor symptoms bradykinesia, resting tremor, rigidity and postural instability (Fahn 2003), while definite diagnosis can only be made post mortem (Hughes, Daniel et al. 1992). Secondary non motor symptoms include cognitive impairment, hallucinations, illusions, depression, freezing, sleep disorders, odor loss, hypotension, frequent urination, sweating and constipation (Dauer and Przedborski 2003), thus reflecting the multisystemic nature of PD.

Neuropathologically, PD is characterized by the loss of dopaminergic neurons in the substantia nigra pars compacta (SNpc) and the abnormal deposition of proteinaceous inclusions termed Lewy bodies (LBs) and Lewy neurites (LNs) in the surviving neurons and axons, respectively (Forno 1996). These aberrant inclusions are robustly immunoreactive for α-synuclein protein (ASYN) (mainly in the halo of these inclusions) (Spillantini, Schmidt et al. 1997, Baba, Nakajo et al. 1998, Spillantini, Crowther et al. 1998) but also for other proteins such us ubiquitin and neurofilament (Surguchov 2008). Nonetheless, neurodegeneration and LB deposition are not only evident in the dopaminergic system but also extends to other neuronal systems such as the noradrenergic (locus coeruleus), serotonergic (raphe) and cholinergic (nucleus basalis of Meynert and dorsal motor nucleus of the vagus) systems, as well as to the cerebral cortex (especially cingulate and entorhinal cortices), olfactory bulb, and autonomic nervous system. The degeneration of hippocampal structures and cholinergic cortical inputs contributes to the high rate of dementia that accompanies PD, particularly in older patients.

A)
Substantia nigra

Diminished substantia nigra as seen in Parkinson's disease

B)
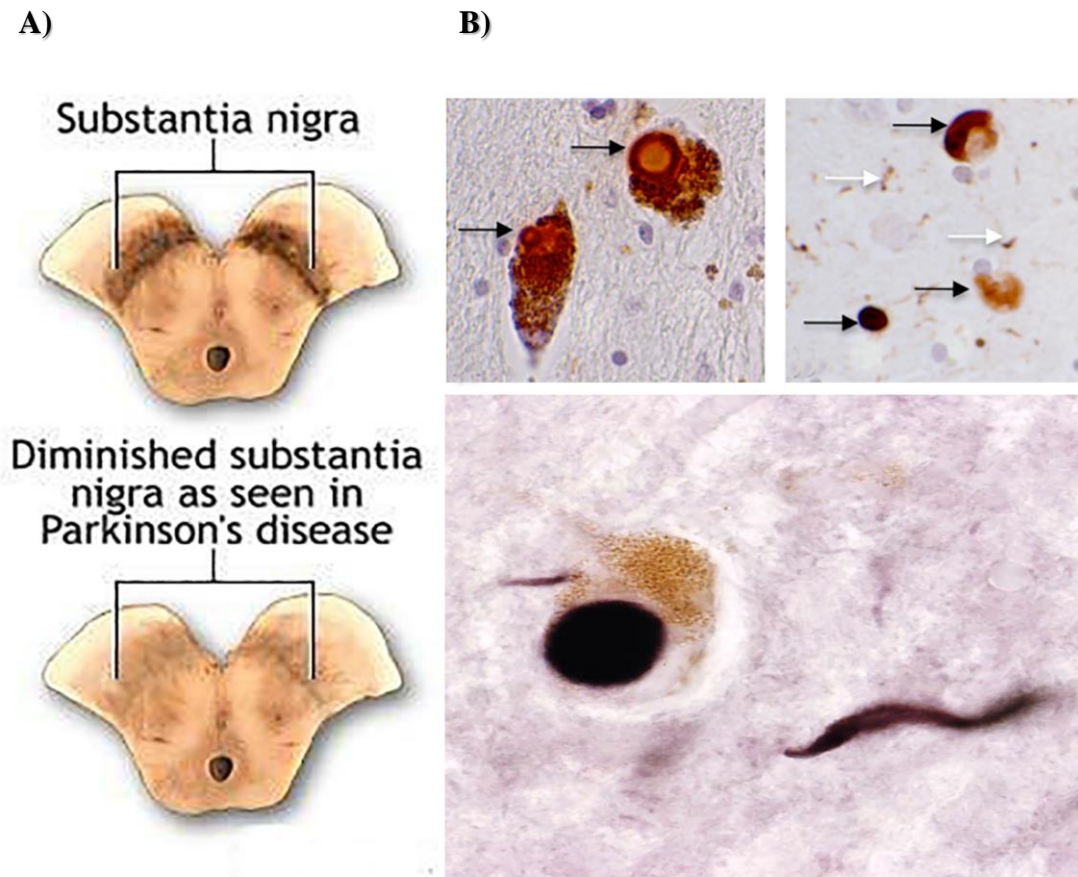
Figure 2. Neuropathological features of PD: A) Depigmentation of SNpc as a result of dopaminergic cell loss in post-mortem material from a PD patient in contrast to the intact substantia nigra of a healthy control. B) LBs and LNs immunolabeled for ASYN in the substantia nigra from a PD brain.

Interestingly, (Braak, Del Tredici et al. 2003) described that LB formation follows an ''ascending course'' in anatomically distinct brain areas and suggested a six-stage scheme in which the pathology appears first in the dorsal vagal nucleus and olfactory bulb (OB stage 1). This corresponds to the premotor symptoms hyposmia and autonomic dysfunction, including constipation (Abbott, Petrovitch et al. 2001, Hawkes 2008, Ross, Petrovitch et al. 2008, Savica, Carlin et al. 2009). At stage 2, pathology appears in the pontine area of the locus coeruleus, raphe nuclei and reticular formation. This brainstem affection may cause rapid eye movement sleep behavior disorder which is one of the most specific indicators for the future development of PD and occurs in 30–50% of PD patients (Gagnon, Postuma et al. 2006, Iranzo, Molinuevo et al. 2006). Stage 3 marks the involvement of the SN and the anterior olfactory nucleus, whereas significant rates of degenerating neurons in the pars compacta are detectable at stage 4. The motor symptoms of PD emerge at stage 4 or later. Stages 5 and 6 are characterized by the involvement of the basal forebrain and cortical regions, including the entorhinal cortex and cornu ammonis regions of the hippocampus. This advanced stage of PD is clinically dominated by complicated control of motor symptoms (e.g., fluctuations, dyskinesias and dysphagia) and severe non motor symptoms like Parkinson's disease dementia (PDD), psychosis and sleep-wake disorders. Dementia

with Lewy bodies (DLB) is clinically accompanied by a predominant dementia syndrome preceding motor symptoms and pathologically by neocortical accentuation of LB pathology (McKeith, Dickson et al. 2005, Halliday, Holton et al. 2011, Irwin, Lee et al. 2013). Although there have been criticisms of this hypothesis (Burke, Dauer et al. 2008) since it does not explain the absence of symptoms in subjects who on autopsy have widespread ASYN pathology, it appears to account for the majority of cases examined in large cohorts of LB cases (Dickson, Uchikado et al. 2010).

Genetically PD is a rather heterogeneous and complex disorder. Epidimiological studies have revealed that approximately 10% of PD cases are familial (Thomas and Beal 2007) and the remaining 90% are sporadic. A plethora of studies and more recently large scale genome-wide association studies (GWAS) (Pankratz, Wilk et al. 2009, Satake, Nakabayashi et al. 2009, Simon-Sanchez, Schulte et al. 2009, Edwards, Scott et al. 2010) have identified genes and gene loci that correlate with PD. These can be classified as rare causal genes, moderate risk common variants and low risk common variants (Houlden and Singleton 2012), which are presented below, in Fig. 3.
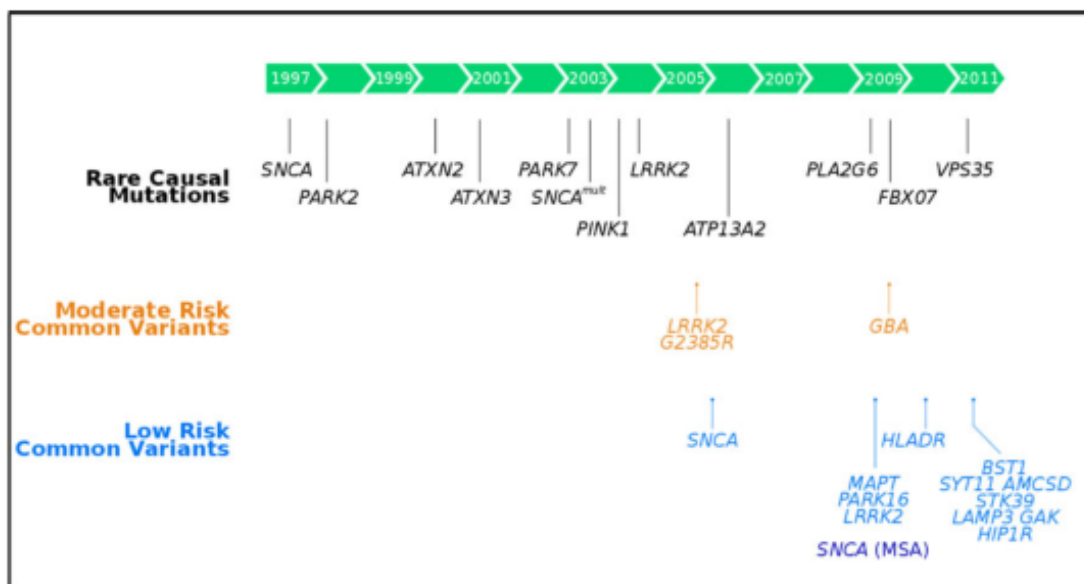
Figure 3. Genetics of PD *(Houlden and Singleton 2012).*

Additionally, besides mutations in specific genes that can cause rare familial PD, complex interactions between several genes encoded by nuclear or mitochondrial DNA (or both), modifying effects of susceptibility alleles and epigenetic factors, impaired proteolytic function, oxidative stress and effects on PD-linked-gene expression that are attributable to environmental agents and aging have also been proposed as risk factors for PD. Their interrelationship in normal aging and PD state is presented below, in Fig.4.
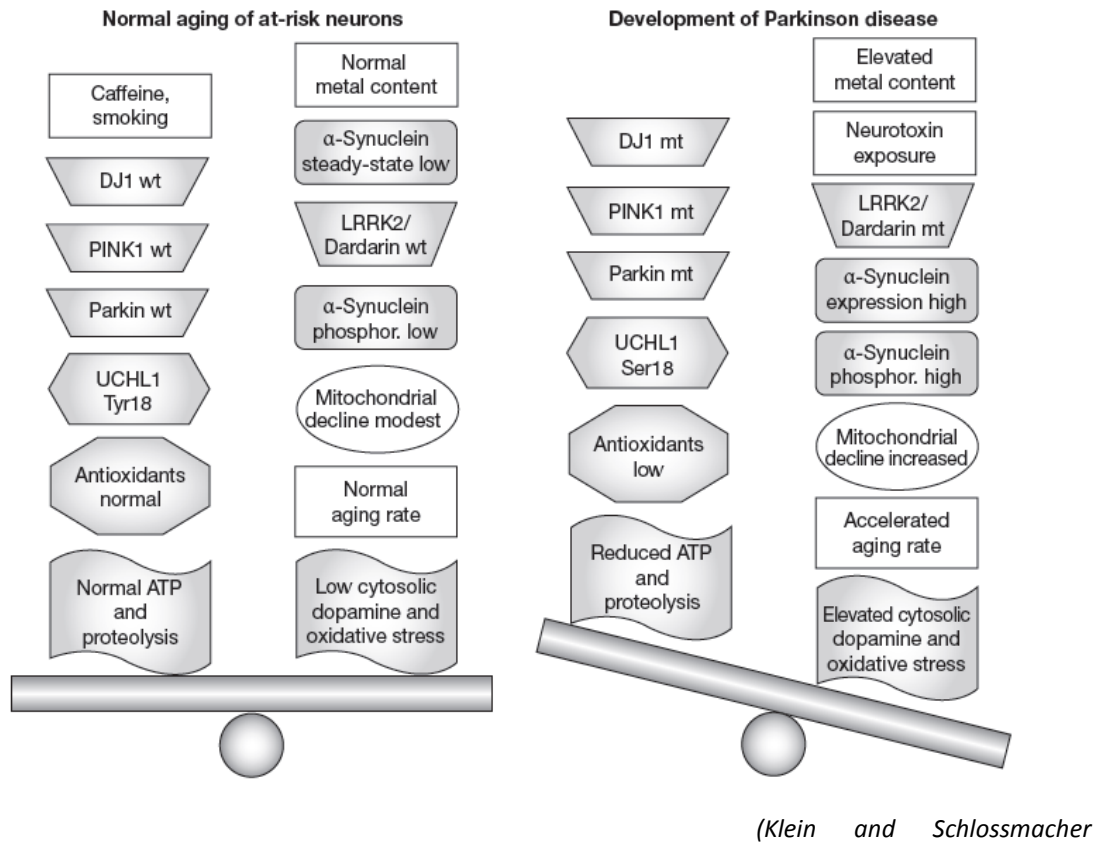
Figure 4. PD as a complex disorder. A model of known pathogenetic events in PD shows a principal imbalance between factors that promote PD (e.g. increased total metal content in the substantia nigra, altered steady-state levels of ASYN protein, including its phosphorylation, rise in dopamine metabolism-related stress, and exposure to neurotoxins) and factors that prevent PD (e.g. cigarette smoking, caffeine consumption, expression of wild-type Parkin, DJ1, and PINK1, and normal levels of glutathione). LRRK2, leucine-rich repeat kinase 2; mt, mutant; phosphor., phosphorylation of ASYN at residue Ser129; PINK1, phosphatase and tensin homolog-induced putative kinase 1; Ser18, serine at residue 18; Tyr, tyrosine at residue 18; UCHL1, ubiquitin carboxyl-terminal esterase L1; wt, wild-type.

Regarding current treatments for PD enormous progress has been made over the past half century due to advances in experimental therapeutics, yet levodopa (L-DOPA), a precursor of dopamine synthesis, still remains the most potent drug for controlling PD symptoms (Jankovic and Aguilar 2008). Nonetheless, it is associated with a variety of side-affects such as a ''wearing off'' effect, levodopa-induced dyskinesias and other motor complications (Stern 2004, Weiner 2004). Fortunately, other drugs are available, amongst these are dopamine agonists as the initial or early form of dopaminergic therapy, catechol-o-methyl-transferase inhibitors to prolong responses to dopamine agonists, and non-dopaminergic agents such as anticholinergics and amantadine, which usually provide satisfactory symptomatic relief in the early phases of anti-PD therapy.

Additionally, adjunctive therapies have been developed, but these must be implemented early (Schapira 2004). For example, ''deprenyl and tocopherol antioxidative therapy of Parkinsonism'' together with L-DOPA has been accompanied with significantly slower decline, less wearing off, on-off motor fluctuations, and less

freezing, but more dyskinesias (Shoulson, Oakes et al. 2002). Rasagiline, a selective, irreversible monoamine oxidase inhibitor, provides a modest benefit as an adjunctive therapy in PD patients experiencing levodopa related motor fluctuations (Stern, Marek et al. 2004).

Regarding neurosurgical approaches for treating PD, neuroablative surgeries include thalamotomy, pallidotomy and subthalotomy. Thalamotomy involves the ablation of a part of the thalamus, generally the ventralis intermedius, to relieve tremor with excellent short- and long-term tremor suppression in 80–90% of patients with PD. Pallidotomy involves destruction of a part of the globus pallidus interna (GPi) leading to significant improvements in each of the cardinal symptoms of PD (tremor, rigidity and bradykinesia), as well as a significant reduction in dyskinesia. Last, subthalamotomy involves destruction of a part of the subthalamic nucleus (STN) leading to significant improvements in the cardinal features of PD, as well as the reduction of motor fluctuations and dyskinesia. Currently, the aforementioned ablative surgeries for PD have largely been replaced by deep brain stimulation (DBS). DBS is a form of stereotactic surgery via electrodes implanted in the ventralis intermedius nucleus of the thalamus, GPi, STN, or other subcortical nuclei. Thalamic stimulation appears to be particularly effective in the treatment of parkinsonian and essential tremor (Ondo et al. 1998). Several studies have demonstrated that DBS of the GPi and STN improves parkinsonian symptoms and prolongs the "on" time (Linazasoro, Van Blercom et al. 2003), as well as other aspects of quality of life (Diamond and Jankovic 2005).
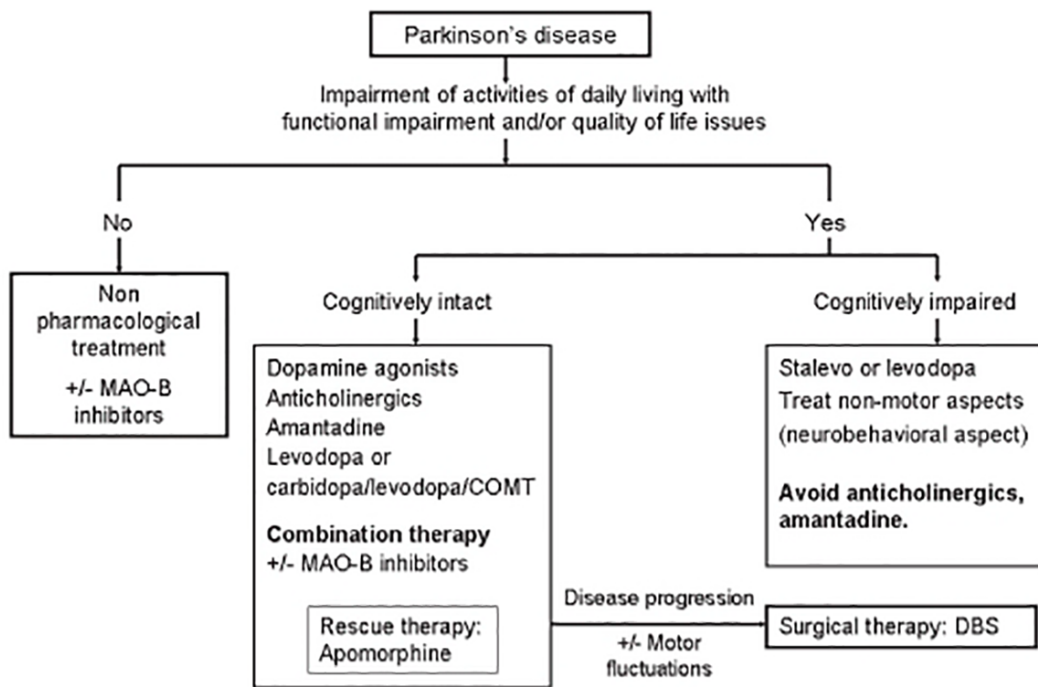
Figure 5. Treatment guidelines for the progressive stages of PD *(Jankovic 2008 REVIEW).*

Promising future therapies include A2α antagonists, such as Istradefylline, Preladenant and SYN115. L-DOPA formulations like levodopa/carbidopa intestinal gel (Duodopa), an aqueous gel that contains 20 mg/mL L-DOPA and 5 mg/mL carbidopais effective to reduce motor fluctuations and dyskinesia in advanced PD (Nyholm 2006, Fernandez and Odin 2011) and PX066, an extended-release oral formulation of carbidopa/levodopa. Other antiparkinsonian medications include XP21279, ND0611, Safinamide and Cogane (PMY50028). Antidyskinesia medications include AFQ056 and Fipamezole. Gene therapy involving the use of CERE-120 (AAV2-NRTN), an adeno-associated virus serotype 2 vector encoding human neurturin is under a phase1/2 clinical trial. Additionally, gene therapy including glutamic acid decarboxylase gene (GAD) transfer in a phase 2, double-blind, randomized trial (LeWitt, Rezai et al. 2011), practically defined OFF UPDRS motor scores improved by 8.1 points in the GAD group and 4.7 points in the sham surgery group at 6 months. Last but not least, speech therapy, exercise and physical therapy and dietary considerations are also an important part of PD therapeutic approaches.

1.3 *SNCA*: a major risk factor for PD

A mutation in the α-synuclein gene (*SNCA*) was the first genetic aberration linked to PD to be reported by Polymeropoulos et al. (1997). The mutation corresponded to a G209A substitution in the *SNCA* gene resulting in an A53T amino acid change in rare families with autosomal dominant inheritance. Following this initial report, two more point mutations were identified and linked to PD, A30P and E46K (Kruger, Kuhn et al. 1998, Zarranz, Alegre et al. 2004). Recently, five additional *SNCA* substitutions (A18T, A29S, H50Q, G51D, and A53E) have been identified (Appel-Cresswell, Vilarino-Guell et al. 2013, Hoffman-Zacharska, Koziorowski et al. 2013, Lesage, Anheim et al. 2013, Proukakis, Dudzik et al. 2013, Pasanen, Myllykangas et al. 2014).

In addition to point mutations, duplications and triplications (Singleton, Farrer et al. 2003, Chartier-Harlin, Kachergus et al. 2004, Miller, Hague et al. 2004) of the *SNCA* gene locus have been reported in familial PD. Interestingly, a gene dosage effect seemed to govern the multiplication cases since subjects carrying a triplication had an earlier onset and more severe symptoms than the duplication carriers. Therefore, increased levels of *SNCA* were directly linked to PD pathogenesis. Consistent with this notion, overexpression of mutant but most importantly wild-type (WT) ASYN in various animal models was able to recapitulate different aspects of PD. Specifically, ASYN-dependent neurodegeneration has been demonstrated in *SNCA* transgenic (Tg) flies (Feany and Bender 2000), *SNCA* Tg mice (Masliah, Rockenstein et al. 2000, van der Putten, Wiederhold et al. 2000, Giasson, Duda et al. 2002, Neumann, Kahle et al. 2002) *SNCA* virus infected rats (Kirik, Rosenblad et al. 2002, Lo Bianco, Ridet et al. 2002), and primates (Kirik, Annett et al. 2003).

Besides familial PD, several lines of evidence have established the presence of a genetic link between *SNCA* and sporadic PD. For instance, a number of polymorphic variants in the 5' and 3' regions of the *SNCA* gene locus reportedly confer susceptibility to developing PD in case/control studies (Farrer, Maraganore et al. 2001, Pals, Lincoln

et al. 2004, Mueller, Fuchs et al. 2005, Mizuta, Satake et al. 2006). One of the most studied *SNCA* polymorphic variants, the Rep-1 dinucleotide repeat site located 10.7 kb upstream from the transcriptional start site of *SNCA* (Xia, Rohan de Silva et al. 1996, Touchman, Dehejia et al. 2001), and certain alleles of this variant have been associated with an increased risk of sporadic PD (Kruger, Vieira-Saecker et al. 1999, Tan, Matsuura et al. 2000, Farrer, Maraganore et al. 2001, Mizuta, Nishimura et al. 2002, Tan, Tan et al. 2003, Tan, Chai et al. 2004). It has to be noted that there were also studies that failed to replicate such an association (Parsian, Racette et al. 1998, Izumi, Morino et al. 2001, Khan, Graham et al. 2001, Spadafora, Annesi et al. 2003, Tan, Tan et al. 2003). However, a large meta-analysis (Maraganore, de Andrade et al. 2006) confirmed that Rep-1 allele-length variability was associated with an increased risk of PD. Nevertheless, it is not still clear whether the Rep-1 variant is responsible for this increased risk or if it is in linkage disequilibrium with the actual causative element within the *SNCA* promoter. Besides, Rep-1 polymorphic variants reportedly act as modulators of *SNCA* transcription (Chiba-Falek and Nussbaum 2001, Chiba-Falek, Touchman et al. 2003, Chiba-Falek, Kowalak et al. 2005), a finding that was further replicated in mice (Cronin, Ge et al. 2009) and even in the human brain (Linnertz, Saucier et al. 2009). Polymorphisms in the 3' region have also been correlated with *SNCA* levels and PD risk (Mueller, Fuchs et al. 2005, Mizuta, Satake et al. 2006, Fuchs, Tichopad et al. 2008, Simon-Sanchez, Schulte et al. 2009, Mata, Shi et al. 2010) in the European and Japanese populations. Four polymorphisms, i.e., rs356219, rs356220, rs35616, and rs356203, were associated prominently with PD in both populations (Mizuta, Takafuji et al. 2013). Intriguingly, risk conferring alleles at the 3' untranslated region (3'-UTR) were associated with the increased expression of an alternatively spliced form of *SNCA* (McCarthy, Linnertz et al. 2011, Rhinn, Qiang et al. 2012), suggesting an alternative mechanism via which gene variations may be linked to disease. Moreover, recent studies have identified the presence of functional non-coding conserved regions in the SNCA gene locus (Sterling, Walter et al. 2014) as well as a CT-rich haplotype in intron 4 of SNCA that confers risk for LB pathology in AD and affects *SNCA* (Lutz, Saul et al. 2015).

Last and of most importance, large unbiased GWAS established single nucleotide polymorphisms (SNPs) in the *SNCA* region as one of the most common risk factors for sporadic PD (Pankratz, Wilk et al. 2009, Satake, Nakabayashi et al. 2009, Simon-Sanchez, Schulte et al. 2009, Edwards, Scott et al. 2010, International Parkinson Disease Genomics, Nalls et al. 2011). The likely impact of disease-associated *SNCA* variants identified by GWAS includes altered control of the level of transcription, regulation of alternative splicing, or altered stability of mRNA through post-transcriptional mechanisms.

1.4 Structure and function of ASYN

ASYN is a small presynaptic predominately neuronal protein that is linked genetically and neuropathologically to PD. Nonetheless, ASYN pathology is not confined only to PD but occurs also in other neurodegenerative disorders such as multiple system atrophy, DLB, LB variant of AD (LBV/AD), neurodegeneration with brain iron accumulation type I, pure autonomic failure and even a subtype of essential tremor disease, which are collectively termed synucleinopathies.

The first member of the family of proteins for which ASYN is named was cloned from the neuromuscular junction of the electric eel (Maroteaux, Campanelli et al. 1988). Antibodies against that protein labeled both synapses and nuclei, leading to the name "synuclein." A related protein was cloned from zebra finch as a protein upregulated during song learning, a period of enormous synaptic plasticity (George, Jin et al. 1995). ASYN is a highly conserved protein of 140 amino acids belonging to a multigene family that includes β-synuclein and γ-synuclein (George 2002). In solution it lacks a defined structure, thus it is described as "natively unfolded." However, ASYN can adopt an α-helical conformation upon binding to negatively charged lipids and can also form β-sheet structures on prolonged periods of incubation. Briefly, the protein is composed of three distinct structures: 1) the N-terminus region (residues 1-60) which contains apolipoprotein binding motifs (KTKEGV), responsible for the formation of α-helical structures; 2) the central hydrophobic region (residues 61-95), termed the NAC domain, which confers β-sheet potential; and 3) the C-terminus domain (residues 96-140), which is highly negatively charged and primarily unstructured (George 2002).

Post-translational modifications (PTMs) in the C-terminal region of ASYN, such as oxidation, nitration and phosphorylation, influence the propensity of ASYN to aggregate (Hashimoto, Hsu et al. 1999, Hashimoto, Takeda et al. 1999, Giasson, Duda et al. 2000). For example, phosphorylation at serine 129 may increase the propensity of ASYN to fibrillize, whereas phosphorylation at tyrosine 125 may prevent ASYN fibrillation (Uversky 2007). Similarly, C-terminal truncation of ASYN accelerates aggregation of the protein in vitro (Crowther, Jakes et al. 1998, Murray, Giasson et al. 2003). Truncated ASYN has been detected in LB in PD and DLB (Baba, Nakajo et al. 1998, Anderson, Walker et al. 2006). Tg mice overexpressing C-terminally truncated ASYN (1–130) have substantial cell loss in the SNpc but not in the ventral tegmental area (Wakamatsu, Ishii et al. 2008), suggesting a toxic function of truncated ASYN in SNpc dopaminergic neurons.
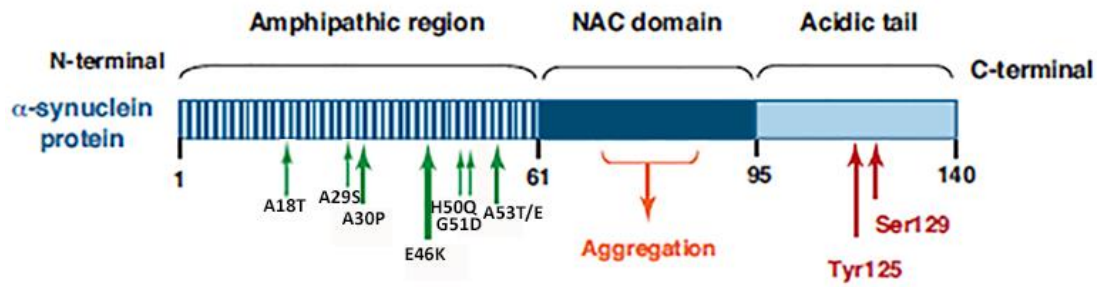
Figure 6. Schematic representation of human ASYN domains. Structurally, ASYN is a 140 amino acid protein and its sequence can be divided into three regions with distinct structural characteristics. The highly conserved N-terminal domain encodes for a series of imperfect 11 amino acid repeats with a consensus motif of KTKEGV reminiscent of the lipid-binding domain of apolipoproteins, which in certain conditions forms amphipathic helices. The eight missense mutations known to cause familial PD (A30P, E46K, A53T, A53E, H50Q, G51D, A18T, and A29S) lie in the amphipathic region, suggesting an important function for this region of the protein. The central hydrophobic region (non-amyloid-b component or NAC domain) of ASYN is associated with an increased propensity of the protein to form fibrils. The acidic C-terminal tail contains mostly negatively charged residues and is largely unfolded. Most common post translational modifications in the C-terminal region of SNCA that influence ASYN propensity to aggregate *in vivo* are phosphorylation at serine 129 (Ser 129) and phosphorylation at tyrosine 125 (Tyr 125) are indicated by the red arrows.

ASYN is expressed abundantly in the nervous system (1% of total cytosolic protein) but its expression has also been detected in peripheral tissues including heart, muscle and blood. Regarding its normal function although ASYN has been implicated in numerous cellular processes, its exact physiological function remains elusive. However, studies have identified various mechanisms in which ASYN interacts with neurotransmitters, lipids, carbohydrates, membrane bound receptors, and other proteins in the brain. Specifically, ASYN has been shown to interact with tubulin (Alim, Hossain et al. 2002) and that ASYN may have activity as a potential microtubule-associated protein, such as Tau (Alim, Ma et al. 2004). Importantly, recent evidence strongly suggests that ASYN functions as a molecular chaperone in the formation of SNARE complexes (Bonini and Giasson 2005, Chandra, Gallardo et al. 2005, Burre, Sharma et al. 2010, Burre, Sharma et al. 2014). In particular, it simultaneously binds to phospholipids of the plasma membrane via its N-terminus domain and to synaptobrevin-2 via its C-terminus domain, with increased importance during synaptic activity (Burre, Sharma et al. 2010). Importantly, a recent study demonstrated that soluble monomeric ASYN assembles into higher-order multimers upon membrane binding and that membrane binding of ASYN is required for its physiological activity in promoting SNARE complex assembly at the synapse (Burre, Sharma et al. 2014). In addition, ASYN has also been shown to be essential for normal cognition, since ASYN knock-out mice showed impaired spatial learning and working memory (Kokhan, Afanasyeva et al. 2012).

1.5 *SNCA* gene

SNCA was first identified as the gene encoding a protein of which a subfragment, termed the non-β-amyloid component of AD amyloid (NAC), was thought to be a component of the AD plaques (Ueda, Fukushima et al. 1993). Human *SNCA* is located on human chromosome 4q21.3–q22. Human SNCA spans a region of 111 kb and consists of 6 exons ranging in size from 42 to 1110 base pairs (bp) (Xia, Saitoh et al. 2001), 5 of which correspond to a coding region that is highly conserved between vertebrates. The translation start codon (ATG) is encoded by exon 2 and the stop codon (TAA) is encoded by exon 6. The NAC component is encoded by exon 4. Exon 1 was found to have different splicing sites, producing different 5'-untranslated sequences in the cDNAs (Xia, Saitoh et al. 2001). Several studies reviewed in Beyer et al. (Beyer 2006) reported alternative isoforms of *SNCA* caused by alternative splicing of exons 3 and 5 to produce 4 variants of different amino acid (aa) length: exons 3+5+ (140 aa; *SNCA* 140), exons 3-5+ (126 aa; *SNCA* 126), exons 3+5- (112 aa; *SNCA* 112) and exons 3-5- (98 aa; *SNCA* 98). *SNCA* 112 is reportedly only found in the brains of patients with LB disease and is upregulated in cell culture models by the parkinsonian neurotoxins MPP+ and rotenone (Kalivendi, Yedlapudi et al. 2010). Each intron is flanked by the canonical GT-AG splice-site nucleotides and introns' sizes range from 1.270 bp (intron 1) to 93.050 bp (intron 4). A 400 bp fragment upstream of the transcriptional start site was found to be sufficient for transcription in a luciferase assay in the human neuroblastoma cell line SHSY5Y and the mouse hypothalamus cell line GT1-7 (Xia, Saitoh et al. 2001) and in the SHSY5Y and 293T cell lines (Chiba-Falek and Nussbaum 2001) and is likely to include the core promoter of *SNCA*. This finding was also confirmed in our laboratory in primary cortical neuronal cultures (Clough, Dermentzaki et al. 2011). Additionally, a highly TC-rich sequence in intron 4 was found to be polymorphic by length and four alleles, A0, A1, A2, and B were identified in a Caucasian population (Xia, Saitoh et al. 2001). A dinucleotide repeat polymorphism located ~10 kb upstream from the SNCA gene called the NACP-Rep-1 repeat, has been shown to regulate *SNCA* expression in neuronal cell culture (Chiba-Falek and Nussbaum 2001) and in a Tg model (Cronin et al. 2009). In the European population, three of the four associated SNPs with the most significant P-values for PD in GWAS were clustered around the 3'-UTR of *SNCA* (rs2736990, rs3857059 and rs11931074) (Simon-Sanchez, Schulte et al. 2009). Additionally, the 3'-UTR of *SNCA* is known to contain target binding sites for two micro RNAs (miRNAs), mir-7 and mir-153, which are expressed predominately in neurons and downregulate *SNCA* expression (Junn, Lee et al. 2009, Doxakis 2010).
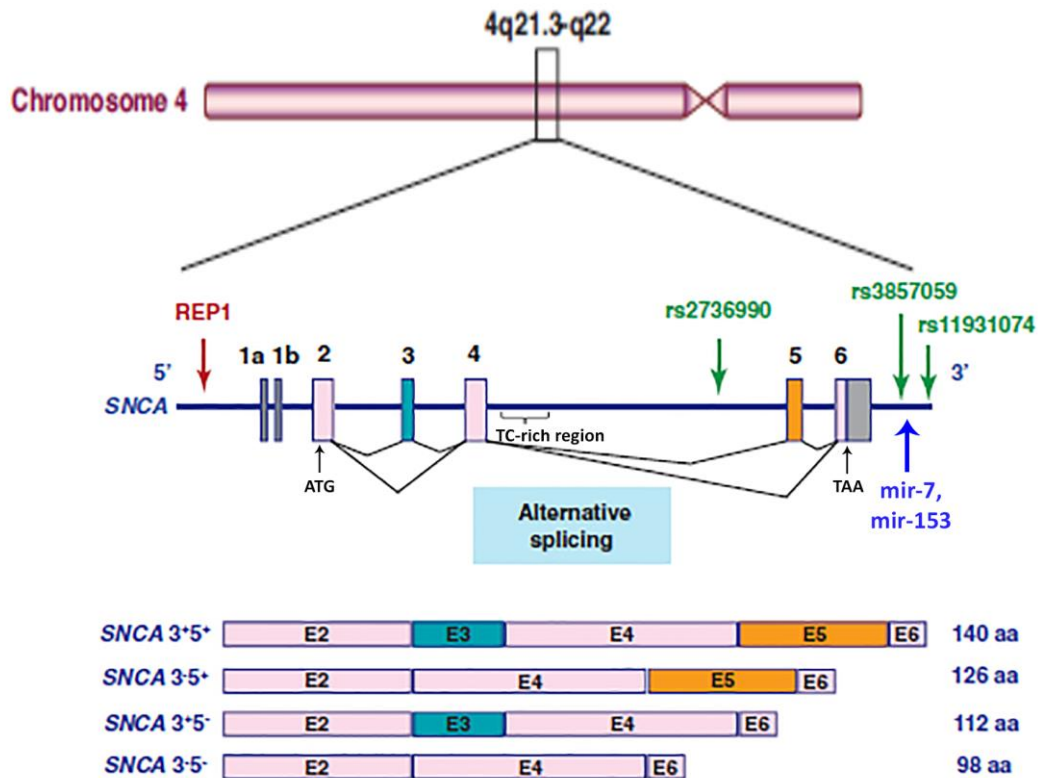
(Venda, Cragg et al. 2010)

Figure 7. Human *SNCA* gene and transcript variants. Human *SNCA* is located at chromosome 4, position 4q21.3-q22. Exons are depicted as numbered boxes and introns as lines. ATG and TAA represent the start and stop codons, respectively. 1a and 1b boxes represent different splicing products of exon 1. Alternative splicing of exons 3 and 5 generates four *SNCA* isoforms of different lengths (140 aa, 126 aa, 112 aa, and 98 aa). The REP 1 repeat in the promoter region is indicated by the red arrow. The three SNPs that were found to be most highly associated with PD (rs2736990, rs3857059 and rs11931074) are indicated by the green arrows. The miRNAs mir-7 and mir-153 which bind to the 3'-UTR of *SNCA* are indicated by the blue arrow. A TC-rich region is located 0.9 kb downstream of the exon 4/intron 4 boundary.

The mouse α-synuclein gene (*Snca*) spans a genomic region of 98 kb, slightly smaller than its human counterpart. Comparison of the genomic and cDNA sequence using the VISTA program (Touchman, Dehejia et al. 2001) revealed that the intron / exon structures of the mouse and human genes are highly conserved, which was expected since the human and rodent proteins are 95.3% identical (Lavedan 1998). This comparison highlighted sequence conservation coinciding with the *SNCA* / *Snca* coding exons 2–5 and the 5' coding portion of exon 6. The 5'-UTR, which is contained almost entirely within the first exon, is not well conserved between human and mouse. In contrast, the 3'-UTR is 80.4% identical up to the first polyadenylation site shared by both species. Nineteen regions within intron 4 achieve an average cross-species identity of at least 75%. These evolutionary conserved regions, do not represent exons but are likely enhancer elements (Sterling, Walter et al. 2014, Lutz, Saul et al. 2015). The segment extending ∼10 kb upstream of exon 1, the region likely to contain the minimal promotor as well as putative regulatory sequences, also shows high sequence similarity.

1.6 Transcriptional gene regulation

1.6a Layers of transcriptional gene regulation

Gene regulation is a fundamental process in every biological system. Reflective of its importance to cell survival and function, the regulatory mechanisms governing gene expression are exquisitely sophisticated. The key concepts of transcriptional control were established in the early 1960s in bacterial systems by Francois Jacob and Jacques Monod (Jacob and Monod 1961). Their pioneering work and many subsequent studies established that regulatory proteins called transcription factors (TFs) act *in trans* to promote or inhibit gene expression by binding to specific DNA sequences in cis-regulatory modules (CRMs) or enhancers. Currently new data and high-throughput technologies have expanded our knowledge regarding the cellular gene expression programs and the mechanisms involved in the global regulation of transcription.

In order to facilitate our understanding of this extremely complex process of eukaryotic transcriptional gene regulation has been dissected into many layers. The first layer of transcriptional regulation can be appreciated at the level of naked DNA. The most basic model dictates that TFs bind to specific DNA binding sites (CRMs or enhancers) to drive or repress gene expression by recruiting cofactors and RNA polymerase II to target genes (Ong and Corces 2011, Lelli, Slattery et al. 2012, Spitz and Furlong 2012). TFs can be separated into two classes based on their regulatory responsibilities: control of initiation versus control of elongation (Yankulov, Blau et al. 1994, Fuda, Ardehali et al. 2009, Rahl, Lin et al. 2010, Adelman and Lis 2012, Zhou, Li et al. 2012). Nonetheless, this distinction is not always clear since some TFs may participate in the control of both initiation and elongation. Cofactors on the other hand, are protein complexes that contribute to activation (coactivators) or repression (corepressors), but do not have DNA-binding properties of their own. These coactivators include the Mediator complex, P300, and general transcription factors, among others (Sikorski and Buratowski 2009, Juven-Gershon and Kadonaga 2010, Malik and Roeder 2010, Taatjes 2010).

Briefly, once the recruited RNA polymerase II molecules initiate transcription, they generally transcribe for a short distance, typically 20–50 bp, and then pause (Adelman and Lis 2012). This process is controlled by the pause control factors DSIF and NELF, which are physically associated with the paused RNA polymerase II molecules. The paused polymerases may transition to active elongation through pause release, or they may ultimately terminate transcription with release of the small RNA species. Pause release and subsequent elongation occur through the recruitment and activation of positive transcription elongation factor b (P-TEFb), which phosphorylates the paused polymerase and its associated pause control factors. P-TEFb can be brought to these sites in the form of a large complex called the super elongation complex (Smith, Lin et al. 2011, Luo, Lin et al. 2012). Additional complexes, such as PAFc, also contribute to the regulation of elongation (Jaehning 2010). TFs such as c-Myc stimulate the P-TEFb-mediated release of RNA polymerase II from these pause sites and thus contribute to the control of transcription elongation (Rahl, Lin et al. 2010).

Recent studies have provided new insights into cofactors that play important roles in DNA loop formation and maintenance, which are key to proper gene control. During transcription initiation, the DNA loop formed between enhancers and core promoter elements is stabilized by cohesin, which is recruited by the NIPBL cohesin-loading protein that is associated with mediator complex (Kagey, Newman et al. 2010). The cohesin complex has circular dimensions capable of encircling two nucleosome-bound molecules of DNA. Although cohesion is recruited to active promoters, it also becomes associated with the DNA-binding factor CTCF, which has been implicated in the formation of insulator elements. Thus, cohesin is thought to have roles in transcription activation at some genes and in silencing at others (Parelho, Hadjur et al. 2008, Wendt, Yoshida et al. 2008, Hadjur, Williams et al. 2009, Phillips and Corces 2009, Schmidt, Schwalie et al. 2010, Dorsett 2011).

The above stripped-down view of DNA, although important for understanding the biophysical properties that govern TF-DNA interactions, ignores all of the complexities of the nuclear environment. DNA in eukaryotic genomes is compacted into chromatin; the basic unit of chromatin, the nucleosome, consists of 147 bp of DNA wrapped around a histone octamer containing 2 copies of each of the core histones H2A, H2B, H3, and H4 (Luger, Mader et al. 1997, Li and Reinberg 2011). DNA associated with histones is less accessible to TFs and RNA polymerase than is naked DNA, making chromatin transcriptionally more repressed than naked DNA. This fundamental unit of chromatin, the nucleosome is regulated by protein complexes that can mobilize the nucleosome or modify its histone compartments. Gene activation is accompanied by the recruitment of ATP-dependent chromatin remodeling complexes of the SWI/SNF family, which mobilize nucleosomes to facilitate access of the transcription apparatus and its regulators to DNA (Clapier and Cairns 2009, Hargreaves and Crabtree 2011). In addition, there is recruitment, by TFs and the transcription apparatus, of an array of histone-modifying enzymes that acetylate, methylate, ubiquitinylate, and otherwise chemically modify nucleosomes in a stereotypical fashion across the span of each active gene (Campos and Reinberg 2009, Bannister and Kouzarides 2011, Gardner, Allis et al. 2011, Li and Reinberg 2011, Rando 2012, Zhu, Adli et al. 2013). These modifications provide interaction surfaces for protein complexes that contribute to transcriptional control. Enzymes that remove these modifications are also typically present at the active genes, producing a highly dynamic process of chromatin modification as RNA polymerase is recruited and goes through the various steps of initiation and elongation of the RNA species.

Repressed genes are embedded in chromatin with modifications that are characteristic of specific repression mechanisms (Moazed 2009, Beisel and Paro 2011, Cedar and Bergman 2012, Jones 2012, Reyes-Turcu and Grewal 2012). One type of repressed chromatin, which contains nucleosome modifications generated by the polycomb complex (e.g., histone H3K27me3), is found at genes that are silent but poised for activation at some later stage of development or differentiation (Orkin and Hochedlinger 2011). Another type of repressed chromatin is found in regions of the genome that are fully silenced, such as those containing retrotransposons and other repetitive elements (Feng, Jacobsen et al. 2010, Lejeune and Allshire 2011). The mechanisms that silence this latter set of genes can involve both nucleosome

modification (e.g., histone H3K9me3) and DNA methylation. Below, transcriptional regulation at the level of naked DNA and the nucleosome is presented schematically in Fig. 8.
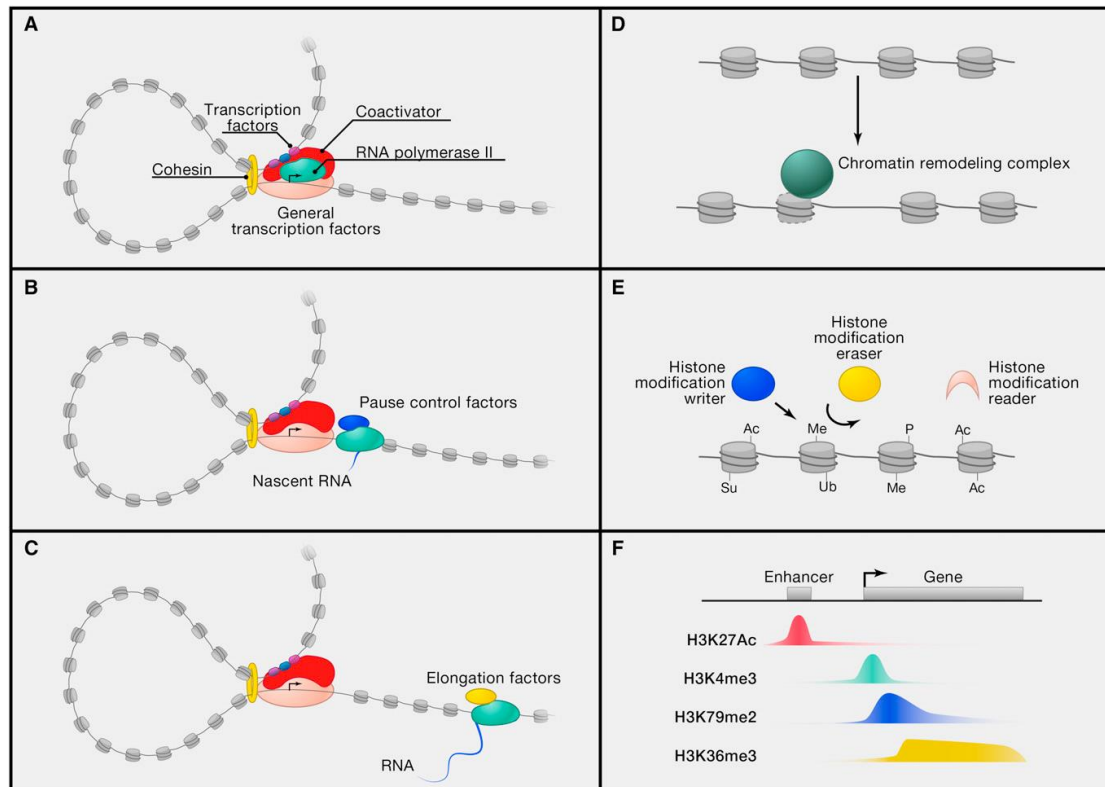
(Lee and Young 2013)

Figure 8. Transcriptional Regulation process. (A) Formation of a preinitiation complex. TFs bind to specific DNA elements (enhancers) and coactivators, which bind to RNA polymerase II, which in turn binds to general TFs at the transcription start site (arrow). The DNA loop formed between the enhancer and the start site is stabilized by cofactors such as the mediator complex and cohesin. (B) Initiation and pausing by RNA polymerase II. RNA polymerase II begins transcription from the initiation site, but pause control factors cause it to stall some tens of bp downstream. (C) Pause release and elongation. Various TFs and cofactors recruit elongation factors such as P-TEFb, which phosphorylates the pause release factors and polymerase, allowing elongation to proceed. (D) Chromatin structure is regulated by ATP-dependent remodeling complexes that can mobilize the nucleosome, allowing regulators and the transcription apparatus increased access to DNA sequences. (E) Transcriptional activity is influenced by proteins that modify and bind the histone components of nucleosomes. Some proteins add modifications (writers), some remove modifications (erasers), and others bind via these modifications (readers). The modifications include acetylation (Ac), methylation (Me), phosphorylation (P), SUMOylation (Su), and ubiquitination (Ub). (F) Histone modifications occur in characteristic patterns associated with different transcriptional activities. As an example, the characteristic patterns observed at actively transcribed genes are shown for histone H3 lysine 27 acetylation (H3K27Ac), histone H3 lysine 4 trimethylation (H3K4me3), histone H3 lysine 79 dimethylation (H3K79me2), and histone H3 lysine 36 trimethylation (H3K36me3).

Until this point we have unfolded a two-dimensional, linear view of DNA and chromatin. Another higher level of transcriptional control can be achieved by high-order chromatin structure and three dimensional organization of chromosomes in the nuclei. Our knowledge of how nuclear architecture and chromosomal conformation are implicated in eukaryotic gene expression has increased dramatically over the past decade due to immense technological advances in chromosome conformation capture (3C) and 3C-bases high-throughput technologies (Dekker, Rippe et al. 2002, de Wit and de Laat 2012) as well as microscopy-based techniques for studying subnuclear DNA or RNA localization (Lieberman-Aiden, van Berkum et al. 2009, Eskiw and Fraser 2011).

Regarding nuclear organization, a general conclusion from the above studies is that the interior of the nucleus is not a uniform compartment. Chromosomes occupy defined spatial regions termed "territories", which are often further organized on the basis of gene density and activity (Vaquerizas, Akhtar et al. 2011, de Wit and de Laat 2012, Dostie and Bickmore 2012, Ethier, Miura et al. 2012, Sexton, Yaffe et al. 2012). Gene-rich regions are found more toward the center of the nucleus, whereas gene-poor regions are located closer to the nuclear periphery. Although the mechanisms are unclear, rearrangements toward the periphery are proposed to be a consequence of interactions with the nuclear envelope (Zuleger, Robson et al. 2011). Additionally, active genes are generally found at the surface of a chromosomal territory, whereas inactive or repressed genes are buried in the interior (Vaquerizas, Akhtar et al. 2011, de Wit and de Laat 2012, Dostie and Bickmore 2012, Ethier, Miura et al. 2012). Highly expressed genes have also been observed to reside in foci that have been termed "transcription factories" (Razin, Gavrilov et al. 2011). These observations and others have led to the idea that colocalization may lead to coregulation (Dai and Dai 2012).

In addition, recent Hi-C data in *Drosophila* further correlate intra- and interchromosomal interactions with transcriptionally active regions, whereas inactive domains remain confined within their respective chromosomal territories (Sexton, Yaffe et al. 2012). For example the identification of the β-globin locus control region and gypsy insulators in *Drosophila* established looping as the predominant paradigm for enhancer-promoter interactions, and there are now many examples of enhancer-promoter communication that occur as a result of looping (Krivega and Dean 2012). Recent experiments in *Drosophila* directly correlate enhancer-promoter interactions with cell type-specific gene expression using a new method called cgChIP (cell- and gene-specific ChIP) (Agelopoulos, McKay et al. 2012). In addition to cis-looping models, enhancers can also interact with promoters *in trans*. In *Drosophila*, this process is called transvection and has been observed between Hox complexes on homologous chromosomes (Duncan 2002). In vertebrates, *trans* enhancer-promoter interactions have been observed during odorant receptor choice in olfactory neurons (Lomvardas, Barnea et al. 2006).

However, other studies using glycocorticoid-inducible gene expression in cell lines did not observe significant chromosomal rearrangements upon activation (Hakim, Sung et al. 2011). Therefore, we must be cautious in making broad interpretations regarding the role of nuclear architecture in gene regulation, as observations can be highly specific to a particular gene or group of genes. New advances in microscopy may help

to sort out data from cross-linking-based studies by visualizing interactions in situ (Joseph, Orlov et al. 2010). Below, all the layers of transcriptional regulation are summarized schematically in Fig. 9.
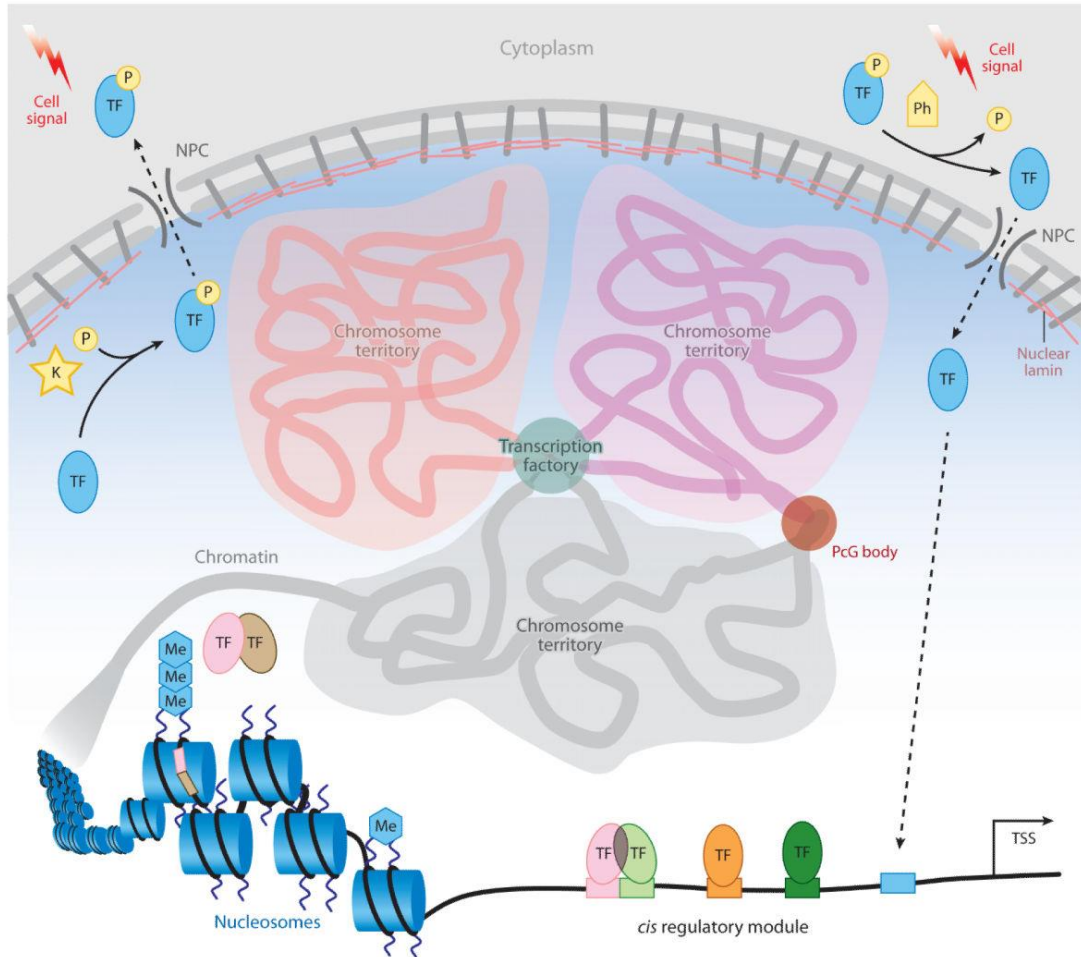
(Lelli, Slattery et al. 2012)

Figure 9. Overview of eukaryotic gene regulation. Within the nucleus of a cell, chromosomes occupy defined spatial regions called territories. Interactions between adjacent territories can correlate with transcriptionally active chromatin in transcription factories or silenced chromatin in polycomb group (PcG) bodies. Posttranslational modification of TFs, such as phosphorylation (P), can influence nuclear import (*dashed arrows*) through nuclear pore complexes (NPCs) in response to extracellular signals. Posttranslational modifications of histones, such as methylation (Me), can also correlate with the transcriptional state of associated genes. The position of nucleosomes can restrict access of TFs by occluding binding sites (*colored rectangles*). Lastly, TF recognition of specific binding sites, either as monomers or as a part of a complex with other proteins, also contributes to proper recruitment or release of RNA polymerase from the transcriptional start site (TSS). Abbreviations: K, kinase; Ph, phosphatase.

Additionally, apart from the established role of TFs and CRMs in the transcriptional gene control recent studies and the ENCODE project have highlighted the substantial role of non-coding RNAs (ncRNAs) in gene expression through modulation of transcriptional and posttranscriptional processes (Bartel 2009, Orom and Shiekhattar 2011, Ebert and Sharp 2012, Lee 2012, Rinn and Chang 2012, Wright and Ciosk 2013). Briefly, miRNAs, which are the best studied of the various classes of ncRNAs, fine tune the levels of target messenger RNAs (mRNAs). Some long ncRNAs (lncRNAs) recruit chromatin regulators to specific regions of the genome and thereby modify gene expression, and some apparently do not have a function but are simply a product of a transcriptional event that is itself regulatory (Latos, Pauler et al. 2012).

1.6b Modes of action of TFs

In prokaryotes, single TFs are able to regulate gene expression. However, this type of gene regulation is usually insufficient for eukaryotic gene regulation. Instead, eukaryotes rely on combinatorial transcriptional inputs into CRMs to regulate gene expression in space and time (Istrail and Davidson 2005). The specific recruitment of many individual factors refines expression on the basis of cellular context, timing of expression, and extracellular signals. For example, the same binding sites in the same CRM of the *Drosophila* nidogen gene have been shown to bind different forkhead domain TFs in different tissues, with distinct regulatory outputs (Zhu, Ahmad et al. 2012). Alternatively, multiple homeobox (Hox) TFs, which have highly similar DNA-binding specificity as monomers, can target the same gene via distinct CRMs in different tissues (Enriquez, Boukhatmi et al. 2010). It also appears that TFs can bind non-canonical motifs in certain contexts, although the mechanism by which these motifs are distinguished from canonical motifs remains unclear (Badis, Berger et al. 2009, Busser, Shokri et al. 2012). Regulation can be further refined by PTMs of TFs, which can affect subcellular localization, DNA binding, and protein-protein interactions (Tootle and Rebay 2005, Benayoun and Veitia 2009, Bernard and Harley 2010, Charlot, Dubois-Pot et al. 2010, Daitoku, Sakamaki et al. 2011). Some researchers propose a PTM code in which multisite PTM events provide an important regulatory mechanism for different signaling pathways to affect TF function and influence gene expression (Benayoun and Veitia 2009). Below, the mechanisms that dictate the assembly of TFs in the CRMs are presented briefly in Fig.10.

a Enhanceosome

Modular cooperativity
Strict grammar

Enhanceosome
cooperativity

b Billboard or TF collective

Local cooperativity
Flexible grammar

c DNA allostery

Gene X

Gene Y

d Classical cooperativity

Latent specificity

Gene X

A + B

Gene Y

A'B'

Multiple partners

+

B

A

+

C

Gene X

A + B

Gene Y

A + C

e Collaborative competition
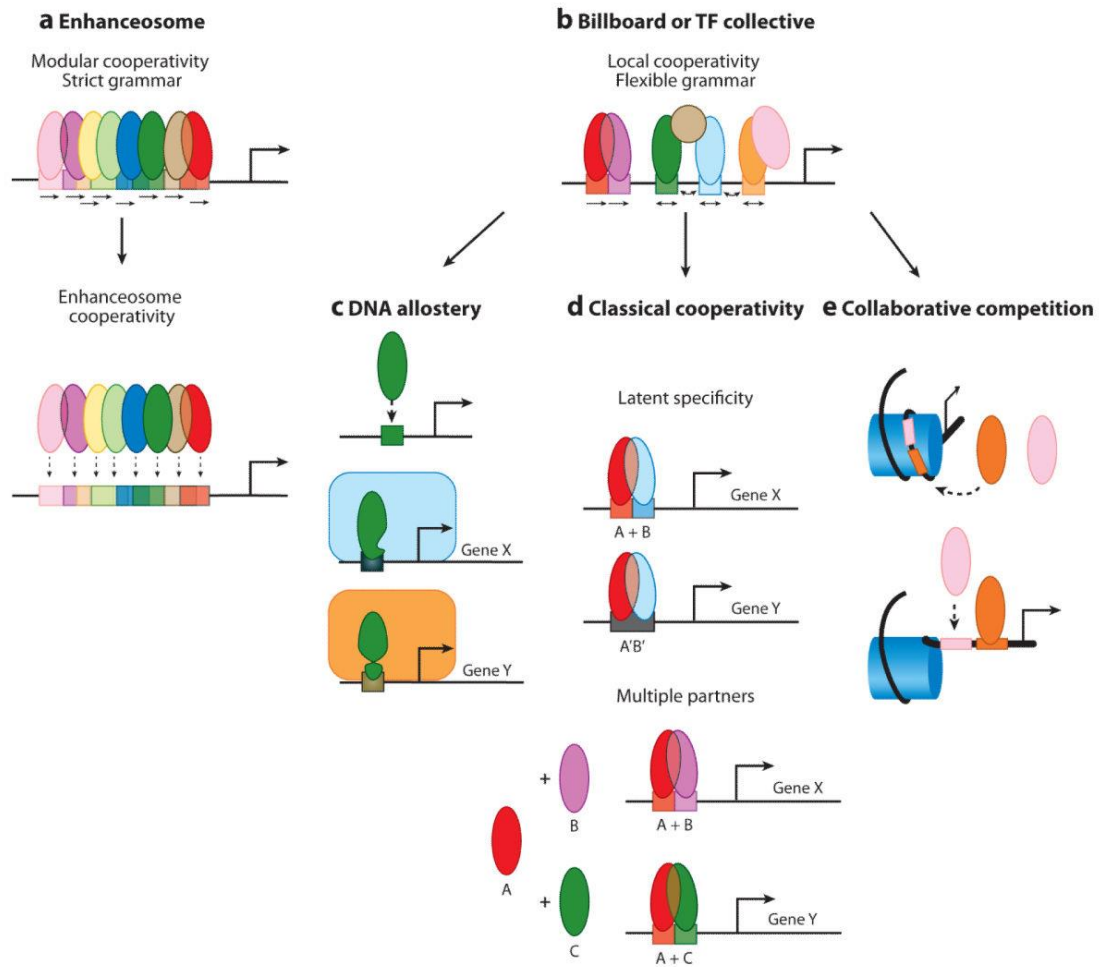
(Lelli, Slattery et al. 2012)

Figure 10. Cis-regulatory module (CRM) assembly and cooperative DNA-binding models. This image depicts three different models of CRM assembly and related cooperativity mechanisms. (*a*) The enhanceosome model requires strict modular cooperativity between all TFs. (*b*) In contrast, the flexibility of the Billboard and TF Collective models permits different cooperativity mechanisms to control CRM assembly. (*c*) In the case of DNA allostery, interactions between the DNA sequence and the TF can facilitate conformational changes in the TF that result in the recruitment of different regulatory complexes (*rounded rectangles*) in a sequence-specific manner. (*e*) Classical cooperativity uses protein-protein interactions between TFs to facilitate cooperative binding. These types of cooperative interactions help to increase TF DNA-binding specificity by restricting recruitment to dimeric sites (A+B). In the case of latent specificity, direct protein-protein interactions alter binding specificities so that TFs recognize novel composite sites (A'B'). (*f*) Lastly, collaborative competition between TFs and nucleosomes can lead to cooperative binding when the binding of one TF provides access for another TF to bind a neighboring site.

1.7 Transcriptional regulation of *SNCA*

As has already been mentioned, genetic alterations in *SNCA* are closely linked to familial and sporadic PD. Briefly, several lines of evidence have directly linked increased levels of WT *SNCA* with dysfunctional and abnormal ASYN deposition and neurodegeneration in humans and in animal models, while polymorphisms within and around the *SNCA* gene locus are correlated to increased PD risk. Collectively, these studies support the over-arching idea that dysregulation of *SNCA* levels, leading to its excess accumulation and aggregation, is a major factor in PD pathogenesis. Nonetheless, to date not much is known about the regulation of *SNCA* in general, let alone about its transcriptional regulation.

From previous studies it is well established that under physiological conditions ASYN protein levels are developmentally induced in the rat brain (Petersen, Olesen et al. 1999) and in rat neuronal cell cultures (Murphy, Rueter et al. 2000, Rideout, Dietrich et al. 2003, Vogiatzi, Xilouri et al. 2008), following determination of neuronal phenotype and establishment of synaptic connections. In contrast, *Snca* mRNA levels follow a different expression pattern. More specifically in the central nervous system (CNS) of rodents the mRNA levels of *Snca* begin to rise at the end of embryonic life and reach their highest level during the first weeks of postnatal life. Following this period, *Snca* mRNA levels drop considerably (Petersen, Olesen et al. 1999), even though protein levels are stable (Li, Lesuisse et al. 2004), suggesting that the protein is regulated in adulthood by additional post-transcriptional and post-translational modifications. The mechanisms involved in the developmental transcriptional regulation of *SNCA* remain elusive to a great extent. Moreover, *Snca* expression levels are modulated in conditions that alter plasticity or confer injury (George, Jin et al. 1995, Kholodilov, Neystat et al. 1999, Vila, Vukosavic et al. 2000, Manning-Bog, McCormack et al. 2002), but again, the mechanisms involved are unclear. It is possible, that the mechanisms involved in the developmental process and in plasticity-induced conditions share common features.

Conversely, under pathological conditions in PD there has been controversy regarding the expression levels of *SNCA* mRNA in the brains of sporadic PD patients, with studies reporting both increased and decreased levels of *SNCA* (Rockenstein, Hansen et al. 2001, Kingsbury, Daniel et al. 2004, Chiba-Falek, Lopez et al. 2006, Dachsel, Lincoln et al. 2007, Papapetropoulos, Adi et al. 2007). However, Grundemann et al. (Grundemann, Schlaudraff et al. 2008), by applying laser-capture microdissection reported increased *SNCA* mRNA levels in the surviving nigral neurons derived from PD brains compared to control samples. Protein levels are not obviously increased overall in PD brains, although clearly there is a transition favoring the insoluble components, including monomeric and oligomeric ASYN. Interestingly, it has been reported that in certain mouse models of neurodegenerative diseases, including an inducible *SNCA* model, reversal of expression of the causative proteins ameliorated neurodegeneration (Yamamoto, Lucas et al. 2000, Zu, Duvick et al. 2004, Nuber, Petrasch-Parwez et al. 2008, Lim, Kehm et al. 2011). Therefore, if *SNCA* levels could

be controlled then certain aspects of the disease phenotype could be halted or even reversed.

Toward that direction, previous work in our laboratory utilizing primarily the rat pheochromocytoma PC12 cell line but also primary neuronal cultures in order to study the mechanisms involved in the transcriptional regulation of *SNCA*, resulted in some interesting novel insights regarding this complex process. PC12 cells is a model system used frequently to study the mechanisms of the neurotrophin-mediated differentiation of proliferating neuronal precursors to post-mitotic, differentiated neuron-like cells that possess many characteristics of sympathetic neurons (Greene and Tischler 1976). Rat cortical cultures is a well-established primary neuronal cell model system that represents an abundant and relatively homogeneous source of post-mitotic neurons from the CNS with at least 95% purity (Rideout and Stefanis 2002) which allow the performance of several biochemical assays and most importantly neurons that are affected in later stages of PD progress (Mattila, Rinne et al. 2000). We have confirmed that *Snca* is induced (mRNA and protein) in differentiated PC12 cells (Stefanis, Kholodilov et al. 2001, Clough and Stefanis 2007) and rat cortical neurons upon maturation of the cultures (Vogiatzi, Xilouri et al. 2008, Clough, Dermentzaki et al. 2011). We have demonstrated that the neurotrophin-mediated upregulation of *SNCA* in PC12 cells involves the extracellular signal- regulated kinase (ERK) and the phosphatidyl-inositol 3 kinase (PI3K) pathways along with transcriptional control elements lying within the intron 1 region of the *SNCA* gene locus (Clough and Stefanis 2007). Notably, in PC12 cells, *SNCA* promoter deletion constructs (related to the full human *SNCA* 10.7-kb promoter construct) including either the core promoter of *SNCA* or the intron 1 region alone demonstrated high transcriptional activity, whereas constructs including both the core promoter and intron 1 were inactive. Strikingly, in rat cortical cultures we observed the exact opposite pattern, deletion constructs including both the core promoter and intron 1 were transcriptionally active, whereas those that contained the core promoter and intron 1 in isolation were inactive. Additionally, these effects were mediated only through the Trk and PI3K signaling pathways. Further, application of exogenous brain-derived neurotrophic factor (BDNF) recapitulated these effects, although inhibition of BDNF did not lead to any appreciable alteration in the levels of *Snca*, suggesting that BDNF, although sufficient for *Snca* mRNA induction, is not the main factor involved in the *Snca* induction with maturation in culture (Clough, Dermentzaki et al. 2011). Below, the differences in *SNCA* transcriptional activity of different *SNCA* promoter constructs between PC12 cells and rat cortical cultures are presented briefly in Fig.11.
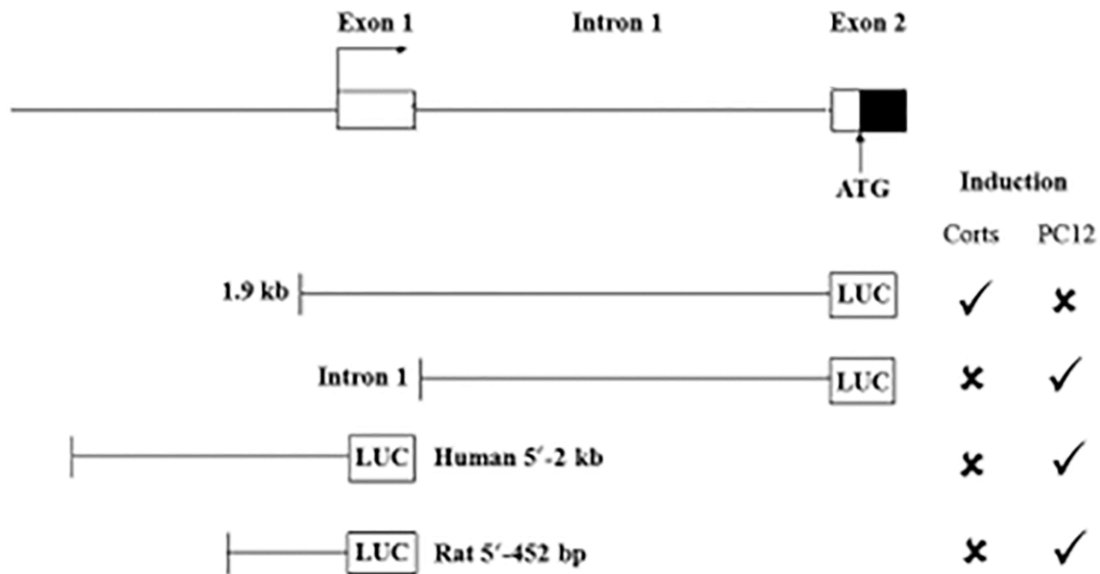
Figure 11. Differential *SNCA* transcriptional activity in PC12 cells and in rat cortical cultures. The top cartoon shows the 5' genomic region of human *SNCA*. Exons are depicted as closed boxes and introns as lines. The canonical 5' transcriptional start site is depicted with an angled arrow at the start of exon 1. ATG marks the translational start site at exon 2. Luciferase constructs for this region are depicted as lines connected to a LUC-labeled box. Activation in the luciferase assay (V) or lack of induction (X) is dependent on the transcriptional elements present (core promoter and intron 1) and the cell system (differentiated PC12 cells and rat cortical cultures [corts]). The constructs Human 5'-2kb and Rat 5'-452bp contain the core promoter of *SNCA*, while the 1.9-kb construct contains both the core promoter and intron1.

In parallel, an independent study by Scherzer et al. (Scherzer, Grass et al. 2008) confirmed the importance of *SNCA* intron 1 region by reporting that the GATA-2 TF can occupy intron 1 and further modulate *SNCA* expression in dopaminergic cells. However, a recent study, by Brenner et al. (Brenner, Wersinger et al. 2015), even though identified through bioinformatics analysis putative binding sites for GATA-2 in *SNCA* intron 1, instead revealed significant occupancy for GATA-2 within intron 2. Additionally, several studies have highlighted the involvement of intron 1 methylation, as an epigenetic mechanism to modulate *SNCA*. Two independent studies (Jowaed, Schmitt et al. 2010, Matsumoto, Takuma et al. 2010) reported that decreased methylation of the CpG islands spanning the intron 1 area of *SNCA* was associated with increased expression of *SNCA*, importantly, intron 1 hypomethylation was observed in postmortem brains of patients with sporadic PD. Interestingly, the CpG islands within intron 1 that were mainly found hypomethylated were the ones located within predicted consensus TF binding sites (TFBSs), suggesting that *SNCA* intron 1 methylation-mediated transcriptional regulation may depend on the binding of specific TFs. Further, Wang et al. (Wang, Wang et al. 2013) also observed increased *SNCA* expression in various cell lines including dopaminergic neurons following intron 1 hypomethylation. Besides neuronal cell lines and brain samples, hypomethylation of *SNCA* intron 1 was also evident in blood samples from PD patients compared to controls (Ai, Xu et al. 2014, Pihlstrom, Berge et al. 2015), suggesting that SNCA intron 1 hypomethylation

could serve as a potential biomarker for PD. Interestingly, *SNCA* intron 1 hypomethylation in blood samples was also associated with the Rep-1 polymorphism located 5' of *SNCA* (Ai, Xu et al. 2014) and rs3756063 polymorphism located 3' of *SNCA* (Pihlstrom, Berge et al. 2015), thus further supporting a link between *SNCA* variability, promoter methylation, and PD risk. Conversely, the methylation status of the SNCA intron 1 CpG islands in peripheral leukocytes is still under debate with other studies reporting *SNCA* intron 1 hypomethylation in PD patients compared with normal controls (Tan, Wu et al. 2014) and studies reporting no difference (Richter, Appenzeller et al. 2012, Song, Ding et al. 2014). Therefore, the potential of *SNCA* methylation as a biomarker in PD warrants further investigations. Further, γ-synuclein, a member of the synuclein family has also been shown to contain critical elements within its first intron (Lu, Gupta et al. 2001, Surgucheva and Surguchov 2008). In a recent study by Sterling et al. (Sterling, Walter et al. 2014) a number of functional non-coding conserved regions, located in the intron 1 region of *SNCA* were also found to be involved in its transcriptional activity. Collectively, the above data further strengthen the importance of the intron 1 region in the transcriptional control of *SNCA*.

Following that notion, we screened for regulatory elements in the intron 1 region of *SNCA*. Through cross-species alignment (Clustal W; Larkin et al 2007) and MatInspector analysis for identifying putative TFBSs (with human, rat and mouse sequences) we identified a novel TF named zinc finger and SCAN domain containing 21 (ZSCAN21) to be at least one of the factors responsible for the observed *SNCA* induction in differentiated PC12 cells (Clough, Dermentzaki et al. 2009). Briefly, we found that a binding site for ZSCAN21 at the very beginning of intron 1 of SNCA is required for its transcriptional activity in PC12 cells, since deletion of this binding site from the human intron 1 construct resulted in significant (~50%) decrease in the luciferase assay. Likewise, *Zscan21*-mediated small-interfering RNA (siRNA) silencing led to decreased luciferase activity from the human intron 1 construct (~50%) when compared with control scrambled siRNA and also significantly inhibited ASYN expression. Additionally, electromobility shift assay (EMSA) analysis revealed the presence of a protein in the nuclear extract of PC12 cells that was able to specifically bind to *Zscan21* DNA probes. Therefore, these results conclusively demonstrated the involvement of ZSCAN21 in the transcriptional regulation of *SNCA* in PC12 cells. At this point we must mention that current analysis utilizing an updated version of MatInspector Software revealed a second putative binding site for ZSCAN21 in the intron 1 region of SNCA 130 bp downstream related to the first ZSCAN21 binding site that we also included in the present study. An additional ZSCAN21 putative binding site located very 5' to the *SNCA* promoter was not included. Below, the basic regulatory elements of intron 1 region of *SNCA* gene are presented schematically in Fig.12.
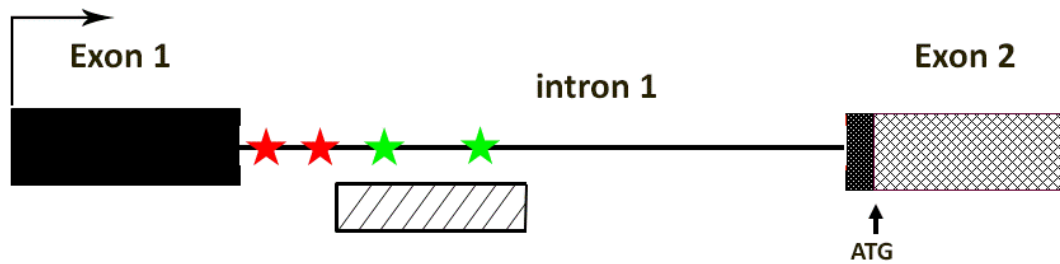
Figure 12. Schematic of human *SNCA* intron 1 regulatory elements. Exons 1 and 2 are depicted as boxes, with the translated regions filled in and the untranslated regions as hatched boxes. The intron 1 is depicted by a line. The bent arrow marks the canonical transcription start site at exon 1 whereas ATG marks the translational start site at exon 2. Red filled stars at the 5' prime of intron 1 represents the putative binding site for the ZSCAN21 TF (Clough, Dermentzaki et al. 2009, Brenner, Wersinger et al. 2015) whereas green stars the putative GATA-2 binding sites (Scherzer, Grass et al. 2008). CpG islands spanning intron 1 region as described in Jowaed et al. (Jowaed, Schmitt et al. 2010) are presented as a white hatched box.

ZSCAN21 (synonyms: Zipro 1, RU49, Zfp38, NY-REN1, CTfin51) is a DNA binding TF that belongs to the Krüppel C2H2-type zinc finger protein family. In general, zinc finger TFs can exert either positive or negative regulation of genes (Laity, Lee et al. 2001). Diversity in the modular multi-finger protein family is determined by the conserved domains found outside the zinc finger region. These domains include BTB/POZ (Bardwell and Treisman 1994), KRAB (Bellefroid, Poncelet et al. 1991), and SCAN (Williams, Blacklow et al. 1999). They usually control selective association of the TFs with other cellular factors essential for regulation, subcellular localization, DNA binding or transcription. In particular, the SCAN domain is restricted to vertebrates and can act as a mediator of both homo and heterodimerization (Williams, Blacklow et al. 1999, Sander, Haas et al. 2000, Schumacher, Wang et al. 2000, Stone, Maki et al. 2002, Sander, Stringer et al. 2003). It is an 82–88 amino acid highly conserved domain (Williams, Blacklow et al. 1999, Sander, Haas et al. 2000, Honer, Chen et al. 2001, Stone, Maki et al. 2002), forming a structurally independent module with 5 distinct α-helices in each monomer (Ivanov, Stone et al. 2005). Human ZSCAN21 shares 82% homology with mouse and rat ZSCAN21 and is primarily localized in the nucleus. An important difference is observed at the N-terminal region where human ZSCAN21 lacks 77 residues of the trans-activation region relative to rodent ZSCAN21 (Carneiro, Silva et al. 2006). Mouse ZSCAN21 (Zfp-38) reportedly function as a TF, containing 3 sequence repeats that show trans-activation activity (Chowdhury, Goulding et al. 1992). It binds to a bipartite motif (5'-AGTAC-3') showing higher affinity to motifs separated by 2–7 nucleotide (Yang, Zhong et al. 1996). Human ZSCAN21 has been shown to form homodimers and also heterodimers with SCAND1 (Carneiro, Silva et al. 2006), a SCAN family protein that lacks the zing finger region (Sander, Haas et al. 2000). Importantly, from high throughput bioinformatics analysis (two-hybrid and high affinity mass spectrometry), human ZSCAN21 has been predicted to interact with many co-repressors or co-activators. Intriguingly mouse ZSCAN21, although sharing 97% amino acid similarity in the SCAN domain with the human protein, has been reported not to form homodimers and to interact only with zinc finger and SCAN containing domain 26 (Williams, Blacklow

et al. 1999). Regarding its role in the CNS it has been shown to participate in the proliferation of granule cell precursors during post-natal development (Alder, Cho et al. 1996, Yang, Zhong et al. 1996, Yang, Wynder et al. 1999). In addition, in the peripheral nervous system it is reportedly involved in the activation of non-myelinating Schwann cells in general, and terminal Schwann cells in particular (Ellerton, Thompson et al. 2008). Regarding *SNCA*, a recent study has shown that overexpression of ZSCAN21 can both repress *SNCA* and increase *SNCB* expression in the SHSY5Y cell line (Wright, McHugh et al. 2013). Moreover, a study by Brenner et al. (Brenner, Wersinger et al. 2015) reported that ZSCAN21 and GATA-2 bind directly to the intron 1 and intron 2 region of *SNCA*, respectively in human brain tissue. Given the important role of ZSCAN21 in the transcriptional regulation of SNCA in neuronal-like cells (PC12 and SHSY5Y) as well as the fact that ZSCAN21 binds to the intron 1 region of *SNCA* in human brain tissue, we wished to investigate further its role in the transcriptional regulation of *SNCA* in primary neuronal cultures, and in particular, *in vivo*.
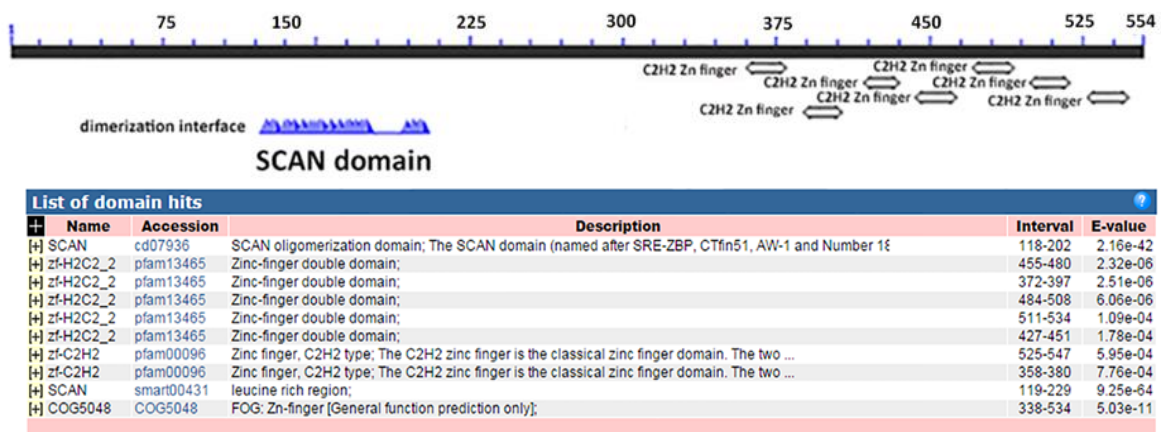
Figure 13. Schematic of ZSCAN21 conserved domains. ZSCAN21 consists of the SCAN oligomerization domain which is found in several vertebrate proteins that contain C2H2 zinc finger motifs, many of which may be TF playing a role in cell survival and differentiation. This protein-interaction domain can mediate homo-and hetero-oligomerization of SCAN-containing proteins. Seven zinc fingers C2H2 type, which is the classical zinc domain. The two conserved cysteine and histidine residues co-ordinate a zinc ion. The C2H2 zinc finger is composed of two short beta strands followed by an alpha helix. The amino terminal part of the helix binds the major groove in DNA binding zinc fingers.

Besides the importance of intron 1 in the transcriptional control of *SNCA*, several lines of evidence have also highlighted the presence of other regulatory elements, including *cis*-regulatory elements of the *SNCA* gene as well as TFs, involved in its transcription. To date, the best characterized polymorphic variant in the *SNCA* gene, that has been reported to act as a modulator of *SNCA* transcription in different cell lines and *in vivo,* is the Rep-1 dinucleotide repeat in the 5'-promoter region of *SNCA* that is also associated with PD risk. Specifically, Rep-1 has been shown to have a reproducible effect on regulating transcriptional SNCA in transiently transfected neuronal cell lines (Chiba-Falek and Nussbaum 2001, Chiba-Falek, Touchman et al. 2003), in a Tg mouse

model (Cronin, Ge et al. 2009) and in human brain (Linnertz, Saucier et al. 2009). In all these studies, the extended Rep-1 PD-"risk" allele was associated with elevated *SNCA* levels compared to the shorter Rep-1 PD-"protective" allele. Interestingly, deletion of the Rep-1 element resulted in a significant reduction of *SNCA* expression compared to the full construct (Touchman, Dehejia et al. 2001, Cronin, Ge et al. 2009). Therefore, these results, suggested that Rep1 might act as an enhancer element to upregulate *SNCA* mRNA levels. However, Fuchs et al (Fuchs, Tichopad et al. 2008), even though they reproduced the Rep-1 effect on *SNCA* levels in human blood, did not detect an effect in the brain. This discrepancy with the study performed by Linnertz et al (Linnertz, Saucier et al. 2009) could be attributed to differences in sample size. Linnertz et al. included 144 brain samples, whereas Fuchs et al. analyzed 24. Further, the Rep-1 repeat has been found to interact with a nuclear protein, the poly (ADP-ribose) polymerase 1 (PARP-1). Formation of this complex led to decreased *SNCA* promoter/enhancer transcriptional activity in luciferase reporter assays in SHSY5Y cells, while inhibition of the enzymatic activity of PARP-1 instead increased *SNCA* Promoter/Enhancer activity (Chiba-Falek, Kowalak et al. 2005), suggesting this regulation might be transcriptionally-driven, at least in part. Interestingly, inhibition of the enzymatic activity of PARP-1 along with deletion of the Rep 1 repeat resulted in decreased SNCA promoter/enhancer activity, indicating the possibility that PARP-1 might interact with other sites along the *SNCA* promoter/enhancer region, thus allowing PARP-1 to play a dualistic role in *SNCA* transcriptional regulation.

Previous work in our laboratory, through luciferase-based assays with different length constructs of the *SNCA* promoter, unveiled a complex network of *cis*-regulatory elements, lying 5' of exon1 and within exon1, that play a role in the transcriptional regulation of *SNCA* in PC12 cells. MatInspector software analysis for the identification of conserved putative TFBSs in this area revealed several TF candidates. Among the TFs tested, only ZNF219 was found to be involved in *SNCA* regulation. Specifically, si-RNA-mediated silencing of ZNF219 resulted in a moderate increase of ASYN levels in PC12 cells. However, the presence of multiple ZNF219 binding sites (3 sites) in the promoter of SNCA as well as the differential response (repressor or activator) observed upon inhibition of ZNF219 in the luciferase assay of different length SNCA promoter constructs indicated that its role in the regulation of *SNCA* is complex (Clough, Dermentzaki et al. 2009).

Furthermore, regarding the 3' *SNCA* region, the SNPs rs356219 and rs365165 located in the 3'-UTR of *SNCA* and which are also in linkage disequilibrium have been shown to influence *SNCA* levels in different brain regions. Fuchs et al. (Fuchs, Tichopad et al. 2008) reported higher *SNCA* mRNA correlated with rs356219 disease allele in the substantia nigra of the midbrain, and with the protective allele in the cerebellum. Conversely, Linnertz et al. (Linnertz, Saucier et al. 2009) reported higher *SNCA* mRNA levels correlated with the rs356219 and rs365165 protective alleles in the temporal cortices and midbrain and were unchanged among the genotypes in the frontal cortices. Additionally, Mizuta et al. (Mizuta, Takafuji et al. 2013) demonstrated no significant differences in *SNCA* mRNA levels in the brain or lymphoblasts from PD patients harboring either the disease or protective rs356219 polymorphism. The discrepancies among these studies might be from the number and variation of samples. In the same

study, Mizuta et al. (Mizuta, Takafuji et al. 2013) also identified that the yin-yang 1 TF (YY1) binds to the protective rs356219 allele and further regulates the expression of lncRNA RP11-115D19.1 located in the 3'-UTR of *SNCA*. Interestingly, a positive correlation was observed among RP11-115D19.1, *SNCA*, and YY1 expression levels in autopsied cortices, suggesting their functional interaction *in vivo* and perhaps unveiling a possible novel mechanism regulating *SNCA* expression.

Recent studies have also reported the presence of conserved non-coding areas around and within the *SNCA* gene that are associated with *SNCA* expression. Sterling et al. (Sterling, Walter et al. 2014) found 12 conserved DNA sequences in the *SNCA* gene locus that either enhanced or reduced the expression of a reporter gene. Briefly, three elements upstream of the *SNCA* gene displayed an approximately 1.5-fold increase in expression. Of the intronic regions, 3 showed a 1.5-fold increase and 2 others indicated a 2- and 2.5-fold increase in expression, respectively. Three elements downstream of the SNCA gene showed a 1.5- and 2.5-fold increase. Lastly, one element downstream of SNCA had a reduced expression of the reporter gene of 0.35-fold of normal activity. Additionally, a study by Lutz et al. (Lutz, Saul et al. 2015) identified a CT-rich region spanning intron 4 of *SNCA* that acts as an enhancer element. Specifically, 4 distinct haplotypes were detected within this highly-polymorphic-low complexity CT-rich region. One of these haplotypes was significantly associated with elevated *SNCA* mRNA levels as well as with increased risk to develop LBV/AD. These results demonstrate that the *SNCA* gene contains *cis*-regulatory regions that might regulate its transcription and expression. Further studies, mainly in disease-relevant tissue types, will be important to understand the functional impact of regulatory regions and specific PD-associated SNPs in the disease process.

1.8 Degradation of ASYN: another level of regulation

Besides transcriptional control, several proteins are further regulated at the post-transcriptional and / or post-translational level. Principally, aggregation-prone proteins including ASYN are reportedly regulated post-translationally via degradation pathways. In general, degradation mechanisms play a major role in the regulation of steady state levels of proteins. Regarding ASYN, its degradation has been controversial. Work in our laboratory as well as other studies have supported that the bulk of degradation of at least monomeric WT ASYN in neuronal cell systems is mediated through the lysosomal pathways of chaperone-mediated autophagy and macroautophagy (Cuervo, Stefanis et al. 2004, Vogiatzi, Xilouri et al. 2008, Alvarez-Erviti, Rodriguez-Oroz et al. 2010) and that dysregulation of these degradation pathways may be a contributing factor to PD pathogenesis. Conversely, soluble ASYN is reportedly degraded by the proteosomal pathway (Bennett MC 1999 (Bennett, Bishop et al. 1999, Tofaris, Layfield et al. 2001, Ebrahimi-Fakhari, Cantuti-Castelvetri et al. 2011). It is possible that the exact species and pools of ASYN determine its degradation pathway since ASYN oligomeric forms cannot be subject to proteasomal degradation and rather inhibit the ubiquitin proteasome system (Lindersson, Beedholm et al. 2004, Zhang, Tang et al. 2008).

Additionally, the distribution of ASYN to different cellular clearing pathways does not only depend on monomeric versus multimeric forms but also depends on PTMs. PTMs of ASYN such as phosphorylation, SUMOylation and ubiquitination are prominent in PD and are primarily involved in ASYN aggregation as well as clearance. In the case of ASYN clearance, PTMs presumably act as molecular switches that determine the fate of the protein and its preference for a certain proteolytic pathway. Regarding ASYN, ubiquitination is one trigger that controls the partitioning of the protein between the proteasomal and autophagy systems. Monoubiquitinated ASYN has been shown to be degraded preferentially by the proteasome, whereas deubiquitinated ASYN was targeted to the autophagy pathway (Rott, Szargel et al. 2011). Another trigger is phosphorylation. Overexpression of the PLK2 kinase increases ASYN phosphorylation and mediates the selective clearance of ASYN through autophagic degradation and accordingly causes reduced ASYN toxicity (Oueslati, Schneider et al. 2013). Further, studies in yeast as PD model have shown that SUMOylated ASYN is primarily targeted to the autophagy pathway, whereas non-SUMOylated ASYN is primarily channeled to the proteasome (Shahpasandzadeh, Popova et al. 2014).

It is well established that protein quality control mechanisms play an essential role for the accumulation of misfolded and oligomeric protein species in neurodegenerative diseases. Therefore, a better understanding of the interplay between ASYN modifications and degradation pathways could provide a more specific targeting of ASYN to cellular clearing pathways as a therapeutic strategy for PD and other synucleinopathies.

2. AIM

SNCA is an established susceptibility gene for familial and sporadic PD, one of the most common human neurodegenerative disorders. Increased *SNCA* levels are also causative for PD. However, to date, the biochemical pathways and transcriptional elements involved in *SNCA* expression are to a great extent elusive. Previous work in our laboratory as well as several other studies have highlighted the importance of the intronic region of *SNCA* in its transcriptional regulation. Specifically, ZSCAN21, whose putative binding sites lie within intron 1, was found to exert a key role in the transcriptional regulation of *SNCA* in neuronal-like cells. Therefore, given the importance of ZSCAN21 in *SNCA* control we undertook this present study in order to extend our findings related to the role of ZSCAN21 in primary neuronal cultures and, in particular, *in vivo*. For this purpose, we utilized virus-mediated approaches to downregulate as well as overexpress *Zscan21* in neurons in order to evaluate its role in *Snca* regulation. We used two different cell-culture systems, cortical and hippocampal neuron cultures and neurosphere cultures. These cultures are *in vitro* systems that mimic different stages of neuronal development, since *Snca* is developmentally regulated. Likewise, *in vivo,* we also assessed the role of *Zscan21* in *Snca* regulation at two different developmental stages: one early in development and one later (adult). The last part of our study included the genetic screening of DNA blood samples from PD and control subjects for putative polymorphisms in the binding site for ZSCAN21 specifically as well as the intron 1 region in general. Such studies may cement ZSCAN21 as an important regulator of *SNCA* transcription, and may provide potential therapeutic targets not only for PD but also for other synucleinopathies.

3. MATERIALS AND METHODS

3.1 Rat cortical and hippocampal neuron cultures

Cultures of Wistar rat (embryonic day 17, E17) cortical or hippocampal neurons were prepared as described previously (Rideout and Stefanis 2002, Dietrich, Rideout et al. 2003). Dissociated cells were plated onto poly-D-lysine-coated 12-well dishes at a density of approximately 5.5×10^5 cells / well. The cells were maintained in Neurobasal medium (Gibco, Rockville, MD, USA; Invitrogen, Carlsbad, CA, USA), with B27 serum-free supplements (Gibco; Invitrogen), L-glutamine (0.5 mM), and penicillin/streptomycin (1%). More than 95% of the cells cultured under these conditions represent postmitotic neurons (Rideout and Stefanis 2002). The time in culture of cells was calculated using days in vitro (DIV), with the day of plating designated as 0 DIV.

For experiments using the various TRC2-pLKO lentiviruses (shZSCAN21/1, shZSCAN21/2, shZSCAN21/4, shscrambled), cultured cortical or hippocampal neurons were infected at 4 DIV at a multiplicity of infection (MOI) of 1. At 5 or 7 days post-infection cortical or hippocampal cultures were processed for RNA and protein isolation respectively. Additionally, cultures were visualized for infection efficiency under an inverted microscope and representative images were recorded (Leica DMIRE 2 microscope). For experiments using the adenoviruses (AV) (ZSCAN21, EGFP) cultured cortical cultures were infected at 4 DIV with an MOI of 100 and collected at 5 days post-infection. For the luciferase assays, cortical cultures were infected at 4 DIV with an MOI of 1 with the above lentiviruses. At 3 days post-infection, the cultures were transfected with a variety of luciferase constructs and processed for luciferase activity at 48 h post-infection.

3.2 Rat neurosphere cultures

Neurosphere cultures were prepared from rat cortical and hippocampal tissue from E16 Wistar rat embryos and maintained in suspension in full medium + growth factors (+GFs): 1:1 mixture of Dulbecco's modified Eagle's medium (1 g/L D-Glucose, L-Glutamine, Pyruvate; Sigma) and F12 nutrient mixture (Sigma), plus 20 ng/mL human epidermal growth factor (hEGF; R&D Systems) and 20 ng/mL human basic fibroblast growth factor (bFGF; R&D Systems), 20 μg/mL insulin (Sigma), 1x B27 supplement (Gibco), 0.25 mM L-glutamine and 1% penicillin/streptomycin to promote the production of the neurospheres. The neurospheres were passaged 2–3 times before plating in poly-D-lysine-coated plates in the presence of full medium (Kaltezioti, Kouroupi et al. 2010, Kaltezioti, Antoniou et al. 2014). The next day, the cultures were infected with lentiviruses overnight, and the following day, the medium was changed with full medium -growth factors (-GFs): the same as the full medium +GFs without hEGF and bFGF in order to promote differentiation. The cultures were then harvested on the 5th day of differentiation.

3.3 Western immunoblotting

Primary neuron or neurosphere cultures were washed twice in phosphate-buffered saline (PBS) and then harvested in RIPA lysis buffer (150 mM NaCl, 50 mM Tris PH 8.0, 0.1% sodium dodecyl sulfate, 1% NP-40; Sigma, 2 mM EDTA). Brain tissues were homogenized again in RIPA lysis buffer and clear lysate was isolated following centrifugation at $50.000 \times g$ in 4°C. Protein concentrations were determined using the Bradford method (Bio-Rad Laboratories, Hercules, CA, USA). A variable amount of protein in the lysates was mixed with $4 \times$ Laemmli buffer prior to running on 12% sodium dodecyl sulfate polyacrylamide gels. Following transfer to a nitrocellulose membrane, the blots were probed with antibodies directed against: ASYN (1:1000; BD Biosciences, Sparks, MD, USA), ZSCAN21 (GenScript or home-made), ERK (loading control; 1:5000; Santa Cruz Biotechnology), β-actin (1:5000; Sigma), and GAPDH (1:1000; Santa Cruz Biotechnology). Blots were probed with horseradish peroxidase-conjugated secondary antibodies (mouse and rabbit), visualized with a LumiSensor HRP kit (GenScript) and exposed to Super RX film (Fuji Film). Following scanning of the images with Adobe Photoshop, Gel Analyzer software version 1 was used to quantify the intensity of the bands. In all cases, the levels of ASYN and ZSCAN21 were normalized to those of ERK or β-actin for quantification and statistical analysis.

3.4 Immunocytochemistry

Neurosphere cultures grown on 24-well plates with coverslips were fixed with 3.7% formaldehyde for 25 min at 4°C. Blocking was with 10% normal goat serum and 0.4% Triton X-100 for 1 h at room temperature (RT). Primary antibodies including ASYN (1:600; BD Biosystems), ZSCAN21 (1:400; Santa Cruz, ZNF-38 [H-68]: sc-98315 or GenScript; home-made) and TUJ1 (1:2000; Sigma), were applied overnight at 4°C, followed by fluorescent secondary antibodies: 1:250; rabbit Cy2, 1:250; mouse Cy3, 1:250; mouse Cy2 (Jackson ImmunoResearch) for 1 h at RT. The fluorescent marker Hoechst (1 mM; Sigma) or TO-PRO (1mM) was used to assess cell nuclei. Cultures were visualized under a confocal upright microscope (LEICA TCS SP5) and representative images were recorded.

3.5 Immunohistochemistry

Wistar rats were perfused intracardially through the ascending aorta with physiological saline under pentobarbital anaesthesia, followed by ice cold 4% paraformaldehyde. The brains were removed and post-fixed overnight in the same preparation of paraformaldehyde, then transferred to 15% sucrose overnight, and then to 30% sucrose overnight. The brains were frozen with isopentane under dry ice. The brains were cryosectioned through the coronal plane in 20 mm increments, and every section throughout the hippocampus was collected. Immunohistochemical staining was carried out on embedded sections and on slides.

Regarding the fluorescent immunohistochemistry (FI) assay, the sections were first washed with PBS, followed by antigen retrieval with 10 mM citrate buffer, blocking in 2% normal goat serum (NGS) and 0.1% Triton-X-100 and incubation for 48 h at 4°C with the following primary antibodies: ASYN (1:600; BD Biosystems), ZSCAN21 (1:400; Santa Cruz), and NeuN (1:300; Millipore). They were then incubated with the following secondary antibodies: rabbit Cy3 (1:250), mouse Cy3 (1:250), mouse Cy2 (1:250) (Jackson ImmunoResearch) for 1 h incubation at RT. Sections were visualized under a confocal upright microscope (LEICA TCS SP5) and representative images were recorded.

Regarding 3,3′-diaminobenzene (DAB) staining, the sections were first quenched for 10 min in 3% H_2O_2/10% methanol mixture and subsequently blocked with 10% NGS for 1 h at RT. The monoclonal ASYN antibody (1:600; BD Biosystems) was added for 48 h, followed by incubation with a biotinylated anti-rabbit antibody (1:1500; Vector Laboratories) in 1% NGS for 1 h and avidin–biotin peroxidase complex for 1 h in RT (ABC Elite; Vector Laboratories). Staining was visualized using diaminobenzidine (Sigma) as a chromogen. Specificity was tested in adjacent sections with the primary or the secondary antibody omitted. The sections were stained with cresyl violet (Nissl staining), and then dehydrated in graded ethanol and cover slipped. The sections were visualized under a bright field microscope (DML S2) and representative images were recorded.

3.6 Dissociation and fluorescence-activated cell sorting (FACS) of rat adult brain

For dissociation and debris removal of rat adult brain tissue prior to FACS analysis we followed the protocol of Guez-Barber et al. (Guez-Barber, Fanous et al. 2012). In more detail, AAV-transduced rat brains were extracted under ice and washed with PBS to remove remaining blood. GFP-positive areas of the brains (identified under a stereoscope) were isolated, minced with razorblades, and placed in a 15-mL tube with Hibernate A (BrainBits) (Brewer, Torricelli et al. 1993, Brewer 1997) medium. The supernatant was discarded and 4 mL of Accutase solution (Sigma, A6964) supplemented with 8 μL DNase (10 mg/mL stock) were added. The tissue was triturated gently (10-20 times) and placed on a shaker at 4°C for 1 h for enzymatic dissociation. Afterwards, the digested tissue was centrifuged at 1400 rpm for 10 min at 4°C. The pellet was resuspended in 5 mL Hibernate A medium and further processed with fire polished Pasteur pipettes of decreasing diameter until single cell level. The clear supernatant was first passed through a 70-μm cell strainer (Falcon, 352350) (pre-wet / to remove cell clusters and large debris) in a 50 mL tube and centrifuged at 1500-2000 rpm for 10 min at 4°C. The procedure was repeated using a 40-μm cell strainer (Falcon, 352340).

Percoll (P1644; Sigma), removal of debris: Small cellular debris that was not restrained by the cell strainers was reduced by density centrifugation through a three-density step gradient of Percoll. One milliliter of each solution (high density solution: 3.426 mL

Hibernate + 824.5 μL Percoll + 97.8 μL of 1M NaCl; Medium density solution: 3.600 mL Hibernate + 650.5 μL Percoll + 76.5 μL of 1M NaCl; Low density solution: 3.770 mL Hibernate + 480.3 μL Percoll + 59.5 μL of 1M NaCl) was layered carefully in a 15-mL tube, with the highest density solution at the bottom. The filtered cell suspension was applied to the top of this gradient and centrifuged at 430 x g for 3min. The cloudy top layer (~2 mL) containing debris was removed and discarded. Cells in the remaining layers were pelleted by centrifugation at 550 × g for 5min (the cells are not actually pelleted, they gather in an interphase). The cells were resuspended in Cell Sorting Buffer (2% FBS, 2 mM EDTA in PBS/filtered through a 0.2-μm filter) in a 15-mL tube and centrifuged at 1400 rpm for 10 min at 4°C.

The pellet was resuspended again in the Cell Sorting Buffer for labelling with the following primary antibodies: cell surface markers PE mouse anti-rat CD24 (clone HIS50; BD Biosciences, 562104) and alexa fluor 647 anti-rat C90.1 (Thy-1.1) (Biolegends, 202507). These antibodies have been reported to label neuronal cells (Pruszak, Ludwig et al. 2009, Yuan, Martin et al. 2011). For labelling, 2 μg of each antibody were added to 5 mL total sample (0.4 μg/mL) and incubated in the dark for approximately 1 h at 4°C (with shaking every 10-15min). The cells were centrifuged at 1400 rpm for 10 min at 4°C, washed once in Cell Sorting Buffer and incubated with the dye DAPI (0.5 – 1 μg/mL) for 5 min. Cells were then centrifuged at 1400 rpm for 10 min at 4°C, resuspended in Cell Sorting Buffer and passed through a 50-μm pre-wetted filter to the specified sorting tubes for FACS analysis.

For FACS analysis the Fluorescence-Activated Cell Sorter ARIA IIu was used. The cells were passed through a 70-μm nozzle, with a starting flow rate of 1 that was gradually increased to 4. The filters used were Blue (488 nm) for GFP, Yellow-Green (561 nm) for PE CD24, Red (638 nm) for Alexa 647 CD90 and Violet (405 nm) for DAPI. A small portion of the sample was incubated without antibodies to gate the cells according to their light scattering characteristics. Duplet exclusion was also included. Non-transduced tissue was used (control) to set the threshold for the GFP-positive signal. Importantly, a small portion of test samples labeled with fluorescent dyes were used to identify the neuronal subpopulation. Colocalozation of GFP (+), CD24 (+) and CD90 (+) marked our population of interest that was further sorted in RNase-free tubes at 4°C for RNA isolation. Colocalization of GFP (-), CD24 (+), and CD90 (+) marked our negative neuronal population that served as the internal control in our study. This population was also sorted.

3.7 RNA extraction and cDNA synthesis

Total RNA was extracted from different brain regions, primary neuronal cultures and neurosphere cultures using TRIzol (Invitrogen). DNase (Promega, 1U/μg) was added to remove any remaining DNA. RNA concentration was determined spectrophotometrically at 260 nm, while the quality of purification was determined by a 260 nm / 280 nm ratio that showed values between 1.7 and 2.0, indicating high RNA

quality. cDNA was generated with the M-MLV Reverse Transcription System (Promega). For the reaction we used: 1–2 µg total RNA, 1× Buffer, 500 ng oligo-dT primer, 2 mM dNTPs, 40 U RNasin, and 200 U M-MLV enzyme.

Regarding the FACS assay, total RNA was extracted using an RNeasy Kit (QIAGEN) according to the manufacturer's instructions and cDNA was synthesized using the Superscript II Reverse Transcription System (Invitrogen, 18064). For the reaction we used: 80 ng RNA, 1× Buffer, 500 oligo-dT primer, 0.5 mM dNTPs, 0.01 M DDT, 40 U RNasin, and 200 U Superscript II enzyme.

3.8 Reverse transciption PCR

Semi-quantitative reverse-transcription PCR was performed using cDNA as a template from different brain areas. For the PCR reaction we used the Thermopol Taq polymerase system (New England Biolab, M0267). For the reaction we used: 1× Buffer, 0.5 mM dNTPs, 0.5 µM primers, 1.25 U enzyme, 0.08 µg cDNA template. The primers used to perform the PCR were: ZSCAN21-F', ZSCAN21-R', SNCA-F', SNCA-R', β-actin-F', β-actin-R' (details in the Primer List). The PCR conditions were: 95°C for 4 min, 94°C for 30 s, 56°C for 30 s, 72°C for 30 s (30 cycles), and 72°C for 5 min. Products were subsequently resolved on agarose gels stained with ethidium bromide

3.9 Real Time PCR

In most cases we utilized a Platinum Taq Kit (Invitrogen, 10966) along with home-made Cyber Green solution. Duplicates or triplicates of each sample were assayed by relative quantitative real-time PCR using the Light Cycler Roche 96 machine to determine the levels of expression of different mRNAs. As a reference gene for normalization we used β-actin. The primers used for each target (SNCA RT-F', SNCA RT-R', ZSCAN21 RT-F', ZSCAN21 RT-R', OVERZSCAN21 RT-F', OVERZSCAN21-RT-R', β-ACTIN RT-F', β-ACTIN RT-R') are listed below in 3.21

Each cDNA sample, derived from 1–1.5 µg total RNA from primary neuronal and neurosphere cultures, was diluted 1/20 before use for the amplification assay. At least 3 independent runs (overall $\geq$ 6 repeats) were assessed for each mRNA target. The reaction conditions were: 1× Buffer (-Mg), 1.5 mM $MgCl_2$, 0.2 mM dNTPs, 0.2 µM primers, template < 500 ng, 2 U Platinum Taq, and Cyber Green (home-made). The PCR conditions were: 95°C for 180 s, 95°C for 10 s, 60°C for 15 s, 72°C for 15 s (45 cycles), and 95°C for 60 s, 65°C for 60 s, 95°C for 10s, and 37°C for 30s.

As a negative control for the specificity of amplification, we used no template samples in each plate. No amplification product was detected in the control reactions. Data were analyzed automatically with a threshold set in the linear range of amplification. The cycle number at which any particular sample crossed that threshold (Ct) was then used to determine fold difference, whereas the geometric mean of the control gene (β-actin)

served as a reference for normalization. Fold difference was calculated as 2-ΔΔCt (Livak and Schmittgen 2001).

Regarding the FACS assay and the chromatin immunoprecipitation assay (CHIP) we used the Bio-Rad kit instead of the home made Cyber Green as it is more sensitive for low concentration-starting material. The PCR settings were: 95°C for 30 s, 55°C for 50 s (repeat 45 cycles), and 55°C for 10 min, 95°C for 10 s, 55°C for 60 s, and 98°C for 1 s.

3.10 Transfection and luciferase assay

All 5'-promoter constructs of SNCA utilized in this study are inserted in the pGL3-empty vector (Promega). The 10.7-kb construct used in this study was a kind gift from Drs Nussbaum and Chiba-Falek (Chiba-Falek and Nussbaum 2001). The 1.9-kb and intron 1 constructs were generated as described previously (Clough and Stefanis 2007, Clough, Dermentzaki et al. 2009). The constructs lacking the first putative ZSCAN21 binding site (1.9d), the second putative ZSCAN21 binding site (1.9sec) as well as both (1.9dd) were constructed using the 1.9kb construct as a template via site-directed mutagenesis with a QuikChange Lightning Site-Directed Mutagenesis Kit (Promega, 210518). All transfections were performed using Lipofectamine 2000 (Invitrogen) according to the manufacturer's instructions and as described previously (Clough and Stefanis 2007). Briefly, for the luciferase assay all transfections were performed in 12-well tissue culture dishes with 5.5×10^5 cells/well with 1.6 μg per well of target vector and 1/50 (of the target vector) of TK-Renilla (internal control) (Promega). Four μL of lipofectamine per well were determined to give the best transfection efficiency in primary neurons. All transfections were performed for 4 h in plain Neurobasal medium for cortical cultures and plain neurosphere buffer for differentiated neurosphere cultures. Next, complete medium was added. In all luciferase assays, the cells were harvested at 48 h after the addition of complete medium to the cells. Luciferase activity was detected with the Dual Luciferase Assay (Promega) according the manufacturer's instructions. This particular "dual" system allows the use of two enzymes, luciferase (experimental) and Renilla (control) within a single system. Typically, the "experimental" reporter is correlated with the effect of specific experimental conditions, while the activity of the co-transfected "control" reporter provides an internal control that serves as the baseline response. Normalizing the activity of the experimental reporter to the activity of the internal control minimizes experimental variability caused by differences in cell viability or transfection.

3.11 3' Rapid amplification of cDNA ends

Total RNA extraction was performed with TRIzol (Ambion) from rat embryonic cortical cultures treated with the lentivirus shZSCAN21/4 or control (without any treatment). Then, DNase treatment (Promega) removed any remaining DNA contamination. Following this, ~ 2.5 μg of total RNA were converted into cDNA using

a Reverse Transcriptase Superscript II system (Invitrogen) and an oligo-dT adapter primer (1× Buffer, 0.5 μM AP primer, 0.5 mM dNTPs, 0.01 M DDT, 40 U RNasin, and 200 U Superscript II). Next we treated our samples with RNase H in order to remove the original RNA template.

Subsequently, cDNA was amplified by PCR using the Platinum Tag Polymerase Kit (Invitrogen), a gene-specific primer (GSP) that anneals to a ZSCAN21 exon sequence, and a reverse universal amplification primer (UAP) that contains only the unique sequence of the oligo-dT adapter primer and not the oligo-dT sequence (Primer list). The reaction conditions were: 1× PCR Buffer (-Mg), 1.5 mM $MgCl_2$, 0.2 mM dNTPs, 0.2 μM primers, and 2 U Platinum Tag. The PCR conditions were: 94°C for 2 min, 94°C for 30 s, 62°C for 30 s, 72°C for 1 min, (30 cycles), and 72°C for 5 min. Next, the PCR products were separated in a 2% agarose gel and evaluated further by sequencing. In the present study we utilized the primers below (section 3.21).

3.12 Chromatin immunoprecipitation assay

CHIP experiments were performed according to Kaltezioti et al. (Kaltezioti, Kouroupi et al. 2010, Kaltezioti, Antoniou et al. 2014). In detail, for every independent experiment, ~5–6 10-cm plates (1.0×10^7 cortical neurons /plate) were used. The cultures were processed for the CHIP assay on the 8th day of culture. The cells were fixed with formaldehyde, 1% final concentration, in the medium for 10 min at RT. The reaction was stopped by adding 0.137 M glycine while shaking for 1–2 min at RT. The medium was discarded, the cells were washed twice with PBS, collected in PBS, and finally centrifuged at 1.500 rpm for 10 min at 4°C. The pellet was resuspended in 1 mL cell lysis buffer (5 mM HEPES pH: 8.0, 85 mM KCl, 0.5% NP-40, 1× protease inhibitors (PI), 10 μL/mL phenylmethanesulfonylfluoride [PMSF]) and left on ice 30 min to lyse. The lysate was centrifuged at 5000 rpm for 10 min at 4°C and the pellet (containing the nuclei) was resuspended in 1 mL nuclei lysis buffer (50 mM Tris-HCl, pH: 8.0, 10 mM EDTA pH: 8.0, 1% SDS, 1× PI, 10 μL/mL PMSF) and incubated on ice for 10 min.

An aliquot (40μL) from the lysate was kept to check chromatin before sonication and the rest of the sample was sonicated (30% amplitude 1 s on / 1 s off, total time 9 min on ice the whole time). Following sonication, phenol:chloroform purification in 40 μL of sample before and after sonication was performed as well as agarose gel separation (1.5%) to check the size of the chromatin fragments in both conditions. We expected fragments between 800–200 bp. Next, the sonicated sample was centrifuged at 13.000 rpm for 15min at 4°C, and the supernatant was kept (contains the chromatin). The absorbance was measured (OD 260/280 nm) and aliquots of 100 μg per CHIP reaction were made.

Next, agarose beads were pre-cleared (here we used agarose A beads (Santa Cruz) since they work better for polyclonal antibodies). The beads were washed three times with PBS prior to the pre-clearing reaction: beads, 0.35 mg/mL bovine serum albumin (BSA), 0.55 μg/mL t-RNA, and CHIP buffer w/o SDS (16.7 mM Tris-HCl pH:8.0,

167mM NaCl, 1.2mM EDTA pH:8.0, 1.1% Triton-X-100, 1× PI, 10 μL/mL PMSF) to a final volume of 1 mL, under rotation at RT for 2 h.

Subsequently, 4 volumes of CHIP full buffer (16.7 mM Tris-HCl pH: 8.0, 167 mM NaCl, 1.2 mM EDTA pH: 8.0, 1.1% Triton-X-100, 0.01% SDS, 1× PI, 10 μL/mL PMSF) were added to the chromatin samples (100 μg each) along with 30 μL of pre-cleared agarose beads and rotated for 1 h at 4°C. Next, the samples were centrifuged at 3000 rpm for 5 min at 4°C and the supernatant was collected (10% of the supernatant from one sample was kept aside as INPUT). For the CHIP reaction, to each pre-cleared chromatin sample were added: either 10 μg of the antibody of interest; here ZSCAN21 (GenScript) or 10 μg of the same isotype (rabbit polyclonal) irrelevant antibody (c-myb; Santa Cruz) as a negative control (IgG control), 0.01 mg/mL BSA, 0.02 μg/mL t-RNA, 30 μL magnetic beads (Dynabeads Protein G / Invitrogen) until a final volume of 1 mL. The samples were rotated overnight at 4°C.

Next day, the beads were collected (using a magnet) and the supernatant was discarded. Sequential washes under rotation for 7 min at 4ºC with Low Salt Wash buffer (20 mM Tris-HCl pH: 8.0, 2 mM EDTA pH:8.0, 500 mM NaCl, 1% Triton-X-100, 0.1% SDS, 1 μL/mL PMSF), High Salt Wash buffer (20 mM Tris-HCl pH:8.0, 2 mM EDTA pH: 8.0, 150 mM NaCl, 1% Triton-X-100, 0.1% SDS, 1 μL/mL PMSF/ 1 mL/tube) and LiCl Wash buffer (10 mM Tris-HCl pH:8.0, 1 mM EDTA pH:8.0, 250 mM LiCl, 1% deoxycholic acid, 0.1% SDS, 1% NP-40, 1 μL/mL PMSF). The beads were washed again twice with TE buffer (10 mM Tris-HCl pH: 8.0, 1 mM EDTA pH: 8.0) and finally eluted in 125 μL Elution buffer (100 Mm NaHCO3, 1% SDS) and a 15 min incubation at 65°C (twice / final volume 250 μL).

For reverse cross-linking, a final concentration of 0.2 M NaCl was added to every sample and incubated at 65°C overnight. The same procedure was also applied to the INPUT samples. The next day, 2 μL RNase A (10 μg/μL) were added followed by incubation at 37°C for 1 h. Then, 1 μL/tube Proteinase K (20 mg/mL) was added followed by incubation at 55°C for 2 h. Finally, the samples were purified via column purification (PCR clean up Kit; Macherey-Nagel) in a total volume of 50 μL.

For Real-Time PCR we diluted the purified samples 1/10 and used the CHIP ZSCAN21-F', CHIP ZSCAN21-R', CHIP 3' SNCA-F', CHIP 3' SNCA-R', CHIP OLIG2-F' and CHIP OLIG2-R' primers (Primer list).

3.13 ZSCAN21 deletion constructs

ZSCAN21 binding site deletion constructs were constructed via site-directed mutagenesis with a QuikChange Lightning Site-Directed Mutagenesis Kit (Agilent). The deletion constructs were 1.9d ZSCAN21, which lacks the first ZSCAN21 binding site, 1.9dd ZSCAN21, which lacks both binding sites and 1.9 sec ZSCAN21, which lacks the second ZSCAN21 binding site. The primers were designed using the

QuikChange   Primer   Design   Program   available   online   at:
www.agilent.com/genomics/qcpd (Primer list).

The reaction conditions were: 1× Buffer, 50 ng ds DNA, 1.25 ng sense and antisense
primers, 1 μL dNTPs (kit), 1.5 μL Quick Solution, 1 μL enzyme. The PCR conditions
were: 95°C for 2 min, 95°C for 20 s, 60°C for 10 s, 68°C for 4 min (30 s/kb of plasmid
length), (17 cycles), and 68°C for 5 min.

3.14 Lentiviral vector construction and virus production

The small hairpin RNAs (shRNAs) against ZSCAN21 (3 targets) and scrambled were
cloned into the TRC2-pLKO vector (Sigma) containing the U6 promoter, the selection
marker puromycin and the woodchuck hepatitis post-transcriptional regulatory element
(WPRE). The shRNAs were inserted in the *Age*I/*Eco*RI multiple cloning site. The
sense/antisense primers that were used for each shRNA were pLKO ZSCAN21/1
sense/antisense, pLKO ZSCAN21/2 sense/antisense, pLKO ZSCAN21/4
sense/antisense and pLKO SCRAMBLED sense/antisense (Primer list). Additionally
we cloned the EGFP sequence from another vector using PCR with *Bam*HI-EGFP-F'
and *Bam*HI-EGFP-R' (Primer list) before the puromycin sequence in the TRC2-pLKO
vector by digesting the vector and the EGFP PCR product with *Bam*HI enzyme and
then ligating both pieces. Subsequently, for the production of the viral particles,
HEK293 cells (10, 150-mm dishes for each lentivirus) grown to approximately 70–
80% confluence were transfected using the calcium-phosphate method with the TRC2-
pLKO-EGFP-shRNA vector, the pCMV delta R8.2 plasmid (encoding the HIV-1
GAG/POL, Tat and Rev regulatory genes), and the pMD2.G plasmid (encoding the
VSVG packaging gene). After 3 days incubation, the supernatant was collected,
centrifuged to discard cell debris, passed through a 0.45-μm filter and centrifuged at
26.000 rpm in a Sorvall Discovery 100SE ultra-centrifuge with a TH-641 rotator for 3
h at 4°C. The pellet was then resuspended in filtered 1× HBSS in PBS with 0.5% BSA
under mild vortexing for 30min at 4°C, centrifuged at 2.000 rpm for 30 s, aliquoted
into sterile Axygen tubes, and kept at -80°C. The titration of the viral preparation was
performed in HeLa cells following serial dilutions of each lentivirus by FACS analysis
of the GFP signal. The titer was then calculated by the mathematical equation: % GFP
positive cells × dilution of virus × no. of cells infected / 100. In general the titer of the
lentiviruses were ~ 1–2 ×10^8 transduction units (TU)/mL.

3.15 Adeno-associated vector (AAV) construction and virus production

The shRNAs of interest (ZSCAN21/2 and scrambled) were cloned into an rAAV
backbone plasmid containing the synapsin-1 promoter, WPRE, and bovine growth
hormone polyA site. The shRNA primers were the pLL3.7 ZSCAN21/2 sense and
antisense and the pLL3.7 SCRAMBLED sense and antisense (Primer list). The
expression cassette is flanked by AAV2 inverted terminal repeats. The shRNAs were
inserted in the *Hpa*I/*Xho*I multiple cloning site. The sense/antisense primers that were
used for each shRNA were the pLL3.1 ZSCAN21/2 sense/antisense and the pLL3.1

SCRAMBLED sense/antisense (Primer list). Subsequently, for the production of viral particles, HEK293 cells grown to approximately 70–80% confluence were double-transfected using the calcium-phosphate method with the rAAV plasmid and helper plasmids encoding essential AV packaging and AAV6 capsid genes. After 3 days incubation, the cells were harvested and lysed by performing 3 freeze-thaw cycles in a dry ice/ethanol bath. After treatment with Benzonase nuclease (Sigma), the lysate was purified using a discontinuous iodixanol gradient followed by Sepharose Q column chromatography, and finally concentrated with a 100-kD cut-off column (Millipore Amicon Ultra). To determine the titer of the viral stock solutions quantitative PCR with primers and probes targeting the inverted terminal repeat sequence was performed (Grimm, Kern et al. 1998, Zolotukhin, Byrne et al. 1999, Xilouri, Brekk et al. 2013). The titer for AAV/shZSCAN21/2 was: 3×10^{14} TU/mL and 1.8×10^{14} TU/mL for AAV/shscrambled.

3.16 Adenoviral vector (AV) construction and virus production

The rat ZSCAN21 overexpression AV vector was generated using the following steps. We first performed PCR from cDNA of rat cortical cultures with the OVERZSCAN21-F' and OVERZSCAN21-R' primers (Primer list) to isolate the coding sequence of ZSCAN21. Next, the rat ZSCAN21 sequence was cloned first into a modified version of the PENTR.GD entry vector and then introduced into the pAd/ PL-DEST Gateway vector (Invitrogen). Second-generation E1, E3, and E2a-deleted recombinant human serotype 5 adenoviruses (rAd) were generated, as described previously (He, Zhou et al. 1998, Xilouri, Kyratzi et al. 2012). Viral vector stocks were amplified from plaque isolates in order to guarantee homogeneity. Final vector stocks were purified and concentrated using double discontinuous and continuous CsCl gradients. Viral titers of purified vector stocks were determined in infected HEK 293A cells following serial dilutions of the viral preparation using an Adeno-X Rapid Titer Kit (Clontech) following the mathematical equation: infected cells/field $\times$ 38.2 $\times$ dilution factor / viral volume. The titer was expressed as viral particles/mL and it was calculated as 1.97×10^{11} viral particles /mL for rAd-ZSCAN21. As a negative control we used rAd-GFP with a titer of 1.55×10^{11} viral particles/mL, which had already been made in our laboratory.

3.17 Animals

Post-natal P3 or 2-month old adult Wistar rats (180-200 g) were housed in a cage (2–3 animals per cage for adults) with free access to food and water under a 12 h light/dark cycle. All experimental procedures performed were approved by the Institutional Animal Care and Use Committee of the Biomedical Research Foundation of the Academy of Athens.

3.18 Stereotaxic surgical procedure

For adult rats all surgical procedures were performed under general anesthesia using isoflurane. After placing the animal into a stereotaxic frame (Kopf Instruments), 4 μL recombinant AAV solution was injected unilaterally into the dentate gyrus of hippocampus at 2 different sites. The coordinates of the first injection site were -3.0 mm anteroposterior (AP) from the bregma, -1.5 mm mediolateral (ML) from the bregma, and -3.6 mm dorsoventral (DV) from the scalp, and the coordinates of the second injection site were -4.56 mm AP from the bregma, -2.6 mm ML from the bregma, and -3.2 mm DV from the scalp, according to the rat stereotaxic atlas (Paxinos and Watson, 1998). The tooth bar was adjusted to 2.3 mm. Injection was performed using a pulled glass capillary (diameter of 60–80 mm) attached to a Hamilton syringe with a 22 s gauge needle. After delivery of the viral vector using an injection rate of 0.1 mL/15s, the capillary was held in place for 5min, retracted 0.1 mm, and, after 1 min, was slowly withdrawn from the brain

For post-natal day 3 rats (P3 rats) we used a specific stereotaxic unit (model 900 small animal stereotaxic unit; Kopf Instruments). We first anesthetized the pups under ice and then placed them in the stereotaxic frame that was kept cold during the surgical procedure with dry ice and ethanol. We performed bilateral stereotaxic injections in the ventricles (2 μL / ventricle, titer: 7.0×10^{13} TU/mL). We targeted the ventricles by calculating approximately two-fifth of the distance between the lambda and each eye (Kim, Ash et al. 2013).

3.19 Control and PD patient samples for intron 1 genomic analysis

Control and PD patient blood samples were collected by the Special Outpatient Clinic of Mobility and Memory Disorders of Attikon Hospital, as well as from the General Hospital of Syrou, within the framework of the Parkinsonian patients Biobank creation program that was funded by the General Secretariat for Research and Technology, Greece. To date, approximately 500 samples have been collected in 3:1 ratio of patients versus controls. Both groups were age and gender matched. Detailed clinical records following the participants' consent were included. The protocols regarding the collection and analysis of the samples have been filed and approved from the corresponding hospital committees. In the present study, for screening the intron 1 region of the SNCA gene we performed PCR with specific primers (INTRON 1 F', INTRON 1 R' / primer list) that bind to the 5'-region within the first exon of SNCA and to the 3'-region in intron 1 (the final product includes approximately two thirds of the intron 1 region of SNCA from its start) in collaboration with Professor Thomas Gasser (University of Tubingen). The resulting 917-bp PCR products were further processed with sequence analysis. In total, 400 samples were sequenced (~200 control and ~200 PD).

3.20 Statistical analysis

Statistical analysis was performed using unpaired t-test for single analyses. Where multiple testing was required, a one-way analysis of variance (ANOVA) test was utilized, with a post hoc Tukey's HSD test. P-values < 0.05 were considered significant. All statistical analyses were performed using GraphPad Prism 5 Demo suite software.

3.21 Primer List

ZSCAN21-F′: 5′- CAGAAGCAGTCTTGGGAGAAA-3′

ZSCAN21-R′: 5′-TCTCCCTTTCCAGGTTGTTG-3′

SNCA-F′: 5′-CTGCCACTGGTTTTGTCAAG-3′

SNCA-R′: 5′-TGTACGCCATGGAAGAACAC-3′

β-ACTIN-F′: 5′-TGGCTCCTAGCACCATGA-3′

β-ACTIN-R′: 5′-CCACCAATCCACACAGAG-3′

SNCA RT-F′: 5′-GCCTTTCACCCCTCTTGCAT-3′

SNCA RT-R′: 5′-TATCTTTGCTCCACACGGCT-3′

ZSCAN21 RT-F′: 5′-CGGTTGTGCTATGGTTCAGC-3′

ZSCAN21 RT-R′: 5′-ACACTCCAAACCTGGGACTC-3′

OVERZSCAN RT-F′: 5′-CTGTGGATGCCAGCCCTAAA-3′

OVERZSCAN RT-R′: 5′-CGCTTTCTTGGGTCCTGAGT-3′

β-ACTIN RT-F′: 5′-TGGCTCCTAGCACCATGA-3′

β-ACTIN RT-R′: 5′-CCACCAATCCACACAGAG-3′

AP: 5′-CAGGACCGATTAACCAGGGTCGAACACTTTTTTTTTTTTTTTT-3′

UAP: 5′-CAGGACCGATTAACCAAGGGTCGAACAC-3′

GSP: 5′-TGGGAAGGCTTTCAGCCACAGCTCCAAC-3′

2nd GSP: 5′-CAGCGTCTGCTAGGCCTGCTCCAGGAGA -3′

pLKO ZSCAN21/1 SENSE: 5′-
CCGGGCCAGCCCTAAATATGAGTTTCTCGAGAAACTCATATTTAGGGCTGGCTTTTTG-3′

pLKO ZSCAN21/1 ANTISENSE: 5′-
AATTCAAAAAGCCAGCCCTAAATATGAGTTTCTCGAGAAACTCATATTTAGGGCTGGC-3′

pLKO ZSCAN21/2 SENSE: 5′-
CCGGGCTCCAACCTTACCCTTCATTCTCGAGAATGAAGGGTAAGGTTGGAGCTTTTTG-3′

pLKO ZSCAN21/2 ANTISENSE: 5′-
AATTCAAAAAGCTCCAACCTTACCCTTCATTCTCGAGAATGAAGGGTAAGGTTGGAGC-3′

pLKO ZSCAN21/4 SENSE: 5′-
CCGGGTGTAAGGAGTGTGGCAAAGCCTCGAGGCTTTGCCACACTCCTTACACTTTTTG-3′

pLKO ZSCAN21/4 ANTISENSE: 5′-
AATTCAAAAAGTGTAAGGAGTGTGGCAAAGCCTCGAGGCTTTGCCACACTCCTTACAC-3′

pLKO SCRAMBLED SENSE: 5′-
CCGGCAACAAGATGAAGAGCACCAACTCGAGTTGGTGCTCTTCATCTTGTTGTTTTTG-3′

pLKO SCRAMBLED ANTISENSE :5′-AATTCAAAAACAACAAGATGAAGAGCACCAACTCGAGTTGGTGCTCTTCATCTTGTTG-3′

pLL3.7 ZSCAN21/2 SENSE: 5′-TGCTCCAACCTTACCCTTCATTTTCAAGAGAAATGAAGGGTAAGGTTGGAGCTTTTTTC-3′

pLL3.7 ZSCAN21/2 ANTISENSE: 5′-TCGAGAAAAAAGCTCCAACCTTACCCTTCATTTCTCTTGAAAATGAAGGGTAAGGTTGGAGCA-3′

pLL3.7 SCRAMBLED SENSE: 5′-TGCTGATTCCGCCTAAAGATTCAAGAGATCTTTAGGCGGAATCAGCTTTTTTC-3′

pLL3.7 SCRAMBLED ANTISENSE: 5′-TCGAGAAAAAAGCTGATTCCGCCTAAAGATCTCTTGAATCTTTAGGCGGAATCAGCA-3′

BamHI-EGFP-F′: 5′-GAGAGGATCCCGCCACCATGGTGAGCAAGGGC-3′

BamHI-EGFP-R′: 5′-GAGAGGATCCTCACTTGTACAGCTCGTCCATGCCGAGA-3′

OVERZSCAN21 F′: 5′-CAGAGATCTATGACCAAGGTGGTGGGCATGG-3′

OVERZSCAN21 R′: 5′-CAGGAATTCTTACTGTACCTCTCCCTCTCCA-3′

CHIP ZSCAN F′: 5′-GAAGCCTAGAGAGCCGGTAAG-3′

CHIP ZSCAN R′: 5′-CCGAGTGATGTACTTTCCAGTCA-3′

3′ CHIP Snca F′: 5′-AGATGGGCAAGGTATGGCTG-3′

3′ CHIP Snca R′: 5′-CCCAAGGAAAACAGTGCATCG-3′

CHIP OLIG 2 F′: 5′-AGCCTAGGGGGATTACAGGG-3′

CHIP OLIG 2 R′: 5′-ACCAGGTTCTGGAGCGAATG-3′

EGFP F′: 5′-CCCGACAACCACTACCTGAG-3′

EGFP R′: 5′-GTCCATGCCGAGAGTGATCC-3′

1.9 DEL ZSCAN21 SENSE: 5′-AGCAGAGGGACTCAGGTTGTGGATCTAAACGG-3′

1.9 DEL ZSCAN21 ANTISENSE: 5′-CCGTTTAGATCCACAACCTGAGTCCCTCTGCT-3′

1.9 DEL SEC ZSCAN21 SENSE: 5′-GTCTCTGGGAGGTGGTCCCTTTGGGGAG-3′

1.9 DEL SEC ZSCAN21 ANTISENSE: 5′-CTCCCCAAAGGGACCACCTCCCAGAGAC-3′

INTRON 1 F′:5′-GCGGAGAACTGGGAGTGGCCATTC-3′

INTRON 1 R′: 5′-GCTAACAGGTTGATGGTGGAAAGG-3′

4. RESULTS

4.1 Expression of ZSCAN21 in the central nervous system

As has already been mentioned, experiments in our laboratory have highlighted ZSCAN21 as an important regulator of *SNCA* expression in the PC12 cell line. Therefore, in the present study, we wished to characterize further the role of ZSCAN21 in primary neuronal cultures and most importantly *in vivo*. Toward this direction, we first checked whether ZSCAN21 is expressed *in vivo* in different brain areas, where ASYN is known to be expressed (midbrain, striatum, olfactory bulbs, hippocampus, cortex, and cerebellum) and which are linked to varying degrees with PD pathology. Of note, previous experiments in our laboratory using semiquantitative RT-PCR demonstrated the expression of *Zscan21* in different neuronal cells, including cortical and sympathetic neuronal cultures (Clough, Dermentzaki et al. 2009). Thus, we isolated different rat brain areas (as aforementioned) from two developmental stages, i.e., embryonic (E17) and adult (~2 months), to test for ZSCAN21 mRNA and protein expression, since limited information regarding ZSCAN21 was available. Regarding mRNA expression, we performed a TRIzol-based RNA extraction, cDNA synthesis, and RT-PCR assay. For PCR amplification we used specific primers for *Zscan21*, *Snca*, and β-actin (control) (Primer list). Regarding protein expression, following homogenization and lysis of the tissues we performed western blot analysis using a polyclonal antibody we generated against ZSCAN21 (GenScript), which in limited exposures of the film led to the appearance of a single specific band at the expected molecular weight. We detected the expression of ZSCAN21, both mRNA and protein, in all brain areas tested (Fig. 14). Additionally, the expression of ASYN was also verified in these areas in agreement with previous studies (Neystat, Lynch et al. 1999, Chiba-Falek, Lopez et al. 2006, Grundemann, Schlaudraff et al. 2008, Linnertz, Saucier et al. 2009). Interestingly, we also noticed that ZSCAN21 was more robustly expressed at the embryonic stage compared to adult brain (with a more profound difference at the protein level) following a reverse pattern to that of ASYN expression.
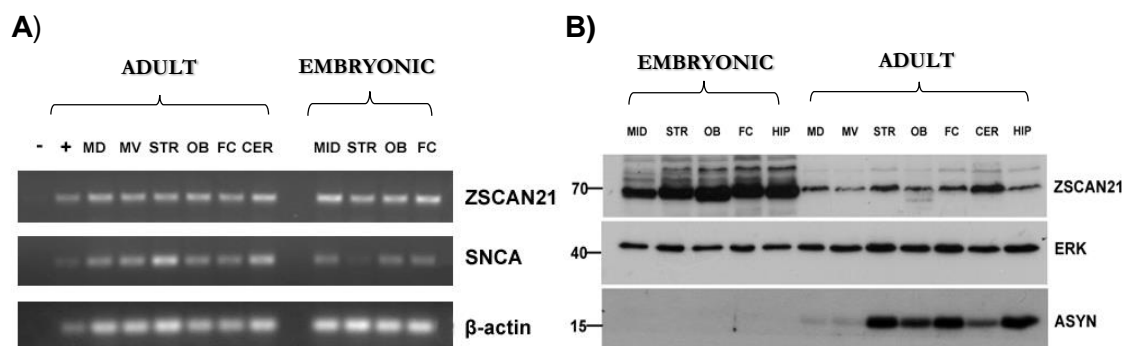
Figure 14. ZSCAN21 expression (mRNA and protein) in different brain areas from embryonic and adult rats. Different brain areas were isolated from embryonic (E18) and adult rats. The brain areas were: midbrain (MID) or midbrain dorsal (MD) and midbrain ventral (MV), striatum (STR), olfactory bulbs (OB), frontal cortex (FC), cerebellum (CER) and hippocampus (HIP). Following homogenization, RNA or protein isolation was performed. A) RT-PCR for *Zscan21*, *Snca,* and β-actin (loading ctl); (-) : negative ctl, (+) : PC12 cell lysate. B) Western blot for ZSCAN21, ASYN, and β-actin (loading ctl). Expression of ZSCAN21 (mRNA, protein) was detected in all tested brain areas, both embryonic and adult. Similarly, the expression of ASYN was also verified as expected.

4.2 Developmental expression profile of ZSCAN21 in the central nervous system

To establish a complete picture of the expression profile of ZSCAN21 during development and by extension of ASYN we further analyzed additional developmental stages from the rat brain including: E17, P1, P3, P5, P7 or P8, P10, P12 or P13, P16 and adult (~2 months). The brain region we decided to focus mainly our study on was the hippocampus. First, ZSCAN21 is highly and selectively expressed in the granule cells of the dentate gyrus (DG) of the hippocampus (Yang, Zhong et al. 1996). Second and most important, increasing lines of evidence involve the hippocampus mainly with the non-motor symptoms of PD, including primarily cognitive impairment and dementia that affect a high percentage of PD patients. Following the same protocol, we performed RNA and protein extraction from different developmental stages of the hippocampus. At the mRNA level, *Zscan21* was increased developmentally until the P10 stage and then its levels started to decrease. Likewise, *Snca* was also increased developmentally during the first weeks of postnatal life, but its levels dropped later in the adult stage, verifying previous studies (Petersen, Olesen et al. 1999) (Fig. 15A). At the protein level, ZSCAN21 decreased gradually (following the mRNA expression pattern), whereas ASYN increased developmentally (in contrast to the mRNA expression pattern) (Fig. 15B). Similar results were obtained for the cortex (data not shown). In conclusion, there was no clear correlation between the expression levels of ZSCAN21 and ASYN during development *in vivo*. However, we were interested in investigating the involvement of ZSCAN21 in *Snca* transcription at different developmental stages *in vitro* and *in vivo*, in order to verify whether this differential ZSCAN21 expression during development could diversely regulate *Snca* expression levels.
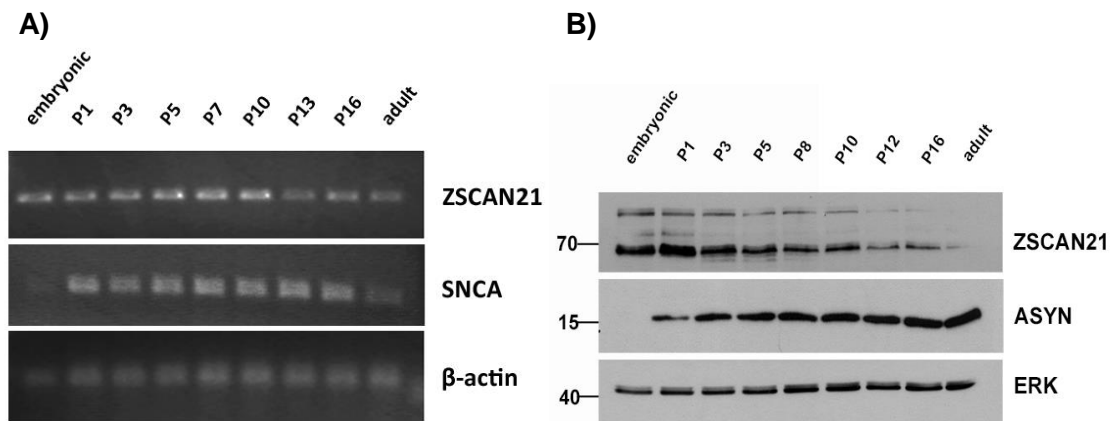
Figure 15. ZSCAN21 (mRNA and protein) expression profile at different developmental stages. The hippocampus was isolated from different developmental stages of rat brain: E17, P1, P3, P5, P7 or P8, P10, P12 or P13, P16, and adult (`2months). Then, the tissues were homogenized and processed for RT-PCR or western blot analysis. A) RT-PCR for the amplification of *Zscan21*, *Snca*, and β-actin (loading control) with specific primers. *Zscan21* mRNA expression was developmentally increased until the P10 stage and then its levels started to decrease. Accordingly, *Snca* mRNA levels increased during the first weeks of postnatal life and then were significantly reduced during adulthood. B) Western blot against ZSCAN21, ASYN and ERK (loading control). ZSCAN21 protein was reduced during development (following the mRNA expression pattern) while ASYN increased (in contrast to the mRNA expression pattern).

We additionally performed FI in cryostat-cut sections from rat brain of different developmental stages (P5, P10, P15, and adult) with a specific antibody against ZSCAN21 (Santa Cruz). This antibody gave a more specific staining compared to the home-made GeneScript antibody and was used for all immunohistochemistry experiments presented here. Similarly, we verified the same pattern of expression for ZSCAN21 during development. Representative images are shown in Fig. 16.

A)

B)
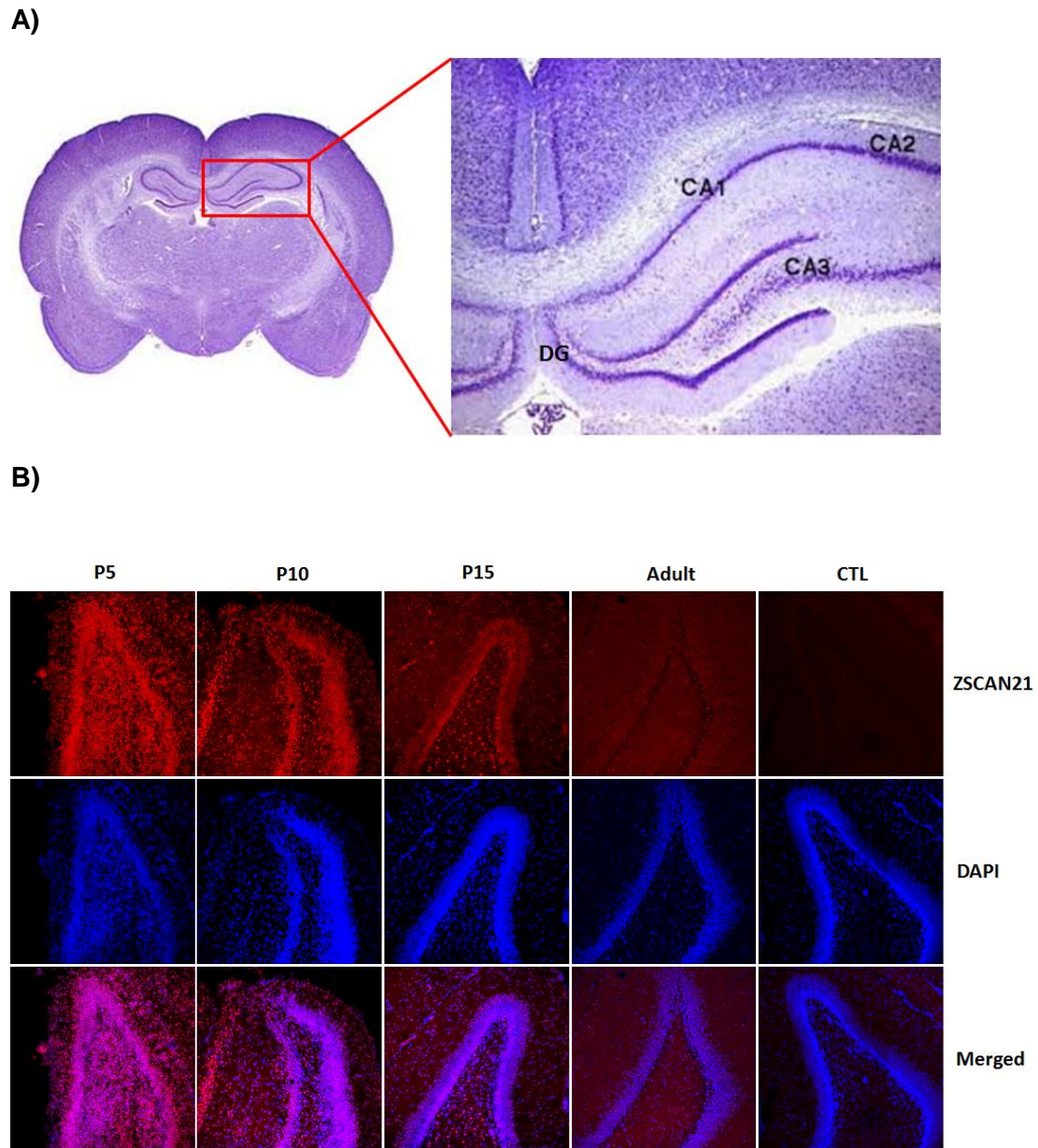
Figure 16. ZSCAN21 expression at different developmental stages in the hippocampus. A) Coronal section of the rat brain. The hippocampus is denoted with a red box. Higher magnification highlights the DG, cornu ammonis 1 (CA1), cornu ammonis 2 (CA2), and cornu ammonis 3 (CA3) areas of the hippocampus. B) Cryostat-cut sections (20 µm) from different developmental stages of the rat brain were immunolabeled with a fluorescent specific antibody against ZSCAN21 (Santa Cruz/red) and the nuclear marker TO-PRO (blue). As a secondary antibody, Cy3-rb was used. In addition, sections that were not incubated with a primary antibody (CTL) were also used as a negative control. A gradual reduction of the ZSCAN21 FI signal can be observed clearly as the age of the animal increases. The CTL condition represents the background signal of the tissue. Representative images from the DG of the hippocampus (20 ×) via an upright confocal microscope.

4.3 Neuronal expression of ZSCAN21

We next assessed whether ZSCAN21 is expressed in neurons. Therefore, we performed an FI assay using cryostat-cut sections, from P5 and P10 rat brains where ZSCAN21 is expressed robustly, with specific antibodies against ZSCAN21 and the neuronal marker NeuN (Millipore). We observed co-localization of ZSCAN21 and NeuN expression in nuclei in different brain areas, indicating that ZSCAN21, as expected for a TF, has a nuclear localization, and is indeed expressed in neurons. Representative images are shown in Fig.17.
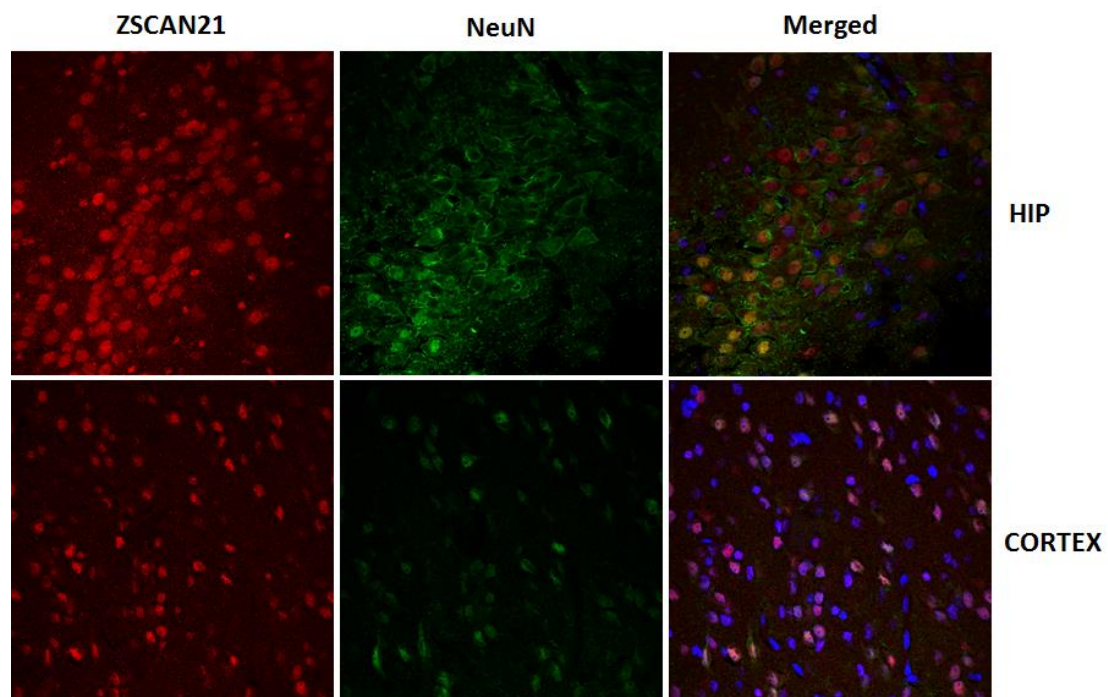
Figure 17. Neuronal expression of ZSCAN21 in the rat brain. Cryostat-cut sections (20 μm) from P10 rat brain were immunolabeled with a fluorescent specific antibody against ZSCAN21 (Santa Cruz/red) and the neuronal marker NeuN (green). TO-PRO (blue) is indicative of nuclear staining. Cy3-rb and Cy2-ms were used as a secondary antibody. Co-localization of ZSCAN21 and NeuN is evident in the merged pictures. Representative images from the DG of the hippocampus (HIP) and cortex (63×) via an upright confocal microscope.

4.4 Co-expression of ZSCAN21 and ASYN in postnatal rat brain.

Several studies has shown that ASYN presents a cell soma staining pattern early in development, whereas in the adult brain it exhibits a diffuse pattern of reactivity throughout the neuropil (Bayer, Jakala et al. 1999, Galvin, Schuck et al. 2001, Raghavan, Kruijff et al. 2004, Kahle 2008). Therefore, we selectively used cryostat-cut sections from different postnatal stages from rat brain (P5, P10, P15, and P22) to verify the cell soma staining of ASYN and also to check for co-localization between ASYN and ZSCAN21 via FI analysis. In parallel we used sections that were not incubated with a primary antibody (CTL) as a negative control (data not shown). We detected cell soma staining of ASYN until P15, as well as co-expression with ZSCAN21. Representative images are shown in Fig. 18.
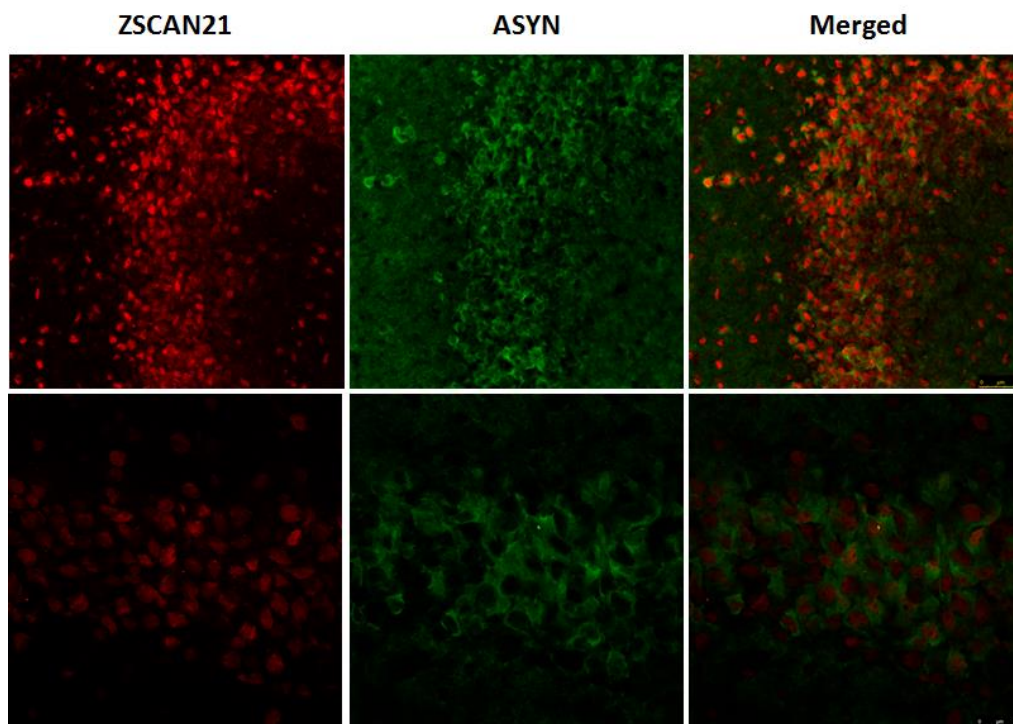
Figure 18. Co-expression of ZSCAN21 and ASYN in postnatal rat brain. Cryostat-cut sections (20 µm) from P5 rat brain were immunolabeled with fluorescent specific antibodies against ASYN (BD Biosciences), ZSCAN21 (Santa Cruz/red) and the nuclear marker TO-PRO (blue). As secondary antibodies Cy3-rb and Cy2-ms were used. ASYN was expressed in the cell soma of neurons and co-expressed with ZSCAN21 (merged) in early developmental stages. Representative images from the DG of the hippocampus (40×, 63×) via a confocal upright microscope.

To eliminate the possibility of non-specificity regarding the cell soma staining for ASYN, we further performed an immunohistochemistry assay based on the organic substance DAB in cryostat-cut sections from P5 and adult (negative control) rat brains. ASYN was immunolabeled with a specific antibody and NISSL staining served as a cell soma marker for neurons. In parallel, we performed competition experiments for ASYN by incubating the ASYN antibody together with an excess of recombinant ASYN in order to neutralize the binding capacity of the antibody (negative control). Similarly, we again detected the cell soma staining pattern of ASYN in P5 rat brain sections in contrast to the adult brain, thus verifying the presence of cell soma staining of ASYN in the postnatal brain. Representative images are shown in Fig.19
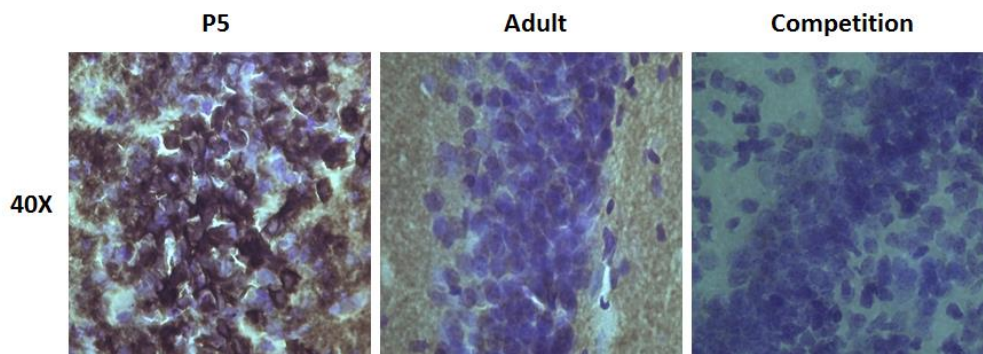
Figure 19. Verifying cell soma staining of ASYN in the early postnatal rat brain via DAB staining. Cryostat-cut sections (20 μm) from P5 and adult rat brain were immunolabeled with specific antibodies against ASYN (BD Biosciences/brown). NISSL staining was used as a marker of neuronal cell soma staining (blue). ASYN was expressed in the cell soma of neurons in the P5 brain, but not in the adult (neuropil staining). Competition experiment served as a negative control. Representative images from the DG of the hippocampus (40×) via a bright field microscope.

4.5 *Zscan21* downregulation upregulates *Snca* in rat neuronal primary cultures

Since we verified, at least in certain developmental stages, ZSCAN21 co-expression in different brain areas with ASYN *in vivo*, our next step involved the construction of shRNA lentiviruses selectively silencing *Zscan21* in order to evaluate its involvement in the regulation of *Snca*. Lentiviruses constitute a useful tool for transducing dividing as well as non-dividing cells with high efficiency and allow the stable expression of a transgene or short hairpin (shRNA). In the current study, we designed 3 shRNAs against *Zscan21* (shZSCAN21/1, shZSCAN21/2, and shZSCAN21/4) as well as scrambled shRNA (control virus) that targets no known sequence in the rat genome. The above shRNAs were cloned in the TRC2-pLKO lentivirus-vector (Invitrogen), which is widely used for downregulating different proteins in primary cultures as well as in *in vivo* systems with high efficacy (Zufferey, Nagy et al. 1997, Zufferey, Dull et al. 1998, Stewart, Dykxhoorn et al. 2003, Moffat, Grueneberg et al. 2006, Yamamoto and Tsunetsugu-Yokota 2008). In addition, we incorporated the EGFP reporter protein in the vector for monitoring the efficiency of transduction. Of note, we had also utilized the pLL3.7 lentivirus-vector in initial experiments, but unfortunately we were unable to achieve efficient downregulation of *Zscan21* repeatedly.

As a first step toward evaluating potential alterations of *Snca* expression due to *Zscan21* downregulation, we infected rat embryonic cortical cultures with the shZSCAN21-expressing lentiviruses. As already mentioned, this is a well-established primary neuronal cell model system that represents an abundant and relatively homogeneous source of post-mitotic neurons from the CNS with at least 95% purity (Rideout and Stefanis 2002). The efficiency of infection was monitored with the EGFP reporter protein. We were able to achieve almost 100% efficiency of infection in the rat cortical cultures for the shZSCAN21/1, shZSCAN21/2 and shscrambled lentiviruses (Fig. 20A). At 5 days post-infection, the cultures were harvested and processed either for RNA or protein isolation. The mRNA and protein levels of ZSCAN21 and ASYN were evaluated with real-time PCR and western blotting, respectively. We observed significant downregulation of ZSCAN21 of ~50% at both the mRNA and protein level (for both *Zscan21* targets). Regarding ASYN we observed a significant increase at both mRNA and protein (for both *Zscan21* targets), a reverse expression pattern compared to PC12 cells (Clough, Dermentzaki et al. 2009). Similar results were also obtained from primary hippocampal cultures (tested only with shZSCAN21/2), thus further validating the specificity of these results. We should also mention that different time points were assessed for ZSCAN21 and ASYN expression levels from the ones shown. Shorter time points (<96 h) had no effect upon ASYN and later time points (>5 days) demonstrated comprised cell integrity.

A)

	SCRAMBLED	ZSCAN21/2	ZSCAN21/1
Phase			
GFP			

B)

Corticals

ZSCAN21/2

SNCA

C)

Corticals
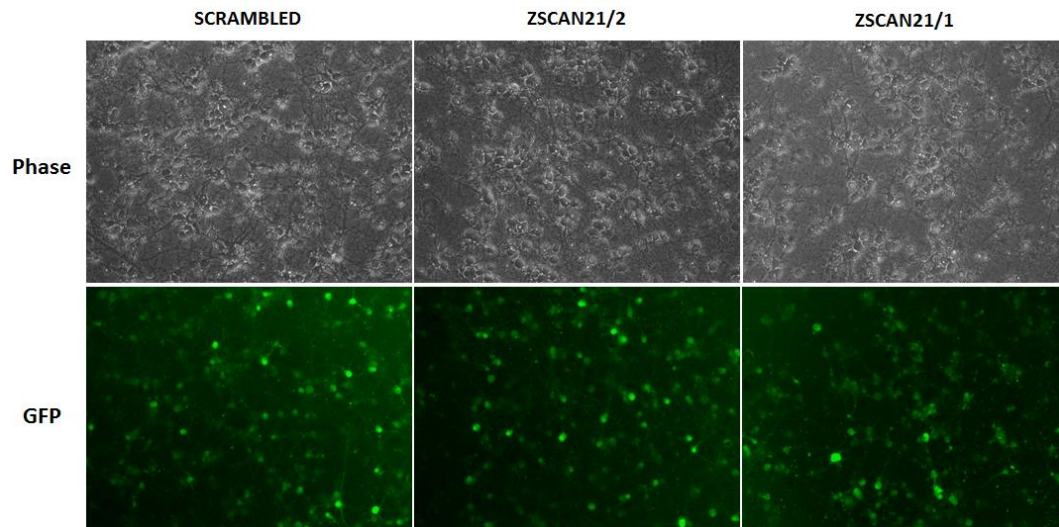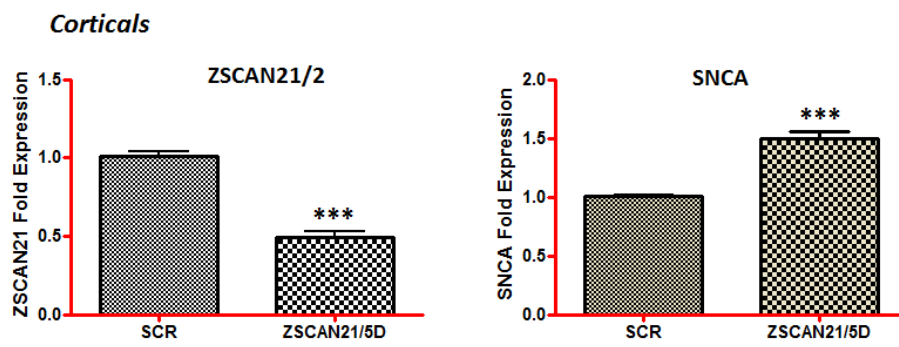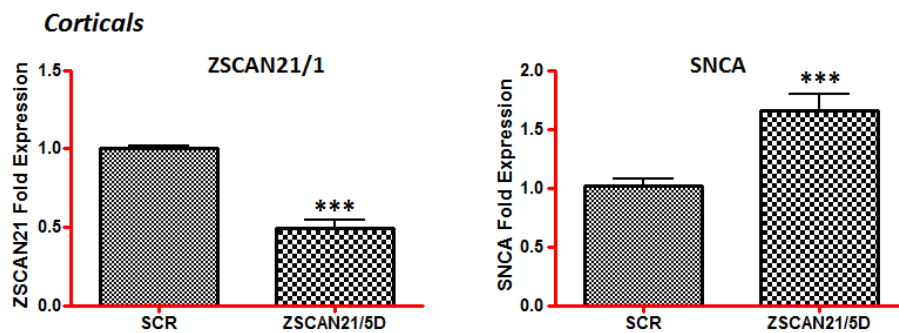
ZSCAN21/1

SNCA

D)
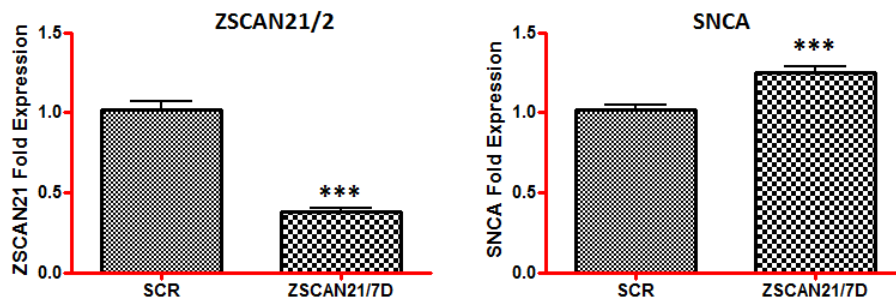
Hippocampal

Figure 20. *Snca* **mRNA is increased following downregulation of** *Zscan21* **(shZSCAN21/2 and shZSCAN21/1) in rat primary neuronal cultures.** Cortical or hippocampal cultures were prepared from embryonic day 17 (E17) rats. The neurons were infected at day 4 of culture with shZSCAN21/2, shZSCAN21/1, or shscrambled (control) lentiviruses at an MOI of 1. At 5 (for cortical cultures) or 7 days (for hippocampal cultures) post-infection, the cultures were assessed for *Zscan21* and *Snca* mRNA expression with real-time PCR. A) Efficiency of transduction in rat cortical cultures (20×) (the same efficiency was observed in hippocampal cultures / data not shown). B) Quantification of results from 5 independent experiments performed in triplicate. Results are presented as a mean, ±SEM (n = 15). Statistical analysis was performed via an unpaired t-test. Downregulation of *Zscan21* (shZSCAN21/2) leads to statistical significant increase of *Snca* (P < 0.0001) in rat embryonic cortical cultures. D) Quantification of results from 2 independent experiments. Results are presented as a mean, ±SEM (n = 8). Statistical analysis was performed via an unpaired t-test. Downregulation of *Zscan21* (shZSCAN21/1) led to statistically significant increase of *Snca* expression (P < 0.0001) in rat embryonic cortical cultures. C) Quantification of results from 4 independent experiments performed in triplicate. Results are presented as a mean, ±SEM (n = 12). Statistical analysis was performed via an unpaired t-test. Similarly, downregulation of *Zscan21* (shZSCAN21/2) led to a statistically significant increase of *Snca* expression (P < 0.0001) in rat embryonic hippocampal cultures. β-actin, loading control.
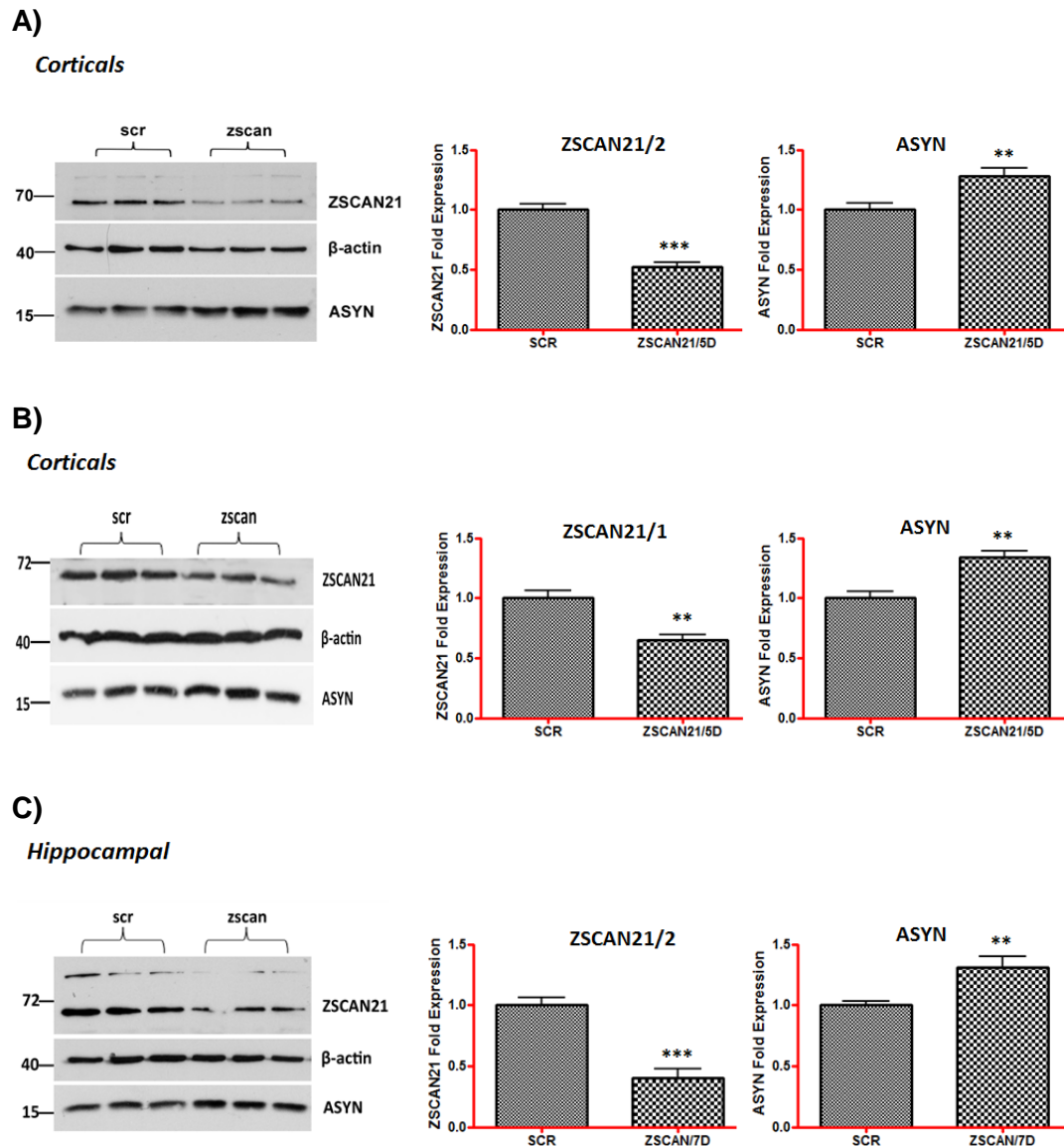
Figure 21. ASYN protein is increased following downregulation of *Zscan21* in rat primary neuronal cultures. Cortical or hippocampal cultures were prepared from E17 rats. The neurons were infected at day 4 of their culture with shZSCAN21/2, shZSCAN21/1, or shscrambled (control) lentiviruses at an MOI of 1. At 5 (for cortical cultures) or 7 days (for hippocampal cultures) post-infection, the cultures were assessed for ZSCAN21 and ASYN protein expression with western blot analysis. A) Western blot analysis and quantification of results from 4 independent experiments performed in triplicate. Results are presented as a mean, ±SEM (n = 12). Statistical analysis was performed via an unpaired t-test. Downregulation of *Zscan21 (*shZSCAN21/2) led to a statistically significant increase of ASYN expression (P < 0.01) in rat embryonic cortical cultures. β-actin, loading control. B) Western blot analysis and quantification of results from 1 independent experiment in quadruplicate. Results are presented as a mean, ±SEM (n = 4). Statistical analysis was performed via unpaired t-test. Downregulation of *Zscan21* (shZSCAN21/1) led to a statistically significant increase of ASYN expression (P < 0.05) in rat embryonic cortical cultures. β-actin, loading control. C) Western blot analysis and quantification of results from 3 independent experiments performed in triplicate. Results are presented as a mean, ±SEM (n = 9). Statistical analysis was performed via an unpaired t-test. Similarly, downregulation of *Zscan21* (shZSCAN21/2) led to a statistically significant increase of ASYN expression (P < 0.01) in rat embryonic hippocampal cultures. β-actin, loading control.

4.6 Promoter activity assay of *SNCA* following downregulation of *Zscan21* in rat primary cultures.

To measure the transcriptional activity of the *SNCA* promoter following *Zscan21* silencing, we utilized the Dual Luciferase Reporter assay (Promega), a genetic reporter system widely used to study eukaryotic gene expression and cellular physiology. Different deletion constructs of the 5' promoter of *SNCA* have been systematically examined for transcriptional activity in differentiated PC12 as well as in cortical primary cultures in previous experiments in our laboratory (Clough and Stefanis 2007, Clough, Dermentzaki et al. 2009, Clough, Dermentzaki et al. 2011). These experiments showed that the 1.9-kb deletion construct (which includes the core promoter and the 1st intron of *SNCA*) and the intron 1 construct demonstrated a reverse pattern of transcriptional activity in the above cell systems.

In the present study, given the fact that *Zscan21*-mediated downregulation upregulates ASYN at the mRNA and protein level, we wished to evaluate further whether this induction results from increased transcriptional activity of the *SNCA* promoter. To address this issue, we utilized the 1.9-kb luciferase construct, which is highly induced in the luciferase assay (in contrast to intron 1) in rat cortical cultures, intron 1 construct and the 10.7-kb luciferase construct. The 10.7-kb construct is also induced in the luciferase assay in rat cortical cultures (Clough, Dermentzaki et al. 2011) and most importantly contains the NACP/Rep-1 polymorphism that has been correlated with PD risk in several studies (Chiba-Falek and Nussbaum 2001, Maraganore, de Andrade et al. 2006, Cronin, Ge et al. 2009, Linnertz, Saucier et al. 2009). Therefore, we infected rat embryonic cortical cultures with either the shZSCAN21/2, shZSCAN21/1 or shscrambled lentiviruses. At 3 days post-infection we transfected these cultures with the 10.7-kb, 1.9-kb, intron1 and pGL3-empty (control vector) luciferase constructs, and we performed the luciferase assay at 48 h later. Notably, we observed significant induction in the luciferase assay following *Zscan21* downregulation with the shZSCAN21/2 and shZSCAN21/1 targets compared to shscrambled for the 1.9-kb promoter construct that contains the core promoter of *SNCA*. Therefore, *Zscan21* silencing increases *SNCA* transcription at the promoter level. However, we did not observe any significant alterations for the 10.7-kb construct or the intron 1 construct.
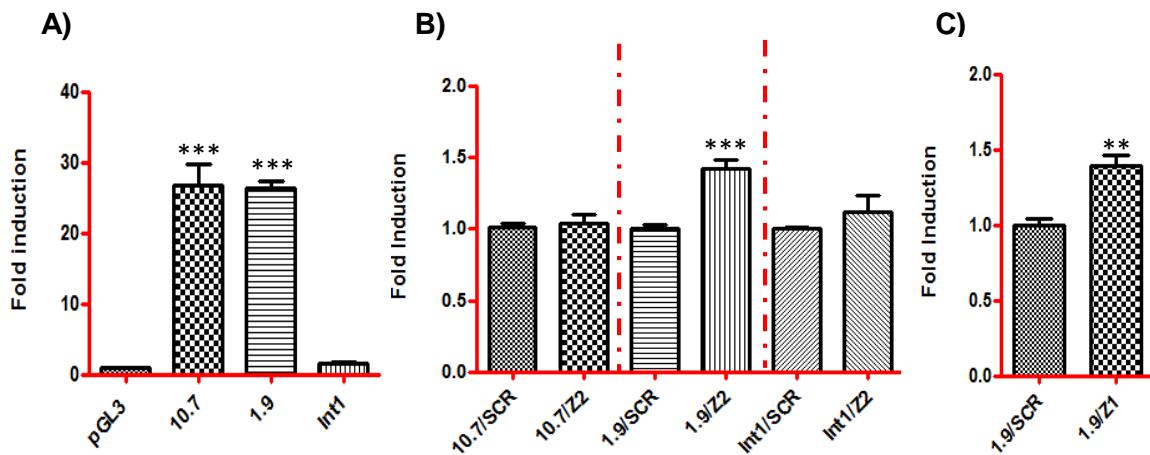
Figure 22. Increased transcriptional activity of the *SNCA* promoter following *Zscan21* downregulation in rat cortical cultures. Cortical cultures were prepared from E17 rats. The neurons were infected at day 4 of their culture with shZSCAN21/2, shZSCAN21/1, or shscrambled (control) lentiviruses at an MOI of 1. At 3 days post-infection, the cultures were transfected with the 10.7 (kb), 1.9 (kb), intron 1 (Int1), and pGL3 basic -empty vector luciferase constructs. At 48 hours post-transfection, the cells were lysed and assessed for the luciferase assay. A) Relative luciferase activity of the 10.7-kb (P < 0.0001), 1.9-kb (P < 0.0001), and intron 1 (Int1) luciferase constructs compared to pGL3-empty vector in naïve cortical cultures. Quantification of results from 4 independent experiments performed in duplicate. Results are presented as a mean, ±SEM (n = 8). Statistical analysis was performed via an unpaired t-test. B) Quantification of results from 5 independent experiments performed in duplicate for 1.9-kb and 10.7-kb and 3 independent experiments performed in duplicate for intron1 (Int1). Results are presented as a mean, ±SEM (n = 10, n = 6, respectively). Statistical analysis was performed via an unpaired t-test. Significant induction in the luciferase assay following *Zscan21* downregulation (shZSCAN21/2, Z2) compared to scrambled (fold induction set as 1 for each construct in the scrambled condition) for the 1.9-kb construct (P < 0.0001), but not for the 10.7-kb and intron 1 (Int1) constructs. C) Quantification of results from 1 experiment performed in triplicate for the 1.9-kb construct. Results are presented as a mean, ±SEM (n = 3). Statistical analysis was performed via an unpaired t-test. Significant induction in the luciferase assay following *Zscan21* downregulation (shZSCAN21/1, Z1) compared to scrambled (fold induction set as 1 for each construct) for the 1.9-kb construct (P < 0.01).

4.7 Assessment of ZSCAN21 mode of *SNCA* transcriptional regulation in rat cortical cultures.

So far, our data indicated the involvement of ZSCAN21 in the transcriptional regulation of SNCA at the level of its promoter in rat primary neuronal cultures, though they could not provide sufficient information as to whether this regulation was direct or indirect. Previous experiments in our laboratory have shown that ZSCAN21 directly regulates SNCA via its binding site in the intron 1 area of *SNCA* in differentiated PC12 cells (Clough, Dermentzaki et al. 2009), but most important, a recent study by Brenner et al. (Brenner, Wersinger et al. 2015) reported that ZSCAN21 binds to the intron 1 region *in vivo* in human brain tissue. Therefore, there was enough evidence to support the hypothesis that ZSCAN21 regulates *SNCA* transcription by binding to its intron 1 region. To validate this conjecture, first we performed a CHIP assay in rat cortical cultures to examine whether ZSCAN21 binds directly to the predicted consensus sites in the intron 1 region. In the intron 1 region of *SNCA*, there are two predicted binding sites for ZSCAN21 conserved in human and rat (MatInspector), one at the very beginning of intron 1 and one approximately 130 bases downstream. For the CHIP assay, we designed specific primers to include the region (~150 bases) with both putative ZSCAN21 binding sites. For the immunoprecipitation we used the ZSCAN21 GenScript antibody as well as a negative control (IgG control) irrelevant antibody of the same isotype (c-myb). Additionally, we used primers amplifying either a distant region in the same gene (an area in the exon / intron 4 region of *Snca* / 3' SNCA) or a region in another gene (in this case the OLIG2 gene) as negative controls. We found an increase of approximately 15-fold in the case of the ZSCAN21 antibody compared to the irrelevant IgG control for the 150 bp designated region in the intron 1 region in the real-time PCR assay. Regarding the negative control regions for 3' SNCA and OLIG2, we observed an approximately 4- and 2-fold signal, respectively. These data indicate that it is very likely that ZSCAN21 binds to the intron 1 region of *Snca* in rat cortical neuronal cultures. Further, we designed constructs lacking the first putative ZSCAN21 binding site (1.9d), the second putative ZSCAN21 binding site (1.9sec), as well as both binding sites (1.9dd), using the 1.9kb construct (which is highly induced in the luciferase assay in cortical cultures) as a template via site-directed mutagenesis. Then, we performed luciferase assays in primary cortical cultures. The 1.9-kb construct again, like before, demonstrated robust induction of luciferase activity. Interestingly, overall, we did not detect a significant alteration between the 1.9-kb construct and the 1.9-kb deletion constructs.

A)
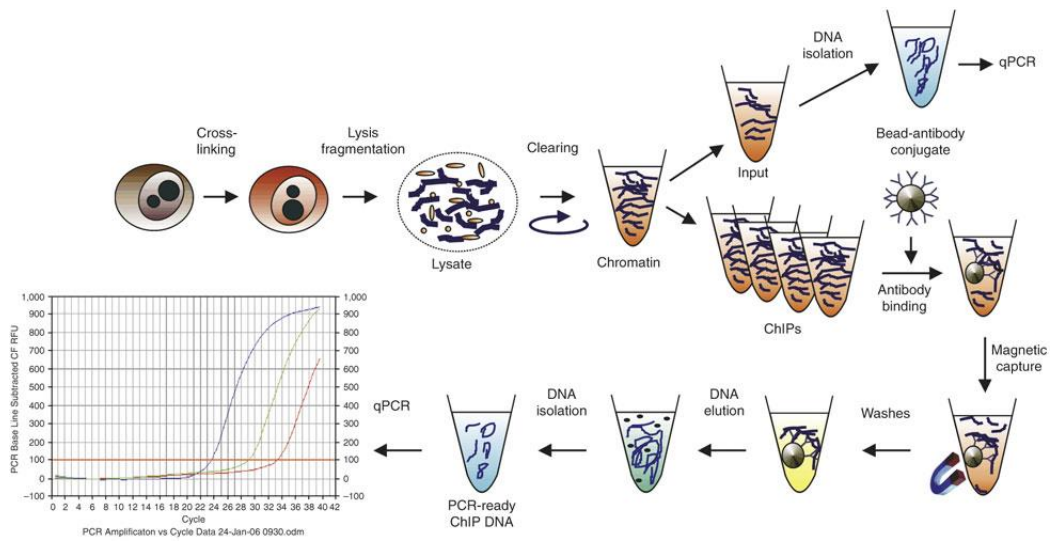
(Dahl and Collas 2008)

B)

C)

71
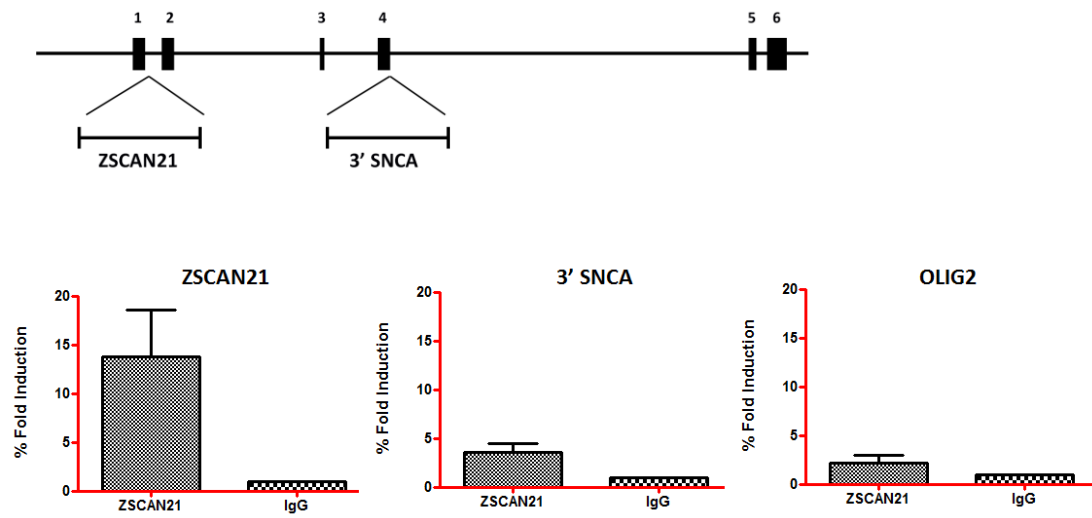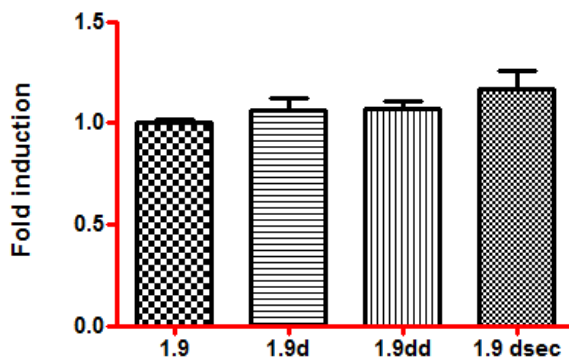
Figure 23. CHIP assay and *SNCA* promoter activity following deletion of ZSCAN21 binding sites in intron 1. A) Schematic of a CHIP assay. Cross-linking is performed directly in cell culture followed by cell lysis and chromatin fragmentation. Next, chromatin pre-clearing is performed to reduce non-specific binding. A small portion of the pre-cleared sample is kept as input (positive ctl) and the rest undergoes CHIP either with a specific antibody for the protein of interest, or an irrelevant antibody of the same isotype (IgG/negative ctl) along with magnetic beads. The immunoprecipitated protein-DNA complex is disrupted, and the DNA is eluted and further amplified with specific primers (real-time PCR). If CHIP is successful, there will be a significant difference between the number of cycles for the sample of interest (specific antibody) and the negative ctl (irrelevant IgG antibody) denoted by the exponential curves in the PCR software. B) Schematic of the rat *Snca* gene: exons are depicted as boxes and introns as lines. The specific location in the rat *Snca* gene of the amplified area containing the two ZSCAN21 putative binding sites (ZSCAN21) as well as the amplified non-specific area (3' SNCA) are presented. Rat cortical cultures were harvested at day 8 and processed for the CHIP assay. The antibodies used for immunoprecipitation were ZSCAN21 (10 µg; Genscript antibody) and c-myb (10 µg; irrelevant antibody). We observed a 15-fold increase for ZSCAN21 compared to the irrelevant antibody (IgG). For 3' SNCA (negative control on the same gene locus) we detected an approximately 4-fold induction and a 2.5-fold induction for OLIG2 (negative control on a different gene) compared to IgG. Quantification of results (real time-PCR) from 3 independent experiments. C) Cortical cultures were transfected at day 7 with the 1.9-kb construct, ZSCAN21 deletion constructs (1.9d, 1.9dd, and 1.9 sec), and pGL3 basic empty vector (control). At 48 h post-transfection, the cells were lysed and assessed for luciferase assay. Quantification of results from 4 independent experiments performed in duplicate and normalized according to the pGL3 empty vector. Results are presented as a mean, ±SEM (n = 8). Statistical analysis was performed via one way ANOVA and post hoc Tukey's test. We observed no statistically significant differences between the 1.9-kb and the ZSCAN21 deletion constructs.

4.8 Silencing of *Zscan21* in differentiated cultures derived from neurospheres.

We also examined the interplay between ZSCAN21 and SNCA in free-floating cultures of neural stem cells termed neurospheres (Reynolds and Weiss 1992). Neurospheres represent an early developmental model system, and since ZSCAN21 demonstrates the highest levels of expression very early in development, it seemed plausible to examine its role upon *Snca* regulation in that system. Generally, neurospheres are derived from a single-cell suspension of neural stem and progenitor cells isolated from the fetal or adult CNS. In our case, we isolated the cortex and hippocampus from embryonic (E16) rat brains, and following mechanical dissociation, we cultured the starting population as a single cell suspension in medium containing EGF and FGF which drive the neurosphere formation (Vescovi, Reynolds et al. 1993, Morshead, Reynolds et al. 1994, Gritti, Parati et al. 1996, Reynolds and Weiss 1996, Tropepe, Sibilia et al. 1999). Next, following a few passages (usually P2-P3), these neurospheres were dissociated and plated in poly-D-lysine-coated plates either in the presence of the above growth factors as proliferating cultures or in the absence of these factors as differentiated mixed cultures that consist of neurons, astroglia and oligodendroglia. The percent of neurons in the cultures is approximately 15-20%. We must mention that the maturation state of the differentiated cultures is completely different from that of primary cultures. These differentiated neurons derived from neurospheres are positive for beta-III tubulin (TUJ1 / early neuronal marker) and almost negative for NeuN (mature neuronal

marker). In our study, we utilized the differentiated cultures, since ASYN is not detected in the proliferating cultures (data not shown). Immunohistochemistry against ZSCAN21, ASYN, and TUJ1 verified the co-expression of ZSCAN21 and TUJ1 as well as ASYN and TUJ1 (Fig 24).

A)
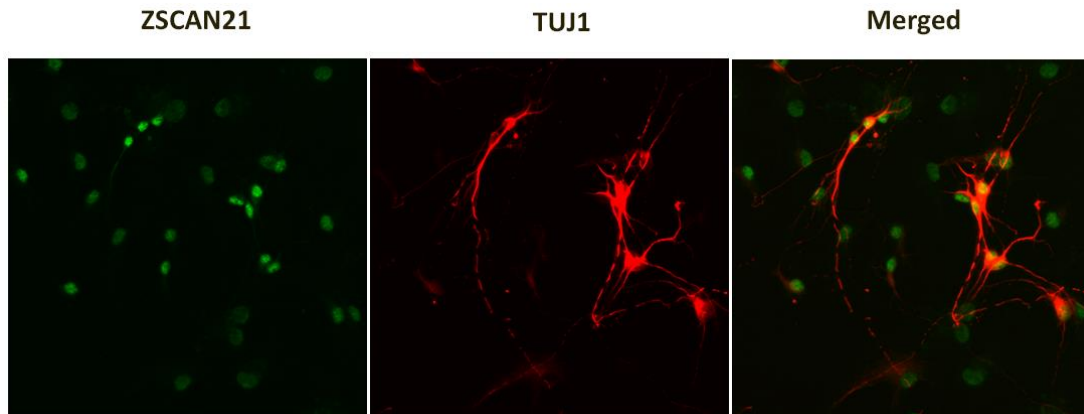
B)
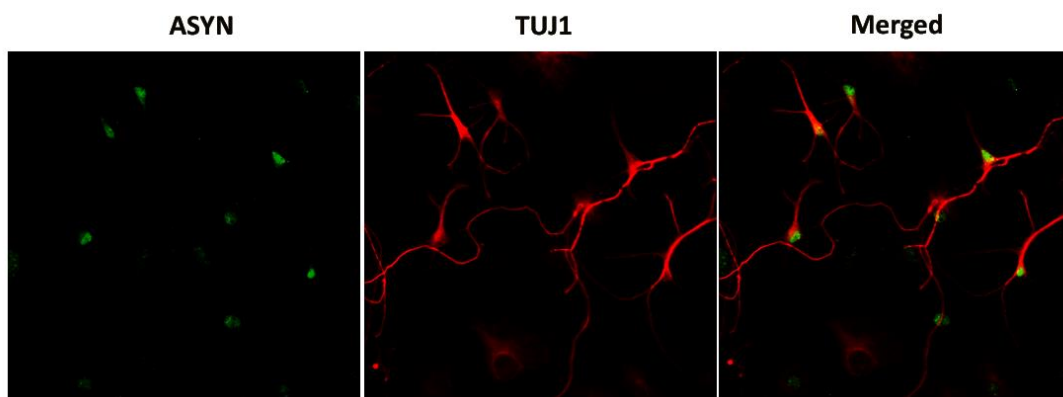
Figure 24. Neuronal expression of ZSCAN21 and ASYN in differentiated neurospheres. Neurosphere cultures derived from the cortex and hippocampus of E16 rat embryos following 2 passages were dissociated and plated for differentiation. On the 3rd day of differentiation, the cultures were immunolabeled with antibodies against TUJ1 (early neuronal marker) ZSCAN21 (GenScript), and ASYN (C20). As secondary antibodies, Cy3-ms (red) and Cy2-rb (green) were used. We detected co-localization A) of TUJ1 with ZSCAN21 and B) of TUJ1 with ASYN. Representative images for each antibody separately and merged from an upright microscope (40×).

We next infected these differentiated cultures with the shZSCAN21 lentiviruses (shZSCAN21/1 and shZSCAN21/2) and shscrambled (control) and assessed them for ZSCAN21 and ASYN expression levels at 5 days post-infection. We observed high infection efficiency for all lentiviruses (Fig. 25A). Significant silencing of *Zscan21* with both lentiviruses surprisingly led to decreased levels of ASYN at both the mRNA and protein level (Fig 25 B, C, and D). This finding is in contrast to previous results in the primary neuronal cultures, where we detected increased ASYN levels.

A)
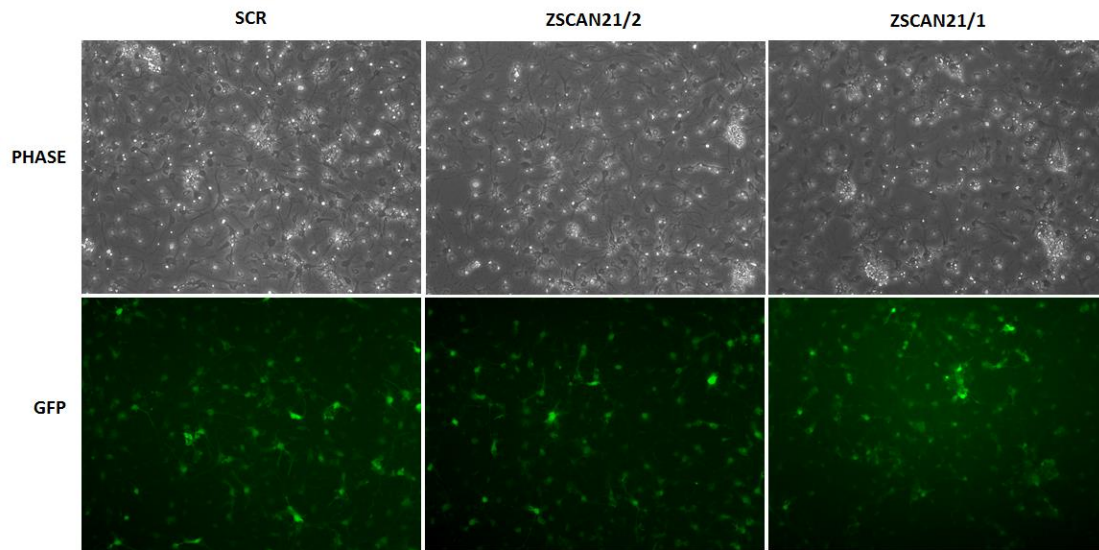
B)
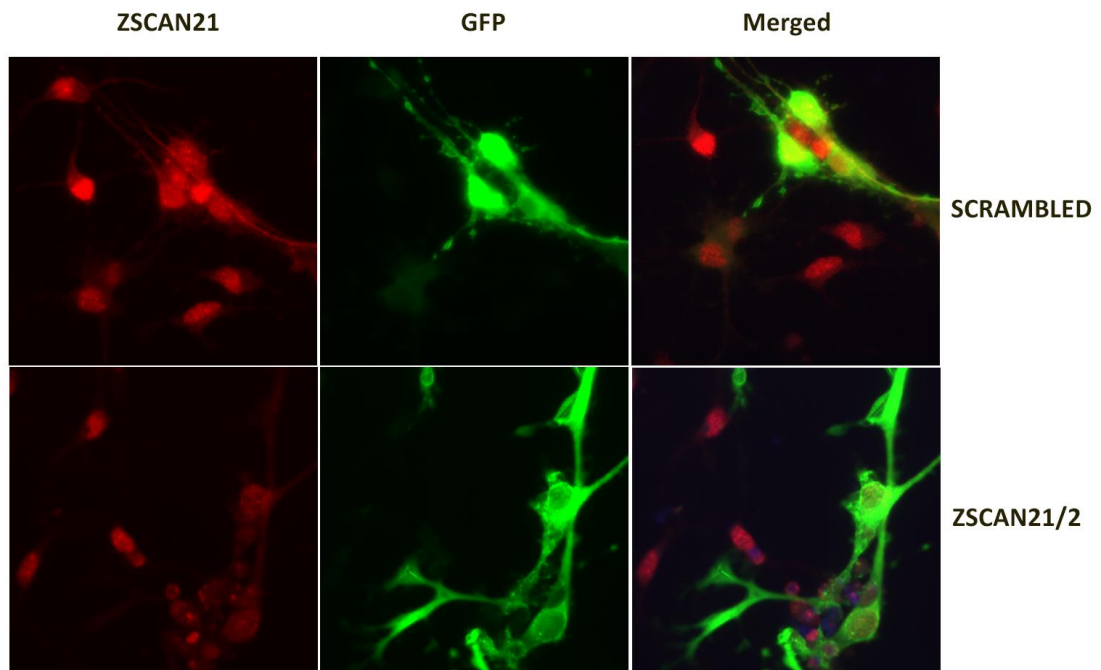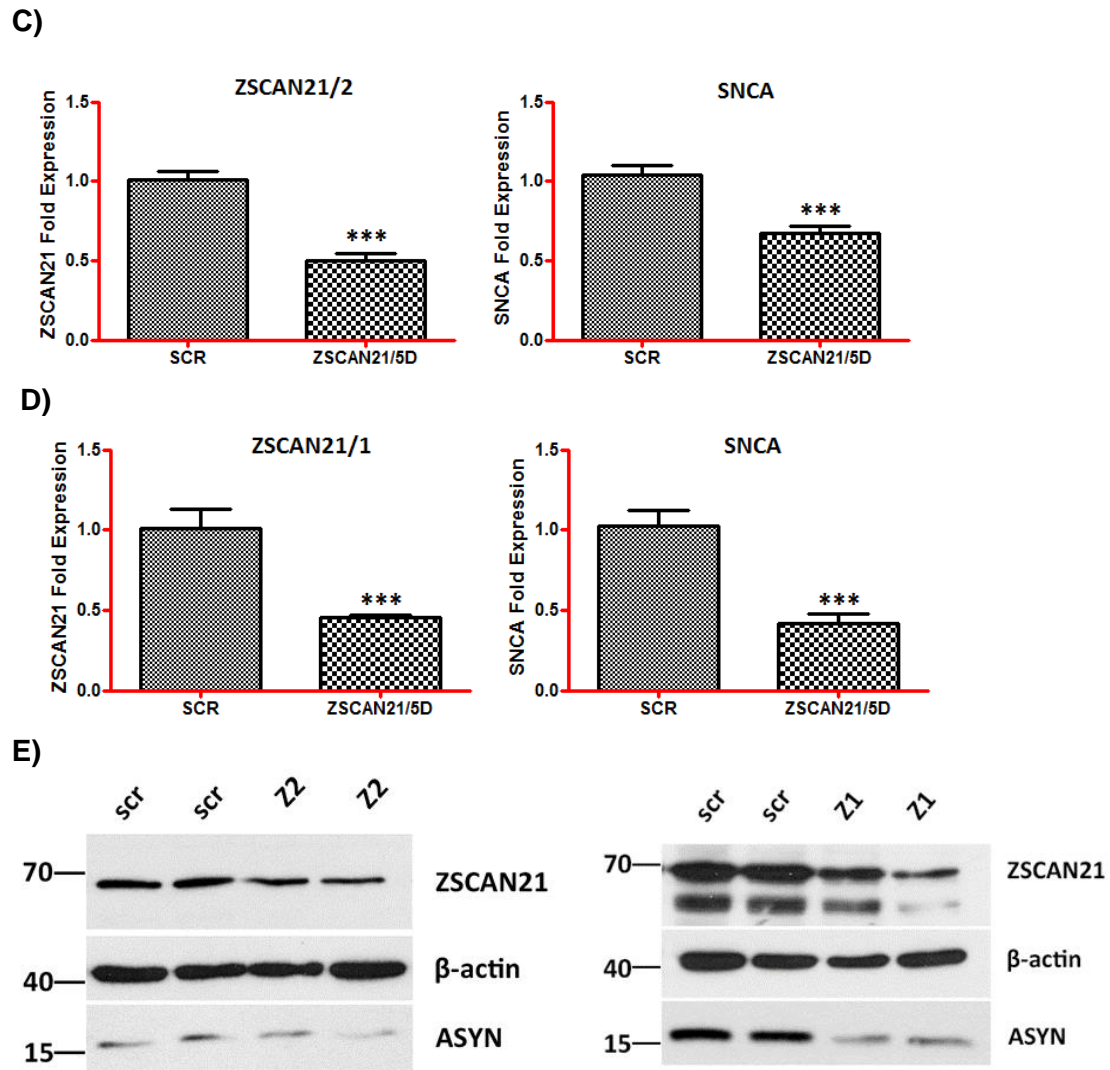
Figure 25. Lentivirus-mediated silencing of *Zscan21* (shZSCAN21/2 and shZSCAN21/1) leads to decreased levels of ASYN in differentiated neurosphere cultures. Neurosphere cultures derived from the cortex and hippocampus of E16 rat embryos following 2 passages were dissociated and plated for differentiation. On the 1st day of differentiation, the cultures were infected with shZSCAN21/2, shZSCAN21/1, or shscrambled lentiviruses. At 5 days post-infection, the cultures were harvested and assessed for immunocytochemistry, real-rime PCR, and western blotting. A) Efficiency of transduction for shZSCAN21/2, shZSCAN21/1 and shscrambled lentiviruses (20×). B) Immuno-labeling against ZSCAN21 in both shZSCAN21/2 and shscrambled conditions. Cy3-rb (red) was used as a secondary antibody. GFP is the reporter marker of the lentiviruses. Downregulation was noted in the shZSCAN21 condition compared to shscrambled. Representative images from a confocal microscope (63×). C) Quantification of mRNA results from 3 independent experiments performed in triplicate. Results are presented as a mean, ±SEM (n = 9). Statistical analysis was performed via an unpaired t-test. Downregulation of *Zscan21 (*shZSCAN21/2) led to a statistically significant decrease of *Snca* expression (P < 0.001). β-actin, loading control. D) Quantification of mRNA results from 2 independent experiments performed in quadruplet. Results are presented as a mean, ±SEM (n = 8). Statistical analysis was performed via an unpaired t-test. Downregulation of *Zscan21* (shZSCAN21/1) led to a statistically significant decrease of *Snca* expression (P < 0.001). β-actin, loading control E) Representative western blot. *Zscan21* downregulation (shZSCAN21/2 [Z2] and shZSCAN21/1 [Z1]) led to decreased ASYN levels. β-actin, loading control.

We also tried to test whether *Zscan21* silencing reduces *SNCA* transcription at the promoter level in the differentiated neurosphere cultures by performing luciferase assays. Again, we utilized the 1.9-kb *SNCA* promoter construct for this assay. We observed a great variation among independent experiments (data not shown), that overall indicated no significant effect upon *SNCA* promoter activity following shZSCAN21/2 silencing. However, in the differentiated neurosphere cultures, we know that only a small percentage of cells represents early neurons (15-20%) and most cells are glia thus, since transfection of the 1.9-kb promoter construct is random, we do not know what percentage of neurons are transfected each time and we also cannot exclude the possibility that the 1.9-kb construct can also be affected in unpredictable ways by the other cell populations present. Concluding, it is rather difficult to test directly whether *Zscan21* silencing indeed reduces *SNCA* promoter activity in these cultures.

4.9 Evaluating the role of ZSCAN21 upon *Snca* regulation in different developmental stages *in vivo*.

For the *in vivo* experiments we produced AAVs targeting *Zscan21* expression. The reason we utilized AAVs over lentiviruses is due to their increased transduction efficacy in *in vivo* settings (with the TRC2-pLKO lentiviruses we were unable to transduce neuronal cells *in vivo*). Specifically, for the AAVs used in the current study, shRNA expression was driven by a synapsin promoter that ensures the selective transduction of neurons. In addition, a GFP selection marker was also incorporated in the AAV vector sequence for the visualization of the signal. We focused on studying the role of ZSCAN21 on *Snca* regulation *in vivo* in two developmental stages due to the differential regulation of *Snca* transcription following *Zscan21* silencing in the neurosphere cultures (early developmental stage) and the rat primary neuronal cultures (representing a more mature stage). The shZSCAN21 target that was cloned in the AAV vector was shZSCAN21/2. We achieved high neuronal transduction efficiency in both developmental stages with AAV/shZSCAN21/2 and AAV/shscrambled. Regarding the early developmental stage, we performed stereotaxic delivery of both AAVs in the lateral ventricles of postnatal day 3 (P3) rat brains using a specific stereotaxic unit for pups according to Kim et al. (Kim, Ash et al. 2013). We followed this approach as it is particularly difficult to target a specific brain area at such a young age. The AAVs, due to the small diameter of their viral particles (~20-30 nm), have the ability to spread efficiently through the lateral ventricles and transduce proximal brain areas, including the hippocampus, which was of most interest to us in the present study. The amount of the AAVs injected was 7.0×10^{13} TU/mL (2 μL/ventricle) for both AAVs. The animals were sacrificed at 1 month post-infection and the brain samples were processed either for FI or cell sorting for RNA analysis. Immunohistochemistry of cryostat-cut brain sections with the neuronal NeuN marker revealed sufficient neuronal transduction mainly in the areas surrounding the ventricles, such as the striatum, cortex and hippocampus. In most cases, neuronal transduction was more evident in the hippocampus. In parallel, brain samples were processed for cell sorting in order to isolate the infected neurons for mRNA analysis of *Zscan21* and *Snca*

expression for both AAVs. To achieve efficient cell sorting we utilized the GFP reporter marker of the AAVs along with antibodies for neuronal cell surface markers. The neuronal cell surface markers used were the PE-CD24 (BD Biosciences) and Alexa Fluor 647 CD90.1 (BioLegend) antibodies. For each animal (AAV/shZSCAN21 or AAV/shscrambled) we sorted two different cell populations, the transduced population that was positive for GFP, CD24 and CD90 and the non-transduced population that was negative for GFP and positive for CD24 and CD90. The non-transduced population served as an internal control for the endogenous cargo. We assessed these sorted samples for *Zscan21* and *Snca* mRNA expression. We achieved robust downregulation of *Zscan21* in the case of the AAV / shZSCAN21-treated animals versus AAV/shscrambled and ctl (non-transduced population) according to real-time PCR analysis. Additionally, the animals that demonstrated the highest downregulation were also highly enriched for the GFP signal, thus substantiating the effectiveness of the sorting assay utilized. Nevertheless, *Snca* levels remained unchanged following *Zscan21* downregulation. Of note, from the total of 11 animals (5 AAV/shZSCAN21, 6 AAV/shscrambled) that underwent sorting, only 3 were highly enriched for the GFP signal in the case of AAV/ shZSCAN21 and 3 in the case of AAV /shscrambled viruses. This was due to variation in the transduction efficiency of both AAVs following stereotaxic injection in the ventricles (also evident in the immunohistochemistry assay) of P3 rats.

A)

B)

Scramble.GFP
Zscan.GFP

Brain

Dissociation

Percoll

+

*Immunolabelling
(CD24, CD90)*

SSC

FSC

Debris

Cell bodies

Doublet exclusion

SSC-W

SSC-H

FSC-W

FSC-H

Cell surface markers

CD24

CD90 (Thy-1)

Sorted Cells → RNA

Untransfected

Scramble.GFP

Zscan.GFP

GFP

0

11,3%

18,3%
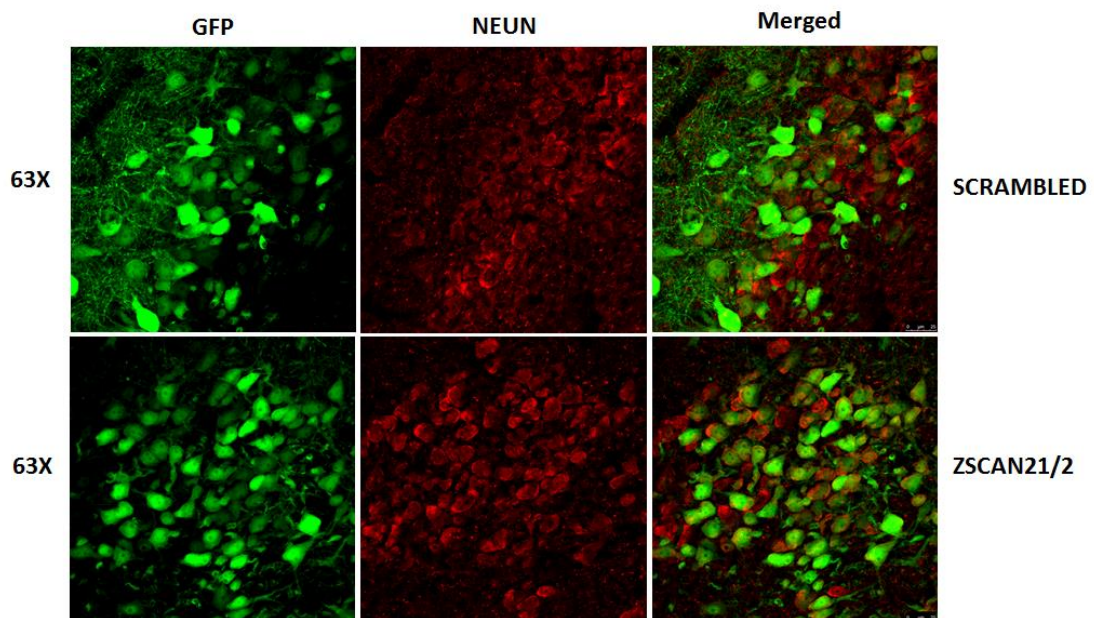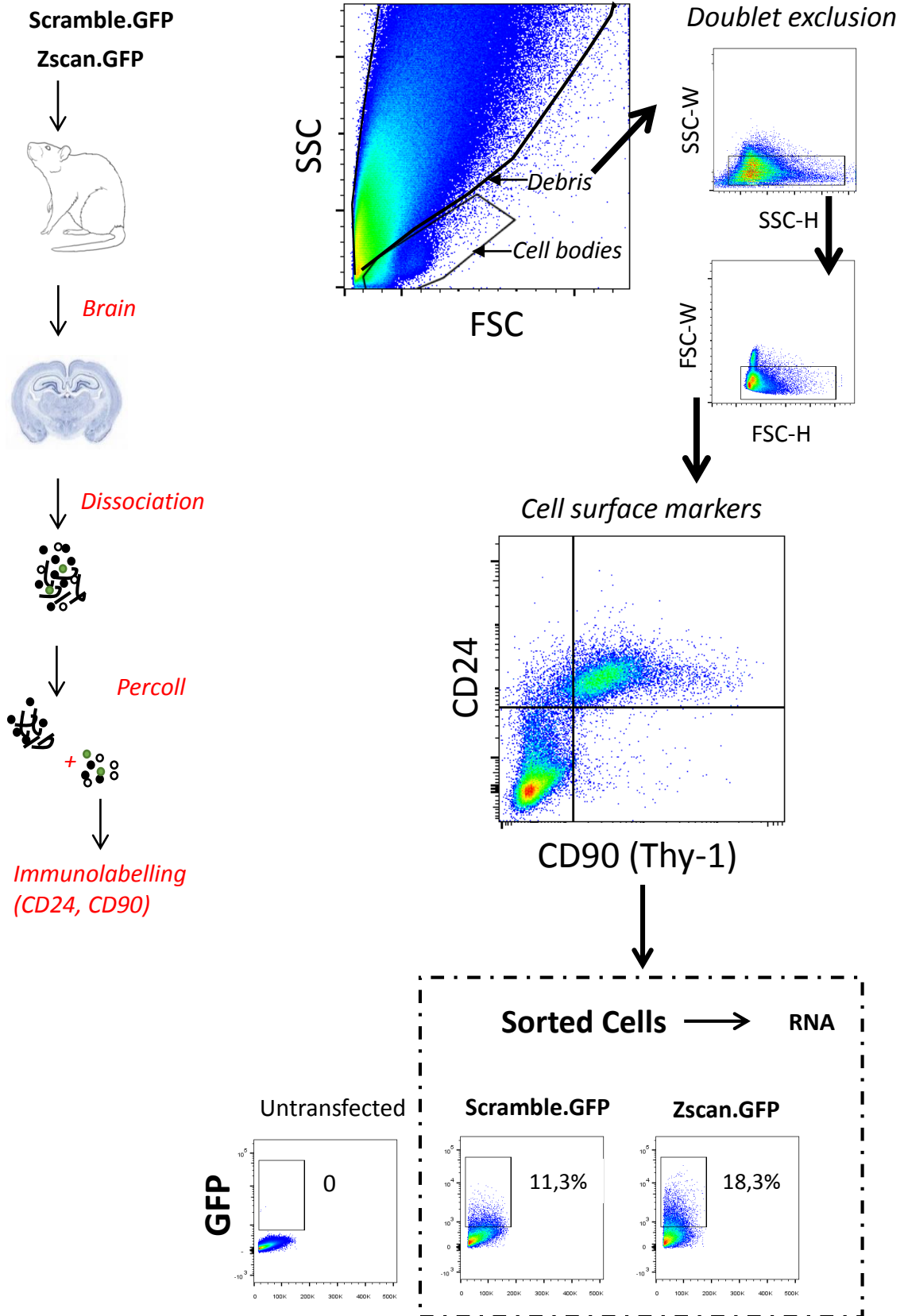
C)
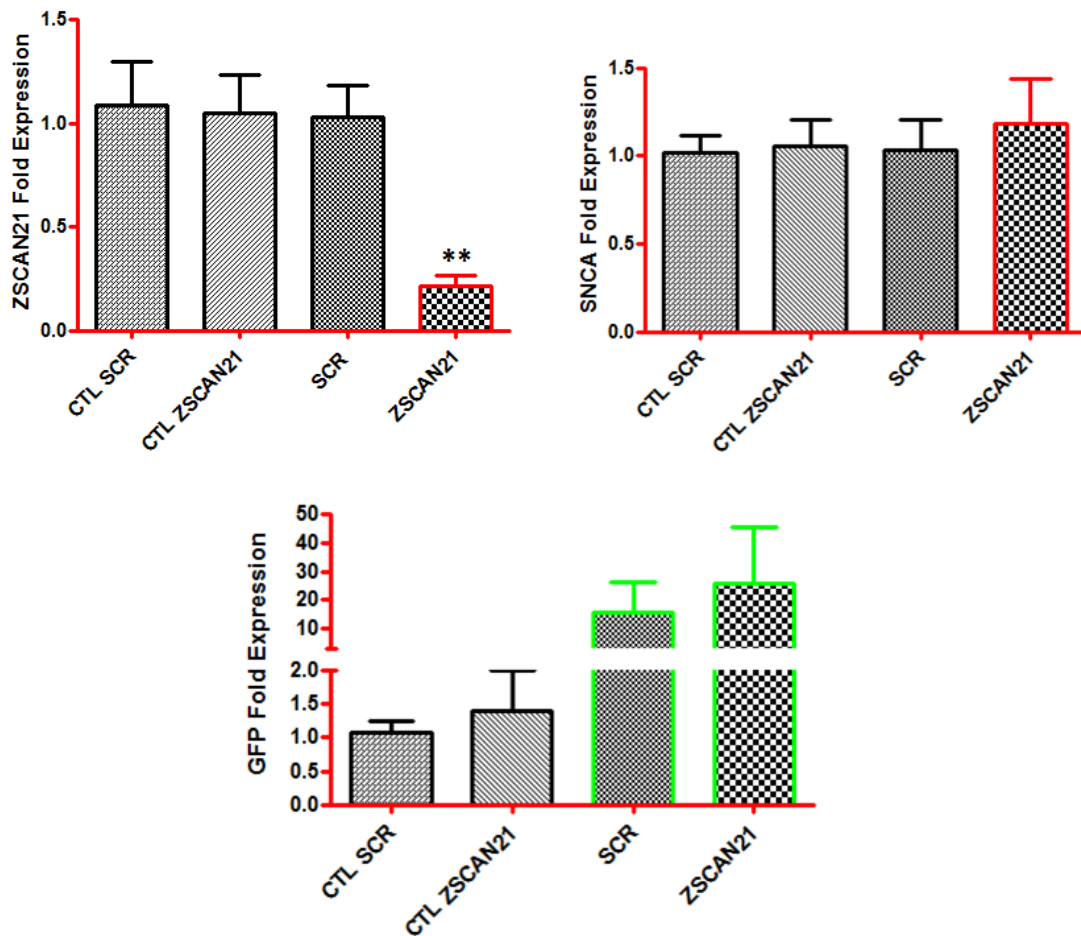
Figure 26. **AAV-mediated silencing of *Zscan21* did not alter *Snca* levels in the early postnatal rat brain.**
A) Cryostat-cut sections (20μm) from 1-month-old rat brains stereotaxically injected with AAV/shZSCAN21 or AAV/shSCRAMBLED (at P3) were immunolabeled with the NeuN neuronal marker. The Cy3-rb was used as a secondary antibody. The GFP reporter marker of the AAVs demonstrated the efficiency of transduction in both the AAV/shZSCAN21 and AAV/shSCRAMBLED condition. Co-localization of NeuN (red) and GFP (green) was observed in the merged picture. Representative images from the DG of the hippocampus (63×) via a confocal microscope. B) Schematic of FACS protocol including dissociation of tissue to a cell suspension, removal of debris by filtration and Percoll gradient centrifugation, immunolabeling of cells with cell surface neuronal markers (CD24, CD90), and purification of GFP-positive neurons using FACS analysis. A typical light scatter plot showing distinct clusters for debris and cells is presented. Each dot represents one event detected by the laser. Forward scatter (FSC) represents the size of the event while side scatter (SSC) represents granularity of the event. The box indicates the area of mainly cell bodies that was sorted for subsequent RNA extraction and downstream use in quantitative real-time PCR. Criteria set for sorting were duplet exclusion, colocalization of the CD45/CD90 signal and positive GFP signal. From the gated area we had approximately 11% positive cells that were sorted for the AAV/shSCRAMBLED samples and approximately 18% positive cells that were sorted for the AAV/ZSCAN21 samples. C) Quantification of results from real-time PCR. β-actin, loading control. Results are presented as a mean, ±SEM (n = 5 for control scrambled [CTL SCR], n = 4 for control ZSCAN21 [CTL ZSCAN21], n = 3 for AAV/shscrambled [SCR] and n = 3 for AAV/shZSCAN21 [ZSCAN21]. Statistical analysis was performed via an unpaired t-test. Significant downregulation of *Zscan21* expression (P < 0.01) did not significantly affect *Snca* levels.

Although we did not observe any significant change in the *Snca* levels following downregulation of *Zscan21* expression in the early developmental stages of the rat brain where ZSCAN21 is expressed robustly, we were nevertheless interested in further investigating whether (in contrast) the low expression levels of ZSCAN21 observed in the adult brain could be involved in *Snca* transcription. For this purpose, we again performed stereotaxic injections utilizing the above AAVs targeting the DG of the hippocampus in 2-month-old rats. For this assay we used a total of 12 adult rats (6 AAVshZSCAN21, 6 AAVshSCRAMBLED). The injections were performed at 2 distinct sites of the DG of the hippocampus in the right hemisphere of the brain in order to transduce efficiently a more extended area. The coordinates of the injection sites were: 1st AP: -3.0, ML: -1.5, and DV: -3.6, and 2nd AP: -4.56, ML: -2.6, and DV: -3.3. The amount of the virus injected for both AAVs was 7.0×10^{13} TU/mL (2μL / injection site). The animals were sacrificed at 2-months post-infection and the brain samples were processed either for FI or biochemical assays. Immunohistochemistry of cryostat-cut brain sections with the neuronal NeuN marker revealed widespread neuronal transduction of the DG of the hippocampus. The immunohistochemistry assay was performed in 1 animal per group. The remaining 5 animals in each group were processed for *Zscan21* and *Snca* mRNA levels. We also isolated the right infected area of the DG of the hippocampus through a stereoscope by visualizing the GFP signal. We also isolated the same area from the left hemisphere (non-injected) that represents the endogenous levels of expression for each animal. We then isolated total RNA (TRIzol-based) and performed real-time PCR. We observed significant *Zscan21* downregulation in the group of AAV/shZSCAN21 animals compared to AAV/shscrambled. Similarly to the early postnatal stage, we were not able to detect significant alterations in *Snca* levels between the two groups.

A)
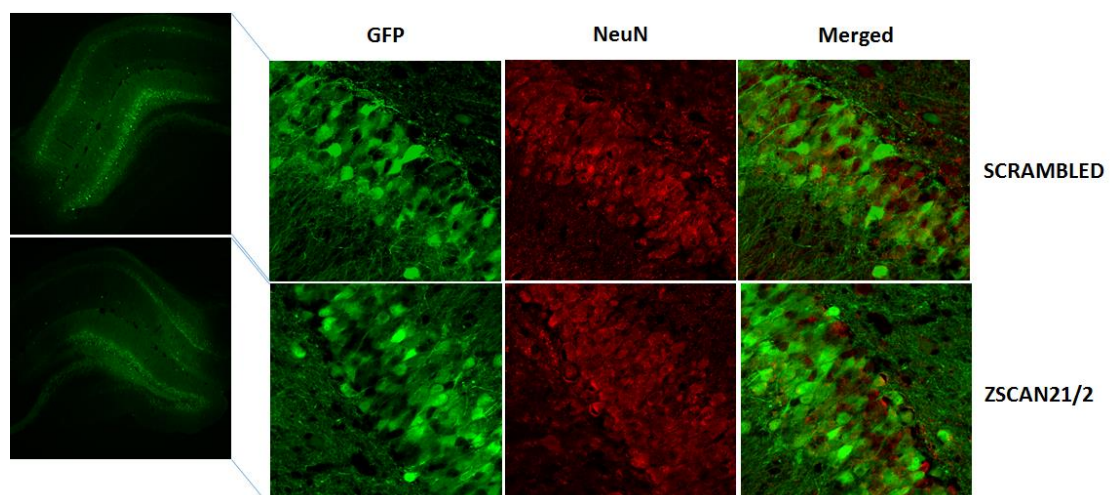
B)
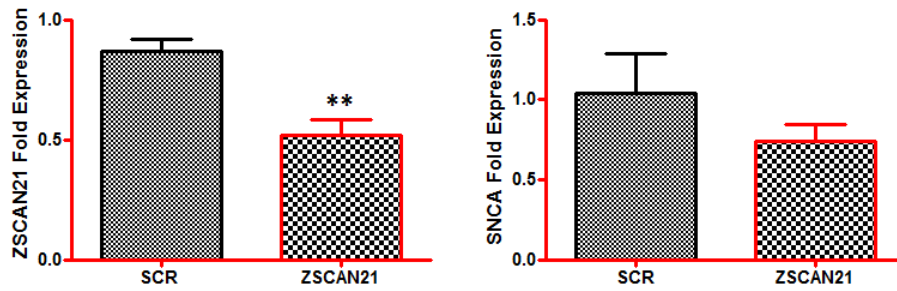
Figure 27. AAV-mediated silencing of *Zscan21* did not alter *Snca* levels in the DG of the hippocampus in adult rat. A) Cryostat-cut sections (20 µm) from 4-month-old rat brains stereotaxically injected with AAV/shZSCAN21 or AAV/shSCRAMBLED (at 2-months of age) were immunolabeled with the NeuN neuronal marker. The Cy3-rb was used as a secondary antibody. The GFP reporter marker of the AAVs demonstrated the efficiency of transduction in both the AAV/shZSCAN21 and AAV/shSCRAMBLED condition. Co-localization of NeuN (red) and GFP (green) was observed in the merged picture. Representative images from the DG of the hippocampus (5×, 63×) via a confocal microscope. B) Quantification of the results from real-time PCR. β-actin, loading control. Results are presented as a mean, ±SEM (n = 5 for AAV/shZSCAN21 and n = 4 for AAV/shscrambled). Statistical analysis was performed via an unpaired t-test. Significant downregulation of *Zscan21* expression (P < 0.01) did not significantly affect *Snca* levels.

4.10 Overexpression of *Zscan21* in cortical neuronal cultures

Since *Zscan21* silencing increased *Snca* at its promoter, mRNA, and protein level in cultured E17 cortical neurons, we were interested in examining whether *Zscan21* overexpression could suppress *Snca* expression. For this purpose, we produced AVs expressing the rat *Zscan21* coding sequence to overexpress *Zscan21* in rat cortical neuronal cultures. AVs, similarly to lentiviruses, have the ability to transduce post-mitotic cells with high efficiency. *Zscan21* coding sequence cloning as well as the AV production are summarized in the Materials and Methods section. We first tested for ZSCAN21 overexpression in HEK293T cells, and indeed, we had a high rate of overexpression (Fig. 28A). Regarding cortical neuronal cultures we detected high efficiency of transduction in the case of the AV/GFP control virus (Fig. 28B). On the contrary, the AV/ZSCAN21 virus does not contain a GFP reporter; therefore, we could not visualize its overexpression directly. Surprisingly, following a western blot assay, we were able to detect only slight ZSCAN21 overexpression that was evident at early time points (24 and 48 h) (Fig. 28D). We tested different MOIs (50-400), but overall, there was no substantiated difference in the ZSCAN21 overexpression profile. For further experiments we chose to work with an MOI of 100 since it gave efficient transduction and conferred no toxicity. Conversely, at the mRNA level, we could detect robust *Zscan21* overexpression starting from an approximately 15-fold difference compared to endogenous levels at the early time point of 24 h, then 10-fold at 48 h, 5-fold at 72 h and lastly 3.5-fold at 5 days. The gradual reduction seen in the overexpressed *Zscan21* mRNA levels over time is expected, due to the episomal nature of the AV expression. Additionally we excluded the possibility that this mRNA overexpression detected with real-time PCR could be attributed to *Zscan21* AV cDNA, as cDNA from OVERZSCAN21 samples had an almost 32-64 fold difference compared to cDNA samples that were not reverse transcribed (negative control). As expected, since ZSCAN21 overexpression was not evident at the protein level, we did not detect any alteration in *Snca* mRNA and protein levels at any of the time points tested.

The fact that *Zscan21* mRNA overexpression is not followed by subsequent ZSCAN21 protein overexpression, suggests that ZSCAN21 protein levels must be under tight regulation either at the post-transcriptional or post-translational level, or perhaps a combination of both.

A)
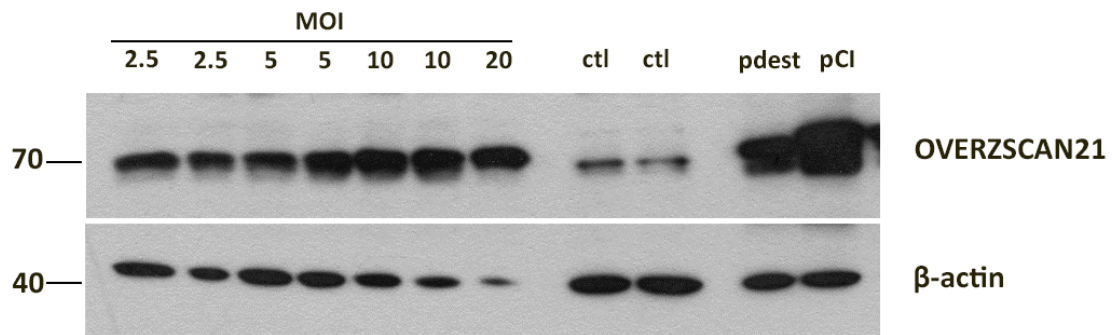
B)
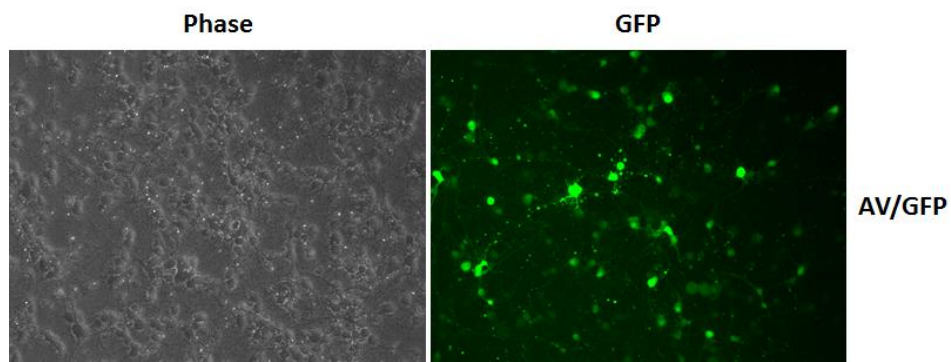
C)
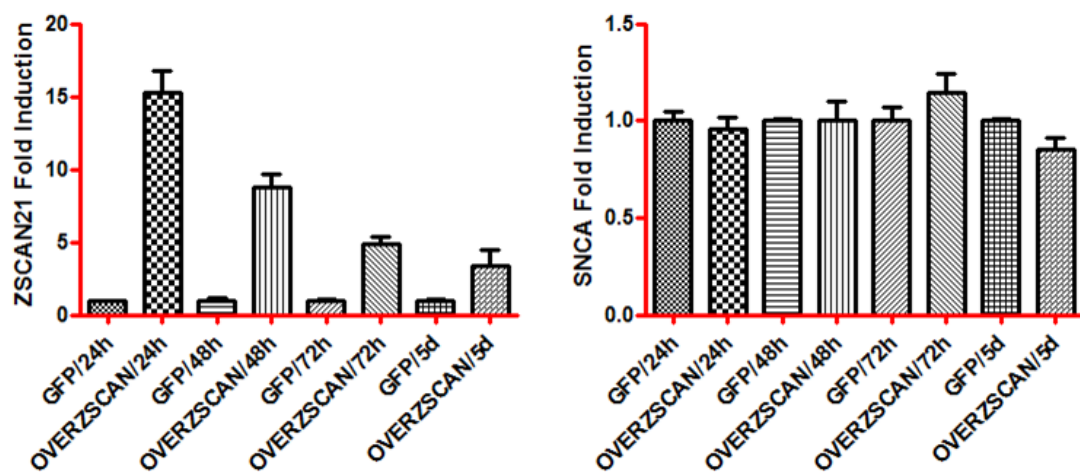
D)
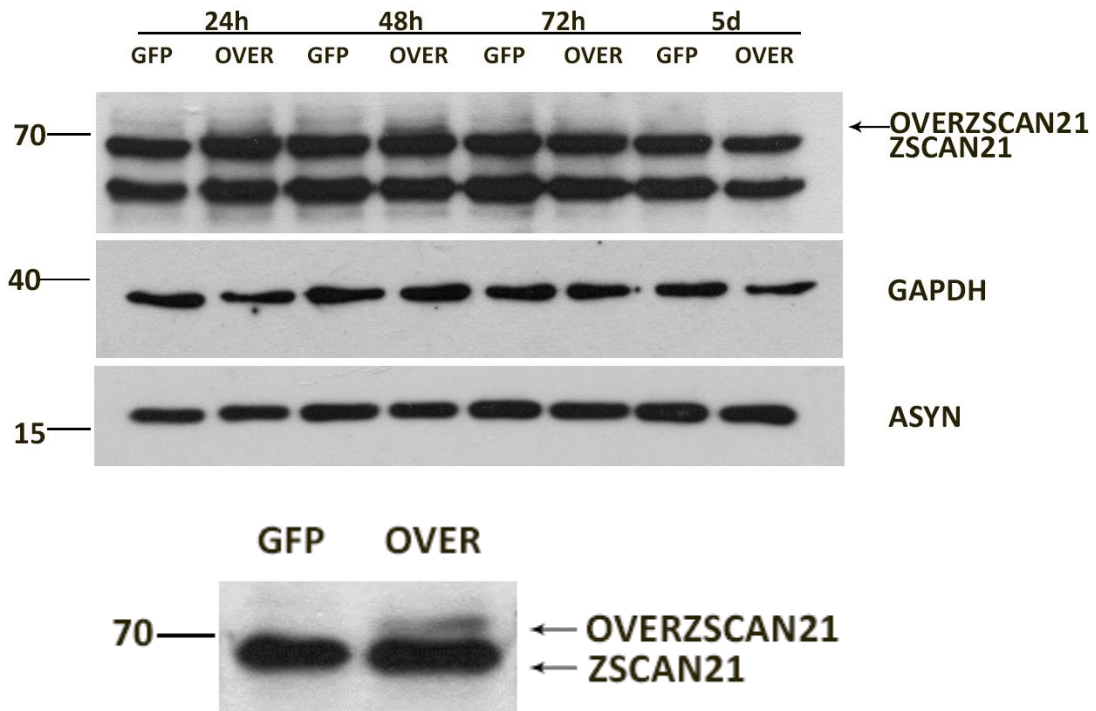
Figure 28. ZSCAN21 protein levels are under tight regulation in rat cortical neuronal cultures. A) HEK293T cells were infected with the AV/OVERZSCAN21 AV at serial MOIs (2.5, 5, 10, and 20) or transfected with the calcium phosphate method with the adenoviral plasmid pDEST / ZSCAN21 (pdest / positive control) and another plasmid overexpressing the murine *Zscan21*, the 3'-FLAG pCI mouse *Zscan21* (pCI / positive control). Uninfected cells were also used as negative control (ctl). Overexpression of ZSCAN21 was evident following infection of HEK293T cells even at the lowest MOI. Cortical neuron cultures were prepared from E17 rats. The neurons were infected at day 4 of their culture with the AV/OVERZSCAN21 or AV/GFP (control) AVs at an MOI of 100. The cultures were collected at different time points (24h, 48h, 72h, and 5 days) and assessed for *Zscan21* and *Snca* mRNA and protein levels with real-time PCR and western blot analysis, respectively. B) Efficiency of transduction of AV/GFP virus in rat cortical cultures (20×). C) Quantification of results from real time PCR (2 experiments). β-actin, loading control. Overexpression of *Zscan21* mRNA was evident at all time points tested. *Snca* mRNA levels remained unaltered. D) Representative western blots: one with all time points and one magnified on the 48 h time point where ZSCAN21 slight overexpression was more evident. This slight overexpression of ZSCAN21 was observed only at early time points (24 h and 48 h), and ZSCAN21 ran slightly higher on the blot compared to endogenous protein, suggesting that overexpressed ZSCAN21 is possibly subjected to post-translational modifications.

4.11 Another target for silencing *Zscan21* (shZSCAN21/4) strongly reduced *Snca* expression in rat cortical cultures.

From the above experiments it was evident that *Zscan21* downregulation with 2 shRNA targets leads to increased ASYN levels at both the mRNA and protein level in cortical neuron cultures. In parallel we also used another shZSCAN21 target, shZSCAN21/4. This target was able to downregulate *Zscan21* expression in rat cortical cultures as efficiently as the other two targets. In contrast though, we noticed that the expression levels of ASYN instead of being increased like the other two targets, were significantly decreased both at the mRNA and protein level (Fig. 29B, C). Notably, ASYN protein was almost completely depleted (Fig 29C). *SNCA* transcriptional activity, measured through luciferase assays based on the 1.9- and 10.7-kb constructs, was also significantly decreased (Fig 29D).

A)
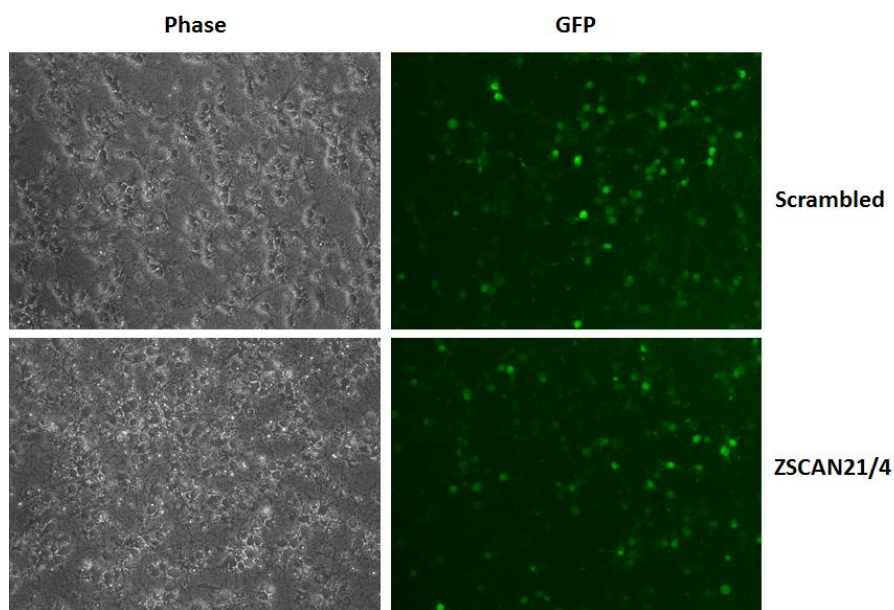
B)
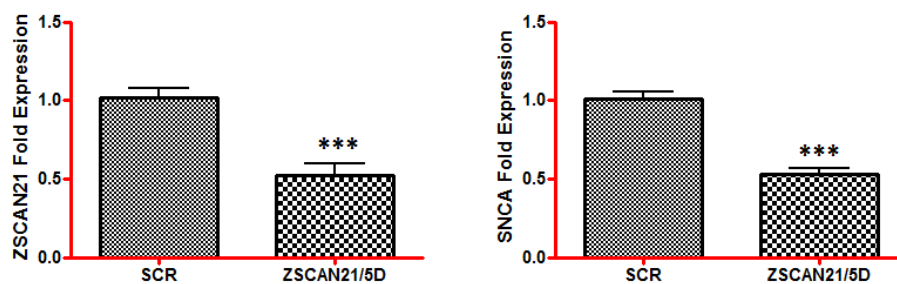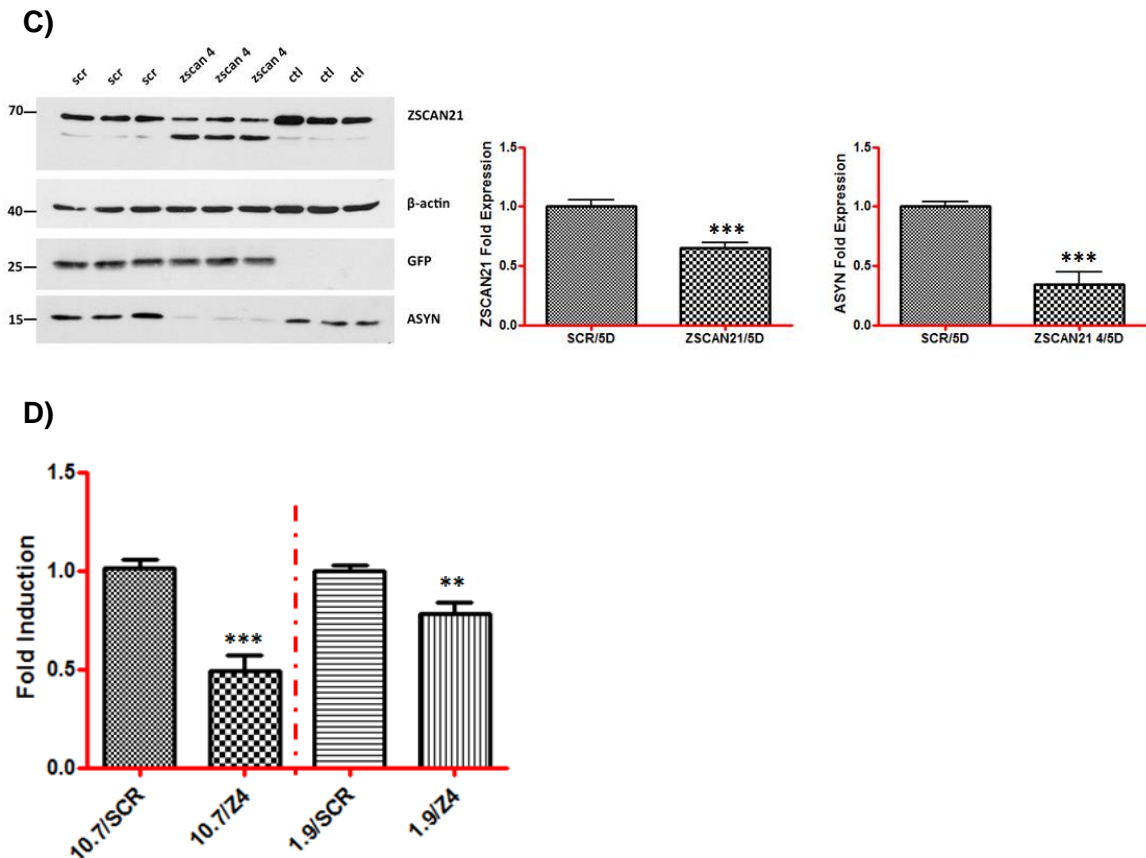
Figure 29 ASYN is significantly decreased following *Zscan21* downregulation with shZSCAN21/4 in rat cortical cultures. Cortical cultures were prepared from E17 rats. The neurons were infected at day 4 of their culture with shZSCAN21/4 or shscrambled (control) lentiviruses, at an MOI of 1. At 5 days post-infection, the cultures were assessed for ZSCAN21 and ASYN mRNA and protein expression with real-time PCR and western blotting, respectively, or at 3 days post-infection the cultures were transfected with the 10.7 -kb, 1.9-kb, intron 1, and pGL3 basic -empty vector luciferase constructs. At 48 h post-transfection, the cells were lysed and assessed for the luciferase assay A) Efficiency of transduction (20×). B) Quantification of mRNA results from 4 independent experiments performed in triplicate. Results are presented as a mean, ±SEM (n = 12). Statistical analysis was performed via an unpaired t-test. Downregulation of *Zscan21* led to a statistically significant decrease of *Snca* expression (P < 0.0001). β-actin, loading control C) Western blot analysis and quantification of results from 3 independent experiments performed in triplicate. Results are presented as a mean, ±SEM (n = 9). Statistical analysis was performed via an unpaired t-test. Downregulation of *Zscan21* led to a statistically significant decrease of ASYN expression (P < 0.0001) in rat embryonic hippocampal cultures. β-actin, loading control. D) Quantification of results from 3 independent experiments performed in duplicate for 1.9-kb and 10.7-kb constructs. Results are presented as a mean, ±SEM (n = 6). Statistical analysis was performed via an unpaired t-test. Significant reduction in the luciferase assay following *Zscan21* downregulation compared to scrambled (fold induction set as 1 for each construct) for the 1.9-kb (P < 0.01) and 10.7-kb (P < 0.001) constructs.

Interestingly, in addition to the downregulation of ZSCAN21, we also observed an increase of another band below ZSCAN21 in western blot analysis. This band in the experiments with the shZSCAN21/2 target was either decreased or unchanged. Therefore, we wondered whether this band that was detected with the ZSCAN21 polyclonal antibody (GenScript) and was increased in the case of shZSCAN21/4, could potentially play a role in the observed downregulation of *Snca*. The predominant scenario that we wanted to test was whether this protein represents a truncated ZSCAN21 protein that arises from alternative splicing of the basic *Zscan21* mRNA product. In that case, this putative alternative splicing product could be increased in a compensatory manner to the downregulation of ZSCAN21 and further decrease *Snca* expression. Supporting evidence towards this hypothesis was the fact that shZSCAN21/4 binds more 3' to the last exon (exon 4) of *Zscan21* mRNA compared to shZSCAN21/2 and shZSCAN21/1. Additionally, the protein that would result from that difference matches the size of the other band in the western blot with the ZSCAN21 GenScript antibody. Conversely, with the Santa Cruz ZSCAN21 antibody, we were unable to detect the second band, but since this antibody recognizes an epitope more 3' in the ZSCAN21 protein than the GenScript antibody, it is possible that it may not target the putative truncated ZSCAN21 protein. Therefore, in order to shed more light on this assumption we decided to utilize the 3' RACE assay.

A)

gi|219273450|ref|NM_001012021.2| *Rattus norvegicus* **zinc finger and SCAN domain containing 21 (*Zscan21*), mRNA**

```
ATGACCAAGGTGGTGGGGCATGGCCACAGTTCTGGGCCCCAGGCCACCTCAGGAGTCTATGGGACCTTCGCCCATTAAAGTTGAAGAGGATGAAGAAAAAGAC
AAGTGCCGCCCTAGCCTAGAGCTATCCCGAAAGCGCTTCAGGCAGTCTAGAAACCAGGACACTCTTGAGCCAATGGGACCTTCAACCATTAAAGCTGAAGAGG
AGGAAGACAAGGACAAGGGCCACCCTAGCCTAGAGCTATCCCGTAAGAGCTTCAAGCAGTTTGGGTACCATGACACTTTGGAACAGTTGGGACCTTCGACTGT
TAAAGCTGAAGAGGATGAAGAGAAGGACAAGGGCCGCCCTAGCCTAGAGATATCCCGTCAGCGCTTCAGGCAGTTTGGGTACCATGACACTCCTGGGCCCCG
AGAGGCACTGAGCCAGCTTCGGGTGCTCTGCTGTGAGTGGCTACAGCCTGAGATCCACACCAAGGAGCAGATTCTAGAGCTACTGGTTCTGGAGCAGTTCCTG
ACCATCCTGCCCCGAGAGCTCCAGGCCTGGGTACAGCAGCACTGCCCTGAGAGTGCAGAGGAGGCCGTCACTCTCCTGGAAGACCTGGAGCAAGAACTGGAT
GAGCCTGGACTGCAGGTCTCATCTCCAAATGAACAGAAGCAGTCTTGGGAGAAAATATCAACTTCAGGAACTGCAATGGAGTCCTTAAGCAGCACTGAGACCC
AGCCTGTGGAT GCCAGCCCTAAATATGAGTTT TGGGGGCCCCTGTACATCCAAGAGACTGGTGAAGAGGAGGTTTTCACTCAGGACCCAAGAAAGCGCCAAG
GTTTTAAATTGAATCCGCAGAAGGAGGACTCAGCAGATGAGCAGAGAAGTTCTGAAGAAGAGTCTCATGCAGGTGGACTCAAAAGAAACATCATGCCCATGAT
CACTGCCAATAAGTATGGATCGAGGTCAGAAAGGCAGTGGGCCAACAACCTGGAAAGGGAGAGAGGGGCAAAAGCCTCTCTTCAAGACACGGGATCCAGGA
AAGGGGCAGAACCAGCGTCTGCTAGGCCTGCTCCAGGAGAGAAACGTTACATATGTGCAGAGTGTGGGAAGGCCTTTAGCAATAGCTCAAACCTCACTAAACA
CCGGAGAACACACACTGGGGAGAAGCCTTACGTGTGCACCAAGTGTGGGAAGGCTTTCAGCCACA GCTCCAACCTTACCCTTCATT ACCGGACACATCTGGTG
GACCGGCCCTATGACTGTAAGTGTGGGAAAGCCTTTGGGCAGAGCTCAGACCTCCTTAAACATCAGAGGATGCACACAGAAGAGGCGCCCTATCAGTGTAAAG
ACTGTGGGAAAGCCTTCAGTGGGAAGGGCAGCCTCATTCGACACTATCGCATCCACACAGGGGAGAAGCCCTATCAGTGCAATGAGTGTGGAAAGAGTTTTA
GTCAGCATGCAGGTCTCAGTTCCCATCAACGCCTGCATACAGGGGAGAAACCCTATAA GTGTAAGGAGTGTGGCAAAGC CTTCAACCATAGTTCGAATTTTAAT
AAGCATCACAGAATCCATACTGGTGAAAAACCCTATTGGTGTAACCACTGTGGGAAAACCTTCTGTAGCAAGTCAAATCTTTCCAAGCATCAGAGAGTCCACAC
TGGAGAGGGAGAGGTACAG TAA
```

B)

RAT ZSCAN21 AMINO ACID SEQUENCE

```
MTKVVGMATVLGPRPPQESMGPSPIKVEEDEEKDKCRPSLELSRKRFRQSRNQDTLEPMGPSTIKAEEEEDKDKGHPSLELSRKSFKQFGYHDTLEQLGPSTVKAEEDEE
KDKGRPSLEISRQRFRQFGYHDTPGPREALSQLRVLCCEWLQPEIHTKEQILELLVLEQFLTILPRELQAWVQQHCPESAEEAVTLLEDLEQELDEPGLQVSSPNEQKQSW
EKISTSGTAMESLSSTETQPVDASPKYEFWGPLYIQETGEEEVFTQDPRKRQGFKLNPQKEDSADEQRSSEEESHAGGLKRNIMPMITANKYGSRSERQWANNLERER
GAKASLQDTGSRKGAEPASARPAPGEKRYICAECGKAFSNS SNLTKHRRTHTGEKPY VCTKCGKAFSHS SNLTLHYRTHLVDRPYDCKCGKAFGQSSDLLKHQRMHTEE
APYQCKDCGKAFSGKGSLIRHYRIHTGE KPYQCNECGKSFSQHAGLSSHQRLHTGEKPYKCKECGKAFNHSSNFNKHHRIHTGEKPYWCNHCGKTFCSKSNLSKHQRV
HTGEGEVQ
```

Figure 30. *Zscan21* shRNAs and GenScript antibody target sites. A) *Zscan21* mRNA coding sequence. The translation start site (ATG) and end site (TAA) are highlighted in gray. The shZSCAN21/1, shZSCAN21/2, and shZSCAN21/4 target sites are highlighted with yellow, purple, and green, respectively. B) ZSCAN21 protein sequence. The antigen recognition site for the ZSCAN21 GenScript and ZSCAN21 Santa Cruz antibodies are denoted in red and blue, respectively.

4.12 3' Rapid amplification of cDNA ends of *Zscan21*

As aforementioned, we wanted to test the scenario of an alternatively spliced *Zscan21* variant that could explain the discrepancy observed in *Snca* expression following *Zscan21* downregulation with the two different shRNA targets (shZSCAN21/2 and shZSCAN21/4). Therefore, we performed 3' RACE. In general, RACE is a procedure for the amplification of nucleic acid sequences from a messenger RNA template between a defined internal site and either the 3' or the 5' end of the mRNA. Specifically, 3' RACE takes advantage of the natural poly(A) tail found in mRNA as a generic priming site for PCR, thus, mRNAs are converted into cDNA using reverse transcriptase and an oligo-dT adapter primer that also bears a unique sequence in its 5' region that does not target any known sequence in the genome; here, the rat genome. Specific cDNA is then amplified by PCR using a GSP that anneals to exon sequences and a reverse UAP that contains only the unique sequence of the oligo-dT adapter primer. This permits the capture of unknown 3' mRNA sequences that lie between the exon and the poly (A) tail. These unknown 3' mRNA sequences can be visualized in an agarose gel and further evaluated by sequencing.

We used 2 GSPs termed GSP and 2ndGSP for *Zscan21* in exon 4 around the binding site of the first shRNA target (shZSCAN21/2), in order to be certain of the specificity of the result. We extracted total RNA from cortical cultures in naïve conditions (CTL) or infected with the shZSCAN21/4 lentivirus (Z4). In the second condition, if our hypothesis regarding the presence of an alternative splicing variant of *Zscan21* was true, we should detect a PCR product smaller in length and increased in expression compared to CTL. Accordingly, as demonstrated in the gel below (Fig. 31), there was a predominant band detected at approximately 900 and 1000 bp for GSP/UAP and 2nd GSP/UAP, respectively, which matches the size expected for the basic transcript. Moreover, we observed a significant downregulation in the Z4 condition both for the GSP/UAP and 2nd GSP/UAP primer sets at this molecular weight compared to CTL. In addition, the difference between the GSP and 2ndGSP PCR product was approximately 100 bp. Additionally, we noticed in the Z4 condition, both for the GSP/UAP and 2nd GSP/UAP primer sets a band with increased intensity compared to CTL that was lower in the gel, which could possibly represent the hypothetical alternatively spliced variant of *Zscan21*. Therefore, we gel extracted these bands and sent for sequencing the intense bands that represent the basic *Zscan21* transcript from CTL samples and the bands that might represent the putative alternative *Zscan21* transcript from Z4 samples, from both the GSP/UAP and 2nd GSP/UAP conditions. From the sequencing reaction, we had a 100% positive match for the basic *Zscan21* transcript in both the GSP/UAP and 2nd GSP/UAP conditions, whereas we had a match for the transmembrane mRNA tetraspanin for the putative *Zscan21* alternative

transcript band. To eliminate the possibility of contamination with other non-specific products in the case of the putative *Zscan21* alternative transcript PCR product (the bands were more faint), we further cloned the PCR product from the 2nd GSP/UAP Z4 condition (the band was more evident and tight than the band in the GSP/UAP) in the TOPO-TA vector and assessed different clones with sequencing. Again, the sequencing result was positive in most cases for tetraspanin mRNA and in one case for phosphoglucomutase 1 mRNA. Therefore, *Zscan21* does not seem to be alternative spliced, at least not in the 3' region of exon 4 that we examined. One explanation for the shZSCAN21/4 target could be that it might mediate an off-target effect on another molecule that in turn mediates the reduction of *Snca* expression. shRNA interference can reportedly disturb endogenous microRNA biogenesis, which again can result in off-target effects (Pan, de Ruiter et al. 2011). Alternatively, the lower band recognized by the ZSCAN21 antibody may represent a perhaps closely related cross-reacting protein that may also have modulatory effects on *Snca* regulation.

A)

gi|219273450|ref|NM_001012021.2| *Rattus norvegicus* **zinc finger and SCAN domain containing 21 (*Zscan21*), mRNA**

CCGGTTGTGCTATGGTTCAGCCGCTGTGAGGATTCCAGACTCCAAAGCGGTTCTGAGTCACGGTGAGCCTGCGAGTCCCAGGTTTGGAGTGTGGCACTTTAAGAA
CCAGAAACCCAAAGGCTCCAGGCCTACTCCTAAGAGTCCTGCTGGTTCTGGAGTCTGTGTCATGACCAAGGTGGTGGGCATGGCCACAGTTCTGGGCCCCAGGCC
ACCTCAGGAGTCTATGGGACCTTCGCCCATTAAAGTTGAAGAGGATGAAGAAAAAGACAAGTGCCGCCCTAGCCTAGAGCTATCCCGAAAGCGCTTCAGGCAGT
CTAGAAACCAGGACACTCTTGAGCCAATGGGACCTTCAACCATTAAAGCTGAAGAGGAGGAAGACAAGGACAAGGGCCACCCTAGCCTAGAGCTATCCCGTAAG
AGCTTCAAGCAGTTTGGGTACCATGACACTTTGGAACAGTTGGGACCTTCGACTGTTAAAGCTGAAGAGGATGAAGAGAAGGACAAGGGCCGCCCTAGCCTAGA
GATATCCCGTCAGCGCTTCAGGCAGTTTGGGTACCATGACACTCCTGGGCCCCGAGAGGCACTGAGCCAGCTTCGGGTGCTCTGCTGTGAGTGGCTACAGCCTGA
GATCCACACCAAGGAGCAGATTCTAGAGCTACTGGTTCGGAGCAGTTCCTGACCATCCTGCCCCGAGAGCTCCAGGCCTGGGTACAGCAGCACTGCCCTGAGA
GTGCAGAGGAGGCCGTCACTCTCCTGGAAGACCTGGAGCAAGAACTGGATGAGCCTGGACTGCAGGTCTCATCTCCAAATGAACAGAAGCAGTCTTGGGAGAA
AATATCAACTTCAGGAACTGCAATGGAGTCCTTAAGCAGCACTGAGACCCAGCCTGTGGATGCCAGCCCTAAATATGAGTTTTGGGGGCCCCTGTACATCCAAGA
GACTGGTGAAGAGGAGGTTTTCACTCAGGACCCAAGAAAGCGCCAAGGTTTTAAATTGAATCCGCAGAAGGAGGACTCAGCAGATGAGCAGAGAAGTTCTGAA
GAAGAGTCTCATGCAGGTGGACTCAAAAGAAACATCATGCCCATGATCACTGCCAATAAGTATGGATCGAGGTCAGAAAGGCAGTGGGCCAACAACCTGGAAA
GGGAGAGAGGGGCAAAAGCCTCTCTTCAAGACACGGGATCCAGGAAAGGGGCAGAAC<mark>CAGCGTCTGCTAGGCCTGCTCCAGGAGA</mark>GAAACGTTACATATGTGC
AGAGTGTGGGAAGGCCTTTAGCAATAGCTCAAACCTCACTAAACACCGGAGAACACACACTGGGGAGAAGCCTTACGTGTGCACCAAGTG<mark>TGGGAAGGCTTTCA
GCCACAGCTCCAAC</mark>CTTACCCTTCATTACCGGACACATCTGGTGGACCGGCCCTATGACTGTAAGTGTGGGAAAGCCTTTGGGCAGAGCTCAGACCTCCTTAAACA
TCAGAGGATGCACACAGAAGAGGCGCCCTATCAGTGTAAAGACTGTGGGAAAGCCTTCAGTGGGAAGGGCAGCCTCATTCGACACTATCGCATCCACACAGGG
GAGAAGCCCTATCAGTGCAATGAGTGTGGAAAGAGTTTTAGTCAGCATGCAGGTCTCAGTTCCCATCAACGCCTGCATACAGGGGAGAAACCCTATAAGTGTAA
GGAGTGTGGCAAAGCCTTCAACCATAGTTCGAATTTTAATAAGCATCACAGAATCCATACTGGTGAAAAACCCTATTGGTGTAACCACTGTGGGAAAACCTTCTGT
AGCAAGTCAAATCTTTCCAAGCATCAGAGAGTCCACACTGGAGAGGGAGAGGTACAG<mark>TAA</mark>GTGTCCATTTCTGTCTGTTGTTATTGTTGTAAACGTTAGAATGTG
AATGCTAGGAAGAAGCTCTGTAATGCATTTCATGTTTGATAGTAGGTTTGGCTCTAGTCATCGAGGGGTGCCTTGGAGGGAGAGCTCCACAGCAATAGAGTAGA
CAAGAGAGGTCTACAGAGCAGCCGGGAGCTCCACACTGGTCACCTCTACCAGCAGGGTCCCTCCTCACACTCCAGGCTCCAGTGTACTGTGTGTCCAGTATAGTT
AAGGAAGAGACATTAAAATTGTTTAACTGTTTTAACATGTATTCCACAGTTGTAGTTTGTAAAGAATTGAGCCACCTTGAACAGTCTGATTCAGAATAAACGTATA
GCATCATGTAAAAAAAAAAAAAAAAAAAA

B)
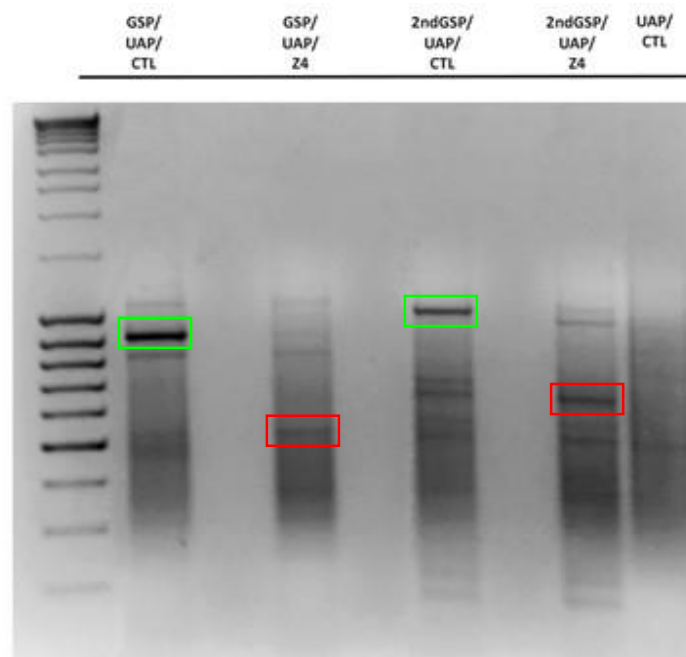
Figure 31. 3' RACE for *Zscan21*. A) Rat *Zscan21* mRNA sequence as well as the positions of the GSP (green) and 2ndGSP (blue) primers. TAA in gray is the stop codon and the remaining 3' area is the 3'UTR that ends at the poly (A) tail. B) The 3' RACE PCR products in an agarose gel; the basic *Zscan21* transcript is denoted by a green box for GSP/UAP (~900 bp) and 2ndGSP/UAP (~1000 bp) in the CTL condition and the putative *Zscan21* alternative transcript is denoted by a red box for GSP/UAP (~550 bp) and 2ndGSP/UAP (~650 bp) in the Z4 condition.

4.13 Genomic analysis of the intron 1 region in PD patients and control samples.

Previous and current work in our laboratory has established the intron 1 region of the *SNCA* gene locus and by extent the ZSCAN21 as key regulatory elements of *Snca* transcription in the PC12 cell line as well as in primary neurons. Therefore, it is plausible that polymorphisms within intron 1, and more specifically, in the ZSCAN21 binding site could potentially be correlated with PD susceptibility. In order to address this issue, we collected and screened DNA samples from PD and control subjects for SNPs following sequencing analysis of part of intron 1. We screened approximately 200 DNA samples from PD and control patients in collaboration with Professor Thomas Gasser (Tubingen University). The sequenced intron 1 region included the two putative ZSCAN21 binding sites, the GATA-2 binding site (Scherzer, Grass et al. 2008) and the CpG methylated islands (Jowaed, Schmitt et al. 2010) (Fig. 32A). Regarding the ZSCAN21 first binding site that we chose to focus mainly on in the present study, only one rare variant was identified that nonetheless had the same incidence in the PD and control samples. Likewise, several common and rare variants were detected in the sequenced area of intron 1 that also exhibited no difference in incidence between the PD and control samples (Fig. 32 B).

A)

SNCA INTRON 1

```
GCTGCAGGGAAAGCAGCGAGCGCCGGGAGAGGGGCGGGCAGAAGCGCTGACAAATCAGCGGTGGGGGCGGAGAGCCGAGGAGAAGGAGAAGGAGGAGGAC
TAGGAGGAGGAGGACGGCGACGACCAGAAGGGGCCCAAGAGAGGGGGCGAGCGACCGAGCGCCGCGACGCGGAAGTGAGGTGCGTGCGGGCTGCAGCGCA
GACCCCGGCCCGGCCCCTCCGAGAGCGTCCTGGGCGCTCCCTCACGCCTTGCCTTCAAGCCTTCTGCCTTTCCACCCTCGTGACGGAGAACTGGGAGTG
GCCATTCGACGACAGGTTAGCGGGTTTGCCTCCCACTCCCCCAGCCTCGCGTCGCCGGCTCACAGCGGCCTCCTCTGGGGACAGTCCCCCCCGGGTGCCG
CCTCCGCCCTTCCTGTGCGCTCCTTTTCCTTCTTCTTTCCTATTAAATATTATTTGGGAATTGTTTAAATTTTTTTTTTTAAAAAAAGAGAGAGGCGGGGA
GGAGTCGGAGTTGTGGAGAAGCAGAGGGACTCAGGTAAGTACCTGTGGATCTAAACGGGCGTCTTTGGAAATCCTGGAGAACGCCGGATGGGAGACGAAT
GGTCGTGGGCACCGGGAGGGGGTGGTGCTGCCATGAGGACCCGCTGGGCCAGGTCTCTGGGAGGTGAGTACTTGTCCCTTTGGGGAGCCTAAGGAAAGAG
ACTTGACCTGGCTTTCGTCCTGCTTCTGATATTCCCTTCTCCACAAGGGCTGAGAGATTAGGCTGCTTCTCCGGGATCCGCTTTTCCCCGGGAAACGCGA
GGATGCTCCATGGAGCGTGAGCATCCAACTTTTCTCTCACATAAAATCTGTCTGCCCGCTCTCTTGGTTTTTCTCTGTAAAGTAAGCAAGCTGCGTTTGG
CAAATAATGAAATGGAAGTGCAAGGAGGCCAAGTCAACAGGTGGTAACGGGTTAACAAGTGCTGGCGCGGGGTCCGCTAGGGTGGAGGCTGAGAACGCCC
CCTCGGGTGGCTGGCGCGGGGTTGGAGACGGCCCGCGAGTGTGAGCGGCGCCTGCTCAGGGTAGATAGCTGAGGGCGGGGGTGGATGTTGGATGGATTAG
AACCATCACACTTGGGCCTGCTGTTTGCCTGAGTTTGAACCACACCCCGAGTGAGCAGTTAGTTCTGTTGCCTACGCCTTTCCACCATCAACCTGTTAGC
CTTCTTCTGGGATTCATGTTAAGGATACCCCTGACCCTAAGCCTCCAGCTTCCATGCTTCTAACTCATACTGTTACCCTTTAGACCCCGGGAATTTAAAA
AAGGGGTTAATCTTTTCATGCAACTCCACTTCTGAAATGCAGTAATAACAACTCAGAGGATTCATCCTAATCCGTGGTTAGGTGGCTAGACTTTTACTAG
CCAAGATGGATGGGAGATGCTAAATTTTTAATGCCAGAGCTAAAAATGTCTGCTTTGTCCAATGGTTAAATGAGTGTACACTTAAAAGAGTCTCACACTT
TGGAGGGTTTCTCATGATTTTTCAGTGTTTTTTGTTTATTTTTCCCCGAAAGTTCTCATTCAAAGTGTATTTTATGTTTTCCAGTGTGGTGTAAAGGAAT
TCATTAG
```

B)

DNA change (hg	rs ID	genotypes controls			genotypes PD			MAF con	MAF PD	HWE contr	p allelic	p TREND	p rec (carri
90758009G>T		189	1	0	193	1	0	0,26%	0,26%	0,971	1,000	0,988	0,988
90757885C>G		188	3	0	195	3	0	0,79%	0,76%	0,913	1,000	0,965	0,965
90757845G>A	rs2619362	96	77	19	94	88	18	29,95%	31,00%	0,540	0,749	0,750	0,552
90757840A>G	rs2245801	113	70	9	129	64	7	22,92%	19,50%	0,658	0,242	0,236	0,250
90757805T>C		190	2	0	198	1	0	0,52%	0,25%	0,942	0,652	0,541	0,541
90757735G>T	rs2619361	99	73	19	96	86	18	29,06%	30,50%	0,313	0,659	0,664	0,449
90757636G>C		192	0	0	200	1	0	0,00%	0,25%	NA	1,000	0,328	0,328
90757505A>G	rs1372520	110	72	10	125	68	7	23,96%	20,50%	0,686	0,244	0,236	0,293
90757394C>G	rs3756063	53	100	39	54	100	46	46,35%	48,00%	0,513	0,644	0,640	0,893
90757312G>A	rs2870027	181	11	0	183	15	1	2,86%	4,27%	0,683	0,290	0,299	0,368
90757310C>T		191	1	0	198	1	0	0,26%	0,25%	0,971	1,000	0,980	0,980
90757309T>C	rs1372519	111	70	10	124	67	8	23,56%	20,85%	0,809	0,363	0,359	0,397
90757294T>G	rs1372518	111	72	8	119	68	12	23,04%	23,12%	0,383	0,979	0,979	0,735

total cohort	controls	PD
N	197	204
%female	57,87%	46,57%

Fig 32. SNPs in the intron 1 region of *SNCA* in PD and control samples. A) Regulatory elements of *SNCA* intron 1. The boundaries of the area sequenced are highlighted in red. The start and end of *SNCA* intron 1 region are highlighted in yellow. The two putative ZSCAN21 binding sites are indicated in purple, the GATA-2 putative binding site in green and the CpG islands are included in the area highlighted in blue. B) In total, 197 control and 204 PD samples were screened for putative SNPs in intron 1 of *SNCA* that could confer PD risk. The first column demonstrates the variants that were identified. (rs) stands for common variants, whereas the other represent rare polymorphisms. We have highlighted the polymorphism in the ZSCAN21 binding site in green and the numbers of individuals that carried this polymorphism in control and PD samples are indicated with red boxes. Three individuals shared the polymorphism in the ZSCAN21 binding site in the control and PD group; thus no correlation with PD was identified for polymorphism. Regarding the rest of the intron 1 region, no correlation with PD was achieved for the common and rare variants. The small table demonstrates the total number of PD and control samples tested as well as the percentage of females in each group.

5. DISCUSSION

Although *SNCA* levels play a critical role in familial and sporadic PD, and potentially in other neurodegenerative conditions, and under normal conditions in the control of synaptic neurotransmission, the mechanisms that regulate *SNCA* transcription are not well understood. Previous experiments in our laboratory mainly used the model system of PC12 cells to examine such mechanisms. This stemmed from our original observation that SNCA mRNA and protein levels increase following treatment with growth factors (NGF and bFGF) in this system, in parallel to the well-known phenomenon of induced neuronal differentiation (Stefanis, Kholodilov et al. 2001). In this earlier work, we found that cultured cortical neurons also showed marked *Snca* induction with maturation in culture, mimicking a phenomenon observed during development (Rideout, Dietrich et al. 2003).

In particular, in PC12 cells, we were able to map out the signaling pathways and transcriptional elements involved in NGF and bFGF-mediated *SNCA* induction with the use of varying lengths of human *SNCA* promoter region via luciferase based assays. Briefly, pharmacological and molecular modulation of the ERK and PI3-K signaling pathways inhibited *SNCA* induction, indicating the involvement of these pathways in *SNCA* transcriptional control. Such control was achieved, at least in part, through elements in intron 1 of *SNCA* and, specifically, within its first and third quadrants (Clough and Stefanis 2007). Subsequent work has shown that the element within the first quadrant represents the binding site for the TF ZSCAN21, and that the transcriptional control region is quite complex, involving additional TFs, such as ZNF219 (Clough, Dermentzaki et al. 2009). Specifically, regarding ZSCAN21 it was conclusively shown to be involved in *Snca* regulation since *Zscan21*-mediated down-regulation via RNA interference as well as deletion of its binding site in the intron 1 region significantly suppressed *Snca* levels in (Clough, Dermentzaki et al. 2009).

Most important, previous work in rat cortical cultures revealed important similarities and differences with the PC12 cell line. There were significant differences in activity between constructs of varying length throughout almost the extent of the promoter region, indicating the existence of multiple transcriptional control regions. A basic difference, however, between the PC12 cells and the primary cortical neurons was that in the former case the intron 1 region was sufficient for the induction of *SNCA* transcriptional activity, whereas in the latter both intron 1 and the core promoter were necessary. This finding indicated that these regions contained important regulatory elements that interacted in a different fashion in each system (Clough, Dermentzaki et al. 2011). Differences and similarities were also noted in terms of the biochemical signaling pathways involved. In PC12 cells, the ERK pathway was involved in the transcriptional control of *SNCA* (Clough and Stefanis 2007), but that was not the case in cultured cortical neurons. In contrast, the PI3-K pathway was required in both models for *SNCA* transcriptional activation.

In parallel, further downstream within intron 1, another group has mapped out another important element for *SNCA* transcriptional control, the TF GATA-2 (Scherzer, Grass et al. 2008). Additionally, several studies have reported that *SNCA* intron 1 methylation can modulate *SNCA* expression and most importantly decreased methylation in intron 1 is evident in PD brain and blood specimens compared to healthy controls (Jowaed, Schmitt et al. 2010, Matsumoto, Takuma et al. 2010, Richter, Appenzeller et al. 2012, Wang, Wang et al. 2013, Ai, Xu et al. 2014, Tan, Wu et al. 2014, Pihlstrom, Berge et al. 2015). Besides, a number of conserved non-coding genomic regions in the *SNCA* gene, including the intron 1 region, have been shown to contribute to *SNCA* transcriptional activity (Sterling, Walter et al. 2014). Overall, these data reinforce the importance of the intron 1 regulatory region in the transcriptional control of *SNCA*.

In the present study, we focused on the ZSCAN21 TF and its potential involvement in *Snca* transcription in primary neuronal cultures and *in vivo*. Since ZSCAN21 is an important regulator of *Snca* transcription in differentiated PC12 cells (ZSCAN21-mediated downregulation significantly reduced *Snca* levels), we wished to validate further this scenario for isolated neurons and notably, *in vivo*. Importantly, a study by Yang et. al. (Yang, Wynder et al. 1999) demonstrated no significant phenotypic or functional alterations in *Zscan21*$^{-/-}$ BAC transgenic mice; thus, if *Zscan21* silencing could successfully reduce *Snca* levels *in vivo,* as in PC12 cells, it would not only establish its important role in *Snca* transcription but it could also serve as a potential therapeutic target for PD.

Toward this direction, we first verified ZSCAN21 expression both at the mRNA and protein level in different rat brain areas where ASYN is also present. Interestingly, we noticed that ZSCAN21 (mRNA and protein) is present at high levels developmentally until the P10 stage and then its levels start to decrease, in different brain regions including the cortex and hippocampus. Additionally, we verified the expression of ZSCAN21 in neuronal cells, since ASYN is expressed in neurons. While we were interested in using the *Zscan21*$^{-/-}$ BAC transgenic mice (Yang, Wynder et al. 1999) for our study, unfortunately we were informed that these mice were no longer available due to technical issues. Therefore, we switched direction toward constructing shRNA-expressing lentiviruses against *Zscan21* that could efficiently silence ZSCAN21 in post-mitotic neurons. We utilized the TRC2-pLKO lentivirus vector (Invitrogen), which is used widely to downregulate different proteins in primary cultures as well as *in vivo* systems with high efficacy (Zufferey, Nagy et al. 1997, Zufferey, Dull et al. 1998, Stewart, Dykxhoorn et al. 2003, Moffat, Grueneberg et al. 2006, Yamamoto and Tsunetsugu-Yokota 2008). We constructed 3 lentiviruses against *Zscan21* (shZSCAN21/1, shZSCAN21/2, and shZSCAN21/4) as well as scrambled (control virus) that targets no known sequence in the rat genome. We found that significant downregulation of ZSCAN21 at the mRNA and protein level (for shZSCAN21/1 and shZSCAN21/2 target), surprisingly led to an increase of ASYN expression at both the mRNA and protein level, the opposite expression pattern to that observed in differentiated PC12 cells. Similar results were obtained from primary hippocampal cultures, thus further validating the specificity of the result. In the same way, *Zscan21* silencing was also found to further increase the activity of the 1.9-kb *SNCA* promoter construct in the luciferase assay compared to scrambled conditions. It should be noted

here that the third lenti-shRNA targeted against *Zscan21*, shZSCAN21/4, gave an opposite profile to the others, most likely due to off-target effects, although the possibility of the compensatory upregulation of an alternate *Zscan21* transcript could not be discarded completely, despite the negative results with the 3' RACE analysis. Therefore, *Zscan21* silencing leads to increased *SNCA* promoter transcriptional activity that subsequently results in elevated ASYN mRNA and protein levels in rat primary neuronal cultures. As already mentioned, rat cortical cultures and PC12 cells share important differences in the transcriptional activity of different *SNCA* promoter constructs, with the most basic one being that the 5' of exon 1 (core promoter) and intron 1 regions act synergistically in primary cultures (1.9-kb construct includes both elements and presents promoter activity), whereas in PC12 cells they elicit activity in isolation (intron 1, core promoter, present promoter activity alone). Therefore, the observed differences in the activity of the *SNCA* promoter constructs between these two cell systems could possibly account for the discrepancy observed in *Snca* levels following *Zscan21* downregulation.

Next, since there was evidence indicating that ZSCAN21 binds to the intron 1 region of *SNCA* in differentiated PC12 cells (Clough, Dermentzaki et al. 2009) and *in vivo* in human brain tissue (Brenner, Wersinger et al. 2015), we performed a CHIP assay for ZSCAN21 in rat cortical neuronal cultures to verify this finding. Indeed we found that the region containing the two putative binding sites for ZSCAN21 was significantly enriched (~15 fold) in the sample that was chromatin-immunoprecipitated with an antibody specific to ZSCAN21 compared to an irrelevant antibody, suggesting that ZSCAN21 either binds directly to the intron 1 region of *Snca* or interacts as a co-factor with a TF that binds to this region. To discriminate further whether ZSCAN21 directly or indirectly regulates *SNCA* transcription, we designed constructs lacking the putative binding sites for ZSCAN21 in the intron 1 area of *SNCA* in isolation as well as in combination. As a template we used the 1.9-kb construct that is highly induced in the luciferase assay in cortical cultures to introduce the binding site deletions. Intriguingly, overall we did not detect any significant alterations between the 1.9 kb construct and the 1.9-kb deletion constructs. Therefore, one explanation is that ZSCAN21 may not directly regulate *SNCA* transcription by binding to its predicted binding sites but rather indirectly as a co-factor. Nonetheless, since the luciferase assay is actually an artificial platform that involves distinct promoter elements, therefore it lacks the whole genomic context and genomic interactions present in the endogenous environment and we cannot exclude the possibility that due to these limitations we are unable to detect any alterations in the luciferase assay in the constructs lacking the ZSCAN21 binding sites.

In parallel, we also studied the role of ZSCAN21 upon *Snca* transcription in neurosphere cultures, since ZSCAN21 is expressed robustly early in development. Neurospheres are free-floating cultures of neural stem cells that can be differentiated toward neurons, astroglia and oligodendroglia by the application of growth factors. In our study we used differentiated cultures, since ASYN was not detected in the proliferating state. At this point we must mention that differentiated neurospheres cultures and cortical cultures are *in vitro* systems that mimic different stages of neuronal development. Neurons in differentiated neurospheres cultures represent early neurons (TUJ1 [+], NeuN [-]) whereas neurons in cortical cultures represent mature post-mitotic

neurons (TUJ1 [+], NeuN [+]). To our surprise, we found that significant silencing of *Zscan21* with both lentiviruses led to decreased levels of ASYN at both the mRNA and protein level, in contrast to the increased ASYN levels in primary neuronal cultures. The inability to perform trustworthy luciferase assays in neurosphere cultures limits the comparison of these cultures with the PC12 and cortical neuron cell culture systems, but, with the available data, it would seem that *Zscan21*-mediated regulation of *Snca* mRNA may be more similar in neurospheres and PC12 cells, where ZSCAN21 silencing also leads to decreased *Snca* expression (Clough, Dermentzaki et al. 2009). This differential *Snca* regulation by ZSCAN21 in the above cell systems could be attributed to different reasons. The most likely scenario is that this difference in *Snca* transcription reflects the different developmental stages that these two systems, cortical neurons and neurosphere cultures, represent. Specifically, it is well known that defined sets of TFs are expressed during development to orchestrate specific regulatory functions and interactions that are distinct to each developmental stage. Additionally, many TFs can act as either activators or repressors of transcription depending on the co-factors associated. ZSCAN21 is known to form homo- and heterodimers with other TFs via its SCAN protein-protein interaction domain (Williams, Blacklow et al. 1999, Carneiro, Silva et al. 2006). In general, ZSCAN21 is associated with positive regulation of transcription (Chowdhury, Goulding et al. 1992). However, recent data from affinity capture mass spectometry and two-hybrid assays (Woods, Mesquita et al. 2012, Rolland, Tasan et al. 2014, Huttlin, Ting et al. 2015) have shown that ZSCAN21 can physical interact with many TFs, being either co-activators or co-repressors. RCOR1 (REST corepressor 1), ZSCAN3, and Zkscan4 are examples of TFs that function as repressors. Therefore, we could posit that ZSCAN21 can either activate or repress a gene target; here *Snca*, depending on the TF associated. Therefore, early in development ZSCAN21 could interact with a co-activator (ZSCAN21 silencing leads to decreased *Snca* levels), while later in development it could interact with a co-repressor (ZSCAN21 silencing leads to increased *Snca* levels) to regulate *Snca*. Moreover, this difference in *Snca* regulation could also be attributed to the type of culture itself, differentiated neurospheres are mixed neural cultures, whereas primary neuronal (cortical and hippocampal) cultures represent more than 95% pure neurons; thus, different cell type interactions could lead to different expression phenotypes.

Regarding the *in vivo* experiments we produced AAVs targeting ZSCAN21 expression. The reason we utilized AAVs over lentiviruses is due to their increased transduction efficacy *in vivo* (with the TRC2-pLKO.1 lentiviruses we were unable to transduce neuronal cells *in vivo*). Specifically, for the AAVs used in the current study, shRNA expression is driven by the synapsin promoter that ensures the selective transduction of neurons. Since we detected an opposite pattern of *Snca* regulation following *Zscan21* downregulation in neurospheres (early neurons / reduced *Snca*) and in primary neuronal cultures (mature neurons / increased *Snca*), we decided to study the role of ZSCAN21 in *Snca* regulation *in vivo* at two different developmental stages, one early post-natal and one young adult. Regarding the early developmental stage, we performed injections targeting the lateral ventricles of P3 rat brain and assessed animals for *Zscan21* and *Snca* mRNA levels at 1-month post-injection. We achieved robust downregulation of *Zscan21* in the case of the AAV/shZSCAN21 treated animals versus to

AAV/shscrambled and ctl (non-transduced population) according to real-time PCR analysis. However, *Snca* levels remained unchanged following *Zscan21* downregulation.

Although we did not observe any significant changes in *Snca* levels following downregulation of *Zscan21* in the early developmental stages of the rat brain where ZSCAN21 is expressed robustly, we further examined whether (in contrast) the low expression levels of ZSCAN21 present in the adult brain are involved in *Snca* transcription. We again performed stereotaxic injections utilizing the above AAVs targeting the DG area of the hippocampus in 2-months-old rats.

The DG of the hippocampus was chosen for different reasons. First, ZSCAN21 is highly and selectively expressed in the granule cells of the DG (Yang, Zhong et al. 1996). Secondly, we observed significant co-localization of ZSCAN21 and ASYN in this region (Figure 5). Additionally, the involvement of the hippocampus in the non-motor symptoms of PD has gained increasing attention. Fatigue and depression have been related to hippocampal serotonergic dysfunction by positron emission tomography with specific metabolites of serotonergic metabolism (Pavese, Metta et al. 2010, Ballanger, Klinger et al. 2012). Besides, the hippocampus is modulated by dopaminergic input from the ventral tegmental area and the olfactory bulb and by noradrenergic input from the locus coeruleus and may thus be involved in drive and mood regulation (Goto and Grace 2005). Cognitive deficits in PD are heterogeneous and may include cholinergic and noradrenergic dysfunction impacting hippocampal functions reviewed in (Kehagia, Barker et al. 2010). The extent of hippocampal LB pathology has also been correlated with the degree of dementia in PD patients (Churchyard and Lees 1997). Significant hippocampal atrophy has been observed on magnetic resonance imaging of patients with PDD when compared to non-demented PD patients reviewed in (Calabresi, Castrioto et al. 2013). Additionally, alterations of hippocampal connectivity by diffusion tensor imaging in PD patients predicted the emergence of declarative memory deficits (Carlesimo, Piras et al. 2012). Notably, selective hyposmia in PD is related to hippocampal and striatal dopamine denervation (Bohnen, Gedela et al. 2008). Therefore, hippocampal dysfunction is common in PD patients and most possibly contributes to different non-motor symptoms of PD. Further, regarding ASYN and hippocampal alterations it has been reported that truncated human ASYN (1-120) on a mouse ASYN null background leads to cognitive alterations before the occurrence of motor abnormalities (Costa, Sgobio et al. 2012). Additionally, hippocampal slices treated with ASYN oligomers have impaired long-term potentiation (Diogenes, Dias et al. 2012). In the same way, preformed fibrils generated from full-length and truncated recombinant ASYN can penetrate hippocampal primary neurons and promote the formation of insoluble PD-like LBs (Volpicelli-Daley, Luk et al. 2011). In an inducible transgenic ASYN mouse model, the abnormal accumulation of ASYN in the hippocampus is associated with cognitive loss and causes synaptic deficits (Lim, Kehm et al. 2011). Importantly, it has also been reported that reduced neurogenesis in the DG could have a crucial role in the pathogenesis of depression and other non-motor symptoms of PD. Accordingly, a study by Kohl et al (Kohl, Winner et al. 2012) reported that the expression of transgenic A53T ASYN in developing DG neurons severely impaired neurogenesis. This body

of work highlights the importance of the hippocampal accumulation of ASYN in the pathogenesis of PD and other synucleinopathies, and suggests that the regulation of SNCA expression in this region may be of critical importance.

In the present study even though we were able to detect significant *Zscan21* downregulation in the hippocampus of AAV/shZSCAN21-injected adult animals compared to AAV/shscrambled, we were unable to detect significant alterations in *Snca* mRNA levels, similarly to the early postnatal stage. This lack of effect in *Snca* levels in both developmental stages possibly indicates the presence of compensatory mechanisms that regulate *Snca* transcription *in vivo*. Additionally, it could also mean that ZSCAN21 might have a role in earlier developmental regulation of *Snca* levels, where ZSCAN21 is expressed robustly, but to examine this will require manipulating ZSCAN21 levels earlier than 1-month. Ideally, this could be achieved with the use of a *Zscan21* knock-out animal that would allow us to assess *Snca* expression throughout development. In contrast, an AAV-driven *Zscan21* silencing approach is limited due to the fact that it requires long intervals (>15 days) for efficient downregulation of the target gene.

Next, since *Zscan21* silencing increased *Snca* levels in rat cortical cultures, we decided to examine further whether *Zscan21* overexpression could suppress *Snca*. For this purpose, we produced AVs expressing rat *Zscan21*. Interestingly, we found that even though we had robust *Zscan21* mRNA overexpression, we could only detect a small amount of ZSCAN21 protein that was only evident at the early time points (24 h and 48 h). However, in parallel, we also tested if ZSCAN21 could be significantly overexpressed at the protein level in HEK293T cells. Therefore, it seemed plausible that *Zscan21* mRNA could be regulated at the post-transcriptional or post-translational level so that its protein levels remain steady. Supporting evidence toward this hypothesis was a study by Yang et al (Yang, Wynder et al. 1999), where BAC transgenic mice overexpressing ZSCAN21 presented increased proliferation and at the same time increased cell death in the internal granule layer of the cerebellum, thus indicating that increased levels of ZSCAN21 can be toxic to neurons, and that neurons, to prevent this, should have its levels under tight control. Additionally, several zinc finger TFs that play important role in proliferation and differentiation during development are known to be under tight post-transcriptional or post-translational control, since deregulation of their expression can lead to pathological phenotypes (Rebollo and Schmitt 2003, Mingot, Vega et al. 2009, Yien and Bieker 2013). ZSCAN21 has a role in the proliferation of progenitor cells in the cerebellum (Yang, Wynder et al. 1999); thus, its levels could also be strictly regulated. To date, post-transcriptional regulation for steady-state protein levels involves many mechanisms, including RNA-binding proteins that play a critical role in RNA nuclear export, mRNA stability, modification, turnover and regulation of the translation process as reviewed in (Glisovic, Bachorik et al. 2008), miRNAs that regulate translational repression or mRNA degradation as reviewed in (Filipowicz, Bhattacharyya et al. 2008, Valinezhad Orang, Safaralizadeh et al. 2014) and epigenetic regulation at the RNA level where mRNA is subjected to chemical modifications that can affect protein expression as reviewed in (Yue, Liu et al. 2015). Conversely, a signal dictating increased protein synthesis (e.g., viral-mediated overexpression of a protein) could also be poised post-

translationally by increased clearance of the overexpressed protein via the proteasome system through ubiquitination as reviewed in (Wang, Pattison et al. 2013). Supporting evidence toward this hypothesis is the fact that the slightly overexpressed ZSCAN21 protein was detected a little higher than the endogenous ZSCAN21 protein on the western blot, indicating that perhaps the overexpressed protein is post-translationally modified with ubiquitin, which subsequently leads to its clearance. However, this needs to be investigated further. It is interesting to note that although the mRNA levels of *Zscan21* remain stable beyond P13, its protein levels continue to fall, especially in adulthood (Fig.15), suggesting that such tight post-transcriptional regulation of ZSCAN21 levels also occurs *in vivo.* Interestingly, a study by Wright et al. (Wright, McHugh et al. 2013) revealed that overexpression of ZSCAN21 was able to significantly reduce *SNCA* levels in SHSY5Y cells. The fact that we could also detect overexpression of ZSCAN21 in another cell line, i.e., HEK293T cells, but not in cortical neuron cultures, suggests that ZSCAN21 protein levels must be selectively under tight regulation in neurons and not in cell lines.

Collectively, our data indicate that ZSCAN21 is a TF diversely involved in the process of SNCA transcriptional regulation dependent upon the neuronal culture system tested (cortical cultures and neurospheres). However, the fact that no alteration of *Snca* levels was evident following ZSCAN21 downregulation *in vivo*, implies that ZSCAN21 is not a main regulator of *Snca* transcription *in vivo*, at least at the developmental stages that were tested. These data imply the presence of alternative or perhaps compensatory mechanisms that regulate SNCA transcription in such settings. In combination with the inability to overexpress ZSCAN21 in post-mitotic neurons, likely due to its strict post-transcriptional / post-translational control, it would appear that, in the context of synucleinopathies, attempts to modulate *SNCA* transcription based on ZSCAN21 manipulation may not be fruitful.

The last part of our study involved the examination of possible alterations in *SNCA* intron 1 sequences that may be involved in PD, given the accumulating evidence from our own laboratory and others regarding the importance of this region in *SNCA* transcriptional control. We were especially interested to see whether the 5' ZSCAN21 binding site we had identified with a regulatory role in *SNCA* transcription in PC12 cells would show genetic variability that could be related to the development of PD. To this end, we sequenced a large part of intron 1, including this ZSCAN21 binding site, in DNA derived from controls and PD patients. Although a number of polymorphic variants were detected, including a rare one within the 5' ZSCAN21 binding site, none were associated with the disease in this cohort. For that reason, we did not further aim to match the remaining common and rare variants with the second ZSCAN21 binding site, the GATA-2 binding site, as well as the CpG islands. Additionally, Brenner et al (Brenner, Wersinger et al. 2015) reported that TFBSs of ZSCAN21 and GATA-2 were not polymorphic by analyzing 300 DNA samples from PD patients. Currently, we are assessing more PD and control samples in order to verify conclusively that the lack of a possible correlation was not due to small sample limitations.

Although further studies are needed, these data collectively suggest that genetic variability within the ZSCAN21 binding sites in intron 1 is not linked to PD pathogenesis. It may be worthwhile to investigate genetic variability within the *ZSCAN21* gene itself and possible links to PD risk; however further evidence regarding the importance of ZSCAN21 in *SNCA* transcriptional control would need to be provided to make this endeavor worthwhile.

At this point we must mention that targeted therapeutic gene modulation is the practice of altering the expression of a gene transcriptionally or post-transcriptionally, with a view to alleviate some form of ailment. Specifically, TF-involved therapeutic strategies for modulating the expression of a gene can be achieved either at the transcriptional level with the use of designer zinc-finger proteins or post-transcriptionally with RNA-interference. In the first case zinc-finger proteins capitalize on the DNA-binding capacity of natural zinc-finger domains to modulate the expression of specific target areas of the genome (Choo, Sanchez-Garcia et al. 1994, Kang and Kim 2000, Carvin, Parr et al. 2003, Snowden, Zhang et al. 2003, Urnov, Miller et al. 2005, Papworth, Kolasinska et al. 2006, Lara, Wang et al. 2012), while in the latter case of RNA-interference, it aims to selectively silence a TF whose levels are implicated in dysregulation (Kim and Rossi 2007, Peer, Park et al. 2008, Darcan-Nicolaisen, Meinicke et al. 2009, de Franca, Mesquita Junior et al. 2010, Rettig and Behlke 2012). In our case, since *Zcscan21*$^{-/-}$ mice (Yang, Wynder et al. 1999) reportedly bear no systematic or phenotypic abnormality, we were keen to test whether ZSCAN21 could regulate *Snca* levels *in vivo*, as in that case, ZSCAN21 could be used as a novel therapeutic approach for modulating *SNCA* levels and possibly even treat PD and/or other synucleinopathies. Nevertheless, despite its significant involvement in regulating *Snca* levels in primary neuronal cells this finding could not be replicated *in vivo*, possibly due to compensatory mechanisms that govern the more complex *in vivo* systems. Therefore, ZSCAN21 is not a main regulator of *Snca in vivo*. Notwithstanding, another hypothesis could be that the transcriptional regulation of *SNCA* in not driven by a master regulator but instead involves a network of interactions between TFs and cis regulatory elements within and around *SNCA*. Supporting evidence toward this scenario is the very complicated transcriptional architecture of the promoter of *SNCA* and the fact that *SNCA* is transcriptionally induced in the luciferase assay in cortical neuronal cultures only when the core promoter and the intron 1 region act synergistically and not in isolation. Therefore, given the complex nature of this control, perhaps strategies aiming at signaling pathways or more directly targeting the specific gene in other regulatory regions involved in *SNCA* transcription would be more worthwhile. Conversely, the basic control of ASYN levels in adulthood occurs post-transcriptionally, as mRNA levels are very low; hence, strategies addressing ASYN clearance may be more fruitful in this setting.

6. REFERENCES

Abbott, R. D., H. Petrovitch, L. R. White, K. H. Masaki, C. M. Tanner, J. D. Curb, A. Grandinetti, P. L. Blanchette, J. S. Popper and G. W. Ross (2001). "Frequency of bowel movements and the future risk of Parkinson's disease." Neurology **57**(3): 456-462.

Adelman, K. and J. T. Lis (2012). "Promoter-proximal pausing of RNA polymerase II: emerging roles in metazoans." Nat Rev Genet **13**(10): 720-731.

Agelopoulos, M., D. J. McKay and R. S. Mann (2012). "Developmental regulation of chromatin conformation by Hox proteins in Drosophila." Cell Rep **1**(4): 350-359.

Ai, S. X., Q. Xu, Y. C. Hu, C. Y. Song, J. F. Guo, L. Shen, C. R. Wang, R. L. Yu, X. X. Yan and B. S. Tang (2014). "Hypomethylation of SNCA in blood of patients with sporadic Parkinson's disease." J Neurol Sci **337**(1-2): 123-128.

Alder, J., N. K. Cho and M. E. Hatten (1996). "Embryonic precursor cells from the rhombic lip are specified to a cerebellar granule neuron identity." Neuron **17**(3): 389-399.

Alim, M. A., M. S. Hossain, K. Arima, K. Takeda, Y. Izumiyama, M. Nakamura, H. Kaji, T. Shinoda, S. Hisanaga and K. Ueda (2002). "Tubulin seeds alpha-synuclein fibril formation." J Biol Chem **277**(3): 2112-2117.

Alim, M. A., Q. L. Ma, K. Takeda, T. Aizawa, M. Matsubara, M. Nakamura, A. Asada, T. Saito, H. Kaji, M. Yoshii, S. Hisanaga and K. Ueda (2004). "Demonstration of a role for alpha-synuclein as a functional microtubule-associated protein." J Alzheimers Dis **6**(4): 435-442; discussion 443-439.

Alvarez-Erviti, L., M. C. Rodriguez-Oroz, J. M. Cooper, C. Caballero, I. Ferrer, J. A. Obeso and A. H. Schapira (2010). "Chaperone-mediated autophagy markers in Parkinson disease brains." Arch Neurol **67**(12): 1464-1472.

Anderson, J. P., D. E. Walker, J. M. Goldstein, R. de Laat, K. Banducci, R. J. Caccavello, R. Barbour, J. Huang, K. Kling, M. Lee, L. Diep, P. S. Keim, X. Shen, T. Chataway, M. G. Schlossmacher, P. Seubert, D. Schenk, S. Sinha, W. P. Gai and T. J. Chilcote (2006). "Phosphorylation of Ser-129 is the dominant pathological modification of alpha-synuclein in familial and sporadic Lewy body disease." J Biol Chem **281**(40): 29739-29752.

Appel-Cresswell, S., C. Vilarino-Guell, M. Encarnacion, H. Sherman, I. Yu, B. Shah, D. Weir, C. Thompson, C. Szu-Tu, J. Trinh, J. O. Aasly, A. Rajput, A. H. Rajput, A. Jon Stoessl and M. J. Farrer (2013). "Alpha-synuclein p.H50Q, a novel pathogenic mutation for Parkinson's disease." Mov Disord **28**(6): 811-813.

Baba, M., S. Nakajo, P. H. Tu, T. Tomita, K. Nakaya, V. M. Lee, J. Q. Trojanowski and T. Iwatsubo (1998). "Aggregation of alpha-synuclein in Lewy bodies of sporadic Parkinson's disease and dementia with Lewy bodies." Am J Pathol **152**(4): 879-884.

Badis, G., M. F. Berger, A. A. Philippakis, S. Talukder, A. R. Gehrke, S. A. Jaeger, E. T. Chan, G. Metzler, A. Vedenko, X. Chen, H. Kuznetsov, C. F. Wang, D. Coburn, D. E. Newburger, Q. Morris, T. R. Hughes and M. L. Bulyk (2009). "Diversity and complexity in DNA recognition by transcription factors." Science **324**(5935): 1720-1723.

Ballanger, B., H. Klinger, J. Eche, J. Lerond, A. E. Vallet, D. Le Bars, L. Tremblay, V. Sgambato-Faure, E. Broussolle and S. Thobois (2012). "Role of serotonergic 1A receptor dysfunction in depression associated with Parkinson's disease." Mov Disord **27**(1): 84-89.

Bannister, A. J. and T. Kouzarides (2011). "Regulation of chromatin by histone modifications." Cell Res **21**(3): 381-395.

Bardwell, V. J. and R. Treisman (1994). "The POZ domain: a conserved protein-protein interaction motif." Genes Dev **8**(14): 1664-1677.

Bartel, D. P. (2009). "MicroRNAs: target recognition and regulatory functions." Cell **136**(2): 215-233.

Bayer, T. A., P. Jakala, T. Hartmann, R. Egensperger, R. Buslei, P. Falkai and K. Beyreuther (1999). "Neural expression profile of alpha-synuclein in developing human cortex." Neuroreport **10**(13): 2799-2803.

Beisel, C. and R. Paro (2011). "Silencing chromatin: comparing modes and mechanisms." Nat Rev Genet **12**(2): 123-135.

Bellefroid, E. J., D. A. Poncelet, P. J. Lecocq, O. Revelant and J. A. Martial (1991). "The evolutionarily conserved Kruppel-associated box domain defines a subfamily of eukaryotic multifingered proteins." Proc Natl Acad Sci U S A **88**(9): 3608-3612.

Benayoun, B. A. and R. A. Veitia (2009). "A post-translational modification code for transcription factors: sorting through a sea of signals." Trends Cell Biol **19**(5): 189-197.

Bennett, M. C., J. F. Bishop, Y. Leng, P. B. Chock, T. N. Chase and M. M. Mouradian (1999). "Degradation of alpha-synuclein by proteasome." J Biol Chem **274**(48): 33855-33858.

Bernard, P. and V. R. Harley (2010). "Acquisition of SOX transcription factor specificity through protein-protein interaction, modulation of Wnt signalling and post-translational modification." Int J Biochem Cell Biol **42**(3): 400-410.

Bertram, L. and R. E. Tanzi (2005). "The genetic epidemiology of neurodegenerative disease." J Clin Invest **115**(6): 1449-1457.

Beyer, K. (2006). "Alpha-synuclein structure, posttranslational modification and alternative splicing as aggregation enhancers." Acta Neuropathol **112**(3): 237-251.

Bohnen, N. I., S. Gedela, P. Herath, G. M. Constantine and R. Y. Moore (2008). "Selective hyposmia in Parkinson disease: association with hippocampal dopamine activity." Neurosci Lett **447**(1): 12-16.

Bonini, N. M. and B. I. Giasson (2005). "Snaring the function of alpha-synuclein." Cell **123**(3): 359-361.

Braak, H., K. Del Tredici, U. Rub, R. A. de Vos, E. N. Jansen Steur and E. Braak (2003). "Staging of brain pathology related to sporadic Parkinson's disease." Neurobiol Aging **24**(2): 197-211.

Bredesen, D. E., R. V. Rao and P. Mehlen (2006). "Cell death in the nervous system." Nature **443**(7113): 796-802.

Brenner, S., C. Wersinger and T. Gasser (2015). "Transcriptional regulation of the alpha-synuclein gene in human brain tissue." Neurosci Lett **599**: 140-145.

Brewer, G. J. (1997). "Isolation and culture of adult rat hippocampal neurons." J Neurosci Methods **71**(2): 143-155.

Brewer, G. J., J. R. Torricelli, E. K. Evege and P. J. Price (1993). "Optimized survival of hippocampal neurons in B27-supplemented Neurobasal, a new serum-free medium combination." J Neurosci Res **35**(5): 567-576.

Burke, R. E., W. T. Dauer and J. P. Vonsattel (2008). "A critical evaluation of the Braak staging scheme for Parkinson's disease." Ann Neurol **64**(5): 485-491.

Burre, J., M. Sharma and T. C. Sudhof (2014). "alpha-Synuclein assembles into higher-order multimers upon membrane binding to promote SNARE complex formation." Proc Natl Acad Sci U S A **111**(40): E4274-4283.

Burre, J., M. Sharma, T. Tsetsenis, V. Buchman, M. R. Etherton and T. C. Sudhof (2010). "Alpha-synuclein promotes SNARE-complex assembly in vivo and in vitro." Science **329**(5999): 1663-1667.

Busser, B. W., L. Shokri, S. A. Jaeger, S. S. Gisselbrecht, A. Singhania, M. F. Berger, B. Zhou, M. L. Bulyk and A. M. Michelson (2012). "Molecular mechanism underlying the regulatory specificity of a Drosophila homeodomain protein that specifies myoblast identity." Development **139**(6): 1164-1174.

Calabresi, P., A. Castrioto, M. Di Filippo and B. Picconi (2013). "New experimental and clinical links between the hippocampus and the dopaminergic system in Parkinson's disease." Lancet Neurol **12**(8): 811-821.

Campos, E. I. and D. Reinberg (2009). "Histones: annotating chromatin." <u>Annu Rev Genet</u> **43**: 559-599.

Carlesimo, G. A., F. Piras, F. Assogna, F. E. Pontieri, C. Caltagirone and G. Spalletta (2012). "Hippocampal abnormalities and memory deficits in Parkinson disease: a multimodal imaging study." <u>Neurology</u> **78**(24): 1939-1945.

Carneiro, F. R., T. C. Silva, A. C. Alves, T. Haline-Vaz, F. C. Gozzo and N. I. Zanchin (2006). "Spectroscopic characterization of the tumor antigen NY-REN-21 and identification of heterodimer formation with SCAND1." <u>Biochem Biophys Res Commun</u> **343**(1): 260-268.

Carvin, C. D., R. D. Parr and M. P. Kladde (2003). "Site-selective in vivo targeting of cytosine-5 DNA methylation by zinc-finger proteins." <u>Nucleic Acids Res</u> **31**(22): 6493-6501.

Cedar, H. and Y. Bergman (2012). "Programming of DNA methylation patterns." <u>Annu Rev Biochem</u> **81**: 97-117.

Chandra, S., G. Gallardo, R. Fernandez-Chacon, O. M. Schluter and T. C. Sudhof (2005). "Alpha-synuclein cooperates with CSPalpha in preventing neurodegeneration." <u>Cell</u> **123**(3): 383-396.

Charlot, C., H. Dubois-Pot, T. Serchov, Y. Tourrette and B. Wasylyk (2010). "A review of post-translational modifications and subcellular localization of Ets transcription factors: possible connection with cancer and involvement in the hypoxic response." <u>Methods Mol Biol</u> **647**: 3-30.

Chartier-Harlin, M. C., J. Kachergus, C. Roumier, V. Mouroux, X. Douay, S. Lincoln, C. Levecque, L. Larvor, J. Andrieux, M. Hulihan, N. Waucquier, L. Defebvre, P. Amouyel, M. Farrer and A. Destee (2004). "Alpha-synuclein locus duplication as a cause of familial Parkinson's disease." <u>Lancet</u> **364**(9440): 1167-1169.

Chiba-Falek, O., J. A. Kowalak, M. E. Smulson and R. L. Nussbaum (2005). "Regulation of alpha-synuclein expression by poly (ADP ribose) polymerase-1 (PARP-1) binding to the NACP-Rep1 polymorphic site upstream of the SNCA gene." <u>Am J Hum Genet</u> **76**(3): 478-492.

Chiba-Falek, O., G. J. Lopez and R. L. Nussbaum (2006). "Levels of alpha-synuclein mRNA in sporadic Parkinson disease patients." <u>Mov Disord</u> **21**(10): 1703-1708.

Chiba-Falek, O. and R. L. Nussbaum (2001). "Effect of allelic variation at the NACP-Rep1 repeat upstream of the alpha-synuclein gene (SNCA) on transcription in a cell culture luciferase reporter system." <u>Hum Mol Genet</u> **10**(26): 3101-3109.

Chiba-Falek, O., J. W. Touchman and R. L. Nussbaum (2003). "Functional analysis of intra-allelic variation at NACP-Rep1 in the alpha-synuclein gene." <u>Hum Genet</u> **113**(5): 426-431.

Choo, Y., I. Sanchez-Garcia and A. Klug (1994). "In vivo repression by a site-specific DNA-binding protein designed against an oncogenic sequence." <u>Nature</u> **372**(6507): 642-645.

Chowdhury, K., M. Goulding, C. Walther, K. Imai and H. Fickenscher (1992). "The ubiquitous transactivator Zfp-38 is upregulated during spermatogenesis with differential transcription." <u>Mech Dev</u> **39**(3): 129-142.

Churchyard, A. and A. J. Lees (1997). "The relationship between dementia and direct involvement of the hippocampus and amygdala in Parkinson's disease." <u>Neurology</u> **49**(6): 1570-1576.

Clapier, C. R. and B. R. Cairns (2009). "The biology of chromatin remodeling complexes." <u>Annu Rev Biochem</u> **78**: 273-304.

Clough, R. L., G. Dermentzaki, M. Haritou, A. Petsakou and L. Stefanis (2011). "Regulation of alpha-synuclein expression in cultured cortical neurons." <u>J Neurochem</u> **117**(2): 275-285.

Clough, R. L., G. Dermentzaki and L. Stefanis (2009). "Functional dissection of the alpha-synuclein promoter: transcriptional regulation by ZSCAN21 and ZNF219." <u>J Neurochem</u> **110**(5): 1479-1490.

Clough, R. L. and L. Stefanis (2007). "A novel pathway for transcriptional regulation of alpha-synuclein." <u>FASEB J</u> **21**(2): 596-607.

Costa, C., C. Sgobio, S. Siliquini, A. Tozzi, M. Tantucci, V. Ghiglieri, M. Di Filippo, V. Pendolino, A. de Iure, M. Marti, M. Morari, M. G. Spillantini, E. C. Latagliata, T. Pascucci, S. Puglisi-Allegra,

F. Gardoni, M. Di Luca, B. Picconi and P. Calabresi (2012). "Mechanisms underlying the impairment of hippocampal long-term potentiation and memory in experimental Parkinson's disease." Brain **135**(Pt 6): 1884-1899.

Cronin, K. D., D. Ge, P. Manninger, C. Linnertz, A. Rossoshek, B. M. Orrison, D. J. Bernard, O. M. El-Agnaf, M. G. Schlossmacher, R. L. Nussbaum and O. Chiba-Falek (2009). "Expansion of the Parkinson disease-associated SNCA-Rep1 allele upregulates human alpha-synuclein in transgenic mouse brain." Hum Mol Genet **18**(17): 3274-3285.

Crowther, R. A., R. Jakes, M. G. Spillantini and M. Goedert (1998). "Synthetic filaments assembled from C-terminally truncated alpha-synuclein." FEBS Lett **436**(3): 309-312.

Cuervo, A. M., L. Stefanis, R. Fredenburg, P. T. Lansbury and D. Sulzer (2004). "Impaired degradation of mutant alpha-synuclein by chaperone-mediated autophagy." Science **305**(5688): 1292-1295.

Dachsel, J. C., S. J. Lincoln, J. Gonzalez, O. A. Ross, D. W. Dickson and M. J. Farrer (2007). "The ups and downs of alpha-synuclein mRNA expression." Mov Disord **22**(2): 293-295.

Dahl, J. A. and P. Collas (2008). "A rapid micro chromatin immunoprecipitation assay (microChIP)." Nat Protoc **3**(6): 1032-1045.

Dai, Z. and X. Dai (2012). "Nuclear colocalization of transcription factor target genes strengthens coregulation in yeast." Nucleic Acids Res **40**(1): 27-36.

Daitoku, H., J. Sakamaki and A. Fukamizu (2011). "Regulation of FoxO transcription factors by acetylation and protein-protein interactions." Biochim Biophys Acta **1813**(11): 1954-1960.

Darcan-Nicolaisen, Y., H. Meinicke, G. Fels, O. Hegend, A. Haberland, A. Kuhl, C. Loddenkemper, M. Witzenrath, S. Kube, W. Henke and E. Hamelmann (2009). "Small interfering RNA against transcription factor STAT6 inhibits allergic airway inflammation and hyperreactivity in mice." J Immunol **182**(12): 7501-7508.

Dauer, W. and S. Przedborski (2003). "Parkinson's disease: mechanisms and models." Neuron **39**(6): 889-909.

de Franca, N. R., D. Mesquita Junior, A. B. Lima, F. V. Pucci, L. E. Andrade and N. P. Silva (2010). "RNA interference: a new alternative for rheumatic diseases therapy." Rev Bras Reumatol **50**(6): 695-702.

de Wit, E. and W. de Laat (2012). "A decade of 3C technologies: insights into nuclear organization." Genes Dev **26**(1): 11-24.

Dekker, J., K. Rippe, M. Dekker and N. Kleckner (2002). "Capturing chromosome conformation." Science **295**(5558): 1306-1311.

Diamond, A. and J. Jankovic (2005). "The effect of deep brain stimulation on quality of life in movement disorders." J Neurol Neurosurg Psychiatry **76**(9): 1188-1193.

Dickson, D. W., H. Uchikado, H. Fujishiro and Y. Tsuboi (2010). "Evidence in favor of Braak staging of Parkinson's disease." Mov Disord **25 Suppl 1**: S78-82.

Dietrich, P., H. J. Rideout, Q. Wang and L. Stefanis (2003). "Lack of p53 delays apoptosis, but increases ubiquitinated inclusions, in proteasomal inhibitor-treated cultured cortical neurons." Mol Cell Neurosci **24**(2): 430-441.

Diogenes, M. J., R. B. Dias, D. M. Rombo, H. Vicente Miranda, F. Maiolino, P. Guerreiro, T. Nasstrom, H. G. Franquelim, L. M. Oliveira, M. A. Castanho, L. Lannfelt, J. Bergstrom, M. Ingelsson, A. Quintas, A. M. Sebastiao, L. V. Lopes and T. F. Outeiro (2012). "Extracellular alpha-synuclein oligomers modulate synaptic transmission and impair LTP via NMDA-receptor activation." J Neurosci **32**(34): 11750-11762.

Dorsett, D. (2011). "Cohesin: genomic insights into controlling gene transcription and development." Curr Opin Genet Dev **21**(2): 199-206.

Dostie, J. and W. A. Bickmore (2012). "Chromosome organization in the nucleus - charting new territory across the Hi-Cs." Curr Opin Genet Dev **22**(2): 125-131.

Doxakis, E. (2010). "Post-transcriptional regulation of alpha-synuclein expression by mir-7 and mir-153." J Biol Chem **285**(17): 12726-12734.

Duncan, I. W. (2002). "Transvection effects in Drosophila." <u>Annu Rev Genet</u> **36**: 521-556.

Ebert, M. S. and P. A. Sharp (2012). "Roles for microRNAs in conferring robustness to biological processes." <u>Cell</u> **149**(3): 515-524.

Ebrahimi-Fakhari, D., I. Cantuti-Castelvetri, Z. Fan, E. Rockenstein, E. Masliah, B. T. Hyman, P. J. McLean and V. K. Unni (2011). "Distinct roles in vivo for the ubiquitin-proteasome system and the autophagy-lysosomal pathway in the degradation of alpha-synuclein." <u>J Neurosci</u> **31**(41): 14508-14520.

Edwards, T. L., W. K. Scott, C. Almonte, A. Burt, E. H. Powell, G. W. Beecham, L. Wang, S. Zuchner, I. Konidari, G. Wang, C. Singer, F. Nahab, B. Scott, J. M. Stajich, M. Pericak-Vance, J. Haines, J. M. Vance and E. R. Martin (2010). "Genome-wide association study confirms SNPs in SNCA and the MAPT region as common risk factors for Parkinson disease." <u>Ann Hum Genet</u> **74**(2): 97-109.

Ellerton, E. L., W. J. Thompson and M. Rimer (2008). "Induction of zinc-finger proliferation 1 expression in non-myelinating Schwann cells after denervation." <u>Neuroscience</u> **153**(4): 975-985.

Enriquez, J., H. Boukhatmi, L. Dubois, A. A. Philippakis, M. L. Bulyk, A. M. Michelson, M. Crozatier and A. Vincent (2010). "Multi-step control of muscle diversity by Hox proteins in the Drosophila embryo." <u>Development</u> **137**(3): 457-466.

Eskiw, C. H. and P. Fraser (2011). "Ultrastructural study of transcription factories in mouse erythroblasts." <u>J Cell Sci</u> **124**(Pt 21): 3676-3683.

Ethier, S. D., H. Miura and J. Dostie (2012). "Discovering genome regulation with 3C and 3C-related technologies." <u>Biochim Biophys Acta</u> **1819**(5): 401-410.

Fahn, S. (2003). "Description of Parkinson's disease as a clinical syndrome." <u>Ann N Y Acad Sci</u> **991**: 1-14.

Farrer, M., D. M. Maraganore, P. Lockhart, A. Singleton, T. G. Lesnick, M. de Andrade, A. West, R. de Silva, J. Hardy and D. Hernandez (2001). "alpha-Synuclein gene haplotypes are associated with Parkinson's disease." <u>Hum Mol Genet</u> **10**(17): 1847-1851.

Feany, M. B. and W. W. Bender (2000). "A Drosophila model of Parkinson's disease." <u>Nature</u> **404**(6776): 394-398.

Feng, S., S. E. Jacobsen and W. Reik (2010). "Epigenetic reprogramming in plant and animal development." <u>Science</u> **330**(6004): 622-627.

Fernandez, H. H. and P. Odin (2011). "Levodopa-carbidopa intestinal gel for treatment of advanced Parkinson's disease." <u>Curr Med Res Opin</u> **27**(5): 907-919.

Filipowicz, W., S. N. Bhattacharyya and N. Sonenberg (2008). "Mechanisms of post-transcriptional regulation by microRNAs: are the answers in sight?" <u>Nat Rev Genet</u> **9**(2): 102-114.

Forno, L. S. (1996). "Neuropathology of Parkinson's disease." <u>J Neuropathol Exp Neurol</u> **55**(3): 259-272.

Fuchs, J., A. Tichopad, Y. Golub, M. Munz, K. J. Schweitzer, B. Wolf, D. Berg, J. C. Mueller and T. Gasser (2008). "Genetic variability in the SNCA gene influences alpha-synuclein levels in the blood and brain." <u>FASEB J</u> **22**(5): 1327-1334.

Fuda, N. J., M. B. Ardehali and J. T. Lis (2009). "Defining mechanisms that regulate RNA polymerase II transcription in vivo." <u>Nature</u> **461**(7261): 186-192.

Gagnon, J. F., R. B. Postuma, S. Mazza, J. Doyon and J. Montplaisir (2006). "Rapid-eye-movement sleep behaviour disorder and neurodegenerative diseases." <u>Lancet Neurol</u> **5**(5): 424-432.

Galvin, J. E., T. M. Schuck, V. M. Lee and J. Q. Trojanowski (2001). "Differential expression and distribution of alpha-, beta-, and gamma-synuclein in the developing human substantia nigra." <u>Exp Neurol</u> **168**(2): 347-355.

Gandhi, S. and N. W. Wood (2010). "Genome-wide association studies: the key to unlocking neurodegeneration?" <u>Nat Neurosci</u> **13**(7): 789-794.

Gardner, K. E., C. D. Allis and B. D. Strahl (2011). "Operating on chromatin, a colorful language where context matters." J Mol Biol **409**(1): 36-46.

George, J. M. (2002). "The synucleins." Genome Biol **3**(1): REVIEWS3002.

George, J. M., H. Jin, W. S. Woods and D. F. Clayton (1995). "Characterization of a novel protein regulated during the critical period for song learning in the zebra finch." Neuron **15**(2): 361-372.

Giasson, B. I., J. E. Duda, I. V. Murray, Q. Chen, J. M. Souza, H. I. Hurtig, H. Ischiropoulos, J. Q. Trojanowski and V. M. Lee (2000). "Oxidative damage linked to neurodegeneration by selective alpha-synuclein nitration in synucleinopathy lesions." Science **290**(5493): 985-989.

Giasson, B. I., J. E. Duda, S. M. Quinn, B. Zhang, J. Q. Trojanowski and V. M. Lee (2002). "Neuronal alpha-synucleinopathy with severe movement disorder in mice expressing A53T human alpha-synuclein." Neuron **34**(4): 521-533.

Glisovic, T., J. L. Bachorik, J. Yong and G. Dreyfuss (2008). "RNA-binding proteins and post-transcriptional gene regulation." FEBS Lett **582**(14): 1977-1986.

Goto, Y. and A. A. Grace (2005). "Dopaminergic modulation of limbic and cortical drive of nucleus accumbens in goal-directed behavior." Nat Neurosci **8**(6): 805-812.

Greene, L. A. and A. S. Tischler (1976). "Establishment of a noradrenergic clonal line of rat adrenal pheochromocytoma cells which respond to nerve growth factor." Proc Natl Acad Sci U S A **73**(7): 2424-2428.

Grimm, D., A. Kern, K. Rittner and J. A. Kleinschmidt (1998). "Novel tools for production and purification of recombinant adenoassociated virus vectors." Hum Gene Ther **9**(18): 2745-2760.

Gritti, A., E. A. Parati, L. Cova, P. Frolichsthal, R. Galli, E. Wanke, L. Faravelli, D. J. Morassutti, F. Roisen, D. D. Nickel and A. L. Vescovi (1996). "Multipotential stem cells from the adult mouse brain proliferate and self-renew in response to basic fibroblast growth factor." J Neurosci **16**(3): 1091-1100.

Grundemann, J., F. Schlaudraff, O. Haeckel and B. Liss (2008). "Elevated alpha-synuclein mRNA levels in individual UV-laser-microdissected dopaminergic substantia nigra neurons in idiopathic Parkinson's disease." Nucleic Acids Res **36**(7): e38.

Guez-Barber, D., S. Fanous, B. K. Harvey, Y. Zhang, E. Lehrmann, K. G. Becker, M. R. Picciotto and B. T. Hope (2012). "FACS purification of immunolabeled cell types from adult rat brain." J Neurosci Methods **203**(1): 10-18.

Hadjur, S., L. M. Williams, N. K. Ryan, B. S. Cobb, T. Sexton, P. Fraser, A. G. Fisher and M. Merkenschlager (2009). "Cohesins form chromosomal cis-interactions at the developmentally regulated IFNG locus." Nature **460**(7253): 410-413.

Hakim, O., M. H. Sung, T. C. Voss, E. Splinter, S. John, P. J. Sabo, R. E. Thurman, J. A. Stamatoyannopoulos, W. de Laat and G. L. Hager (2011). "Diverse gene reprogramming events occur in the same spatial clusters of distal regulatory elements." Genome Res **21**(5): 697-706.

Halliday, G. M., J. L. Holton, T. Revesz and D. W. Dickson (2011). "Neuropathology underlying clinical variability in patients with synucleinopathies." Acta Neuropathol **122**(2): 187-204.

Hargreaves, D. C. and G. R. Crabtree (2011). "ATP-dependent chromatin remodeling: genetics, genomics and mechanisms." Cell Res **21**(3): 396-420.

Hashimoto, M., L. J. Hsu, Y. Xia, A. Takeda, A. Sisk, M. Sundsmo and E. Masliah (1999). "Oxidative stress induces amyloid-like aggregate formation of NACP/alpha-synuclein in vitro." Neuroreport **10**(4): 717-721.

Hashimoto, M., A. Takeda, L. J. Hsu, T. Takenouchi and E. Masliah (1999). "Role of cytochrome c as a stimulator of alpha-synuclein aggregation in Lewy body disease." J Biol Chem **274**(41): 28849-28852.

Hawkes, C. H. (2008). "The prodromal phase of sporadic Parkinson's disease: does it exist and if so how long is it?" Mov Disord **23**(13): 1799-1807.

He, T. C., S. Zhou, L. T. da Costa, J. Yu, K. W. Kinzler and B. Vogelstein (1998). "A simplified system for generating recombinant adenoviruses." Proc Natl Acad Sci U S A **95**(5): 2509-2514.

Hoffman-Zacharska, D., D. Koziorowski, O. A. Ross, M. Milewski, J. Poznanski, M. Jurek, Z. K. Wszolek, A. Soto-Ortolaza, J. Slawek, P. Janik, Z. Jamrozik, A. Potulska-Chromik, B. Jasinska-Myga, G. Opala, A. Krygowska-Wajs, K. Czyzewski, D. W. Dickson, J. Bal and A. Friedman (2013). "Novel A18T and pA29S substitutions in alpha-synuclein may be associated with sporadic Parkinson's disease." Parkinsonism Relat Disord **19**(11): 1057-1060.

Honer, C., P. Chen, M. J. Toth and C. Schumacher (2001). "Identification of SCAN dimerization domains in four gene families." Biochim Biophys Acta **1517**(3): 441-448.

Houlden, H. and A. B. Singleton (2012). "The genetics and neuropathology of Parkinson's disease." Acta Neuropathol **124**(3): 325-338.

Hughes, A. J., S. E. Daniel, L. Kilford and A. J. Lees (1992). "Accuracy of clinical diagnosis of idiopathic Parkinson's disease: a clinico-pathological study of 100 cases." J Neurol Neurosurg Psychiatry **55**(3): 181-184.

Huttlin, E. L., L. Ting, R. J. Bruckner, F. Gebreab, M. P. Gygi, J. Szpyt, S. Tam, G. Zarraga, G. Colby, K. Baltier, R. Dong, V. Guarani, L. P. Vaites, A. Ordureau, R. Rad, B. K. Erickson, M. Wuhr, J. Chick, B. Zhai, D. Kolippakkam, J. Mintseris, R. A. Obar, T. Harris, S. Artavanis-Tsakonas, M. E. Sowa, P. De Camilli, J. A. Paulo, J. W. Harper and S. P. Gygi (2015). "The BioPlex Network: A Systematic Exploration of the Human Interactome." Cell **162**(2): 425-440.

International Parkinson Disease Genomics, C., M. A. Nalls, V. Plagnol, D. G. Hernandez, M. Sharma, U. M. Sheerin, M. Saad, J. Simon-Sanchez, C. Schulte, S. Lesage, S. Sveinbjornsdottir, K. Stefansson, M. Martinez, J. Hardy, P. Heutink, A. Brice, T. Gasser, A. B. Singleton and N. W. Wood (2011). "Imputation of sequence variants for identification of genetic risks for Parkinson's disease: a meta-analysis of genome-wide association studies." Lancet **377**(9766): 641-649.

Iranzo, A., J. L. Molinuevo, J. Santamaria, M. Serradell, M. J. Marti, F. Valldeoriola and E. Tolosa (2006). "Rapid-eye-movement sleep behaviour disorder as an early marker for a neurodegenerative disorder: a descriptive study." Lancet Neurol **5**(7): 572-577.

Irwin, D. J., V. M. Lee and J. Q. Trojanowski (2013). "Parkinson's disease dementia: convergence of alpha-synuclein, tau and amyloid-beta pathologies." Nat Rev Neurosci **14**(9): 626-636.

Istrail, S. and E. H. Davidson (2005). "Logic functions of the genomic cis-regulatory code." Proc Natl Acad Sci U S A **102**(14): 4954-4959.

Ivanov, D., J. R. Stone, J. L. Maki, T. Collins and G. Wagner (2005). "Mammalian SCAN domain dimer is a domain-swapped homolog of the HIV capsid C-terminal domain." Mol Cell **17**(1): 137-143.

Izumi, Y., H. Morino, M. Oda, H. Maruyama, F. Udaka, M. Kameyama, S. Nakamura and H. Kawakami (2001). "Genetic studies in Parkinson's disease with an alpha-synuclein/NACP gene polymorphism in Japan." Neurosci Lett **300**(2): 125-127.

Jacob, F. and J. Monod (1961). "Genetic regulatory mechanisms in the synthesis of proteins." J Mol Biol **3**: 318-356.

Jaehning, J. A. (2010). "The Paf1 complex: platform or player in RNA polymerase II transcription?" Biochim Biophys Acta **1799**(5-6): 379-388.

Jankovic, J. and L. G. Aguilar (2008). "Current approaches to the treatment of Parkinson's disease." Neuropsychiatr Dis Treat **4**(4): 743-757.

Jones, P. A. (2012). "Functions of DNA methylation: islands, start sites, gene bodies and beyond." Nat Rev Genet **13**(7): 484-492.

Joseph, R., Y. L. Orlov, M. Huss, W. Sun, S. L. Kong, L. Ukil, Y. F. Pan, G. Li, M. Lim, J. S. Thomsen, Y. Ruan, N. D. Clarke, S. Prabhakar, E. Cheung and E. T. Liu (2010). "Integrative model of genomic factors for determining binding site selection by estrogen receptor-alpha." Mol Syst Biol **6**: 456.

Jowaed, A., I. Schmitt, O. Kaut and U. Wullner (2010). "Methylation regulates alpha-synuclein expression and is decreased in Parkinson's disease patients' brains." J Neurosci **30**(18): 6355-6359.

Junn, E., K. W. Lee, B. S. Jeong, T. W. Chan, J. Y. Im and M. M. Mouradian (2009). "Repression of alpha-synuclein expression and toxicity by microRNA-7." Proc Natl Acad Sci U S A **106**(31): 13052-13057.

Juven-Gershon, T. and J. T. Kadonaga (2010). "Regulation of gene expression via the core promoter and the basal transcriptional machinery." Dev Biol **339**(2): 225-229.

Kagey, M. H., J. J. Newman, S. Bilodeau, Y. Zhan, D. A. Orlando, N. L. van Berkum, C. C. Ebmeier, J. Goossens, P. B. Rahl, S. S. Levine, D. J. Taatjes, J. Dekker and R. A. Young (2010). "Mediator and cohesin connect gene expression and chromatin architecture." Nature **467**(7314): 430-435.

Kahle, P. J. (2008). "alpha-Synucleinopathy models and human neuropathology: similarities and differences." Acta Neuropathol **115**(1): 87-95.

Kalivendi, S. V., D. Yedlapudi, C. J. Hillard and B. Kalyanaraman (2010). "Oxidants induce alternative splicing of alpha-synuclein: Implications for Parkinson's disease." Free Radic Biol Med **48**(3): 377-383.

Kaltezioti, V., D. Antoniou, A. Stergiopoulos, I. Rozani, H. Rohrer and P. K. Politis (2014). "Prox1 regulates Olig2 expression to modulate binary fate decisions in spinal cord neurons." J Neurosci **34**(47): 15816-15831.

Kaltezioti, V., G. Kouroupi, M. Oikonomaki, E. Mantouvalou, A. Stergiopoulos, A. Charonis, H. Rohrer, R. Matsas and P. K. Politis (2010). "Prox1 regulates the notch1-mediated inhibition of neurogenesis." PLoS Biol **8**(12): e1000565.

Kang, J. S. and J. S. Kim (2000). "Zinc finger proteins as designer transcription factors." J Biol Chem **275**(12): 8742-8748.

Kehagia, A. A., R. A. Barker and T. W. Robbins (2010). "Neuropsychological and clinical heterogeneity of cognitive impairment and dementia in patients with Parkinson's disease." Lancet Neurol **9**(12): 1200-1213.

Khan, N., E. Graham, P. Dixon, C. Morris, A. Mander, D. Clayton, J. Vaughan, N. Quinn, A. Lees, S. Daniel, N. Wood and R. de Silva (2001). "Parkinson's disease is not associated with the combined alpha-synuclein/apolipoprotein E susceptibility genotype." Ann Neurol **49**(5): 665-668.

Kholodilov, N. G., M. Neystat, T. F. Oo, S. E. Lo, K. E. Larsen, D. Sulzer and R. E. Burke (1999). "Increased expression of rat synuclein in the substantia nigra pars compacta identified by mRNA differential display in a model of developmental target injury." J Neurochem **73**(6): 2586-2599.

Kim, D. H. and J. J. Rossi (2007). "Strategies for silencing human disease using RNA interference." Nat Rev Genet **8**(3): 173-184.

Kim, J. Y., R. T. Ash, C. Ceballos-Diaz, Y. Levites, T. E. Golde, S. M. Smirnakis and J. L. Jankowsky (2013). "Viral transduction of the neonatal brain delivers controllable genetic mosaicism for visualising and manipulating neuronal circuits in vivo." Eur J Neurosci **37**(8): 1203-1220.

Kingsbury, A. E., S. E. Daniel, H. Sangha, S. Eisen, A. J. Lees and O. J. Foster (2004). "Alteration in alpha-synuclein mRNA expression in Parkinson's disease." Mov Disord **19**(2): 162-170.

Kirik, D., L. E. Annett, C. Burger, N. Muzyczka, R. J. Mandel and A. Bjorklund (2003). "Nigrostriatal alpha-synucleinopathy induced by viral vector-mediated overexpression of human alpha-synuclein: a new primate model of Parkinson's disease." Proc Natl Acad Sci U S A **100**(5): 2884-2889.

Kirik, D., C. Rosenblad, C. Burger, C. Lundberg, T. E. Johansen, N. Muzyczka, R. J. Mandel and A. Bjorklund (2002). "Parkinson-like neurodegeneration induced by targeted overexpression of alpha-synuclein in the nigrostriatal system." J Neurosci **22**(7): 2780-2791.

Klein, C. and M. G. Schlossmacher (2006). "The genetics of Parkinson disease: Implications for neurological care." Nat Clin Pract Neurol **2**(3): 136-146.

Kohl, Z., B. Winner, K. Ubhi, E. Rockenstein, M. Mante, M. Munch, C. Barlow, T. Carter, E. Masliah and J. Winkler (2012). "Fluoxetine rescues impaired hippocampal neurogenesis in a transgenic A53T synuclein mouse model." Eur J Neurosci **35**(1): 10-19.

Kokhan, V. S., M. A. Afanasyeva and G. I. Van'kin (2012). "alpha-Synuclein knockout mice have cognitive impairments." Behav Brain Res **231**(1): 226-230.

Krivega, I. and A. Dean (2012). "Enhancer and promoter interactions-long distance calls." Curr Opin Genet Dev **22**(2): 79-85.

Kruger, R., W. Kuhn, T. Muller, D. Woitalla, M. Graeber, S. Kosel, H. Przuntek, J. T. Epplen, L. Schols and O. Riess (1998). "Ala30Pro mutation in the gene encoding alpha-synuclein in Parkinson's disease." Nat Genet **18**(2): 106-108.

Kruger, R., A. M. Vieira-Saecker, W. Kuhn, D. Berg, T. Muller, N. Kuhnl, G. A. Fuchs, A. Storch, M. Hungs, D. Woitalla, H. Przuntek, J. T. Epplen, L. Schols and O. Riess (1999). "Increased susceptibility to sporadic Parkinson's disease by a certain combined alpha-synuclein/apolipoprotein E genotype." Ann Neurol **45**(5): 611-617.

Ku, C. S., E. Y. Loy, Y. Pawitan and K. S. Chia (2010). "The pursuit of genome-wide association studies: where are we now?" J Hum Genet **55**(4): 195-206.

Laity, J. H., B. M. Lee and P. E. Wright (2001). "Zinc finger proteins: new insights into structural and functional diversity." Curr Opin Struct Biol **11**(1): 39-46.

Lara, H., Y. Wang, A. S. Beltran, K. Juarez-Moreno, X. Yuan, S. Kato, A. V. Leisewitz, M. Cuello Fredes, A. F. Licea, D. C. Connolly, L. Huang and P. Blancafort (2012). "Targeting serous epithelial ovarian cancer with designer zinc finger transcription factors." J Biol Chem **287**(35): 29873-29886.

Latos, P. A., F. M. Pauler, M. V. Koerner, H. B. Senergin, Q. J. Hudson, R. R. Stocsits, W. Allhoff, S. H. Stricker, R. M. Klement, K. E. Warczok, K. Aumayr, P. Pasierbek and D. P. Barlow (2012). "Airn transcriptional overlap, but not its lncRNA products, induces imprinted Igf2r silencing." Science **338**(6113): 1469-1472.

Lavedan, C. (1998). "The synuclein family." Genome Res **8**(9): 871-880.

Lee, J. T. (2012). "Epigenetic regulation by long noncoding RNAs." Science **338**(6113): 1435-1439.

Lee, T. I. and R. A. Young (2013). "Transcriptional regulation and its misregulation in disease." Cell **152**(6): 1237-1251.

Lejeune, E. and R. C. Allshire (2011). "Common ground: small RNA programming and chromatin modifications." Curr Opin Cell Biol **23**(3): 258-265.

Lelli, K. M., M. Slattery and R. S. Mann (2012). "Disentangling the many layers of eukaryotic transcriptional regulation." Annu Rev Genet **46**: 43-68.

Lesage, S., M. Anheim, F. Letournel, L. Bousset, A. Honore, N. Rozas, L. Pieri, K. Madiona, A. Durr, R. Melki, C. Verny, A. Brice and G. French Parkinson's Disease Genetics Study (2013). "G51D alpha-synuclein mutation causes a novel parkinsonian-pyramidal syndrome." Ann Neurol **73**(4): 459-471.

LeWitt, P. A., A. R. Rezai, M. A. Leehey, S. G. Ojemann, A. W. Flaherty, E. N. Eskandar, S. K. Kostyk, K. Thomas, A. Sarkar, M. S. Siddiqui, S. B. Tatter, J. M. Schwalb, K. L. Poston, J. M. Henderson, R. M. Kurlan, I. H. Richard, L. Van Meter, C. V. Sapan, M. J. During, M. G. Kaplitt and A. Feigin (2011). "AAV2-GAD gene therapy for advanced Parkinson's disease: a double-blind, sham-surgery controlled, randomised trial." Lancet Neurol **10**(4): 309-319.

Li, G. and D. Reinberg (2011). "Chromatin higher-order structures and gene regulation." Curr Opin Genet Dev **21**(2): 175-186.

Li, W., C. Lesuisse, Y. Xu, J. C. Troncoso, D. L. Price and M. K. Lee (2004). "Stabilization of alpha-synuclein protein with aging and familial parkinson's disease-linked A53T mutation." J Neurosci **24**(33): 7400-7409.

Lieberman-Aiden, E., N. L. van Berkum, L. Williams, M. Imakaev, T. Ragoczy, A. Telling, I. Amit, B. R. Lajoie, P. J. Sabo, M. O. Dorschner, R. Sandstrom, B. Bernstein, M. A. Bender, M. Groudine, A. Gnirke, J. Stamatoyannopoulos, L. A. Mirny, E. S. Lander and J. Dekker (2009). "Comprehensive mapping of long-range interactions reveals folding principles of the human genome." Science **326**(5950): 289-293.

Lim, Y., V. M. Kehm, E. B. Lee, J. H. Soper, C. Li, J. Q. Trojanowski and V. M. Lee (2011). "alpha-Syn suppression reverses synaptic and memory defects in a mouse model of dementia with Lewy bodies." J Neurosci **31**(27): 10076-10087.

Linazasoro, G., N. Van Blercom and A. Lasa (2003). "Unilateral subthalamic deep brain stimulation in advanced Parkinson's disease." Mov Disord **18**(6): 713-716.

Lindersson, E., R. Beedholm, P. Hojrup, T. Moos, W. Gai, K. B. Hendil and P. H. Jensen (2004). "Proteasomal inhibition by alpha-synuclein filaments and oligomers." J Biol Chem **279**(13): 12924-12934.

Linnertz, C., L. Saucier, D. Ge, K. D. Cronin, J. R. Burke, J. N. Browndyke, C. M. Hulette, K. A. Welsh-Bohmer and O. Chiba-Falek (2009). "Genetic regulation of alpha-synuclein mRNA expression in various human brain tissues." PLoS One **4**(10): e7480.

Livak, K. J. and T. D. Schmittgen (2001). "Analysis of relative gene expression data using real-time quantitative PCR and the 2(-Delta Delta C(T)) Method." Methods **25**(4): 402-408.

Lo Bianco, C., J. L. Ridet, B. L. Schneider, N. Deglon and P. Aebischer (2002). "alpha - Synucleinopathy and selective dopaminergic neuron loss in a rat lentiviral-based model of Parkinson's disease." Proc Natl Acad Sci U S A **99**(16): 10813-10818.

Lomvardas, S., G. Barnea, D. J. Pisapia, M. Mendelsohn, J. Kirkland and R. Axel (2006). "Interchromosomal interactions and olfactory receptor choice." Cell **126**(2): 403-413.

Lu, A., A. Gupta, C. Li, T. E. Ahlborn, Y. Ma, E. Y. Shi and J. Liu (2001). "Molecular mechanisms for aberrant expression of the human breast cancer specific gene 1 in breast cancer cells: control of transcription by DNA methylation and intronic sequences." Oncogene **20**(37): 5173-5185.

Luger, K., A. W. Mader, R. K. Richmond, D. F. Sargent and T. J. Richmond (1997). "Crystal structure of the nucleosome core particle at 2.8 A resolution." Nature **389**(6648): 251-260.

Luo, Z., C. Lin and A. Shilatifard (2012). "The super elongation complex (SEC) family in transcriptional control." Nat Rev Mol Cell Biol **13**(9): 543-547.

Lutz, M. W., R. Saul, C. Linnertz, O. C. Glenn, A. D. Roses and O. Chiba-Falek (2015). "A cytosine-thymine (CT)-rich haplotype in intron 4 of SNCA confers risk for Lewy body pathology in Alzheimer's disease and affects SNCA expression." Alzheimers Dement.

Malik, S. and R. G. Roeder (2010). "The metazoan Mediator co-activator complex as an integrative hub for transcriptional regulation." Nat Rev Genet **11**(11): 761-772.

Manning-Bog, A. B., A. L. McCormack, J. Li, V. N. Uversky, A. L. Fink and D. A. Di Monte (2002). "The herbicide paraquat causes up-regulation and aggregation of alpha-synuclein in mice: paraquat and alpha-synuclein." J Biol Chem **277**(3): 1641-1644.

Maraganore, D. M., M. de Andrade, A. Elbaz, M. J. Farrer, J. P. Ioannidis, R. Kruger, W. A. Rocca, N. K. Schneider, T. G. Lesnick, S. J. Lincoln, M. M. Hulihan, J. O. Aasly, T. Ashizawa, M. C. Chartier-Harlin, H. Checkoway, C. Ferrarese, G. Hadjigeorgiou, N. Hattori, H. Kawakami, J. C. Lambert, T. Lynch, G. D. Mellick, S. Papapetropoulos, A. Parsian, A. Quattrone, O. Riess, E. K. Tan and C. Van Broeckhoven (2006). "Collaborative analysis of alpha-synuclein gene promoter variability and Parkinson disease." JAMA **296**(6): 661-670.

Maroteaux, L., J. T. Campanelli and R. H. Scheller (1988). "Synuclein: a neuron-specific protein localized to the nucleus and presynaptic nerve terminal." J Neurosci **8**(8): 2804-2815.

Masliah, E., E. Rockenstein, I. Veinbergs, M. Mallory, M. Hashimoto, A. Takeda, Y. Sagara, A. Sisk and L. Mucke (2000). "Dopaminergic loss and inclusion body formation in alpha-synuclein mice: implications for neurodegenerative disorders." Science **287**(5456): 1265-1269.

Mata, I. F., M. Shi, P. Agarwal, K. A. Chung, K. L. Edwards, S. A. Factor, D. R. Galasko, C. Ginghina, A. Griffith, D. S. Higgins, D. M. Kay, H. Kim, J. B. Leverenz, J. F. Quinn, J. W. Roberts, A. Samii, K. W. Snapinn, D. W. Tsuang, D. Yearout, J. Zhang, H. Payami and C. P. Zabetian (2010). "SNCA variant associated with Parkinson disease and plasma alpha-synuclein level." Arch Neurol **67**(11): 1350-1356.

Matsumoto, L., H. Takuma, A. Tamaoka, H. Kurisaki, H. Date, S. Tsuji and A. Iwata (2010). "CpG demethylation enhances alpha-synuclein expression and affects the pathogenesis of Parkinson's disease." PLoS One **5**(11): e15522.

Mattila, P. M., J. O. Rinne, H. Helenius, D. W. Dickson and M. Roytta (2000). "Alpha-synuclein-immunoreactive cortical Lewy bodies are associated with cognitive impairment in Parkinson's disease." Acta Neuropathol **100**(3): 285-290.

McCarthy, J. J., C. Linnertz, L. Saucier, J. R. Burke, C. M. Hulette, K. A. Welsh-Bohmer and O. Chiba-Falek (2011). "The effect of SNCA 3' region on the levels of SNCA-112 splicing variant." Neurogenetics **12**(1): 59-64.

McCarthy, M. I., G. R. Abecasis, L. R. Cardon, D. B. Goldstein, J. Little, J. P. Ioannidis and J. N. Hirschhorn (2008). "Genome-wide association studies for complex traits: consensus, uncertainty and challenges." Nat Rev Genet **9**(5): 356-369.

McKeith, I. G., D. W. Dickson, J. Lowe, M. Emre, J. T. O'Brien, H. Feldman, J. Cummings, J. E. Duda, C. Lippa, E. K. Perry, D. Aarsland, H. Arai, C. G. Ballard, B. Boeve, D. J. Burn, D. Costa, T. Del Ser, B. Dubois, D. Galasko, S. Gauthier, C. G. Goetz, E. Gomez-Tortosa, G. Halliday, L. A. Hansen, J. Hardy, T. Iwatsubo, R. N. Kalaria, D. Kaufer, R. A. Kenny, A. Korczyn, K. Kosaka, V. M. Lee, A. Lees, I. Litvan, E. Londos, O. L. Lopez, S. Minoshima, Y. Mizuno, J. A. Molina, E. B. Mukaetova-Ladinska, F. Pasquier, R. H. Perry, J. B. Schulz, J. Q. Trojanowski, M. Yamada and D. L. B. Consortium on (2005). "Diagnosis and management of dementia with Lewy bodies: third report of the DLB Consortium." Neurology **65**(12): 1863-1872.

Miller, D. W., S. M. Hague, J. Clarimon, M. Baptista, K. Gwinn-Hardy, M. R. Cookson and A. B. Singleton (2004). "Alpha-synuclein in blood and brain from familial Parkinson disease with SNCA locus triplication." Neurology **62**(10): 1835-1838.

Mingot, J. M., S. Vega, B. Maestro, J. M. Sanz and M. A. Nieto (2009). "Characterization of Snail nuclear import pathways as representatives of C2H2 zinc finger transcription factors." J Cell Sci **122**(Pt 9): 1452-1460.

Mizuta, I., M. Nishimura, E. Mizuta, S. Yamasaki, M. Ohta and S. Kuno (2002). "Meta-analysis of alpha synuclein/ NACP polymorphism in Parkinson's disease in Japan." J Neurol Neurosurg Psychiatry **73**(3): 350.

Mizuta, I., W. Satake, Y. Nakabayashi, C. Ito, S. Suzuki, Y. Momose, Y. Nagai, A. Oka, H. Inoko, J. Fukae, Y. Saito, M. Sawabe, S. Murayama, M. Yamamoto, N. Hattori, M. Murata and T. Toda (2006). "Multiple candidate gene analysis identifies alpha-synuclein as a susceptibility gene for sporadic Parkinson's disease." Hum Mol Genet **15**(7): 1151-1158.

Mizuta, I., K. Takafuji, Y. Ando, W. Satake, M. Kanagawa, K. Kobayashi, S. Nagamori, T. Shinohara, C. Ito, M. Yamamoto, N. Hattori, M. Murata, Y. Kanai, S. Murayama, M. Nakagawa and T. Toda (2013). "YY1 binds to alpha-synuclein 3'-flanking region SNP and stimulates antisense noncoding RNA expression." J Hum Genet **58**(11): 711-719.

Moazed, D. (2009). "Small RNAs in transcriptional gene silencing and genome defence." Nature **457**(7228): 413-420.

Moffat, J., D. A. Grueneberg, X. Yang, S. Y. Kim, A. M. Kloepfer, G. Hinkle, B. Piqani, T. M. Eisenhaure, B. Luo, J. K. Grenier, A. E. Carpenter, S. Y. Foo, S. A. Stewart, B. R. Stockwell, N. Hacohen, W. C. Hahn, E. S. Lander, D. M. Sabatini and D. E. Root (2006). "A lentiviral RNAi library for human and mouse genes applied to an arrayed viral high-content screen." Cell **124**(6): 1283-1298.

Morshead, C. M., B. A. Reynolds, C. G. Craig, M. W. McBurney, W. A. Staines, D. Morassutti, S. Weiss and D. van der Kooy (1994). "Neural stem cells in the adult mammalian forebrain: a relatively quiescent subpopulation of subependymal cells." Neuron **13**(5): 1071-1082.

Mueller, J. C., J. Fuchs, A. Hofer, A. Zimprich, P. Lichtner, T. Illig, D. Berg, U. Wullner, T. Meitinger and T. Gasser (2005). "Multiple regions of alpha-synuclein are associated with Parkinson's disease." Ann Neurol **57**(4): 535-541.

Murphy, D. D., S. M. Rueter, J. Q. Trojanowski and V. M. Lee (2000). "Synucleins are developmentally expressed, and alpha-synuclein regulates the size of the presynaptic vesicular pool in primary hippocampal neurons." J Neurosci **20**(9): 3214-3220.

Murray, I. V., B. I. Giasson, S. M. Quinn, V. Koppaka, P. H. Axelsen, H. Ischiropoulos, J. Q. Trojanowski and V. M. Lee (2003). "Role of alpha-synuclein carboxy-terminus on fibril formation in vitro." Biochemistry **42**(28): 8530-8540.

Neumann, M., P. J. Kahle, B. I. Giasson, L. Ozmen, E. Borroni, W. Spooren, V. Muller, S. Odoy, H. Fujiwara, M. Hasegawa, T. Iwatsubo, J. Q. Trojanowski, H. A. Kretzschmar and C. Haass (2002). "Misfolded proteinase K-resistant hyperphosphorylated alpha-synuclein in aged transgenic mice with locomotor deterioration and in human alpha-synucleinopathies." J Clin Invest **110**(10): 1429-1439.

Neystat, M., T. Lynch, S. Przedborski, N. Kholodilov, M. Rzhetskaya and R. E. Burke (1999). "Alpha-synuclein expression in substantia nigra and cortex in Parkinson's disease." Mov Disord **14**(3): 417-422.

Noorbakhsh, F., C. M. Overall and C. Power (2009). "Deciphering complex mechanisms in neurodegenerative diseases: the advent of systems biology." Trends Neurosci **32**(2): 88-100.

Nuber, S., E. Petrasch-Parwez, B. Winner, J. Winkler, S. von Horsten, T. Schmidt, J. Boy, M. Kuhn, H. P. Nguyen, P. Teismann, J. B. Schulz, M. Neumann, B. J. Pichler, G. Reischl, C. Holzmann, I. Schmitt, A. Bornemann, W. Kuhn, F. Zimmermann, A. Servadio and O. Riess (2008). "Neurodegeneration and motor dysfunction in a conditional model of Parkinson's disease." J Neurosci **28**(10): 2471-2484.

Nyholm, D. (2006). "Enteral levodopa/carbidopa gel infusion for the treatment of motor fluctuations and dyskinesias in advanced Parkinson's disease." Expert Rev Neurother **6**(10): 1403-1411.

Ong, C. T. and V. G. Corces (2011). "Enhancer function: new insights into the regulation of tissue-specific gene expression." Nat Rev Genet **12**(4): 283-293.

Orkin, S. H. and K. Hochedlinger (2011). "Chromatin connections to pluripotency and cellular reprogramming." Cell **145**(6): 835-850.

Orom, U. A. and R. Shiekhattar (2011). "Noncoding RNAs and enhancers: complications of a long-distance relationship." Trends Genet **27**(10): 433-439.

Oueslati, A., B. L. Schneider, P. Aebischer and H. A. Lashuel (2013). "Polo-like kinase 2 regulates selective autophagic alpha-synuclein clearance and suppresses its toxicity in vivo." Proc Natl Acad Sci U S A **110**(41): E3945-3954.

Pals, P., S. Lincoln, J. Manning, M. Heckman, L. Skipper, M. Hulihan, M. Van den Broeck, T. De Pooter, P. Cras, J. Crook, C. Van Broeckhoven and M. J. Farrer (2004). "alpha-Synuclein promoter confers susceptibility to Parkinson's disease." Ann Neurol **56**(4): 591-595.

Pan, Q., P. E. de Ruiter, K. J. von Eije, R. Smits, J. Kwekkeboom, H. W. Tilanus, B. Berkhout, H. L. Janssen and L. J. van der Laan (2011). "Disturbance of the microRNA pathway by commonly used lentiviral shRNA libraries limits the application for screening host factors involved in hepatitis C virus infection." FEBS Lett **585**(7): 1025-1030.

Pankratz, N., J. B. Wilk, J. C. Latourelle, A. L. DeStefano, C. Halter, E. W. Pugh, K. F. Doheny, J. F. Gusella, W. C. Nichols, T. Foroud and R. H. Myers (2009). "Genomewide association study for susceptibility genes contributing to familial Parkinson disease." Hum Genet **124**(6): 593-605.

Papapetropoulos, S., N. Adi, D. C. Mash, L. Shehadeh, N. Bishopric and L. Shehadeh (2007). "Expression of alpha-synuclein mRNA in Parkinson's disease." Mov Disord **22**(7): 1057-1059; author reply 1057.

Papworth, M., P. Kolasinska and M. Minczuk (2006). "Designer zinc-finger proteins and their applications." Gene **366**(1): 27-38.

Parelho, V., S. Hadjur, M. Spivakov, M. Leleu, S. Sauer, H. C. Gregson, A. Jarmuz, C. Canzonetta, Z. Webster, T. Nesterova, B. S. Cobb, K. Yokomori, N. Dillon, L. Aragon, A. G. Fisher and M. Merkenschlager (2008). "Cohesins functionally associate with CTCF on mammalian chromosome arms." Cell **132**(3): 422-433.

Parsian, A., B. Racette, Z. H. Zhang, S. Chakraverty, M. Rundle, A. Goate and J. S. Perlmutter (1998). "Mutation, sequence analysis, and association studies of alpha-synuclein in Parkinson's disease." Neurology **51**(6): 1757-1759.

Pasanen, P., L. Myllykangas, M. Siitonen, A. Raunio, S. Kaakkola, J. Lyytinen, P. J. Tienari, M. Poyhonen and A. Paetau (2014). "Novel alpha-synuclein mutation A53E associated with atypical multiple system atrophy and Parkinson's disease-type pathology." Neurobiol Aging **35**(9): 2180 e2181-2185.

Pavese, N., V. Metta, S. K. Bose, K. R. Chaudhuri and D. J. Brooks (2010). "Fatigue in Parkinson's disease is linked to striatal and limbic serotonergic dysfunction." Brain **133**(11): 3434-3443.

Peer, D., E. J. Park, Y. Morishita, C. V. Carman and M. Shimaoka (2008). "Systemic leukocyte-directed siRNA delivery revealing cyclin D1 as an anti-inflammatory target." Science **319**(5863): 627-630.

Petersen, K., O. F. Olesen and J. D. Mikkelsen (1999). "Developmental expression of alpha-synuclein in rat hippocampus and cerebral cortex." Neuroscience **91**(2): 651-659.

Phillips, J. E. and V. G. Corces (2009). "CTCF: master weaver of the genome." Cell **137**(7): 1194-1211.

Pihlstrom, L., V. Berge, A. Rengmark and M. Toft (2015). "Parkinson's disease correlates with promoter methylation in the alpha-synuclein gene." Mov Disord **30**(4): 577-580.

Proukakis, C., C. G. Dudzik, T. Brier, D. S. MacKay, J. M. Cooper, G. L. Millhauser, H. Houlden and A. H. Schapira (2013). "A novel alpha-synuclein missense mutation in Parkinson disease." Neurology **80**(11): 1062-1064.

Pruszak, J., W. Ludwig, A. Blak, K. Alavian and O. Isacson (2009). "CD15, CD24, and CD29 define a surface biomarker code for neural lineage differentiation of stem cells." Stem Cells **27**(12): 2928-2940.

Raghavan, R., L. Kruijff, M. D. Sterrenburg, B. B. Rogers, C. L. Hladik and C. L. White, 3rd (2004). "Alpha-synuclein expression in the developing human brain." Pediatr Dev Pathol **7**(5): 506-516.

Rahl, P. B., C. Y. Lin, A. C. Seila, R. A. Flynn, S. McCuine, C. B. Burge, P. A. Sharp and R. A. Young (2010). "c-Myc regulates transcriptional pause release." Cell **141**(3): 432-445.

Ramanan, V. K. and A. J. Saykin (2013). "Pathways to neurodegeneration: mechanistic insights from GWAS in Alzheimer's disease, Parkinson's disease, and related disorders." Am J Neurodegener Dis **2**(3): 145-175.

Rando, O. J. (2012). "Combinatorial complexity in chromatin structure and function: revisiting the histone code." Curr Opin Genet Dev **22**(2): 148-155.

Razin, S. V., A. A. Gavrilov, A. Pichugin, M. Lipinski, O. V. Iarovaia and Y. S. Vassetzky (2011). "Transcription factories in the context of the nuclear and genome organization." Nucleic Acids Res **39**(21): 9085-9092.

Rebollo, A. and C. Schmitt (2003). "Ikaros, Aiolos and Helios: transcription regulators and lymphoid malignancies." Immunol Cell Biol **81**(3): 171-175.

Rettig, G. R. and M. A. Behlke (2012). "Progress toward in vivo use of siRNAs-II." Mol Ther **20**(3): 483-512.

Reyes-Turcu, F. E. and S. I. Grewal (2012). "Different means, same end-heterochromatin formation by RNAi and RNAi-independent RNA processing factors in fission yeast." Curr Opin Genet Dev **22**(2): 156-163.

Reynolds, B. A. and S. Weiss (1992). "Generation of neurons and astrocytes from isolated cells of the adult mammalian central nervous system." Science **255**(5052): 1707-1710.

Reynolds, B. A. and S. Weiss (1996). "Clonal and population analyses demonstrate that an EGF-responsive mammalian embryonic CNS precursor is a stem cell." Dev Biol **175**(1): 1-13.

Rhinn, H., L. Qiang, T. Yamashita, D. Rhee, A. Zolin, W. Vanti and A. Abeliovich (2012). "Alternative alpha-synuclein transcript usage as a convergent mechanism in Parkinson's disease pathology." Nat Commun **3**: 1084.

Richter, J., S. Appenzeller, O. Ammerpohl, G. Deuschl, S. Paschen, N. Bruggemann, C. Klein and G. Kuhlenbaumer (2012). "No evidence for differential methylation of alpha-synuclein in leukocyte DNA of Parkinson's disease patients." Mov Disord **27**(4): 590-591.

Rideout, H. J., P. Dietrich, M. Savalle, W. T. Dauer and L. Stefanis (2003). "Regulation of alpha-synuclein by bFGF in cultured ventral midbrain dopaminergic neurons." J Neurochem **84**(4): 803-813.

Rideout, H. J. and L. Stefanis (2002). "Proteasomal inhibition-induced inclusion formation and death in cortical neurons require transcription and ubiquitination." Mol Cell Neurosci **21**(2): 223-238.

Rinn, J. L. and H. Y. Chang (2012). "Genome regulation by long noncoding RNAs." Annu Rev Biochem **81**: 145-166.

Rockenstein, E., L. A. Hansen, M. Mallory, J. Q. Trojanowski, D. Galasko and E. Masliah (2001). "Altered expression of the synuclein family mRNA in Lewy body and Alzheimer's disease." Brain Res **914**(1-2): 48-56.

Rolland, T., M. Tasan, B. Charloteaux, S. J. Pevzner, Q. Zhong, N. Sahni, S. Yi, I. Lemmens, C. Fontanillo, R. Mosca, A. Kamburov, S. D. Ghiassian, X. Yang, L. Ghamsari, D. Balcha, B. E. Begg, P. Braun, M. Brehme, M. P. Broly, A. R. Carvunis, D. Convery-Zupan, R. Corominas, J. Coulombe-Huntington, E. Dann, M. Dreze, A. Dricot, C. Fan, E. Franzosa, F. Gebreab, B. J. Gutierrez, M. F. Hardy, M. Jin, S. Kang, R. Kiros, G. N. Lin, K. Luck, A. MacWilliams, J. Menche, R. R. Murray, A. Palagi, M. M. Poulin, X. Rambout, J. Rasla, P. Reichert, V. Romero, E. Ruyssinck, J. M. Sahalie, A. Scholz, A. A. Shah, A. Sharma, Y. Shen, K. Spirohn, S. Tam, A. O. Tejeda, S. A. Trigg, J. C. Twizere, K. Vega, J. Walsh, M. E. Cusick, Y. Xia, A. L. Barabasi, L. M. Iakoucheva, P. Aloy, J. De Las Rivas, J. Tavernier, M. A. Calderwood, D. E. Hill, T. Hao, F. P. Roth and M. Vidal (2014). "A proteome-scale map of the human interactome network." Cell **159**(5): 1212-1226.

Ross, G. W., H. Petrovitch, R. D. Abbott, C. M. Tanner, J. Popper, K. Masaki, L. Launer and L. R. White (2008). "Association of olfactory dysfunction with risk for future Parkinson's disease." Ann Neurol **63**(2): 167-173.

Rott, R., R. Szargel, J. Haskin, R. Bandopadhyay, A. J. Lees, V. Shani and S. Engelender (2011). "alpha-Synuclein fate is determined by USP9X-regulated monoubiquitination." Proc Natl Acad Sci U S A **108**(46): 18666-18671.

Rubinsztein, D. C. (2006). "The roles of intracellular protein-degradation pathways in neurodegeneration." Nature **443**(7113): 780-786.

Sander, T. L., A. L. Haas, M. J. Peterson and J. F. Morris (2000). "Identification of a novel SCAN box-related protein that interacts with MZF1B. The leucine-rich SCAN box mediates hetero- and homoprotein associations." J Biol Chem **275**(17): 12857-12867.

Sander, T. L., K. F. Stringer, J. L. Maki, P. Szauter, J. R. Stone and T. Collins (2003). "The SCAN domain defines a large family of zinc finger transcription factors." Gene **310**: 29-38.

Satake, W., Y. Nakabayashi, I. Mizuta, Y. Hirota, C. Ito, M. Kubo, T. Kawaguchi, T. Tsunoda, M. Watanabe, A. Takeda, H. Tomiyama, K. Nakashima, K. Hasegawa, F. Obata, T. Yoshikawa, H. Kawakami, S. Sakoda, M. Yamamoto, N. Hattori, M. Murata, Y. Nakamura and T. Toda (2009).

"Genome-wide association study identifies common variants at four loci as genetic risk factors for Parkinson's disease." Nat Genet **41**(12): 1303-1307.

Savica, R., J. M. Carlin, B. R. Grossardt, J. H. Bower, J. E. Ahlskog, D. M. Maraganore, A. E. Bharucha and W. A. Rocca (2009). "Medical records documentation of constipation preceding Parkinson disease: A case-control study." Neurology **73**(21): 1752-1758.

Schapira, A. H. (2004). "Disease modification in Parkinson's disease." Lancet Neurol **3**(6): 362-368.

Scherzer, C. R., J. A. Grass, Z. Liao, I. Pepivani, B. Zheng, A. C. Eklund, P. A. Ney, J. Ng, M. McGoldrick, B. Mollenhauer, E. H. Bresnick and M. G. Schlossmacher (2008). "GATA transcription factors directly regulate the Parkinson's disease-linked gene alpha-synuclein." Proc Natl Acad Sci U S A **105**(31): 10907-10912.

Schmidt, D., P. C. Schwalie, C. S. Ross-Innes, A. Hurtado, G. D. Brown, J. S. Carroll, P. Flicek and D. T. Odom (2010). "A CTCF-independent role for cohesin in tissue-specific transcription." Genome Res **20**(5): 578-588.

Schumacher, C., H. Wang, C. Honer, W. Ding, J. Koehn, Q. Lawrence, C. M. Coulis, L. L. Wang, D. Ballinger, B. R. Bowen and S. Wagner (2000). "The SCAN domain mediates selective oligomerization." J Biol Chem **275**(22): 17173-17179.

Sexton, T., E. Yaffe, E. Kenigsberg, F. Bantignies, B. Leblanc, M. Hoichman, H. Parrinello, A. Tanay and G. Cavalli (2012). "Three-dimensional folding and functional organization principles of the Drosophila genome." Cell **148**(3): 458-472.

Shahpasandzadeh, H., B. Popova, A. Kleinknecht, P. E. Fraser, T. F. Outeiro and G. H. Braus (2014). "Interplay between sumoylation and phosphorylation for protection against alpha-synuclein inclusions." J Biol Chem **289**(45): 31224-31240.

Shoulson, I., D. Oakes, S. Fahn, A. Lang, J. W. Langston, P. LeWitt, C. W. Olanow, J. B. Penney, C. Tanner, K. Kieburtz and A. Rudolph (2002). "Impact of sustained deprenyl (selegiline) in levodopa-treated Parkinson's disease: a randomized placebo-controlled extension of the deprenyl and tocopherol antioxidative therapy of parkinsonism trial." Ann Neurol **51**(5): 604-612.

Sikorski, T. W. and S. Buratowski (2009). "The basal initiation machinery: beyond the general transcription factors." Curr Opin Cell Biol **21**(3): 344-351.

Simon-Sanchez, J., C. Schulte, J. M. Bras, M. Sharma, J. R. Gibbs, D. Berg, C. Paisan-Ruiz, P. Lichtner, S. W. Scholz, D. G. Hernandez, R. Kruger, M. Federoff, C. Klein, A. Goate, J. Perlmutter, M. Bonin, M. A. Nalls, T. Illig, C. Gieger, H. Houlden, M. Steffens, M. S. Okun, B. A. Racette, M. R. Cookson, K. D. Foote, H. H. Fernandez, B. J. Traynor, S. Schreiber, S. Arepalli, R. Zonozi, K. Gwinn, M. van der Brug, G. Lopez, S. J. Chanock, A. Schatzkin, Y. Park, A. Hollenbeck, J. Gao, X. Huang, N. W. Wood, D. Lorenz, G. Deuschl, H. Chen, O. Riess, J. A. Hardy, A. B. Singleton and T. Gasser (2009). "Genome-wide association study reveals genetic risk underlying Parkinson's disease." Nat Genet **41**(12): 1308-1312.

Singleton, A. B., M. Farrer, J. Johnson, A. Singleton, S. Hague, J. Kachergus, M. Hulihan, T. Peuralinna, A. Dutra, R. Nussbaum, S. Lincoln, A. Crawley, M. Hanson, D. Maraganore, C. Adler, M. R. Cookson, M. Muenter, M. Baptista, D. Miller, J. Blancato, J. Hardy and K. Gwinn-Hardy (2003). "alpha-Synuclein locus triplication causes Parkinson's disease." Science **302**(5646): 841.

Smith, E. R., C. Lin, A. S. Garrett, J. Thornton, N. Mohaghegh, D. Hu, J. Jackson, A. Saraf, S. K. Swanson, C. Seidel, L. Florens, M. P. Washburn, J. C. Eissenberg and A. Shilatifard (2011). "The little elongation complex regulates small nuclear RNA transcription." Mol Cell **44**(6): 954-965.

Snowden, A. W., L. Zhang, F. Urnov, C. Dent, Y. Jouvenot, X. Zhong, E. J. Rebar, A. C. Jamieson, H. S. Zhang, S. Tan, C. C. Case, C. O. Pabo, A. P. Wolffe and P. D. Gregory (2003). "Repression of vascular endothelial growth factor A in glioblastoma cells using engineered zinc finger transcription factors." Cancer Res **63**(24): 8968-8976.

Song, Y., H. Ding, J. Yang, Q. Lin, J. Xue, Y. Zhang, P. Chan and Y. Cai (2014). "Pyrosequencing analysis of SNCA methylation levels in leukocytes from Parkinson's disease patients." Neurosci Lett **569**: 85-88.

Spadafora, P., G. Annesi, A. A. Pasqua, P. Serra, I. C. Ciro Candiano, S. Carrideo, P. Tarantino, D. Civitelli, E. V. De Marco, G. Nicoletti, F. Annesi and A. Quattrone (2003). "NACP-REP1 polymorphism is not involved in Parkinson's disease: a case-control study in a population sample from southern Italy." Neurosci Lett **351**(2): 75-78.

Spillantini, M. G., R. A. Crowther, R. Jakes, M. Hasegawa and M. Goedert (1998). "alpha-Synuclein in filamentous inclusions of Lewy bodies from Parkinson's disease and dementia with lewy bodies." Proc Natl Acad Sci U S A **95**(11): 6469-6473.

Spillantini, M. G., M. L. Schmidt, V. M. Lee, J. Q. Trojanowski, R. Jakes and M. Goedert (1997). "Alpha-synuclein in Lewy bodies." Nature **388**(6645): 839-840.

Spitz, F. and E. E. Furlong (2012). "Transcription factors: from enhancer binding to developmental control." Nat Rev Genet **13**(9): 613-626.

Stefanis, L., N. Kholodilov, H. J. Rideout, R. E. Burke and L. A. Greene (2001). "Synuclein-1 is selectively up-regulated in response to nerve growth factor treatment in PC12 cells." J Neurochem **76**(4): 1165-1176.

Sterling, L., M. Walter, D. Ting and B. Schule (2014). "Discovery of functional non-coding conserved regions in the alpha-synuclein gene locus." F1000Res **3**: 259.

Stern, M. B. (2004). "Dopamine agonists modify the course of Parkinson disease." Arch Neurol **61**(12): 1969-1971.

Stern, M. B., K. L. Marek, J. Friedman, R. A. Hauser, P. A. LeWitt, D. Tarsy and C. W. Olanow (2004). "Double-blind, randomized, controlled trial of rasagiline as monotherapy in early Parkinson's disease patients." Mov Disord **19**(8): 916-923.

Stewart, S. A., D. M. Dykxhoorn, D. Palliser, H. Mizuno, E. Y. Yu, D. S. An, D. M. Sabatini, I. S. Chen, W. C. Hahn, P. A. Sharp, R. A. Weinberg and C. D. Novina (2003). "Lentivirus-delivered stable gene silencing by RNAi in primary cells." RNA **9**(4): 493-501.

Stone, J. R., J. L. Maki, S. C. Blacklow and T. Collins (2002). "The SCAN domain of ZNF174 is a dimer." J Biol Chem **277**(7): 5448-5452.

Surgucheva, I. and A. Surguchov (2008). "Gamma-synuclein: cell-type-specific promoter activity and binding to transcription factors." J Mol Neurosci **35**(3): 267-271.

Surguchov, A. (2008). "Molecular and cellular biology of synucleins." Int Rev Cell Mol Biol **270**: 225-317.

Taatjes, D. J. (2010). "The human Mediator complex: a versatile, genome-wide regulator of transcription." Trends Biochem Sci **35**(6): 315-322.

Tan, E. K., A. Chai, Y. Y. Teo, Y. Zhao, C. Tan, H. Shen, V. R. Chandran, M. L. Teoh, Y. Yih, R. Pavanni, M. C. Wong, K. Puvan, Y. L. Lo and E. Yap (2004). "Alpha-synuclein haplotypes implicated in risk of Parkinson's disease." Neurology **62**(1): 128-131.

Tan, E. K., T. Matsuura, S. Nagamitsu, M. Khajavi, J. Jankovic and T. Ashizawa (2000). "Polymorphism of NACP-Rep1 in Parkinson's disease: an etiologic link with essential tremor?" Neurology **54**(5): 1195-1198.

Tan, E. K., C. Tan, H. Shen, A. Chai, S. Y. Lum, M. L. Teoh, Y. Yih, M. C. Wong and Y. Zhao (2003). "Alpha synuclein promoter and risk of Parkinson's disease: microsatellite and allelic size variability." Neurosci Lett **336**(1): 70-72.

Tan, Y. Y., L. Wu, Z. B. Zhao, Y. Wang, Q. Xiao, J. Liu, G. Wang, J. F. Ma and S. D. Chen (2014). "Methylation of alpha-synuclein and leucine-rich repeat kinase 2 in leukocyte DNA of Parkinson's disease patients." Parkinsonism Relat Disord **20**(3): 308-313.

Thomas, B. and M. F. Beal (2007). "Parkinson's disease." Hum Mol Genet **16 Spec No. 2**: R183-194.

Tofaris, G. K., R. Layfield and M. G. Spillantini (2001). "alpha-synuclein metabolism and aggregation is linked to ubiquitin-independent degradation by the proteasome." FEBS Lett **509**(1): 22-26.

Tootle, T. L. and I. Rebay (2005). "Post-translational modifications influence transcription factor activity: a view from the ETS superfamily." Bioessays **27**(3): 285-298.

Touchman, J. W., A. Dehejia, O. Chiba-Falek, D. E. Cabin, J. R. Schwartz, B. M. Orrison, M. H. Polymeropoulos and R. L. Nussbaum (2001). "Human and mouse alpha-synuclein genes: comparative genomic sequence analysis and identification of a novel gene regulatory element." Genome Res **11**(1): 78-86.

Trenkwalder, C., J. Schwarz, J. Gebhard, D. Ruland, P. Trenkwalder, H. W. Hense and W. H. Oertel (1995). "Starnberg trial on epidemiology of Parkinsonism and hypertension in the elderly. Prevalence of Parkinson's disease and related disorders assessed by a door-to-door survey of inhabitants older than 65 years." Arch Neurol **52**(10): 1017-1022.

Tropepe, V., M. Sibilia, B. G. Ciruna, J. Rossant, E. F. Wagner and D. van der Kooy (1999). "Distinct neural stem cells proliferate in response to EGF and FGF in the developing mouse telencephalon." Dev Biol **208**(1): 166-188.

Ueda, K., H. Fukushima, E. Masliah, Y. Xia, A. Iwai, M. Yoshimoto, D. A. Otero, J. Kondo, Y. Ihara and T. Saitoh (1993). "Molecular cloning of cDNA encoding an unrecognized component of amyloid in Alzheimer disease." Proc Natl Acad Sci U S A **90**(23): 11282-11286.

Urnov, F. D., J. C. Miller, Y. L. Lee, C. M. Beausejour, J. M. Rock, S. Augustus, A. C. Jamieson, M. H. Porteus, P. D. Gregory and M. C. Holmes (2005). "Highly efficient endogenous human gene correction using designed zinc-finger nucleases." Nature **435**(7042): 646-651.

Uversky, V. N. (2007). "Neuropathology, biochemistry, and biophysics of alpha-synuclein aggregation." J Neurochem **103**(1): 17-37.

Valinezhad Orang, A., R. Safaralizadeh and M. Kazemzadeh-Bavili (2014). "Mechanisms of miRNA-Mediated Gene Regulation from Common Downregulation to mRNA-Specific Upregulation." Int J Genomics **2014**: 970607.

van der Putten, H., K. H. Wiederhold, A. Probst, S. Barbieri, C. Mistl, S. Danner, S. Kauffmann, K. Hofele, W. P. Spooren, M. A. Ruegg, S. Lin, P. Caroni, B. Sommer, M. Tolnay and G. Bilbe (2000). "Neuropathology in mice expressing human alpha-synuclein." J Neurosci **20**(16): 6021-6029.

Vaquerizas, J. M., A. Akhtar and N. M. Luscombe (2011). "Large-scale nuclear architecture and transcriptional control." Subcell Biochem **52**: 279-295.

Venda, L. L., S. J. Cragg, V. L. Buchman and R. Wade-Martins (2010). "alpha-Synuclein and dopamine at the crossroads of Parkinson's disease." Trends Neurosci **33**(12): 559-568.

Vescovi, A. L., B. A. Reynolds, D. D. Fraser and S. Weiss (1993). "bFGF regulates the proliferative fate of unipotent (neuronal) and bipotent (neuronal/astroglial) EGF-generated CNS progenitor cells." Neuron **11**(5): 951-966.

Vila, M., S. Vukosavic, V. Jackson-Lewis, M. Neystat, M. Jakowec and S. Przedborski (2000). "Alpha-synuclein up-regulation in substantia nigra dopaminergic neurons following administration of the parkinsonian toxin MPTP." J Neurochem **74**(2): 721-729.

Vogiatzi, T., M. Xilouri, K. Vekrellis and L. Stefanis (2008). "Wild type alpha-synuclein is degraded by chaperone-mediated autophagy and macroautophagy in neuronal cells." J Biol Chem **283**(35): 23542-23556.

Volpicelli-Daley, L. A., K. C. Luk, T. P. Patel, S. A. Tanik, D. M. Riddle, A. Stieber, D. F. Meaney, J. Q. Trojanowski and V. M. Lee (2011). "Exogenous alpha-synuclein fibrils induce Lewy body pathology leading to synaptic dysfunction and neuron death." Neuron **72**(1): 57-71.

von Campenhausen, S., B. Bornschein, R. Wick, K. Botzel, C. Sampaio, W. Poewe, W. Oertel, U. Siebert, K. Berger and R. Dodel (2005). "Prevalence and incidence of Parkinson's disease in Europe." Eur Neuropsychopharmacol **15**(4): 473-490.

Wakamatsu, M., A. Ishii, S. Iwata, J. Sakagami, Y. Ukai, M. Ono, D. Kanbe, S. Muramatsu, K. Kobayashi, T. Iwatsubo and M. Yoshimoto (2008). "Selective loss of nigral dopamine neurons induced by overexpression of truncated human alpha-synuclein in mice." Neurobiol Aging **29**(4): 574-585.

Wang, X., J. S. Pattison and H. Su (2013). "Posttranslational modification and quality control." Circ Res **112**(2): 367-381.

Wang, Y., X. Wang, R. Li, Z. F. Yang, Y. Z. Wang, X. L. Gong and X. M. Wang (2013). "A DNA methyltransferase inhibitor, 5-aza-2'-deoxycytidine, exacerbates neurotoxicity and upregulates Parkinson's disease-related genes in dopaminergic neurons." CNS Neurosci Ther **19**(3): 183-190.

Weiner, W. J. (2004). "Initial treatment of Parkinson disease: levodopa or dopamine agonists." Arch Neurol **61**(12): 1966-1969.

Wendt, K. S., K. Yoshida, T. Itoh, M. Bando, B. Koch, E. Schirghuber, S. Tsutsumi, G. Nagae, K. Ishihara, T. Mishiro, K. Yahata, F. Imamoto, H. Aburatani, M. Nakao, N. Imamoto, K. Maeshima, K. Shirahige and J. M. Peters (2008). "Cohesin mediates transcriptional insulation by CCCTC-binding factor." Nature **451**(7180): 796-801.

Williams, A. J., S. C. Blacklow and T. Collins (1999). "The zinc finger-associated SCAN box is a conserved oligomerization domain." Mol Cell Biol **19**(12): 8526-8535.

Woods, N. T., R. D. Mesquita, M. Sweet, M. A. Carvalho, X. Li, Y. Liu, H. Nguyen, C. E. Thomas, E. S. Iversen, Jr., S. Marsillac, R. Karchin, J. Koomen and A. N. Monteiro (2012). "Charting the landscape of tandem BRCT domain-mediated protein interactions." Sci Signal **5**(242): rs6.

Wright, J. A., P. C. McHugh, S. Pan, A. Cunningham and D. R. Brown (2013). "Counter-regulation of alpha- and beta-synuclein expression at the transcriptional level." Mol Cell Neurosci **57**: 33-41.

Wright, J. E. and R. Ciosk (2013). "RNA-based regulation of pluripotency." Trends Genet **29**(2): 99-107.

Xia, Y., H. A. Rohan de Silva, B. L. Rosi, L. H. Yamaoka, J. B. Rimmler, M. A. Pericak-Vance, A. D. Roses, X. Chen, E. Masliah, R. DeTeresa, A. Iwai, M. Sundsmo, R. G. Thomas, C. R. Hofstetter, E. Gregory, L. A. Hansen, R. Katzman, L. J. Thal and T. Saitoh (1996). "Genetic studies in Alzheimer's disease with an NACP/alpha-synuclein polymorphism." Ann Neurol **40**(2): 207-215.

Xia, Y., T. Saitoh, K. Ueda, S. Tanaka, X. Chen, M. Hashimoto, L. Hsu, C. Conrad, M. Sundsmo, M. Yoshimoto, L. Thal, R. Katzman and E. Masliah (2001). "Characterization of the human alpha-synuclein gene: Genomic structure, transcription start site, promoter region and polymorphisms." J Alzheimers Dis **3**(5): 485-494.

Xilouri, M., O. R. Brekk, N. Landeck, P. M. Pitychoutis, T. Papasilekas, Z. Papadopoulou-Daifoti, D. Kirik and L. Stefanis (2013). "Boosting chaperone-mediated autophagy in vivo mitigates alpha-synuclein-induced neurodegeneration." Brain **136**(Pt 7): 2130-2146.

Xilouri, M., E. Kyratzi, P. M. Pitychoutis, Z. Papadopoulou-Daifoti, C. Perier, M. Vila, M. Maniati, A. Ulusoy, D. Kirik, D. S. Park, K. Wada and L. Stefanis (2012). "Selective neuroprotective effects of the S18Y polymorphic variant of UCH-L1 in the dopaminergic system." Hum Mol Genet **21**(4): 874-889.

Yamamoto, A., J. J. Lucas and R. Hen (2000). "Reversal of neuropathology and motor dysfunction in a conditional model of Huntington's disease." Cell **101**(1): 57-66.

Yamamoto, T. and Y. Tsunetsugu-Yokota (2008). "Prospects for the therapeutic application of lentivirus-based gene therapy to HIV-1 infection." Curr Gene Ther **8**(1): 1-8.

Yang, X. W., C. Wynder, M. L. Doughty and N. Heintz (1999). "BAC-mediated gene-dosage analysis reveals a role for Zipro1 (Ru49/Zfp38) in progenitor cell proliferation in cerebellum and skin." Nat Genet **22**(4): 327-335.

Yang, X. W., R. Zhong and N. Heintz (1996). "Granule cell specification in the developing mouse brain as defined by expression of the zinc finger transcription factor RU49." Development **122**(2): 555-566.

Yankulov, K., J. Blau, T. Purton, S. Roberts and D. L. Bentley (1994). "Transcriptional elongation by RNA polymerase II is stimulated by transactivators." Cell **77**(5): 749-759.

Yien, Y. Y. and J. J. Bieker (2013). "EKLF/KLF1, a tissue-restricted integrator of transcriptional control, chromatin remodeling, and lineage determination." Mol Cell Biol **33**(1): 4-13.

Yuan, S. H., J. Martin, J. Elia, J. Flippin, R. I. Paramban, M. P. Hefferan, J. G. Vidal, Y. Mu, R. L. Killian, M. A. Israel, N. Emre, S. Marsala, M. Marsala, F. H. Gage, L. S. Goldstein and C. T. Carson (2011). "Cell-surface marker signatures for the isolation of neural stem cells, glia and neurons derived from human pluripotent stem cells." PLoS One **6**(3): e17540.

Yue, Y., J. Liu and C. He (2015). "RNA N6-methyladenosine methylation in post-transcriptional gene expression regulation." Genes Dev **29**(13): 1343-1355.

Zarranz, J. J., J. Alegre, J. C. Gomez-Esteban, E. Lezcano, R. Ros, I. Ampuero, L. Vidal, J. Hoenicka, O. Rodriguez, B. Atares, V. Llorens, E. Gomez Tortosa, T. del Ser, D. G. Munoz and J. G. de Yebenes (2004). "The new mutation, E46K, of alpha-synuclein causes Parkinson and Lewy body dementia." Ann Neurol **55**(2): 164-173.

Zhang, N. Y., Z. Tang and C. W. Liu (2008). "alpha-Synuclein protofibrils inhibit 26 S proteasome-mediated protein degradation: understanding the cytotoxicity of protein protofibrils in neurodegenerative disease pathogenesis." J Biol Chem **283**(29): 20288-20298.

Zhou, Q., T. Li and D. H. Price (2012). "RNA polymerase II elongation control." Annu Rev Biochem **81**: 119-143.

Zhu, J., M. Adli, J. Y. Zou, G. Verstappen, M. Coyne, X. Zhang, T. Durham, M. Miri, V. Deshpande, P. L. De Jager, D. A. Bennett, J. A. Houmard, D. M. Muoio, T. T. Onder, R. Camahort, C. A. Cowan, A. Meissner, C. B. Epstein, N. Shoresh and B. E. Bernstein (2013). "Genome-wide chromatin state transitions associated with developmental and environmental cues." Cell **152**(3): 642-654.

Zhu, X., S. M. Ahmad, A. Aboukhalil, B. W. Busser, Y. Kim, T. R. Tansey, A. Haimovich, N. Jeffries, M. L. Bulyk and A. M. Michelson (2012). "Differential regulation of mesodermal gene expression by Drosophila cell type-specific Forkhead transcription factors." Development **139**(8): 1457-1466.

Zolotukhin, S., B. J. Byrne, E. Mason, I. Zolotukhin, M. Potter, K. Chesnut, C. Summerford, R. J. Samulski and N. Muzyczka (1999). "Recombinant adeno-associated virus purification using novel methods improves infectious titer and yield." Gene Ther **6**(6): 973-985.

Zu, T., L. A. Duvick, M. D. Kaytor, M. S. Berlinger, H. Y. Zoghbi, H. B. Clark and H. T. Orr (2004). "Recovery from polyglutamine-induced neurodegeneration in conditional SCA1 transgenic mice." J Neurosci **24**(40): 8853-8861.

Zufferey, R., T. Dull, R. J. Mandel, A. Bukovsky, D. Quiroz, L. Naldini and D. Trono (1998). "Self-inactivating lentivirus vector for safe and efficient in vivo gene delivery." J Virol **72**(12): 9873-9880.

Zufferey, R., D. Nagy, R. J. Mandel, L. Naldini and D. Trono (1997). "Multiply attenuated lentiviral vector achieves efficient gene delivery in vivo." Nat Biotechnol **15**(9): 871-875.

Zuleger, N., M. I. Robson and E. C. Schirmer (2011). "The nuclear envelope as a chromatin organizer." Nucleus **2**(5): 339-349.

APPENDIX

GEORGIA DERMENTZAKI
Diadohou Konstantinou 47, Paiania
Athens, Greece
Tel: +306934765470
E-mail: gdermentzaki@bioacademy.gr

EDUCATION:

Jan 2011 - present   **PhD Candidate**
Project Title: **«*Transcriptional Regulation of α-synuclein»***
Division of Basic Neurosciences, Biomedical Research Foundation
of the Academy of Athens (BRFAA), Athens, Greece

May 2010 - Dec 2010   Project Title: **« *Correlation of Gaucher Disease with α-synuclein*
and Parkinson's Disease»**
Division of Basic Neurosciences, BRFAA, Athens, Greece

Oct 2006 - Feb 2009   **MSc (Biological Sciences):** Degree: *8.9/10*
Project Title: *«**Transcriptional regulation of α-synuclein in the
PC12 cell line and in primary neuronal cultures**»*
University of Athens / Division of Basic Neurosciences-BRFAA,
Athens, Greece

Oct 2005 - Sept 2006   **B.S. Diploma Student (Research year);** Degree**: *10/10*.**
 **Project Title: «*Correlation of the proteasome with neuronal
death and neurodegeneration*»**
Division of Basic Neurosciences-BRFAA, Athens, Greece

Sept 2002 - Sept 2006   **BSc (Biological Sciences)**; Degree: *7.73/10*
University of Athens, Athens, Greece

EXPERTISE

- Cell culture experience in a big variety of cell lines
- Primary neuronal cultures (cortical, hippocampal, sympathetic)
- Western Blot / Immunoprecipitation assay (IP)
- ELISA assay
- Immunocyto / histochemistry assays
- Stereotactic injections in post-natal and adult rats
- Animal Handling / Perfusion
- Cryostat sectioning
- FACS / Sorting
- Fluorescent and confocal imaging

<u>Molecular techniques</u>

- Cloning Techniques (in general)
- RNA / DNA isolation, RT-PCR, qRT-PCR
- Transfections
- Luciferase assay
- Lenti-virus, Adeno-virus and Adeno-Associated-virus construction and production
- CHIP (Chromatin Immunoprecipitation assay)
- 3'-RACE (3'-Rapid Amplification of cDNA endings)

LANGUAGES:

- **Greek** (native)
- **English** (Certificate of Proficiency in English, University of East London)

SPECIALIZED COMPUTER SKILLS:

- Image analysis software: Image J, Photoshop, Gel Analyzer, GraphPad Prism
- Bioinformatics tools: Blast, Clustal W, Genomatix, MatInspector, Genecoder, Primer design tools

SCHOLARSHIPS-AWARDS-DISTINCTIONS:

2003 - 2004	**State Scholarships Foundation**, Department of Biology, University of Athens, Greece
2004 - 2005	**State Scholarships Foundation**, Department of Biology, University of Athens, Greece
September 2010 - 2013	**Irakleitos II,** National Strategic Reference Framework (NSRF)
June 2011	**FEBS travel grant** (summer school), oral presentation
November 2012	**Hellenic Society for Neuroscience**, poster award

INTERNATIONAL CONFERENCE PARTICIPATION

- 36th **FEBS Congress**, Biochemistry for Tomorrow's Medicine, Lingotto Conference Center, Torino, Italy, June 25-30, 2011, Summer School, Oral and poster presentation

- 8th **FENS Forum** of Neuroscience. Barcelona, Spain. 14 – 18 July 2012, poster presentation

- **Keystone Meeting,** Alzheimer's Disease: From Fundamental Insights to Light at the End of the Translational Tunnel (Q8) joint with the meeting on Parkinson's Disease: Genetics, Mechanisms and Therapeutics (Q7), March 2-7, 2014, Keystone Resort, Keystone, Colorado, USA

- 9th **FENS Forum** of Neuroscience. Milan, Italy. 5 - 9 July 2014, poster presentation

PROFESSIONAL MEMBERSHIPS:

- FEBS Society
- FENS Society
- Hellenic Society for Neuroscience

PUBLICATIONS

- **Dermentzaki G**, Dimitriou E, Xilouri M, Michelakakis H, Stefanis L. (2013) «Loss of β-glucocerebrosidase activity does not affect alpha-synuclein levels or lysosomal function in neuronal cells» *PLoS One* 8;8(4):e60674

- **Dermentzaki G,** Argyriou A, Papasilekas T, Moraitou M, Stamboulis E, Vekrellis K, Michelakakis H, Stefanis L. (2012) «Increased dimerization of alpha-synuclein in erythrocytes in Gaucher disease and aging» *Neurosci. Lett.* 528(2):205-9

- Clough RL, **Dermentzaki G**, Haritou M, Petsakou A, Stefanis L (2011) «Regulation of alpha-synuclein expression in cultured cortical neurons». *J Neurochem.* 117(2):275-85

- Clough RL, **Dermetzaki G**, Stefanis L (2009) «Functional dissection of the alpha-synuclein promoter: ZSCAN21 is a key transcriptional regulator». *J Neurochem.* 110(5):1479-90

- **Dermentzaki G**, Lang-Rollin I, Vekrellis K, Xilouri M, Rideout HJ, Stefanis L., (2008) «A novel cell death pathway that is partially caspase dependent, but morphologically non-apoptotic, elicited by proteasomal inhibition of rat sympathetic neurons». *J Neurochem.* 105(3):653-65

REVIEWS

- Reviewer in the Alzheimer & Dementia Journal
- Reviewer in the F1000 Research Journal

REFERENCES

- **Leonidas Stefanis**, MD, PhD, Professor of Neurology and Neurobiology University of Athens Medical School Director, 2nd Department of Neurology Hospital Attikon, Athens, Greece, **email:** lstefanis@bioacademy.gr

- **Panos Politis**, PhD, Investigator - Assistant Professor Level, Center of Biomedical Research Foundation of the Academy of Athens (BRFAA), Greece, **email:** ppolitis@bioacademy.gr

- **Maria Xilouri**, PhD, Investigator-Lecturer Level, Center of Biomedical Research Foundation of the Academy of Athens (BRFAA), Greece, **email**: mxilouri@bioacademy.gr

A novel cell death pathway that is partially caspase dependent, but morphologically non-apoptotic, elicited by proteasomal inhibition of rat sympathetic neurons

Isabelle Lang-Rollin,*,[1] Georgia Dermentzaki,†,[1] Kostas Vekrellis,†,[1] Maria Xilouri,†
Hardy J. Rideout* and Leonidas Stefanis*,†

*Department of Neurology, Columbia University, New York, USA
†Division of Basic Neurosciences, Biomedical Research Foundation of the Academy of Athens, Athens, Greece

Abstract

Proteasomal dysfunction has been linked to neurodegeneration. Pharmacological proteasomal inhibitors may have pro-survival or pro-death effects in neuronal cells. We have previously found that application of such agents to mouse sympathetic neurons leads to activation of the intrinsic apoptotic pathway. We show here that in rat sympathetic neurons proteasomal inhibition leads to a form of death that is morphologically non-apoptotic, with features of autophagy. The intrinsic apoptotic pathway is activated in a delayed fashion compared with mouse neurons, and is in part responsible for death, as evidenced by the partial protective effects of bcl-xL and the general caspase inhibitor Boc-aspartyl-fluoromethylketone. Death is accompanied by induction of Bim and caspase activation, but caspase 3 activation is lacking; 3-methyl-adenine inhibits macroautophagy, but has a relatively small pro-survival effect. We conclude that a complex array of pro- and anti-apoptotic effects elicited by proteasomal inhibition in rat sympathetic neurons leads to partial engagement of the intrinsic apoptotic pathway and a morphologically non-apoptotic, autophagic form of death. The species difference with mouse neurons is underscored by the fact that proteasomal inhibitors are protective against apoptosis elicited by nerve growth factor deprivation in rat, but not mouse, sympathetic neurons. The type of death described herein may be relevant to neurodegenerative diseases, where morphological evidence for apoptosis has been scant.

Keywords: autophagy, Bim, caspase 3 independent, neurodegeneration, protein degradation.

J. Neurochem. (2008) **105**, 653–665.

There is accumulating evidence that proteasomal dysfunction may occur in neurodegenerative diseases, and that it may play a role in disease pathogenesis (Ciechanover and Brundin 2003). The availability of selective pharmacological proteasomal inhibitors has enabled the modeling of proteasomal dysfunction in neuronal cell cultures. We and others have shown that application of such reagents leads to the formation of cytoplasmic inclusions and cell death in various neuronal cell types (reviewed by Rideout and Stefanis 2006; Lang-Rollin and Stefanis 2006). Cell death in such cases demonstrates the biochemical and morphological features of apoptosis (Qiu *et al.* 2000; Rideout *et al.* 2001; Rideout and Stefanis 2002; Lang-Rollin *et al.* 2004; Rideout *et al.* 2005). In particular, as relates to cultured primary neonatal mouse sympathetic neurons, we have found that application of the proteasomal inhibitors Z-IE(OtBu)Ala-Leu-al (PSI) and lactacystin leads to rapid apoptotic death within 24–48 h. This death is accompanied by cytochrome *c* release and

caspase 3 activation, and can be completely blocked by bcl-2 over-expression, the deletion of Bax or the application of the general caspase inhibitor Boc-aspartyl-fluoromethylketone (BAF) (Lang-Rollin *et al.* 2004).

There is however a body of literature that suggests that application of proteasomal inhibitors may also lead to anti-apoptotic effects (reviewed by Canu and Calissano 2006). It is posited that in certain models an early induction of proteasomal activity is necessary to degrade more rapidly key anti-apoptotic molecules and to thus propagate the apoptotic pathway (Canu and Calissano 2006). One of the first demonstrations of this phenomenon was offered by Sadoul *et al.* 1996, who showed that application of the selective proteasomal inhibitor lactacystin led to inhibition of apoptosis induced by nerve growth factor (NGF) deprivation in rat sympathetic neurons. The differential effects of pharmacological proteasomal inhibitors on survival have been attributed in part to the magnitude of proteasomal inhibition achieved and the time length of the exposure (Lin *et al.* 1998; Canu *et al.* 2000; Canu and Calissano 2006; Lang-Rollin and Stefanis 2006).

In view of our findings in mouse sympathetic neurons mentioned above (Lang-Rollin *et al.* 2004) and the reported protective effects of proteasomal inhibitors in rat sympathetic neurons (Sadoul *et al.* 1996), we were interested to examine the effects of proteasomal inhibitors on rat sympathetic neurons. Initial experiments, described herein, showed that such treatment leads to a delayed cell death that does not demonstrate the morphological features of apoptosis. In this manuscript, we have attempted to characterize this interesting cell death pathway, and to ascertain its differences from the classical apoptotic pathways elicited by NGF deprivation in rat sympathetic neurons and by proteasomal inhibition in mouse sympathetic neurons.

Materials and methods

Culture of rat and mouse sympathetic neurons
For the experiments described herein, C57/bL mice and Wistar or Spague–Dawley rats were used. All procedures were approved and followed the regulations of the Institutional Animal Care Committees of Columbia University or of the Biomedical Research Foundation of the Academy of Athens. Sympathetic neuron cultures were derived from sympathetic ganglia of 0- to 1-day-old mouse or rat pups (Stefanis *et al.* 2004). Following trypsinization, the ganglia were plated on 24 wells or 35 mm dishes, in Roswell Park Memorial Institute 1640 medium containing 5% heat-inactivated horse serum and 100 ng/mL mouse NGF (Sigma, St Louis, MO, USA). One day after plating, the antimitotics uridine and 5-fluorodeoxyridine (10 μmol/L each, Sigma) were added.

Transfections and constructs
Over-expression of various genes of interest was achieved by lipofectamine-mediated transfection, using Lipofectamine 2000 (Invitrogen Life Technologies, Carlsbad, CA, USA). Transfection of rat sympathetic neuron cultures was performed 3–6 days after plating, as described previously for mouse sympathetic neurons (Lang-Rollin *et al.* 2004). The enhanced green fluorescent protein (EGFP), myc-tagged PAI2 and Flag-tagged bcl-xL constructs

utilized have been described previously (Lang-Rollin *et al.* 2004, 2005). In co-transfection experiments, we verified that more than 80% of the neurons expressing EGFP also over-expressed bcl-xL (data not shown). We have also transfected neurons with a GFP-LC3 plasmid, kindly provided by Tamotsu Yoshimori, National Institute of Genetics, Japan.

Induction and assessment of neuronal death
At days 3–6 after plating, the proteasomal inhibitors lactacystin (Fenteany *et al.* 1994) or PSI (Figueiredo-Pereira *et al.* 1994) (Calbiochem, San Diego, CA, USA) or vehicle (control, ctl) were added to the sympathetic neuron cultures, with or without the general caspase inhibitor BAF (Sigma) (100 μmol/L). In experiments with the macroautophagy inhibitor 3-methyl-adenine (3-MA; Sigma), this reagent was added at a concentration of 10 mmol/L 24 h after the application of PSI. The poly-ADP ribose polymerase (PARP) inhibitor benzamide (Sigma, diluted in ethanol), was added concurrently with PSI at concentrations of 50 or 150 nmol/L, whereas the permeability transition pore (PTP) inhibitors cyclosporine A and bongkrekik acid were used at concentrations of 1 and 2 μmol/L, respectively. At defined time points, we labeled living cultures with the dye ethidium homodimer (EH; Molecular Probes, Eugene, OR, USA; 1 μmol/L) and the nuclear dye Hoechst 33342 (Sigma, 1 μg/μL) for 20 min. Cultures were rinsed twice with phosphate-buffered saline (PBS), and then visualized at 40× in an inverted fluorescence microscope (Leica DM IRB, Wetzlar, Germany). EH only accumulates in the nucleus of cells with permeabilized cell membranes, and thus labeling with this dye serves as an index of death. We therefore assessed in each case the percentage of neuronal nuclei (Hoechst-positive) that were also EH positive. At least 100 neurons in each well were assessed for EH uptake. As an alternative to EH, in some experiments we also used in a similar fashion propidium iodide (PI; Sigma) at a final concentration of 5 μmol/L.

To perform NGF deprivation, cultures were rinsed twice with serum-free medium, and then complete medium was added together with anti-NGF antibody (Ab) (Upstate Biotechnology, Waltman, MA, USA 1 : 200). NGF deprivation was performed in mouse or rat sympathetic neurons in the presence or absence of lactacystin (1 or 10 μmol/L). Apoptotic death was quantified by assessing the percentage of sympathetic neurons that showed nuclear condensation and formation of chromatin clumps. Twenty-four hours after NGF deprivation the neurons were rinsed in PBS, and then fixed with 3.7% paraformaldehyde at 4°C for 20 min. They were then labeled with the nuclear dye Hoechst 33342 (Sigma, 1 μg/μL) for 20 min, and then rinsed in PBS and visualized in the inverted fluorescence microscope. At least 100 neurons in each well were assessed for features of nuclear apoptosis.

For the assessment of the effect of bcl-xL on survival, we co-transfected this construct or myc-tagged PAI2 MUT as a negative ctl. Thirty-six hours later we applied the proteasomal inhibitors or vehicle, and, 48–72 h later, labeled the cultures with EH, as above. We then counted the percentage of GFP-positive cells that showed EH uptake. At least 50 neurons were counted in each well.

All counts were performed in three separate wells, and are reported as mean ± SEM. They are representative of at least two independent experiments. Representative images were obtained using a SPOT digital camera (Diagnostic Instruments, Inc., Sterling Heights, MI, USA).

Cell labeling and immunostaining

Immunostaining was performed as described previously (Lang-Rollin et al. 2004, 2005). Briefly, neurons plated in 24-well dishes coated with collagen were fixed with paraformaldehyde, as above, and blocked with 10% normal goat serum in PBS, containing 0.4% Triton X-100, followed by incubation with the primary Ab in 2% goat serum in PBS for 1 h at 25°C. Specific antibodies used were: mouse anti-cytochrome c (BD Biosciences Pharmingen, Palo Alto, CA, USA; 1 : 500), anti-GFP (Synaptic Systems, Goettingen, Germany; 1 : 300), anti-Flag (mouse monoclonal M2, Sigma; 1 : 400), anti-Myc (mouse monoclonal, clone 9E10, derived from a hybridoma, 1 : 10), anti-apoptosis inducing factor (AIF) (mouse monoclonal clone E1, 1 : 200; Santa Cruz Biotechnology, Santa Cruz, CA, USA) and rabbit anti-active caspase 3 (R & D Systems, Minneapolis, MN, USA; 1 : 1000). In certain experiments, an LC3 rabbit polyclonal Ab was utilized (a gift from Tamotsu Yoshimori, National Institute of Genetics, Japan; 1 : 500). In this case, fixation was performed with methanol, at −20°C for 5 min, and all subsequent steps of immunostaining were performed in the absence of Triton X-100. Antigens were detected with fluorescent secondary antibodies (1 : 250; Jackson Immuno-Research, West Grove, PA, USA), and the cultures were visualized using standard epifluorescence microscopy with a 40× objective.

We also used the dye caspACE [FITC-VAD-FMK from Promega (Madison, WI, USA), at a final concentration of 10 μmol/L] for assessment of caspase activation. Cultures were exposed for 30 min at 37°C, and then rinsed three times with PBS prior to fixation, as above.

All counts were performed in three separate wells for each condition, with 100 cells counted in each well. Results are reported as mean ± SEM, and are representative of at least two independent experiments. Representative images were obtained using a SPOT digital camera.

Western immunoblotting

Sympathetic neuron cultures in 35-mm dishes were rinsed with PBS, and then triturated off the dish in PBS. Cells were then spun down, and resuspended in a small volume (50–80 μL) of buffer containing 50 mmol/L Tris (pH 7.6), 150 mmol/L NaCl, 2 mmol/L EDTA, and 1% NP-40, supplemented with protease inhibitors (Roche Molecular Biochemicals Inc., Indianapolis, IN, USA). Lysates were left on ice for 20 min, and then centrifuged at 10 000 g to remove insoluble material. Protein concentrations were measured using the Bradford assay (Bio-Rad Laboratories, Hercules, CA, USA). Lysates were combined with 4× sodium dodecyl sulfate (SDS) sample buffer and separated by SDS–polyacrylamide gel electrophoresis. Immuno-blotting was performed using anti-ERK-2 (rabbit polyclonal, Santa Cruz; 1 : 2000), anti-Bax (mouse monoclonal, Santa Cruz; 1 : 1000), anti-Bim (rabbit polyclonal, StressGen, San Diego, CA, USA; 1 : 1000), anti-caspase-2 (anti-Nedd, Troy et al. 1997; at 1 : 500), or anti-X-linked inhibitor of apoptosis protein (XIAP) (MBL, Woburn, MA, USA; 1 : 1000) antibodies. Blocking, application of secondary antibodies and developing of the blots were performed as described previously (Rideout et al. 2001; Rideout and Stefanis 2002; Lang-Rollin et al. 2004).

DNA ladder detection

Both attached and floating cells from sympathetic neuron cultures were centrifuged (800 g, 10 min) and washed with PBS. The pellet was resuspended in a buffer containing 100 mmol/L Tris–HCl, 200 mmol/L NaCl, 10 mmol/L EDTA; pH 8. After addition of an equal volume of digestion buffer (100 mmol/L Tris–HCl, pH 8, 200 mmol/L NaCl, 10 mmol/L EDTA, 0.4% SDS, and 200 μg proteinase K), the cell lysate was incubated at 55°C overnight. Subsequently, DNA was extracted twice with phenol–chloroform and the aqueous phase was treated with Rnase (20 μg/mL). After incubation for 30 min at 37°C, DNA was precipitated with ice-cold ethanol and resolved in water. Yield and purity of DNA were determined by measuring the optical density at 260 and 280 nm. Electrophoresis was carried out on a 1.0% agarose gel and ladder formation of oligonucleosomal DNA (5 μg of each sample) was detected under ultraviolet light.

Electron microscopy

Rat sympathetic neuron cultures were treated either with no additives or with 10 μmol/L PSI for 60 h. The cultures were then rinsed with PBS, and fixed for one hr at 4°C with 2% glutaraldehyde in 2 mmol/L CaCl$_2$, and 100 mmol/L sodium cacodylate. The samples were then processed for electron microscopy as previously described (Stefanis et al. 2001; Lang-Rollin et al. 2003; Rideout et al. 2004).

Statistical analysis

Comparisons were performed using Student's t-test, with the level of significance set at 0.05.

Results

Application of proteasomal inhibitors to rat sympathetic neurons leads to delayed death that is morphologically non-apoptotic

Given the uncertainties about the pro-survival or pro-death effects of proteasomal inhibition on rat sympathetic neurons, we applied the selective proteasomal inhibitors lactacystin (Fenteany et al. 1994) or PSI (Figueiredo-Pereira et al. 1994), or vehicle (ctl) to such cultures. Concentrations of 1 μmol/L of these reagents failed to induce death even after 72 h of application. At the higher concentrations of 10 μmol/L, we did not observe any death for 16–20 h. Some neurons however started to show some loss of their smooth phase-bright appearance, bloating, blebbing and retraction of neuritic processes during this period. Neuronal death started being apparent first after 24 h after the application of the reagents, and was more marked for PSI. Neuronal death due to NGF deprivation occurred more rapidly and was considerably more robust (Fig. 1a and b). Because some neurons that had extensive vacuolization and neurite retraction did not manifest EH or PI incorporation, whereas others, while maintaining phase brightness, showed EH or PI uptake, we have used EH or PI incorporation as an index of cell death in all subsequent experiments, as a more definitive assay for death, instead of counts of phase bright neurons. Interestingly, the morphology of the nuclei of dying neurons was

(a)
(b)
(c)
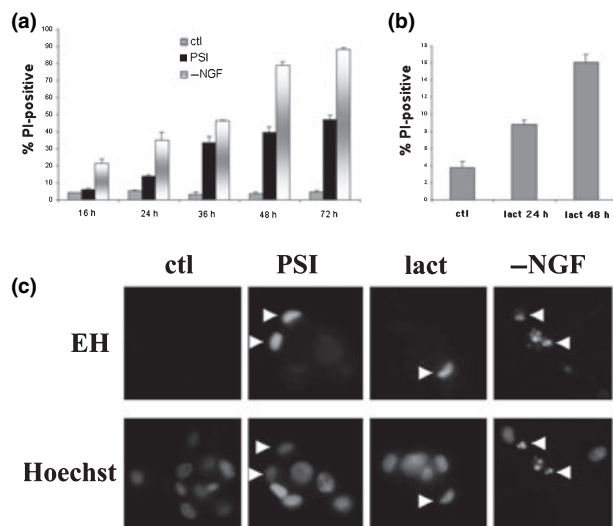
Fig. 1 Application of proteasomal inhibitors to rat sympathetic neurons leads to death with a non-apoptotic nuclear morphology. (a and b) Rat sympathetic neuron cultures were treated either with no additives (control, ctl) or with 10 μmol/L Z-IE(OtBu)Ala-Leu-al (PSI) (a) or 10 μmol/L lactacystin (lact, b), or deprived of nerve growth factor (−NGF, a), as described in Materials and methods. At successive time points after application of the reagents or NGF deprivation, the cultures were incubated with the nuclear dyes propidium iodide (PI) and Hoechst, and the percentage of neurons with Hoechst labeling that showed PI incorporation was assessed ($n = 3$, with at least 100 neurons counted per well for each condition). (c) Rat sympathetic neurons were treated with 10 μmol/L lactacystin or PSI. Sixty hours later the dye ethidium homodimer, together with the nuclear dye Hoechst, was applied to the cultures. Untreated ctl and lactacystin (lact) or PSI-treated cultures were examined in a fluorescence microscope and representative images were obtained. As a positive control for apoptotic morphology of death, cultures were deprived of NGF for 48 h (−NGF). Note the non-apoptotic, ethidium-positive, peanut/crescent-shaped nuclei in the lact and PSI-treated cultures.

largely non-apoptotic. In all experiments, in cultures derived from two different strains of rats (Sprague–Dawley and Wistar), < 10% of dying neurons showed the classical fragmented apoptotic nucleus with apoptotic clumps, that characterizes both the death of mouse sympathetic neurons following proteasomal inhibition (Lang-Rollin *et al.* 2004) and the death of rat sympathetic neurons following NGF deprivation. In contrast, almost all dying neurons displayed uptake of EH in non-apoptotic non-fragmented nuclei that displayed a relatively homogeneous pattern of labelling. Such nuclei were often peanut/crescent shaped. Characteristic examples of lactacystin- and PSI-treated cultures labeled with EH are shown, and contrasted with NGF-deprived cultures (Fig. 1c).

To confirm these results at the ultrastructural level, we assessed cultures treated with PSI by electron microscopy. We were unable to detect any apoptotic profiles in such cultures. However, we detected a significant number of
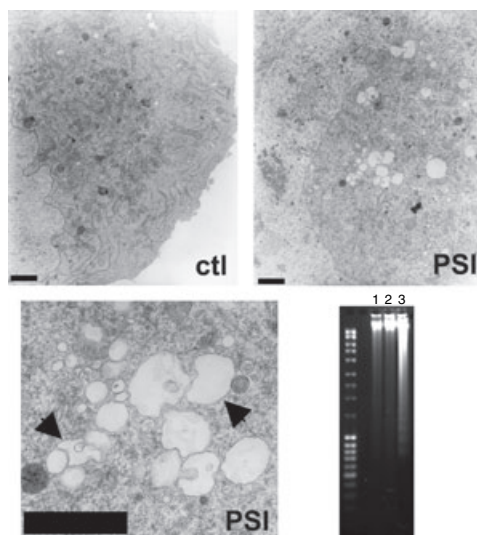

Fig. 2 Z-IE(OtBu)Ala-Leu-al (PSI) application to rat sympathetic neurons leads to non-apoptotic death by ultrastructural criteria. Rat sympathetic neurons were treated with 10 μmol/L PSI or no additives (control, ctl). Sixty hours later the cultures were fixed and processed for electron microscopy. Representative scanned images are shown. The black bar measures 1 μmol/L. Note the peanut/crescent-shaped nucleus in the PSI-treated cultures, with a mild degree of chromatin condensation. The cytoplasm contains a large number of vacuolar structures. A higher power view of these structures is shown in the lower left panel. Arrow heads indicate the presence of double membranes. Bottom left panel: rat sympathetic neuron cultures were treated with 10 μmol/L PSI for 48 h (lane 1), no additives (lane 2), or with 10 μmol/L of the DNA damaging agent camptothecin for 16 h (lane 3). The neurons were then harvested for assessment of DNA laddering, as described in Materials and methods. The lane on the left represents molecular weight markers. Note the appearance of laddering only in the camptothecin-treated cultures (lane 3).

neurons with eccentric, peanut/crescent-shaped nuclei. Such nuclei occasionally showed a small degree of chromatin condensation (Fig. 2, top right panel). In many neurons, extensive vacuolization of the cytoplasm was apparent (Fig. 2, top right panel). On higher power, some, but not all, of the identified vacuolar structures appeared to have double membranes (Fig. 2, bottom left panel). Through random assessment of 20 electron micrograph pictures from PSI-treated cultures and 13 pictures from ctl cultures, we have found that approximately 65% of neurons in PSI-treated cultures exhibit extensive vacuolization, much higher than the background degree of vacuolization seen in ctl cultures.

We also investigated whether the classical hallmark of apoptosis, DNA laddering, was observed in proteasomal inhibitor-treated cultures. Forty-eight hours after PSI application, there was no evidence of DNA laddering (Fig. 2, lower right panel).

We conclude that rat sympathetic neuron cultures treated with PSI or lactacystin die in a delayed fashion, and that this death is morphologically non-apoptotic.

Caspases other than caspase 3 are involved in the death of rat sympathetic neurons exposed to proteasomal inhibitors

Given the evidence for a morphologically non-apoptotic form of death, we were interested to examine next whether caspases participated in this death. Caspase participation is generally synonymous with apoptosis, but there are instances where caspases have been associated with death that is morphologically non-apoptotic (Stefanis 2005). We used two approaches to identify at the single cell level activation of caspases. We labeled the cultures with caspACE, a cell-permeable fluorescence-linked general caspase inhibitor that detects activated caspases that bind to the inhibitor moiety, and then fixed the cultures and performed immunostaining with an Ab specific for the activated form of caspase 3. As a positive ctl, we used NGF-deprived cultures. In such trophic factor-deprived cultures, there was complete concordance between caspACE and caspase 3 activation. In contrast, cultures treated with lactacystin for 50 h showed very little caspase 3 relative to caspACE activation (Fig. 3a–c). Thus, many neurons in lactacystin-treated cultures were caspACE positive, but caspase 3 negative (Fig. 3a). Similar results were achieved with PSI at this time point (data not shown). This was not because of the exact time of sampling because throughout the time course of 16–72 h of exposure to PSI the percentage of neurons with positive staining for activated caspase 3 remained low (Fig. 3d).

Caspase 3-independent death has been linked to death via activation of PARP in the setting of exposure of post-natal cortical neurons to DNA damaging agents (Johnson *et al.* 1999). To ascertain whether PARP activation could be involved in death in this model, we used the well-characterized PARP inhibitor benzamide. At concentrations of 50 and 150 nmol/L, we found no protective effect against PSI-induced death (Fig. 3e). Higher concentrations of benzamide were toxic to the cultures.

To examine whether the caspase activation observed with the caspACE assay was relevant to the death of the cells following proteasomal inhibition, we treated the cultures with the general caspase inhibitor BAF in combination with lactacystin or PSI. We found that BAF, at 100 μmol/L, partially inhibited the death of proteasomal inhibitor-treated neurons (Fig. 4a). BAF diminished the caspACE activation to a commensurate degree (Fig. 4b). We conclude that caspases other than caspase 3 are at least in part involved in death in this model.

Effects of proteasomal inhibitors on mitochondrial function

As caspases appeared to be involved, we wished to examine whether other elements of apoptotic pathways were activated in these cultures following proteasomal inhibition. Events at the level of the mitochondria, such as cytochrome c release and loss of mitochondrial transmembrane potential, are thought to be central in apoptotic pathways (Adams and Cory

2001). We found that both PSI and lactacystin induced these phenomena (Fig. 5a and b). Opening of the PTP, accompanied by release of other pro-apoptotic mitochondrial proteins, such as AIF, is thought to be involved in large-scale DNA fragmentation and non-apoptotic death (Stefanis 2005). We wished to test therefore whether such phenomena could play a role in neuronal death in the current model. We found however that the PTP inhibitors cyclosporine A or bongkrekik acid had no effect on the loss of mitochondrial transmembrane potential or on survival following lactacystin application (Fig. 5c and d). Furthermore, we failed to find evidence for AIF translocation to the nucleus (data not shown).

We conclude that mitochondrial alterations such as cytochrome c release and loss of mitochondrial transmembrane potential occur following proteasomal inhibition of sympathetic neurons. Opening of the PTP and AIF release do not appear to contribute to these phenomena or to neuronal death in this model.

Over–expression of bcl–xL partially protects against cell death and cytochrome *c* release induced by proteasomal inhibitors in rat sympathetic neurons

To examine whether cytochrome c release was regulated, as in other models, by members of the bcl-2 family (Adams and Cory 2001), we over-expressed bcl-xL or a ctl vector, and then treated the cultures with PSI. We found that bcl-xL prevented to a significant extent cytochrome c release (Fig. 6a and b). Furthermore, bcl-xL over-expression was associated with a significant reduction in cell death, commensurate with the effects on cytochrome c release. The effect of bcl-xL on survival was similar to that observed with application of BAF (Fig. 6c and d).

Based on the results with bcl-xL, which showed that bcl-2 family members were involved in death, we wished to examine whether pro-apoptotic members of this family were up-regulated in this model. We found that, similar to mouse sympathetic neurons, the BH3-only protein Bim was up-regulated at the protein level (Fig. 6e). In contrast, Bax levels were unaffected (data not shown). We also wished to examine whether the previously observed lack of caspase 3 activation could be due to induction of an endogenous inhibitor. IAPs, and in particular XIAP, have been shown to play this role (Stefanis 2005). However, we found no induction of XIAP with proteasomal inhibition (Fig. 6e).

We conclude that elements of the intrinsic apoptotic pathway are activated in this model, and are, at least in part, responsible for neuronal cell death.

Macroautophagy occurs in rat sympathetic neurons treated with proteasomal inhibitors, but is not responsible for death

Our electron microscopy results suggested that macroautophagy could be induced in this cell system, given that certain
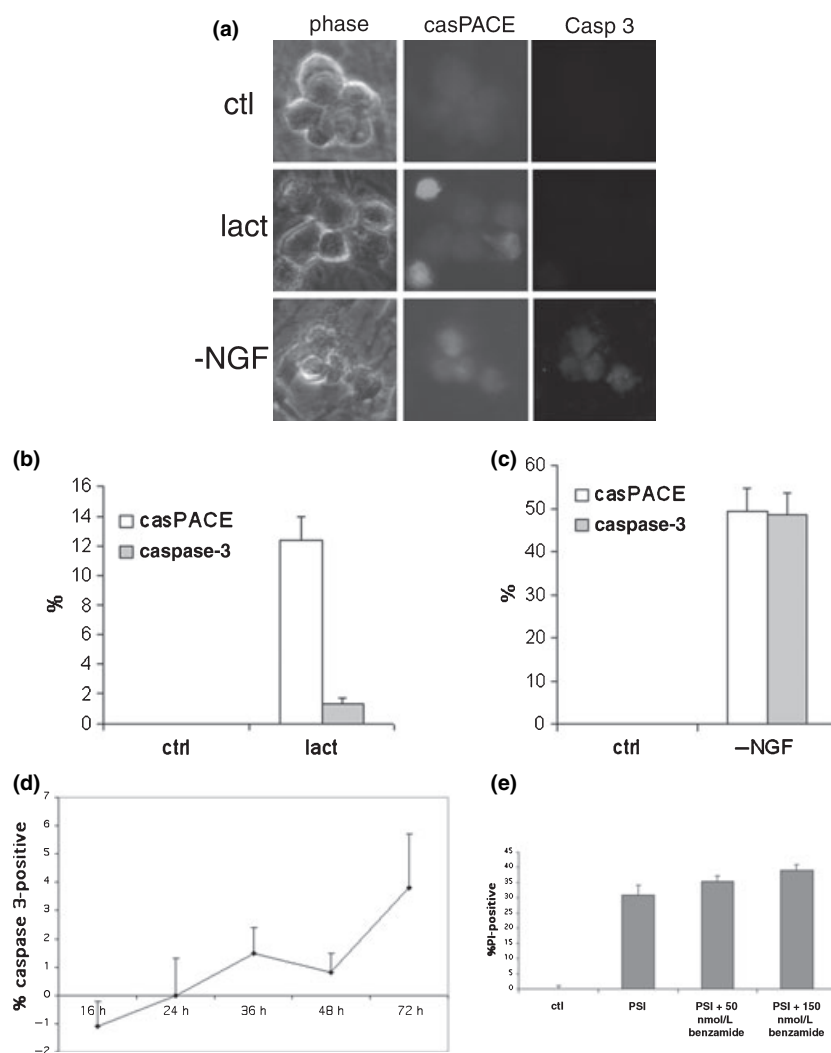
Fig. 3 Application of lactacystin to rat sympathetic neurons leads to activation of caspases other than caspase 3. Rat sympathetic neurons were exposed to no additives (control, ctl) or lactacystin (lact) for 50 h, or deprived of nerve growth factor (NGF) for 40 h, labeled with the caspACE fluorescent compound, and then fixed and immunostained with an antibody (Ab) directed against active caspase 3, and counter-stained with Hoechst. The cultures were then visualized under a fluorescent microscope. In (a), representative images are shown. The percentage of sympathetic neurons that showed caspACE positivity and active caspase 3 immunostaining is reported for lactacystin-treated (b) or NGF-deprived cultures (c). The results reported are the mean ± SEM ($n = 3$, 100 neurons assessed in each of three wells). (d) Rat sympathetic neurons cultures were exposed to either no additives or to 10 μmol/L Z-IE(OtBu)Ala-Leu-al (PSI). At successive time points the cultures were fixed and immunostained with an Ab directed against active caspase 3, and counter-stained with Hoechst. The percentage of activated caspase 3-positive neurons in PSI-treated cultures relative to untreated control cultures is indicated for each time point. (e) Rat sympathetic neurons were exposed for 48 h to either no additives (ctl), 10 μmol/L PSI alone (PSI) or in combination with 50 or 150 nmol/L benzamide, and then assessed for the percentage of neurons with Hoechst labeling that showed propidium iodide (PI) incorporation ($n = 3$, with 100 neurons counted per well for each condition).

of the vacuolar structures identified contained double membranes (Clarke 1990). To examine this further, we first performed transfections with an LC3-GFP vector. LC3 is the mammalian homolog of the yeast autophagy gene Atg8, and is involved in early autophagosome formation. The change of its pattern of localization from a diffuse cytosolic to punctuate indicates conversion of LC3-I to LC3-II, which associates with autophagosomal membranes (Rubinsztein *et al.* 2005). In these experiments we used rapamycin, a known inducer of autophagy (Rubinsztein *et al.* 2005), as a positive ctl. We were unable to see a significant consistent change in the pattern of GFP florescence following the application of rapamycin or proteasomal inhibitors, although in some cases, especially following treatment with PSI, a hint of a punctuate pattern of labeling was observed (data not shown). Immunostaining with a polyclonal LC3 Ab yielded a
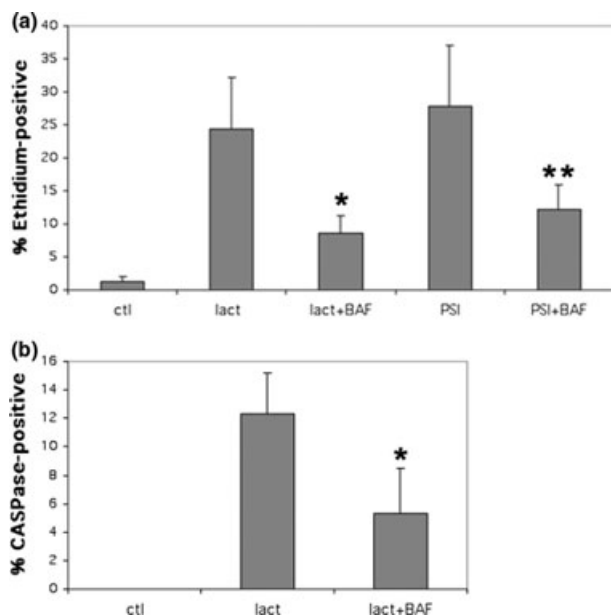
Fig. 4 General caspase inhibition partially prevents death of rat sympathetic neurons exposed to proteasomal inhibition. (a) Rat sympathetic neurons were exposed to no additives (ctl), 10 μmol/L lactacystin or Z-IE(OtBu)Ala-Leu-al (PSI) in the presence or absence of Boc-aspartyl-fluoromethylketone (BAF) (100 μmol/L). Sixty hours later the cultures were assessed for the percentage of neurons that showed ethidium homodimer (EH) uptake. The results reported are the mean ± SEM ($n = 3$, 100 neurons assessed in each of three wells). BAF led to significant inhibition of death induced by lact ($p < 0.05$) or PSI ($p < 0.01$, Student's t-test), *$p < 0.05$ and **$p < 0.01$. (b) Rat sympathetic neurons were exposed to no additives (ctl) or PSI in the presence or absence of BAF (100 μmol/L). Sixty hours later the cultures were labeled with the CASPase compound, and then fixed. The percentage of neurons that showed CASPase positivity was assessed in each case. The results reported are the mean ± SEM ($n = 3$, 100 neurons assessed in each of three wells). BAF led to significant inhibition of CASPase positivity induced by lact ($p < 0.05$, Student's t-test), *$p < 0.05$.

more consistent pattern of punctuate labeling for endogenous LC3 following proteasomal inhibitor application, that was never observed in ctl cultures (Fig. 7a). This pattern however was only seen in a minority of the proteasomal inhibitor-treated cultures. We therefore also used mono-dansyl-cadaverine (MDC) labeling as an alternative method. MDC was thought to label autophagosome structures, but recently it has become clear that it mainly labels late autophagolysosomes (Niemann *et al.* 2000; Rubinsztein *et al.* 2005). We found that in ctl cultures the pattern of MDC labeling was diffuse in all cells. Following rapamycin application, many neurons displayed a punctate pattern of labeling. The application of proteasomal inhibitors led to the appearance of intense labeling of even larger structures. When we applied PSI together with BAF, this labeling pattern was still apparent, indicating that it was not dependent on caspase activation (Fig. 7b).

To examine whether the observed apparent induction of autophagolysosome formation was indeed dependent on macroautophagy, we used the macroautophagy inhibitor 3-MA together with PSI. We indeed observed a 64% reduction in the percentage of neurons that showed globular labeling with MDC compared to cultures treated with PSI alone. Co-administration of 3-MA also significantly ameliorated survival, but the magnitude of this effect was smaller, about 22% (Fig. 7c).

We conclude that there is activation of macroautophagy following proteasomal inhibitor application to sympathetic neurons, but that this activation plays a relatively minor role in death in this model.

Application of proteasomal inhibitors inhibits death induced by NGF deprivation in rat, but not mouse, sympathetic neurons

The above results suggest that in rat sympathetic neurons there is an impediment for the full activation of the apoptotic pathway following proteasomal inhibition. This is likely to manifest at least at two levels, first in the delayed (relative to the mouse system) loss of cytochrome c and second in the relative lack of caspase 3 activation. Sadoul *et al.* (1996) had previously reported that application of lactacystin and PSI to rat sympathetic neurons was actually protective against NGF deprivation-induced death. We wished to examine whether we could reproduce this finding, which has been controversial (Zhai *et al.* 2003), to ascertain whether proteasomal inhibition in these neurons may exert anti-apoptotic effects. In view of the rapid apoptotic death induced by proteasomal inhibitors in mouse sympathetic neurons (Lang-Rollin *et al.* 2004), we have also performed similar experiments in the mouse system, to examine the possibility that there may be a species difference in the induction of such anti-apoptotic responses. In these experiments, we have also used lower doses of lactacystin (1 μmol/L), so as to minimize the induction of pro-death pathways observed with the higher doses.

We find that, as reported by Sadoul *et al.* (1996), proteasomal inhibition with lactacystin leads to an abrogation of the NGF deprivation-induced apoptotic pathway in rat sympathetic neurons. This effect appears to be mediated upstream of cytochrome c release and subsequent caspase 3 activation (Fig. 8a). In contrast, no such effect is discerned in mouse sympathetic neurons (Fig. 8b). If anything, a small additive effect on apoptosis was observed when NGF deprivation and lactacystin were combined.

We conclude that in rat sympathetic neurons application of proteasomal inhibitors leads to an induction of anti-apoptotic signaling, that is likely to play a role in the delayed nature and the altered morphological features of death when proteasomal inhibitors are applied at higher doses. In contrast, in mouse sympathetic neurons, proteasomal inhibition does not lead to an induction of anti-apoptotic effects.
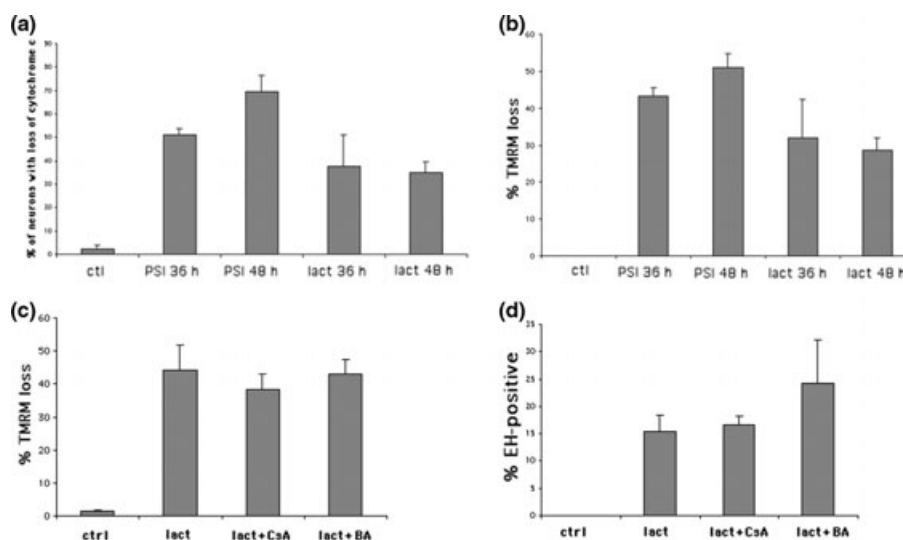
Fig. 5 Proteasomal inhibition in rat sympathetic neurons leads to mitochondrial perturbations. (a and b) Rat sympathetic neurons were treated with no additives, or with 10 μmol/L Z-IE(OtBu)Ala-Leu-al (PSI) or lactacystin for 36 or 48 h. The cultures were then either fixed and immunostained for cytochrome *c* and counter-stained for Hoechst (a), or labeled with the mitochondrial due tetramethylrhodamine methyl ester (TMRM) (b). The percentage of neurons that showed loss of mitochondrial staining for cytochrome *c* (a) or loss of TMRM labeling (b) was assessed for each condition. The results reported are the mean ± SEM (*n* = 3, 100 neurons assessed in each of three wells). (c and d) Rat sympathetic neuron cultures were treated with no additives (ctrl), or with 10 μmol/L lactacystin (lact) alone, or in combination with 1 μmol/L cyclosporine A (CsA) or 2 μmol/L bongkrekik acid (BA). Forty-eight hours later the cultures were labeled with TMRM (c) or EH (d), and the percentage of neurons that showed TMRM loss (c) or EH uptake (d) was assessed in each condition. The results reported are the mean ± SEM (*n* = 3, 100 neurons assessed in each of three wells).

Discussion

The data presented herein indicate that following proteasomal inhibition of rat sympathetic neurons there is an induction of apoptotic signaling, but that the outcome at the morphological level is non-apoptotic death. The morphology that we observe, with the peanut/crescent-shaped nuclei and the cytoplasmic vacuolization, is quite characteristic. We are not aware of similar descriptions of dying cells in the literature. It will be interesting to see whether this, to our knowledge, novel morphology of dying neurons, occurs in other situations, and in particular neuro-degenerative conditions, where proteasomal dysfunction is thought to occur (Ciechanover and Brundin 2003), and where evidence for classical apoptotic morphology has been scant (Stefanis *et al.* 1997). Our findings highlight the discrepancy between morphological apoptosis and apoptotic signaling, and suggest that the lack of morphological apoptosis should not necessarily indicate lack of involvement of apoptotic pathways in neuronal death.

The morphological features of death in this model are likely to be the result of a constellation of effects, but we believe that our data support a scenario in which application of high doses (10 μmol/L) of the proteasomal inhibitors PSI and lactacystin to rat sympathetic neurons leads to the induction of both pro- and anti-apoptotic signaling, as

previously reported in other systems (Lang-Rollin *et al.* 2004; Butts *et al.* 2005; Yew *et al.* 2005). The pro-death signaling eventually prevails, but the death that occurs is delayed, and, when it finally occurs, it is non-apoptotic in morphology. Evidence for this scenario is provided by: (i) the delayed induction of cytochrome *c* release and death in the rat versus the mouse model; (ii) the fact that lactacystin prevents apoptosis induced by trophic deprivation by acting upstream of cytochrome *c* release; and (iii) the dissociation of caspACE versus activated caspase 3 positivity following proteasomal inhibition, but not NGF deprivation. These data point to the idea that following proteasomal inhibition in rat sympathetic neurons, and in parallel to pro-apoptotic signaling, there are at least two anti-apoptotic signals elicited: one that acts at a level prior to cytochrome *c* release, and the other further downstream, at the level of effector caspases.

In experiments in other cellular systems where proteasomal inhibitors have been shown to exert anti-apoptotic functions, their primary site of action has been shown to lie upstream of cytochrome *c* release (Bobba *et al.* 2002). It is likely that proteasomal inhibitors exert these effects, at least in part, by up-regulation of anti-apoptotic factors that are normally degraded by the proteasome. In a recent manuscript, it was proposed that the pro-survival transcription factor MEF2 may be the molecule involved, as it was up-regulated with proteasomal inhibitors in cerebellar granule
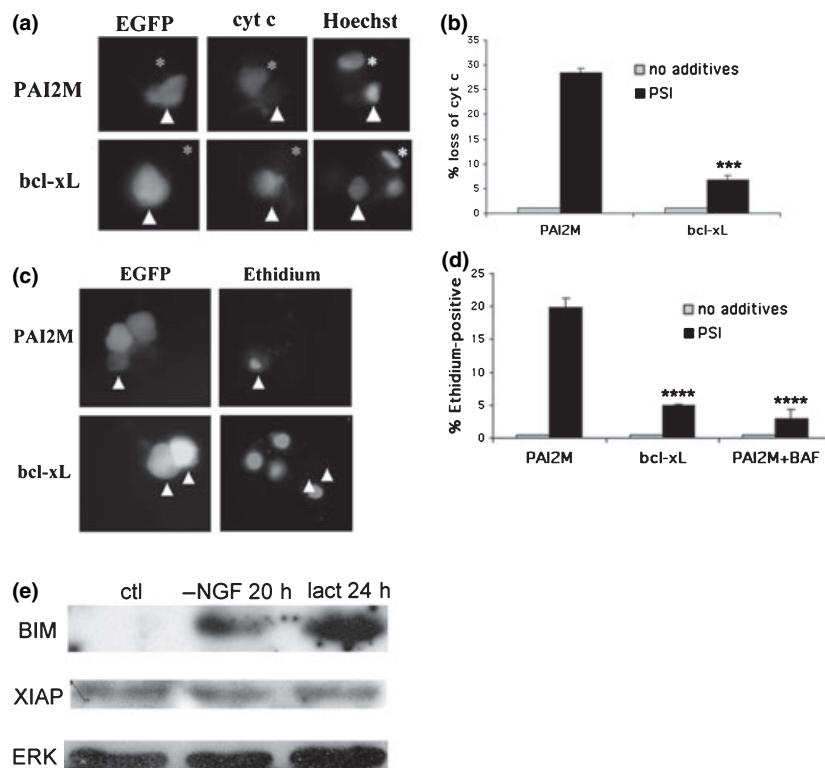
Fig. 6 bcl-xL over-expression prevents cytochrome *c* release and death of proteasomal inhibitor-treated rat sympathetic neurons. (a and b) Rat sympathetic neurons were co-transfected with bcl-xL and EGFP or with PAI2M and EGFP, and 36 h later exposed to either no additives or to 10 μmol/L Z-IE(OtBu)Ala-Leu-al (PSI). Sixty hours later, the cultures were fixed and immunostained for cytochrome *c* and EGFP and counter-stained with the Hoechst nuclear dye. Representative fluorescence photomicrographs of PSI-treated cultures are shown in (a). Arrow heads depict transfected neurons, in the top panel upon co-transfection with PAI2M and in the bottom with bcl-xL. Asterisks depict non-transfected neurons. Note that in the top panel the transfected neuron has lost cyt *c* staining, whereas this is maintained in the bottom panel. The non-transfected neuron in the top panel maintains cyt *c* staining, whereas this is lost in the non-transfected neuron in the bottom panel. The percentage of EGFP-positive neurons that showed loss of mitochondrial staining for cytochrome *c* was assessed for each condition The results reported in (b) are the mean ± SEM ($n = 3$, at least 75 neurons assessed in each of three wells). Bcl-xL co-expression led to significant inhibition of cyt *c* loss induced by PSI when compared to PAI2M ($p < 0.005$, Student's *t*-test), ***$p < 0.005$. (c and d) Rat sympathetic neurons were transfected and treated as above, and 60 h later, the cultures were labeled with ethidium homodimer (EH) and visualized under a fluorescent microscope. EGFP-PAI2M co-transfected cultures were also treated with the combination of PSI and 100 μmol/L BAF. Representative fluorescence photomicrographs of PSI-treated cultures are shown in (c). Arrow heads depict transfected neurons and the corresponding location for the EH dye, in the top panel upon co-transfection with PAI2M and in the bottom with bcl-xL. Note that in the top panel one of the transfected neurons shows EH uptake, whereas this does not occur in the two neurons in the bottom panel. The non-transfected neuron in the top panel maintains cyt *c* staining, whereas this is lost in the non-transfected neuron in the bottom panel. The results reported in (d) are the mean ± SEM ($n = 3$, at least 75 neurons assessed in each of three wells). Bcl-xL co-expression or BAF co-application led to significant inhibition of EH uptake induced by PSI when compared with PAI2M ($p < 0.0005$, Student's *t*-test), ****$p < 0.0005$. (e) Rat sympathetic neurons were treated with no additives or with 10 μmol/L lactacystin for 24 h, and then harvested for western immunoblotting with antibodies (Abs) directed against Bim (top panel) or XIAP (middle panel) or ERK-2 (bottom panel).

neurons induced to undergo death by serum/potassium deprivation (Butts *et al.* 2005). Whatever the nature of these upstream anti-apoptotic effects, they are eventually overwhelmed by pro-death signals, such as the accumulation of Bim, and eventually engagement of the apoptotic pathway at the level of the mitochondria occurs.

The activation of cytochrome *c* release however is not sufficient to fully engage the apoptotic pathway and to lead to an apoptotic morphology in our model. Based on the dissociation between caspase 3 activation and general caspase activation, as judged by caspACE labeling, the lack of apoptotic morphology is likely to be due to an inhibition of specific caspases, including caspase 3. In the absence of such caspase 3-like caspases, other caspases execute death, but this death lacks the morphological features of apoptosis, which likely depend on the presence of caspase 3. This
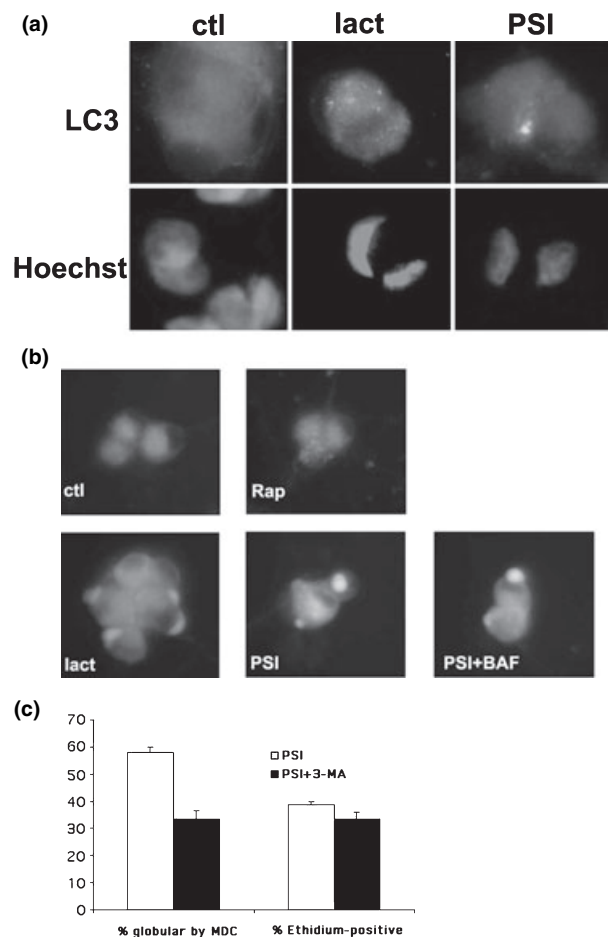
Fig. 7 Macroautophagy induction by application of proteasomal inhibitors to rat sympathetic neurons, but little attenuation of death with a macroautophagy inhibitor. (a) Rat sympathetic neuron cultures were exposed to no additives (control, ctl) or to 10 μmol/L lactacystin (lact) or Z-IE(OtBu)Ala-Leu-al (PSI) for 48 h, and then fixed and immunostained for LC3 (top panel) and co-stained with Hoechst (bottom panel). Cultures were then visualized under a fluorescent microscope. Representative images are depicted. Note the diffuse LC3 staining in control cultures and the appearance of discrete punctate staining in some neurons in cultures treated with proteasomal inhibitors. (b) Rat sympathetic neuron cultures were exposed to rapamycin (rapa, 500 nmol/L), PSI with or without Boc-aspartyl-fluoromethylketone (BAF), or lactacystin (lact) for 48 h, and then labeled with monodansyl-cadaverine (MDC). Cultures were then visualized under a fluorescent microscope. Representative examples are shown. Note the fine, punctuate appearance of the labeling in rapamycin-treated neurons, and the coarser, globular pattern in proteasomal inhibitor-treated neurons. (c) Rat sympathetic neuron cultures were treated with PSI alone, or PSI together with the macroautophagy inhibitor 3-methyl-adenine (3-MA) (10 mmol/L). Of note, 3-MA was added 24 h after PSI application. Sixty hours after PSI application, the cultures were labeled with MDC or ethidium homodimer (EH) and assessed for the percentage of neurons that showed globular-punctate labeling of MDC and EH uptake. The results are the mean ± SEM ($n = 3$, at least 250 neurons assessed per condition in each of three separate experiments); 3-MA significantly inhibited the MDC globular pattern to 36% of cultures treated with PSI alone ($p < 0.01$, paired Student's *t*-test). There was also a significant effect on cell death, as assessed but EH uptake, but the magnitude of this effect was much lower (78% EH-positive neurons compared with cultures treated with PSI alone, $p < 0.01$, paired Student's *t*-test).

scenario is supported by the phenotype in caspase 3 null mice, in which developmental neuronal death does occur, but is morphologically non-apoptotic (Oppenheim *et al.* 2001). In our model, our data with the caspACE labeling and the inhibition of death with BAF indicate that caspases other than caspase 3 are involved in neuronal non-apoptotic death. Whether this is the case in dying neurons in caspase 3 null mice is unknown. We suggest that here again this phenomenon may be due to the up-regulation of a specific caspase 3 (or caspase 9) inhibitor with proteasomal inhibition in rat sympathetic neurons. XIAP was an obvious candidate for such an effect, but immunoblot analysis failed to detect a difference in its expression.

These findings question the absolute link between apoptotic morphology and caspases, and suggest that caspases other than caspase 3 can mediate death that is morphologically non-apoptotic. Similar insights have been gained in other systems. Caspase 2 is an especially interesting candidate in this regard (Yu *et al.* 2003), but in preliminary experiments in our model we have not detected caspase 2 processing by using western immunoblotting (data not shown).

The survival-promoting effects that we have observed with BAF and bcl-xL over-expression have been roughly comparable, and account for an inhibition of 50–75% of death. It is unknown whether the remainder of the dying neurons follow a pathway that is completely different from the classical apoptotic pathway, or whether the lack of a complete effect reflects limitations of the strategies utilized. We believe that the latter possibility is more likely, as BAF did not completely block caspACE labeling in this model, and its effect in this regard was commensurate to its survival-promoting effects.

The vacuoles detected in proteasome inhibitor-treated neurons in our ultrastructural studies suggested the possibility of the induction of macroautophagy in this model. Some of the vacuolar structures appeared to be delimited by double membranes, consistent with this possibility (Clarke 1990; Rubinsztein *et al.* 2005). We performed studies with LC3 immunostaining and LC3-GFP transfections to ascertain whether indeed autophagosomes were formed in this model. The former strategy more consistently showed punctate LC3 labeling with proteasomal inhibition, but this was not a widespread phenomenon. This likely reflects a relative lack of sensitivity of this method in detecting changes, at least in the experimental system that we have utilized, perhaps
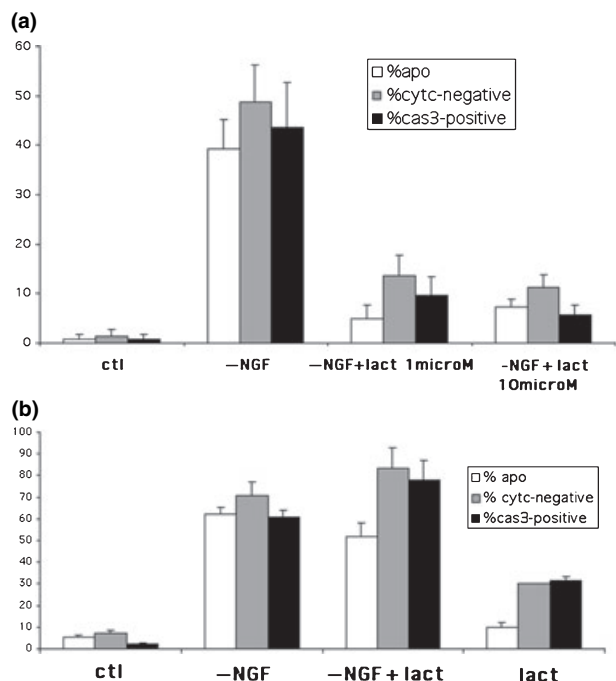
Fig. 8 Proteasomal inhibition prevents nerve growth factor (NGF) deprivation-induced apoptosis in rat, but not mouse sympathetic neurons. (a) Rat sympathetic neuron cultures were either untreated (control, ctl) or deprived of nerve growth factor (−NGF) in the presence or absence of 1 or 10 μmol/L lactacystin. Twenty-four hours later the cells were fixed and immunostained with antibodies against cytochrome *c* and active caspase 3, counter-stained with Hoechst and visualized under a fluorescent microscope. The percentage of sympathetic neurons that showed loss of mitochondrial cytochrome *c* staining, active caspase 3 and apoptotic nuclear morphology is reported for each condition. The results reported are the mean ± SEM ($n = 3$, 100 neurons assessed in each of three wells). (b) Mouse sympathetic neuron cultures were either untreated (ctl) or deprived of NGF in the presence (−NGF + lact) or absence (−NGF) of 1 μmol/L lactacystin, or treated with 1 μmol/L lactacystin alone (lact). Twenty-four hours later the cells were fixed and immunostained with antibodies against cytochrome *c* and active caspase 3, counter-stained with Hoechst and visualized under a fluorescent microscope. The percentage of sympathetic neurons that showed loss of mitochondrial cytochrome *c* staining, active caspase 3 and apoptotic nuclear morphology is reported for each condition. The results reported are the mean ± SEM ($n = 3$, 100 neurons assessed in each of three wells).

because, as suggested by Aviva Tolkovsky, sympathetic neurons may use alternative mammalian isoforms of Atg8 to form autophagosomes (Rubinsztein *et al.* 2005).

To extend the results with LC3 immunolabeling, we also used the dye MDC, which in this cellular system proved to be a more sensitive indicator of macroautophagy induction. Background labeling with this dye in ctl cultures was uniformally diffuse, whereas it became intensely globular and punctate with the application of proteasomal inhibitors.

The use of this reagent to detect autophagosomes is controversial, but, at the very least, it appears to label in part acidic autophagolysosomes (Niemann *et al.* 2000). The fact that the changes observed with proteasomal inhibitors in MDC labeling were in part reversed by the macroautophagy inhibitor 3-MA indicates that these changes reflect ongoing macroautophagy. Despite a marked effect on MDC labeling, 3-MA exerted a relatively smaller effect on death in PSI-treated cultures. This indicates that the process of macro-autophagy has, if anything, a minor impact on death in this model. We have previously achieved similar results in other systems, in which, despite the induction of macroautophagy, macroautophagy inhibition did not impact death (Lang-Rollin *et al.* 2003; Rideout *et al.* 2004). The difference in the results we have obtained and the results of others, that have shown protective effects of 3-MA application in models where macroautophagy occurs (Xue *et al.* 1999; Canu *et al.* 2005), may be that we have always applied 3-MA in a delayed fashion, so as to avoid its non-specific effects on early signaling pathways. In any case, our results in this model indicate that although the morphology of death is autophagic and non-apoptotic, thus qualifying as autophagic, type IIb death, according to the Clarke (1990) nomenclature, the autophagic process is not a major determinant of neuronal death. As we have previously discussed, this does not exclude the possibility that macroautophagy may have a minor role in the current setting, but a more prominent role in neuronal death in other settings.

Our results also show a clear difference between sympathetic neurons derived from mice and rats. This difference cannot be due to different developmental stages, because in both cases we varied the time neurons were cultured prior to the application of proteasomal inhibitors, without any resultant change in the respective death morphologies. The difference was apparent in both the morphology of death and in the differential ability of the proteasomal inhibitors to suppress NGF deprivation-induced death only in the rat cultures. We believe these results can be explained by the presence in the rat, but not the mouse, sympathetic neuron cultures of certain proteins that exert anti-apoptotic effects and that are up-regulated by proteasomal inhibition. Thus, apart from differences in dosing and timing of exposure to proteasomal inhibitors, species differences may account for discrepancies in pro- or anti-apoptotic effects of proteasomal inhibition. It is interesting to note that rat pheochromocytoma PC12 cells, as we have reported (Rideout *et al.* 2001), undergo morphologically apoptotic death when treated with proteasomal inhibitors. However, when these cells are treated with NGF, and assume a neuronal-like phenotype resembling that of sympathetic neurons, and then treated with proteasomal inhibitors, they show a percentage of dying cells with the same non-apoptotic nuclear morphology that we have observed in the rat sympathetic neurons (data not shown). Thus, it is likely that the putative anti-apoptotic

proteins that modify the phenotype of death in rat sympathetic neurons are also induced with neuronal differentiation of PC12 cells.

Acknowledgements

References

Adams J. M. and Cory S. (2001) Life-or-death decisions by the Bcl-2 protein family. *Trends Biochem. Sci.* **26**, 61–66.

Bobba A., Canu N., Atlante A., Petragallo V., Calissano P. and Marra E.(2002) Proteasome inhibitors prevent cytochrome c release during apoptosis but not in excitotoxic death of cerebellar granule neurons. *FEBS Lett.* **515**, 8–12.

Butts B. D., Hudson H. R., Linseman D. A., Le S. S., Ryan K. R., Bouchard R. J. and Heidenreich K. A. (2005) Proteasome inhibition elicits a biphasic effect on neuronal apoptosis via differential regulation of pro-survival and pro-apoptotic transcription factors. *Mol. Cell. Neurosci.* **30**, 279–289.

Canu N. and Calissano P. (2006) Role of the ubiquitin proteasome system during neuronal cell death, in *The Proteasome in Neurodegeneration* (Stefanis L. and Keller J. N., eds), pp. 133–148. Springer, New York.

Canu N., Barbato C., Ciotti M. T., Serafino A., Dus L. and Calissano P. (2000) Proteasome involvement and accumulation of ubiquitinated proteins in cerebellar granule neurons undergoing apoptosis. *J. Neurosci.* **20**, 589–599.

Canu N., Tufi R., Serafino A. L., Amadoro G., Ciotti M. T. and Calissano P. (2005) Role of the autophagic-lysosomal system on low potassium-induced apoptosis in cultured cerebellar granule cells. *J. Neurochem.* **92**, 1228–1242.

Ciechanover A. and Brundin P. (2003) The ubiquitin proteasome system in neurodegenerative diseases: sometimes the chicken, sometimes the egg. *Neuron* **40**, 427–446.

Clarke P. G. (1990) Developmental cell death: morphological diversity and multiple mechanisms. *Anat. Embryol. (Berl.)* **181**, 195–213.

Fenteany G., Standaert R. F., Reichard G. A., Corey E. J. and Schreiber S. L. (1994) A β-lactone related to lactacystin induces neurite outgrowth in a neuroblastoma cell line and inhibits cell cycle progression in an osteosarcoma cell line. *Proc. Natl Acad. Sci. USA* **91**, 3358–3362.

Figueiredo-Pereira M., Berg K. and Wilk S. (1994) A new inhibitor of the chymotrypsin-like activity of the multicatalytic proteinase complex (20S proteasome) induces accumulation of ubiquitin-protein conjugates in a neuronal cell. *J. Neurochem.* **63**, 1578–1581.

Johnson M. D., Kinoshita Y., Xiang H., Ghatan S. and Morrison R. S. (1999) Contribution of p53-dependent caspase activation to neuronal cell death declines with neuronal maturation. *J. Neurosci.* **19**, 2996–3006.

Lang-Rollin I. and Stefanis L. (2006) Mechanisms of neuronal death induced by proteasomal inhibition, in *The Proteasome in Neurodegeneration* (Stefanis L. and Keller J. N., eds), pp. 149–165. Springer, New York.

Lang-Rollin I., Rideout H. J., Noticewalla M. and Stefanis L. (2003) Mechanisms of caspase-independent neuronal death: energy depletion and free radical generation. *J. Neurosci.* **23**, 11015–11025.

Lang-Rollin I., Vekrellis K., Wang Q., Rideout H. J. and Stefanis L. (2004) Application of proteasomal inhibitors to mouse sympathetic neurons activates the intrinsic apoptotic pathway. *J. Neurochem.* **90**, 1511–1520.

Lang-Rollin I., Maniati M., Jabado O., Vekrellis K., Papantonis S., Rideout H. J. and Stefanis L. (2005) Apoptosis and the conformational change of Bax induced by proteasomal inhibition of PC12 cells are inhibited by bcl-xL and bcl-2. *Apoptosis* **10**, 809–820.

Lin K. I., Baraban J. M. and Ratan R. R. (1998) Inhibition versus induction of apoptosis by proteasome inhibitors depends on concentration. *Cell Death Differ.* **5**, 577–583.

Niemann A., Takatsuki A. and Elsasser H-P. (2000) The lysosomotropic agent monodansylcadaverine also acts as a solvent polarity probe. *J. Histochem. Cytochem.* **48**, 251–258.

Oppenheim R. W., Flavell R. A., Vinsant S., Prevette D., Kuan C. Y. and Rakic P. (2001) Programmed cell death of developing mammalian neurons after genetic deletion of caspases. *J. Neurosci.* **21**, 4752–4760.

Qiu J. H., Asai A., Chi S., Saito N., Hamada H. and Kirino T. (2000) Proteasome inhibitors induce cytochrome c-caspase-3-like protease-mediated apoptosis in cultured cortical neurons. *J. Neurosci.* **20**, 259–265.

Rideout H. J. and Stefanis L. (2002) Proteasomal inhibition-induced inclusion formation and death in cortical neurons require transcription and ubiquitination. *Mol. Cell. Neurosci.* **21**, 223–238.

Rideout H. J. and Stefanis L. (2006) Inclusion formation and dissolution following proteasomal inhibition in neuronal cells, in *The Proteasome in Neurodegeneration* (Stefanis L. and Keller J. N., eds), pp. 69–84. Springer, New York.

Rideout H. J., Larsen K. E., Sulzer D. and Stefanis L. (2001) Proteasomal inhibition leads to formation of ubiquitin/α-synuclein immunoreactive inclusions in PC12 cells. *J. Neurochem.* **78**, 899–908.

Rideout H. J., Lang-Rollin I. and Stefanis L. (2004) Involvement of macroautophagy in the dissolution of neuronal inclusions. *Int. J. Biochem. Cell Biol.* **36**, 2551–2562.

Rideout H. J., Lang-Rollin I. C. J., Savalle M. and Stefanis L. (2005) Dopaminergic neurons in rat ventral midbrain cultures undergo selective apoptosis and form fibrillar inclusions, but do not upregulate iHSP70, following proteasomal inhibition. *J. Neurochem.* **93**, 1304–1313.

Rubinsztein D. C., DiFiglia M., Heintz N., Nixon R. A., Qin Z-H., Ravikumar B., Stefanis L. and Tolkovsky A. (2005) Autophagy and its possible role in nervous system diseases, damage and repair. *Autophagy* **1**, 11–22.

Sadoul R., Fernandez P. A., Quiquerez A. L., Martinou I., Maki M., Schroter M., Becherer J. D., Irmler M., Tschopp J. and Martinou J. C. (1996) Involvement of the proteasome in the programmed cell death of NGF-deprived sympathetic neurons. *EMBO J.* **15**, 3845–3852.

Stefanis L. (2005) Caspase-dependent and -independent neuronal death: two distinct pathways to neuronal injury. *Neuroscientist* **11**, 50–62.

Stefanis L., Burke R. E. and Greene L. A. (1997) Apoptosis in neurodegenerative disorders. *Curr. Opin. Neurol.* **10**, 299–305.

Stefanis L., Larsen K. E., Rideout H. J., Sulzer D. and Greene L. A. (2001) Expression of A53T mutant but not wild-type α-synuclein in PC12 cells induces alterations of the ubiquitin-dependent degradation system, loss of dopamine release, and autophagic cell death. *J. Neurosci.* **21**, 9549–9560.

Stefanis L., Wang Q., Oo T., Lang-Rollin I., Burke R. E. and Dauer W. T. (2004) Lack of alpha-synuclein does not alter apoptosis of neonatal catecholaminergic neurons. *Eur. J. Neurosci.* **20**, 1969–1972.

Troy C. M., Stefanis L., Greene L. A. and Shelanski M. (1997) Nedd2 is required for apoptosis after growth factor withdrawal, but not superoxide dismutase (SOD) down-regulation in sympathetic neurons and PC12 cells. *J. Neurosci.* **17**, 1911–1918.

Xue L., Fletcher G. C. and Tolkovsky A. M. (1999) Autophagy is activated by apoptotic signalling in sympathetic neurons: an alternative mechanism of death execution. *Mol. Cell. Neurosci.* **14**, 180–198.

Yew E. H., Cheung N. S., Choy M. S. *et al.* (2005) Proteasome inhibition by lactacystin in primary neuronal cells induces both potentially neuroprotective and pro-apoptotic transcriptional responses: a microarray analysis. *J. Neurochem.* **94**, 943–956.

Yu L. Y., Jokitalo E., Sun Y. F., Mehlen P., Lindholm D., Saarma M. and Arumae U (2003) GDNF-deprived sympathetic neurons die via a novel nonmitochondrial pathway. *J. Cell Biol.* **163**, 987–997.

Zhai Q., Wang J., Kim A., Liu Q., Watts R., Hoopfer E., Mitchison T., Luo L. and He Z. (2003) Involvement of the ubiquitin-proteasome system in the early stages of wallerian degeneration. *Neuron* **39**, 217–225.

Functional dissection of the α-synuclein promoter: transcriptional regulation by ZSCAN21 and ZNF219

Richard Lee Clough,* Georgia Dermentzaki* and Leonidas Stefanis*·†

*Division of Basic Neuroscience, Biomedical Research Foundation of the Academy of Athens, Athens, Greece
†Second Department of Neurology, University of Athens Medical School, Athens, Greece

Abstract

Alpha-Synuclein (SNCA) is an abundant neuronal protein involved in synaptic neurotransmission. SNCA expression levels have been strongly implicated in Parkinson's disease pathogenesis. We have previously demonstrated that in the PC12 cell line elements in intron 1 may mediate SNCA transcriptional regulation in response to neurotrophins. We have now identified transcription factor (TF) binding sites in intron 1 and the 5′-promoter of SNCA. A binding site for the TF zinc finger and SCAN domain containing (ZSCAN)21 in the 5′-region of intron 1 is required for intron 1 transcriptional activity. Small interfering RNA against ZSCAN21 inhibits activation in the luciferase assay and diminishes SNCA protein levels in naïve and neurotrophin-treated PC12 cells and in primary cultured cortical neurons, demonstrating that ZSCAN21 is a novel transcriptional regulator of SNCA in neuronal cells. The 5′-promoter of SNCA has a complex architecture, including multiple binding sites for the TF zinc finger protein (ZNF)219, which functions as both an activator and a repressor. Targeting ZSCAN21 or other TFs controlling SNCA transcriptional activity may provide novel therapeutic avenues not only for Parkinson's disease but also for other synucleopathies.

Keywords: α-synuclein, cortical neurons, neurotrophins, Parkinson's disease, PC12.

J. Neurochem. (2009) 110, 1479–1490.

Parkinson's disease (PD) is a common neurodegenerative disease whose symptoms include tremor, rigidity, bradykinesia and abnormalities of posture and gait (Shastry 2003). Pathologically PD is characterized by substantia nigra neuronal degeneration, leading to striatal dopamine deficiency, although more widespread neuronal degeneration also occurs (Braak et al. 2003). Surviving neurons harbor Lewy bodies containing accumulations of α-synuclein (SNCA), ubiquitin, and neurofilament (Surguchov 2008). Mutations in specific genes leads to familial forms of PD (Cookson et al. 2008); of these genes, SNCA was the first to be linked to PD through the identification of the A53T mutation (Polymeropoulos et al. 1997); two further missense point mutations have been described (Krüger et al. 1998; Zarranz et al. 2004).

In addition to this link between SNCA mutations and PD, there is also evidence indicating that over-expression of wild-type SNCA is sufficient to cause the disease. Over-expression of wild-type SNCA leads to phenotypes resembling PD in various animal models (Feany and Bender 2000; Masliah et al. 2000; Kirik et al. 2002). Triplications (Singleton et al. 2003) and duplications (Chartier-Harlin et al. 2004) of the SNCA gene locus lead to PD in a dose-dependent fashion. Polymorphisms in the promoter sequence, in particular the non-amyloid component of plaques (NACP)-REP1 dinucleotide repeat, located 10.7 kb upstream of the SNCA gene, and in 3′-regions of SNCA confer susceptibility to developing PD in case/control studies (Chiba-Falek and Nussbaum 2001; Farrer et al. 2001; Pals et al. 2004; Mueller et al. 2005; Maraganore et al. 2006). However, it is not known if the non-amyloid component of plaques (NACP)-REP1 polymorphism is responsible for this increased risk or if it is in linkage disequilibrium with the actual causative agent.

There has been controversy regarding the expression levels of SNCA in the brains of sporadic PD patients, with a number

of studies reporting both increased and decreased levels of SNCA (Rockenstein *et al.* 2001; Kingsbury *et al.* 2004; Chiba-Falek *et al.* 2006; Dachsel *et al.* 2007; Papapetropoulos *et al.* 2007). However, in an elegant study, laser-captured microdissection clearly demonstrated significantly elevated SNCA mRNA levels in individual, surviving neuromelanin- and tyrosine hydroxylase-positive substantia nigra dopaminergic neurons from idiopathic PD brains (Gründemann *et al.* 2008).

In certain mouse models of neurodegenerative diseases, reversal of expression of the causative proteins can ameliorate neurodegeneration, including in an inducible model of SNCA over-expression (Yamamoto *et al.* 2000; Zu *et al.* 2004; Nuber *et al.* 2008), indicating that if expression of SNCA can be controlled then certain aspects of the disease phenotype can be halted and even reversed.

We have used the model system of rat pheochromocytoma PC12 cells to examine the transcriptional control of SNCA. This model system is often used to study the mechanisms of neurotrophin-mediated differentiation of proliferating neuronal precursors to post-mitotic, differentiated neuron-like cells, which possess many characteristics of sympathetic neurons (Greene and Tischler 1976). We had initially determined that SNCA was transcriptionally up-regulated in this model (Stefanis *et al.* 2001), and, proposed that intron 1 is an important transcriptional control region of the SNCA gene (Clough and Stefanis 2007), as was independently confirmed (Scherzer *et al.* 2008). In this study, we provide evidence that the transcription factor (TF) zinc finger and SCAN domain containing (ZSCAN)21, which binds to a site within intron 1, is a key regulator of SNCA transcription. We have also expanded our study to the characterization of the 5′-promoter region and identified a role for the TF zinc finger protein (ZNF)219, which can function as both a transcriptional repressor and activator. Such studies further advance our understanding of the transcriptional regulation of SNCA and offer the potential for modulation of SNCA levels within neuronal cells.

Materials and methods

Cell culture

PC12 cells were cultured as previously described (Stefanis *et al.* 2001) on rat-tail collagen coated tissue culture dishes in RPMI-1640 medium (Sigma, St Louis, MO, USA) supplemented with 5% heat-inactivated fetal bovine serum, 10% heat-inactivated horse serum, 200 μM L-glutamine, and 1% penicillin/streptomycin (complete medium). PC12 cells were differentiated in complete medium containing either 50 ng/mL recombinant human nerve growth factor (NGF; a generous gift from RINAT Neuroscience, Paolo Alto, CA, USA) or 50 ng/mL basic fibroblast growth factor (bFGF; Sigma). For experiments using the kinase inhibitors, cells were pre-incubated with the inhibitors for 45 min prior to the addition of the neurotrophins. U0126 was added to the complete media at a concentration of

25 μM. The following inhibitors (Sigma) were also used: LY294002 (25 μM), SP600125 (10 μM), and SB203580 (30 μM).

Primary neuronal cultures

Cultures of Wistar rat (embryonic day 18) cortical neurons were prepared as previously described (Dietrich *et al.* 2003); 1.5×10^6 cells were plated onto poly-D-lysine-coated six-well dishes. Cells were maintained in Neurobasal medium (Gibco, Rockville, MD, USA; Invitrogen, Carlsbad, CA, USA), with B27 serum-free supplements (Gibco; Invitrogen), L-glutamine (0.5 mM), and penicillin/streptomycin (1%). More than 98% of the cells cultured under these conditions represent post-mitotic neurons (Rideout and Stefanis 2002).

Cloning/subcloning

The following clones were generated with a PCR approach from previously cloned constructs (Chiba-Falek and Nussbaum 2001; Clough and Stefanis 2007). Del ZSCAN21 was cloned from intron 1 with the following primers: F, 5′-TACCTGTGGATC-TAAACGGGCGTCTT-3′ and R, 5′-CCTTTACACCACACTG-GAAAAC-3′. The H5′-2 kb (F, 5′-AGGGACACAACATCTGA-GCA-3′), H5′-1 kb (F, 5′-AGGGACACAACATCTGAGCA-3′), and 1.8 kb (F, 5′-CTCCCGATCTCCACAAGAGT-3′) constructs were also cloned via PCR from the previously described constructs (Chiba-Falek and Nussbaum 2001) with a common reverse primer in the first exon (Ex1-R- 5′-AAAGGCA-GAAGGCTTGAAGG-3′). H5′-352 bp was digested from the H5′-2 kb construct in TOPO-TA® (Invitrogen) with the enzymes *Sma*I and *Spe*I. The *Spe*I site was blunt-ended using Klenow (Promega, Madison, WI, USA) and the fragment was then subcloned into the pGL3 basic (Promega) *Sma*I site.

The rat R5′-452 bp promoter was cloned with a PCR approach from genomic DNA extracted from the PC12 cell line (F, 5′-TTCGGGGTTAAAACAAATGG-3′ and R, 5′-TTCCTCCTGTT-TTCCCCAAT-3′). All constructs were sequenced to verify the accuracy of the PCR. All sequences generated by PCR were initially cloned into the TOPO-TA® vector (Invitrogen) and then subcloned into the pGL3-basic luciferase vector (Promega).

Small–scale deletion constructs

Sequential 5′-deletions of the SNCA promoter and intron 1 were made with the Erase-a-Base system (Promega) according to the manufacturer's instructions. Briefly, 10 μg of plasmid was linearized and then digested with exonuclease III in a timed manner to generate deletions of a certain size. Following digestion, plasmids were religated and transformed into bacteria. The end points of the deletions were determined by sequencing. The deleted inserts were then subcloned into the pGL3-basic luciferase vector (Promega) for use in the luciferase assay.

Transfection and luciferase assay

All transfections were performed using Lipofectamine 2000 (Invitrogen) according to the manufacturer's instructions and as previously described (Clough and Stefanis 2007). For the luciferase assays, all promoter sequences were cloned into the pGL3-basic luciferase vector (Promega); this plasmid was also used as the empty-control vector in these assays. Briefly, for the luciferase assay, all transfections were performed in six-well tissue

culture dishes with 2.0×10^5 cells/well with 2.0 µg per well of target vector and 0.5 µg of thymidine kinase-renilla (internal control). In all luciferase assays, the cells were harvested at day 2.5 post-transfection. All transfections were performed overnight and complete medium was added the following day. Samples for western immunoblotting were harvested 48 h post-transfection. For the small interfering RNA (siRNA) experiments, 25 nM siRNA was co-transfected with the target luciferase vector. The following siRNAs were used (all from Qiagen, Valencia, CA, USA): Zipro1 (ZSCAN21; #186910), ZNF219 (#1869160), and All Star Negative Control (#1027281).

Luciferase assays were detected with the Dual Luciferase Assay (Promega) according to the manufacturer's instructions. Graphs show the mean value of at least three experiments with error bars depicting the SEM. All values were calculated relative to the screened vector in untreated PC12 cells.

We (Clough and Stefanis 2007) and others (Madziar *et al.* 2005) have observed a two- to threefold induction for the empty pGL3-basic luciferase vector in the presence of both NGF and bFGF in the PC12 cell line. All statistical analyses were performed to account for the level of activation observed in pGL3-basic.

RT–PCR assay

Total RNA was extracted from PC12 cells on day 3 following the start of treatment using Trizol (Invitrogen). cDNA was generated with the Reverse Transcription System (Promega) according to the manufacturer's instructions. We then performed RT-PCR, using the cDNA as a template. In preliminary experiments, all primer pairs were optimized to be in the log-exponential phase of amplification. The following primers were used to perform the PCR: α-SNCA, F 5′-TTCTGCGGAAGCCTAGAGAG-3′ and R 5′-TCCTCCAA-CATTTGTCACTTGC-3′*; β-actin, F 5′-TCACCATGGATGATGA-TATCGCC-3′* and R 5′-CCACACGCAGCTCATTGTAGAAGG-3′*; ZSCAN21, F 5′-CAGAAGCAGTCTTGGGAGAA-3′ and R 5′-TCTCCCTTTCCAGGTTGTTG-3′; ZNF219, F 5′-CCCCTT-CTGTGGGAAATCTT-3′ and R 5′-CAGGTAGCAGAGGCCT-GAGT-3′; and hepatocyte nuclear factor 4 (HNF4), F 5′-TAG-CAGAGATGAGCCGTGTG-3′ and R 5′-GAGTCATACTGCC-GGTCGTT-3′ (all primers marked * from Baptista *et al.* 2003). Products were subsequently resolved on 1.5% agarose gels stained with ethidium bromide.

Western immunoblotting

PC12 cells were washed twice in phosphate-buffered saline and then harvested in lysis buffer (150 mM NaCl, 50 mM Tris pH 7.6, 0.1% sodium dodecyl sulfate, 1% NP-40 (Sigma), and 2 mM EDTA). Protein concentrations were determined using the Bradford method (Bio-Rad, Hercules, CA, USA). Fifty microgram of lysates were mixed with 2x Laemmli buffer prior to running on 12% sodium dodecyl sulfate–polyacrylamide gels. Following transfer to a nitro-cellulose membrane, blots were probed with antibodies directed against: (i) SNCA (BD Biosciences, San Jose, CA, USA) and (ii) extracellularly regulated kinase (ERK) (Santa Cruz Biotechnol-ogy, Santa Cruz, CA, USA). Blots were probed with horseradish peroxidase-conjugated secondary antibodies and visualized with Western Lightning (Perkin Elmer, Waltham, MA, USA) and exposed to Super RX film (Fuji Film, Fuji USA, Valhalla, NY, USA). Following scanning of the images with Adobe Photoshop (Adobe

Systems Inc., San Jose, CA, USA), IMAGEJ software (Abramoff *et al.* 2004) was used to quantify the intensity of the bands.

Electromobility shift assay

Double-stranded probes were designed for the human TF binding sites identified in MATINSPECTOR (Cartharius *et al.* 2005) for ZSCAN21 (5′-GACGAGGGGTAGGGGGTGGTCCC-3′), ZNF219 (5′-GACGA-GGGGTAGGGGGTGGTCCC-3′), HNF4 (5′-CGAATGTCTCCT-TTGGGCCATGGGA-3′), Sp1 (5′-ATTCGATCGGGGCGGGGC-GAGC-3′), and Oct1 (5′-TGTCAATGCAAATCACTAGAA-3′). Probes were 3′-labeled with biotin (Biotin 3′-End DNA Labeling Kit; Pierce, Rockford, IL, USA). For electromobility shift assay (EMSA), 20 fmol labeled double-stranded oligonucleotides were incubated in Parker buffer (8% Ficoll, 20 mM HEPES, pH 7.9, 50 mM KCl, 1 mM EDTA, and 0.5 mM dithiothreitol), 1 µg poly(dI/dC), 12 µg of nuclear extract and incubated at 21°C for 20 min. Samples were resolved on a 4% non-denaturing acrylamide gel at 4°C, transferred to Hybond N+ membrane (Amersham Biosciences, GE Healthcare, Piscataway, NJ, USA) and developed (LightShift Chemi-luminescent EMSA Kit; Pierce; Clough *et al.* 2004).

Cell sorting

PC12 cells (1.0×10^7 cells) were transiently co-transfected with 25 nM siRNA (ZSCAN21, ZNF219, or scrambled control) and 5 µg enhanced green fluorescent protein (EGFP) in 10 cm tissue culture dishes. Cells were harvested and resuspended in phosphate-buffered saline with 10% fetal bovine serum and 0.5 mM EDTA to a final concentration of 1.0×10^7 cells/mL. Non-transfected PC12 cells were used to choose the starting pool of cells for sorting and to determine the threshold of green fluorescence. By using the 488 nm laser Coherent Sapphire solid state of BD FACSaria Cell Sorter, green cells were detected at the emission spectrum of FITC (515–545 nm), similar to that of EGFP. The sorted samples were used to gen-erate cell lysates for western immunoblotting (Kyratzi *et al.* 2008).

Immunocytochemistry and SNCA quantification

Rat cortical neuron cultures from embryonic day 16 fetuses were plated onto poly-D-lysine-coated 24-well plastic dishes for immuno-cytochemistry at a density of 1.5×10^5 cells/well. Cultured neurons were transiently transfected at day 8 with 0.5 µg EGFP and 25 nM of each siRNA (scrambled control, ZSCAN21, or ZNF219). After 48 h, cells were fixed in 3.7% *p*-formaldehyde for 15 min at 4°C and then blocked for 45 min with 10% normal goat serum with 0.4% Triton X-100, followed by incubation with the following primary antibodies overnight at 4°C: SNCA (BD Biosciences) and GFP rabbit polyclonal (Synaptic Systems, Goettingen, Germany). Following incubation with fluorescent secondary antibodies (Cy2 or Cy3; Jackson Immuno Research, West Grove, PA, USA) for 50 min at 21°C, nuclei were visualized with Hoechst 33258 (1 µM; Sigma). To determine the relative changes in SNCA expression ~100 photos per condition were taken from four wells of EGFP-transfected cells. SNCA levels were measured as intensity mean by the IMAGEJ program for all EGFP-transfected cells per condition. Mean intensities for each siRNA were then binned together for analysis (10 units/bin).

Statistics

Statistical analysis was performed using the Student's *t*-test for single analyses. Where multiple testing was required, a one-way

ANOVA test was utilized, with a *post hoc* Tukey's Honestly Significant Difference (HSD) test. Values of $p < 0.05$ were considered significant. All statistical analyses were performed using the GRAPHPAD PRISM 4 suite of software (GraphPad Software, Inc., San Diego, CA, USA).

Results

Identification and characterization of SNCA intron 1 transcriptional response elements

We had previously identified two regions in the first intron of SNCA that confer the neurotrophin-based luciferase response in PC12 cells by generating large-scale deletion constructs
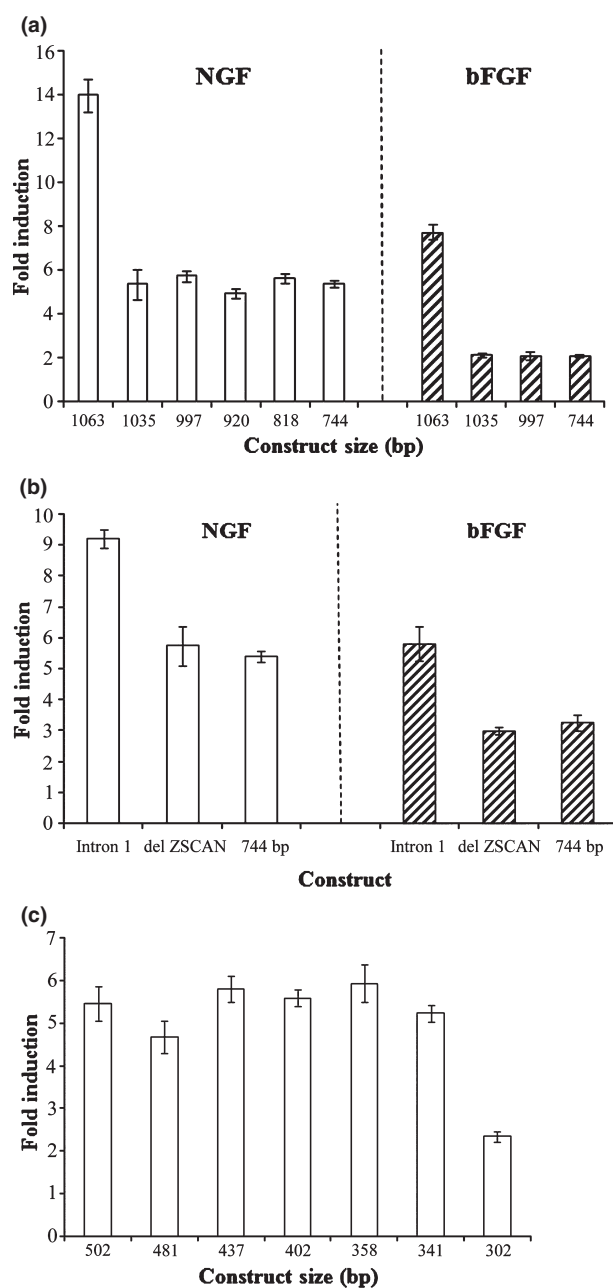
that divided the full-length human intron (1063 bp) into four quadrants: an element that was responsive to both NGF and bFGF treatment was located in the 319 bp first quadrant (1063–744 bp) at the 5′-end of the intron; there was also an NGF-only-responsive element located in the 194 bp third quadrant (502–302 bp) (Clough and Stefanis 2007).

We generated a series of small-scale deletion clones in these areas to localize TF binding sites. For the first quadrant, the level of activation in the luciferase assay upon treatment with NGF or bFGF significantly drops upon deletion of the first 28 bp of this sequence ($p < 0.001$; Fig. 1a). The level of activation observed for this first clone was not significantly different from any of the sequential deletion constructs and is at the same level as when the entire first quadrant is deleted (744 bp construct). These data indicated that both the NGF and bFGF response elements are located in the same 28 bp region and may be the same site.

Cross-species alignment (CLUSTALW; Larkin *et al.* 2007) and MATINSPECTOR analysis in this 28 bp region (with human, rat, and mouse sequences) identified three conserved TF binding sites for the TFs: zinc finger- and scan domain-containing protein 21 (ZSCAN21), paired box gene 1, and forkhead box N1. To identify which of these binding sites was responsible for the induction observed in the luciferase assay, we deleted the 6 bp binding site for

Fig. 1 Localization of intron 1 response elements. Luciferase assays for NGF (open columns) and bFGF (hashed columns) treated PC12 cells. (a) PC12 cells were transfected with a series of deletion constructs, cloned into a luciferase vector, covering the first quadrant of SNCA intron 1; following transfection, the cells were treated with NGF or bFGF and harvested for the luciferase assay 2.5 days later. Induction is shown relative to the same construct in naïve PC12 cells. Fold induction of luciferase activity was reduced for all deletion constructs compared with the full-length intron 1 sequence (1063 bp) for both NGF and bFGF treatment ($p < 0.001$); there were no significant differences between consecutive constructs. (b) PC12 cells transfected with the full-length intron 1 sequence (Intron 1), intron 1 minus the ZSCAN21 binding site (del ZSCAN), or a construct lacking the first quadrant of intron 1 (744 bp). Cells were treated with NGF for 2.5 days and then assayed for luciferase activity. We observed a significant reduction of activation between the full-length intron 1 sequence and the del ZSCAN and 744 bp constructs (NGF: $p < 0.01$ and bFGF: $p < 0.001$). There were no significant differences in the levels of activation between the del ZSCAN and 744 bp constructs for either NGF or bFGF treatment, where Intron 1, full-length intron 1 (1063 bp); del ZSCAN, intron 1 with the ZSCAN21 site deleted; 744 bp, intron 1 lacking the first quadrant. (c) PC12 cells were transfected with a series of deletion constructs covering the third quadrant of SNCA intron 1, cloned into the pGL3-basic luciferase vector, and incubated in the presence of NGF. The results are shown relative to induction for the same construct in naïve PC12 cells. We observed a significant loss of activation, to background levels (as observed for the empty pGL3-basic luciferase vector) between the 341 and 302 bp constructs ($p < 0.001$).

ZSCAN21 from the immediate 5′-end of the intron 1 sequence. In the presence of NGF the luciferase activity of the construct lacking the ZSCAN21 binding site (del ZSCAN) was significantly reduced compared with the full-length intron 1 sequence ($p < 0.001$; Fig. 1b). There was no significant difference between the ZSCAN21 deletion construct and the 744 bp construct. A similar pattern was observed in the presence of bFGF. These data suggest that ZSCAN21 is the TF responsible for the luciferase induction in this region and that both neurotrophins act through the same TF.

Small-scale deletion constructs in the third quadrant of intron 1 were screened to identify the putative binding site for the NGF-responsive element there. As seen in Fig. 1c, a significant drop in luciferase activity was observed between the 341 and 302 bp constructs ($p < 0.001$). Cross-species sequence alignment and MatInspector analysis identified a single conserved binding site for the TF HNF4 that overlaps the 302 bp deletion site.

Electromobility shift assays for the binding sites of ZSCAN21 and HNF4 from this region with nuclear extract from NGF-treated PC12 cells demonstrated specific shifts for both sets of probes (Fig. 2a, lanes 2 and 7) that could be competed out in the presence of excess unlabelled probe (Fig. 2a, lanes 3 and 8). We still observed the shift for both sets of probes in the presence of an excess of unlabelled non-
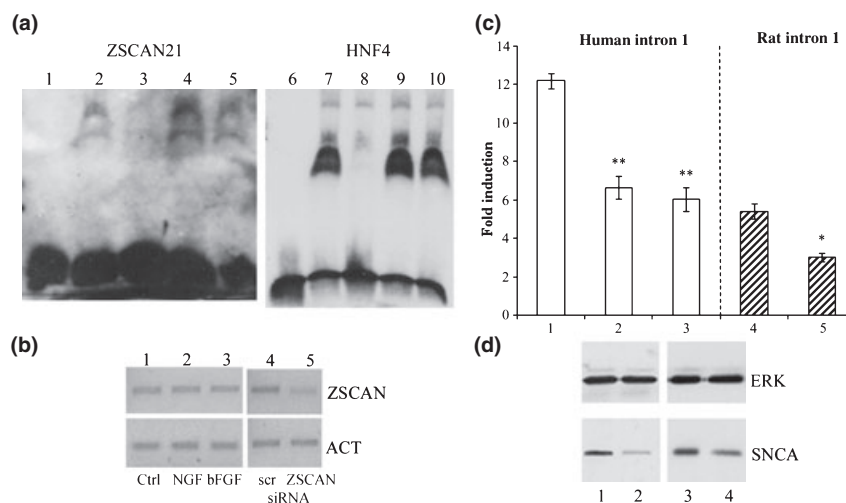

Fig. 2 Characterization of intron 1 transcription factors. (a) EMSA for the ZSCAN21 and HNF4 binding sites from intron 1. ZSCAN21 and HNF4 oligonucleotide probes were incubated with nuclear extracts from NGF-treated and naïve PC12 cells. Double-stranded probes for ZSCAN21 and HNF4 are run in lanes 1 and 6, respectively, in the absence of nuclear extract. A shift is observed for both sets of probes when they are incubated with PC12 nuclear extract from NGF-treated cells (lanes 2 and 7). We observe a reduction of shifted probe in the presence of 100×·molar excess of cold competitor for both probes (lanes 3 and 8); in the presence of 100× molar excess of Oct1 or Sp1 (for ZSCAN21 and HNF4, respectively) non-specific cold competitor the shift is not competed out (lanes 4 and 9). We also observe the shift of both probes in the presence of nuclear extract from naïve PC12 cells (lanes 5 and 10). (b) RT-PCR for ZSCAN21 in PC12 cells. Naïve and neurotrophin-treated PC12 cells express mRNA for the TF ZSCAN21, with no significant difference in levels between the naïve and neurotrophin-treated cells. (1) Naïve (Ctrl), (2) NGF-treated (NGF), and (3) bFGF-treated PC12 cells (bFGF). Transfection of naïve PC12 cells with siRNA against ZSCAN21 (ZSCAN siRNA) reduced the levels of ZSCAN21 mRNA by 54% (± 8%) when compared with scrambled siRNA-treated cells (scr siRNA). (4) Scrambled control siRNA-treated PC12 cells; (5) ZSCAN21 siRNA-treated PC12 cells, where ZSCAN, ZSCAN21; ACT, β-actin loading control. (c) siRNA against ZSCAN21 down-regulate the NGF induction of human (open columns) and rat (hashed columns) intron 1 in the luciferase assay in PC12 cells. (1) Human intron 1 + NGF + scrambled siRNA; (2) human intron 1 + NGF + ZSCAN21 siRNA; (3) human intron 1 lacking the ZSCAN21 binding site + NGF; (4) rat intron 1 + NGF + scrambled siRNA; and (5) rat intron 1 + NGF + ZSCAN21 siRNA. There was significant loss of luciferase activity for both human ($p < 0.001$) and rat ($p < 0.005$) sequences in the presence of siRNA against ZSCAN21. For the human sequence, there was no significant difference in activation between the siRNA-treated intron 1 construct and the construct lacking the ZSCAN21 binding site, where *$p < 0.005$ and **$p < 0.001$ significance when compared with scrambled siRNA-treated cells. (d) Down-regulation of endogenous SNCA expression in the PC12 cell line. PC12 co-transfected with EGFP and siRNA (ZSCAN21 or control scrambled siRNAs) were cell sorted and then probed for SNCA expression with western immunoblotting. (1) PC12 + NGF + control scrambled siRNA; (2) PC12 + NGF + ZSCAN21 siRNA; (3) naïve PC12 + control scrambled siRNA; (4) naïve PC12 + ZSCAN21 siRNA. We observed a reduction of induction of SNCA levels in the presence of NGF and siRNA of 56% (± 5%) when compared with NGF-treated cells in the presence of control scrambled siRNA. There was a reduction of the steady state levels of SNCA in naïve cells in the presence of siRNA against ZSCAN21 of 48% (± 2%) when compared with control scrambled siRNA-treated cells (the apparent higher levels of SNCA in the naïve cells are a result of an over-exposure of the membrane to film), where SNCA, α-synuclein; ERK, loading control.

specific probe (Fig. 2a, lanes 4 and 9). We were also able to detect a specific shift for this probe in nuclear extracts derived from naïve PC12 cells (Fig. 2a, lanes 5 and 10). These data indicate that there is a protein in the nuclear extracts of both naïve and neurotrophin-treated cells that is able to specifically bind to the DNA probes.

ZSCAN21 mRNA was detected in both naïve, NGF- and bFGF-treated PC12 cells with RT-PCR (Fig. 2b, lanes 1, 2, and 3), but we were unable to detect HNF4 (data not shown). There were also no significant changes in the levels of ZSCAN21 mRNA between the naïve and neurotrophin-treated PC12 cells, as determined by this semi-quantitative method. We also verified the expression of ZSCAN21 in cultured sympathetic neurons (data not shown).

We then assessed whether ZSCAN21 was the TF involved in SNCA regulation via its binding site in intron 1. Down-regulation of ZSCAN21 with siRNA (Fig. 2b, lane 5) significantly reduced, by ~50%, the luciferase activity from the human intron 1 construct when compared with control scrambled siRNA (Fig. 2c, bars 1 and 2; $p < 0.001$). There

was no significant difference between the levels of inhibition of intron 1 luciferase activity by ZSCAN21 siRNA and those observed for a construct lacking the ZSCAN21 binding site in the presence of NGF (Fig. 2c, bars 2 and 3). siRNA against ZSCAN21 was also able to significantly inhibit the NGF-activation from the rat intron 1 sequence when compared with scrambled siRNA control-treated cells (Fig. 2c, bars 4 and 5; $p < 0.005$).

Small interfering RNA for ZSCAN21 (or scrambled control siRNA) was co-transfected with an EGFP-expressing vector into PC12 cells which were naïve or subsequently treated with NGF. These cells were cell sorted and the EGFP-positive transfected cells were then analyzed for SNCA levels (Fig. 2d). We observed a clear inhibition of SNCA expression in both the naïve (Fig. 2d, lanes 3 and 4) and in the NGF-treated state (Fig. 2d, lanes 1 and 2) in the presence of siRNA for ZSCAN21 when compared with control scrambled siRNA. These results conclusively demonstrate that ZSCAN21 is a TF involved in the regulation of SNCA in PC12 cells.
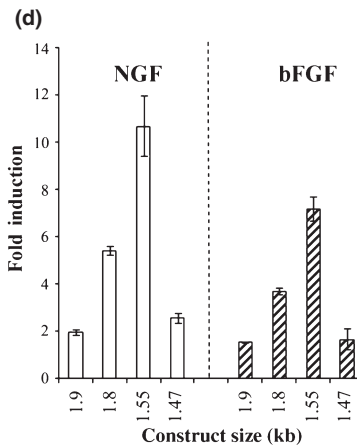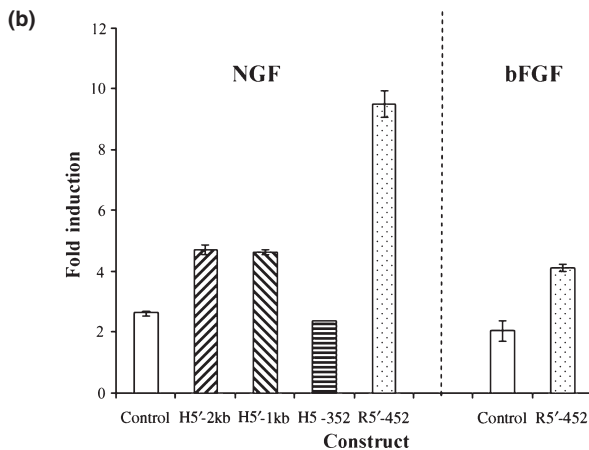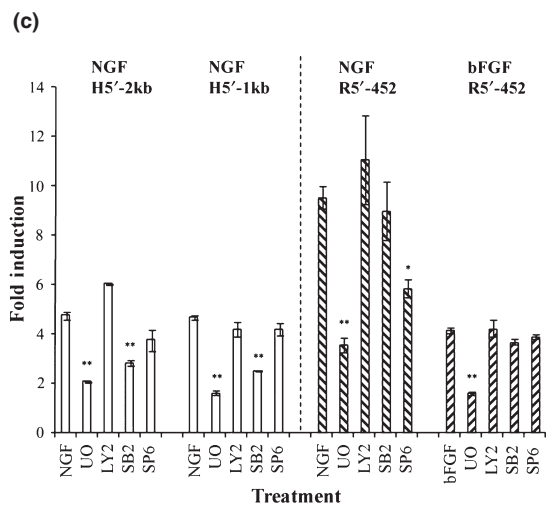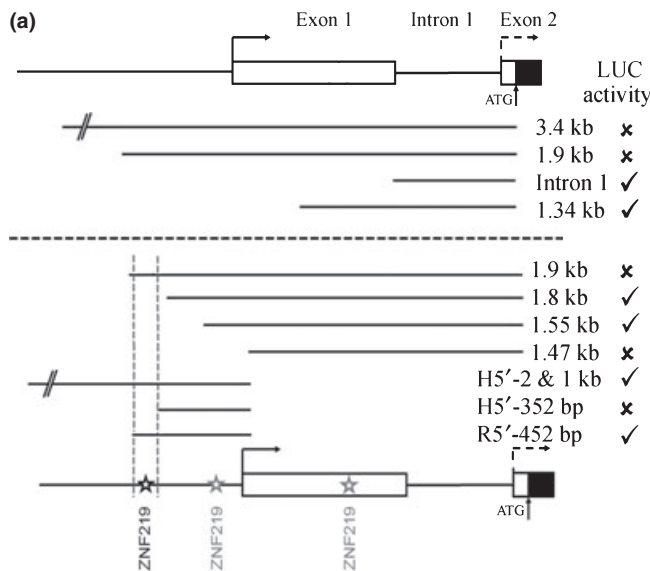
Characterization of the 5′–promoter of SNCA

Our initial analysis of the SNCA promoter showed that the intron 1-based luciferase activity of NGF or bFGF was completely abolished with constructs that contained both intron 1 and the canonical transcriptional start site (TSS) 5′ of exon 1 (3.4 and 1.9 kb in Fig. 3a; Clough and Stefanis 2007). This raised the possibility of an inhibitory interaction between the 5′-promoter and intron 1 leading to the observed loss of luciferase activity. To investigate this further we cloned 2 and 1 kb of the human SNCA 5′-promoter (H5′-2 and 1 kb; Fig. 3a), lacking intron 1 and observed a significant induction of luciferase activity with NGF when compared with the empty pGL3-basic luciferase vector ($p < 0.001$; Fig. 3b) with no significant difference of induction between either of these constructs. There was no significant increase of luciferase activity for the human 2 or 1 kb sequences in the presence of bFGF in this assay (data not shown). To validate this induction for the human sequences we cloned a smaller 452 bp fragment from the rat 5′-promoter (R5′-452 bp; Fig. 3a) and assayed this in the presence of NGF and bFGF; we observed a nine- and sixfold induction of luciferase activity, respectively (NGF: $p < 0.001$; bFGF: $p < 0.005$). The induction for the human 5′-promoter upon treatment with NGF is not solely dependent upon the presence of the core promoter, as a construct containing only 352 bp of the promoter (H5′-352 bp; Fig. 3a) did not have increased luciferase activity in the

presence of either NGF or bFGF (Fig. 3b). Therefore, upon isolation from the regulatory elements in intron 1, the canonical human TSS and 5′-promoter sequences are able to respond to NGF and the rat TSS is able to respond to both NGF and bFGF treatment in the luciferase assay.

We previously identified an essential role for the mitogen-activated protein (MAP)/ERK signaling pathway for both NGF and bFGF induction of the endogenous levels of SNCA and for intron 1 in the luciferase assay (Clough and Stefanis 2007). There is also an involvement of the phosphatidylinositol-3′-kinase/Akt pathway for the endogenous expression of SNCA.

We assessed the kinase pathways implicated in the induction of the 5′-promoter in the luciferase assay for both human and rat sequences. The NGF-induced activation was significantly inhibited using a pharmacological inhibitor of the MAP/ERK kinase pathway, for both the human and rat 5′-sequences (Fig. 3c; U0: $p < 0.001$). For the human 2 and 1 kb 5′-sequences, we also observed a significant inhibition upon application of an inhibitor of p38-mitogen-activated protein kinase (Fig. 3c; SB2: $p < 0.002$). For the rat sequence, we also observed a significant inhibition of induction for NGF upon inhibition of c-Jun N-terminal kinase (JNK) (Fig. 3c; SP6: $p < 0.01$). The differences in the responses of the human and rat sequences may be related to the sizes of the constructs used and/or the presence/absence of TF binding sites. We had previously examined the effects

Fig. 3 SNCA 5′-promoter. (a) Depicts the 5′-genomic structure of human SNCA. Exons are depicted as closed boxes, and introns as lines. The two promoter sites are depicted by bent arrows, with the putative intron 1 promoter as a dashed line. Black box indicates the translational start site in exon 2. Upper panel, luciferase constructs containing both the canonical transcriptional start site and intron 1 sequences (1.9 and 3.4 kb) are not induced in the luciferase assay in the presence of either NGF or bFGF (cross mark). Constructs lacking this 5′-sequence (intron 1 or 1.34 kb) are strongly activated in this assay upon treatment with neurotrophins (tick mark; Clough and Stefanis 2007). Lower panel, conserved TF binding sites in the 5′-promoter and exon 1. Conserved ZNF219 binding sites (indicated by stars) within the promoter of SNCA. We identified a critical region involved in the repression of the 1.9 kb construct, as the observed induction with the smaller 1.8 kb construct allowed us to localize this element to a 141 bp region. The human 5′-constructs of 2 and 1 kb, containing this critical area, were activated in the luciferase assay, as was the rat 5′-452 bp construct (R5′-452 bp). A lack of activation from a smaller human 5′-construct (H5′-352 bp) narrowed this critical area down to 62 bp. There was only one conserved binding site in this area; ZNF219. Two other ZNF219 sites were detected in this area and are depicted with gray stars. (b) Luciferase induction for the 5′-promoter sequence in the absence of intron 1. Human 5′-sequence containing the 5′-promoter (H5′-2 and 1 kb) are significantly induced in the presence of NGF, but not bFGF (data not shown; $p < 0.001$), when compared with neurotrophin-treated empty pGL3-basic luciferase vector (Control); this activation was lost for a smaller 352 bp fragment of the 5′-promoter (H5′-352). There was also signifi-

cant activation from a 452 bp fragment of the rat 5′-promoter (R5′-452) in the presence of NGF ($p < 0.001$) and for bFGF ($p < 0.005$) when compared with the levels of activation observed for the empty luciferase vector. (c) Pharmacological inhibition of the MEK/ERK pathways (U0) significantly reduces the neurotrophin induction of luciferase activity for human (open bars, H5′-2 and 1 kb) and rat (hashed bars, R5′-452) sequences for both NGF and bFGF when compared with control-treated cells. Inhibition with this compound is to the same level as that observed for the empty pGL3-basic vector in the presence of either neurotrophin. Induction from the human sequences was also significantly repressed with an inhibitor of the p38-MAPK pathway (SB2), but this was not replicated for the rat sequences. There was also a significant inhibition of luciferase activity for the rat sequences with NGF in the presence of an inhibitor of the c-Jun N-terminal kinase (JNK) pathway (SP6), which was not replicated for the human sequences. Inhibitors: U0, MAP/ERK; LY2, phosphatidylinositol-3′-kinase; SB2, p38-MAPK; SP6, c-Jun N-terminal kinase (JNK); $*p < 0.01$ and $**p < 0.001$. (d) Serial deletion constructs for the human 5′-promoter region reveal the presence of additional regulatory elements. The induction observed for NGF (clear bars) or bFGF (hashed bars) for each construct is shown relative to the level of induction observed for the same construct in naïve PC12 cells. We observe significant luciferase activity for the 1.8 kb construct, which contains 273 bp of the 5′-promoter, when compared with the 1.9 kb construct. There is a further significant increase in activation for the 1.55 kb construct (that contains 70 bp of the 5′-core promoter). This activation is then lost for the next smallest construct that terminates 7 bp inside exon 1 (1.47 kb).

of these inhibitors on the total levels of SNCA mRNA and protein and had only observed an effect with inhibitors of the MAP/ERK and phosphatidylinositol-3′-kinase pathways. We also examined the signaling pathways involved in the bFGF induction of the luciferase assay for the rat 5′-promoter sequences, where only inhibition of the MAP/ERK pathway was able to inhibit luciferase induction (Fig. 3c; U0: $p < 0.001$). These data indicate that the 5′-canonical promoter is regulated, like intron 1, primarily through the MAP/ERK signaling pathway.

We generated a series of 5′-deletions from the human 1.9 kb luciferase construct to identify the elements in the 5′-promoter of SNCA that were responsible for the inhibition of the luciferase assay (Fig. 3a). In the presence of NGF or bFGF, we observed significant activation after deleting 141 bp from the 5′-end of the 1.9 kb construct (1.8 kb; Fig. 3a and d), indicating the presence of a repressor element in this region. There was a further increase in luciferase activity with the next construct (1.55 kb; Fig. 3a and d), which terminates 70 bp 5′ from the start of exon 1 and includes the core promoter. Intriguingly, once the core promoter is removed (1.47 kb; Fig. 3a and d), the luciferase activation for both NGF and bFGF falls to background levels.

We examined constructs that contained only the 5′-SNCA promoter sequence and not intron 1. We observed a different pattern of activation for this same region, as constructs that contained the region between 1.9 and 1.8 kb (H5′-2 kb, H5′-1 kb, and R5′-452 bp) were active in the luciferase assay (Fig. 3b). However, we observed no luciferase induction by NGF for the H5′-352 bp construct that terminates 3′ of this region (Fig. 3b). This construct narrowed the critical region down to 62 bp. There was only one conserved binding site for the TF zinc finger protein 219 (ZNF219; Sakai *et al.* 2000, 2003) in this region (Fig. 3a).

Electromobility shift assay with the ZNF219 binding site in the human 5′-promoter generated specific shifts for the probe in the presence of nuclear extract from NGF-treated PC12 cells (Fig. 4a, lane 2) that could be competed out in the presence of an excess of the unlabelled specific probe (Fig. 4a, lane 3), but not the non-specific probe (Fig. 4a, lane 4). We also detected a specific shift for this probe in nuclear extracts from naïve PC12 cells (Fig. 4a, lane 5).

Expression of ZNF219 in the PC12 cell line was detected with RT-PCR in both naïve and NGF-treated cells with no difference in the levels of ZNF219 in these two conditions (Fig. 4b, lanes 1–3). ZNF219 was also expressed in cultured sympathetic neurons (data not shown). Co-transfection of naïve PC12 cells with siRNA against ZNF219 reduced the levels of ZNF219 mRNA by 50% (± 3%; Fig. 4b, lane 5) when compared with control scrambled siRNA-treated cells (Fig. 4b, lane 4). siRNA for ZNF219 (or scrambled control) were co-transfected with the pCMS-EGFP vector in PC12 cells, which were subsequently treated with NGF for 2 days

followed by cell sorting. We observed a moderate induction of SNCA protein levels in the presence of the siRNA against ZNF219 of 39% (± 6%; Fig. 4c, lane 2) when compared with scrambled control siRNA transfected cells (Fig. 4c, lane 1; $p < 0.05$).

We co-transfected the 1.9 kb luciferase construct with siRNA against either ZNF219 or scrambled control in the presence of NGF. As seen in Fig. 4d, we did not observe any induction in the luciferase assay for this construct as would be expected from our deletion data. However, the full-length 1.9 kb construct contains three putative binding sites for ZNF219 and it is possible that there are interactions between these multiple sites that may be responsible for the observed repression/activation of luciferase levels. For the human 1 kb and the rat 452 bp 5′-promoter sequences, siRNA against ZNF219 significantly repressed luciferase induction in the presence of NGF when compared with control scrambled siRNA-treated cells ($p < 0.01$).

These data indicate that ZNF219 is involved in the transcriptional regulation of SNCA. The presence of multiple binding sites for ZNF219 in the promoter of SNCA and the differential responses observed upon inhibition of the expression of ZNF219 indicate that its role in the regulation of SNCA is complex. The available data suggest a scenario in which ZNF219, by inducing 5′-promoter elements, inhibits SNCA transcription via intron 1.

Down-regulation of SNCA in primary cortical neurons with ZSCAN21 and ZNF219 siRNA.

We then extended our findings to primary neuron cell cultures. Cortical neuron cultures were selected because they represent a homogenous source of near-pure post-mitotic neurons. We verified by RT-PCR the expression of ZSCAN21 and ZNF219 mRNA in these neurons (data not shown). These cultures were then co-transfected with an EGFP-expressing vector and siRNA against either scrambled control, ZSCAN21 or ZNF219. Immunofluorescence staining for SNCA revealed a clear down-regulation of SNCA levels in the presence of siRNA against ZSCAN21 and ZNF219 when compared against scrambled control siRNA (Fig. 4e). There is a clear increase of the percentage of cells in the lower intensity bins (11–20 and 21–30 units), in ZNF219 (57.3%) and ZSCAN21 (61.1%) siRNA-treated cultures compared with control scrambled siRNA (15.9%). These data indicate that the majority of ZSCAN21 and ZNF219 siRNA-transfected cells were expressing lower levels of SNCA protein than control scrambled siRNA-treated cells. Therefore, both TFs appear to act as positive regulators of SNCA transcription in this primary neuronal cell culture setting.

Discussion

There is now a large body of evidence to indicate that dysregulation of SNCA is a risk factor in developing PD. To
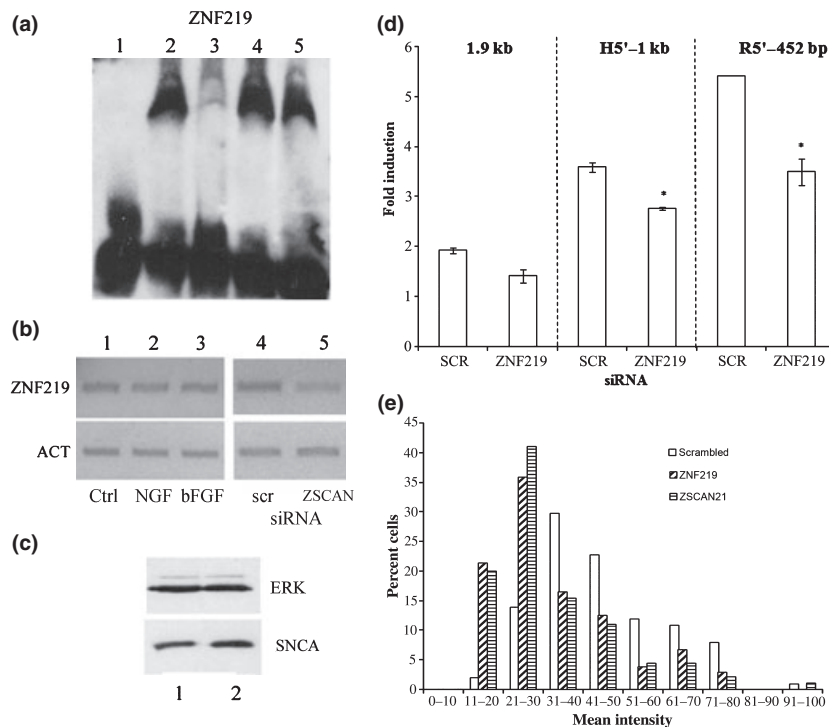
Fig. 4 ZNF219 and SNCA transcriptional regulation. (a) EMSA for the 5′-TF binding site of ZNF219 with nuclear extracts from NGF-treated and naïve PC12 cells. (1) Double-stranded probes for ZNF219 in the absence of nuclear extract. (2) A shift is observed when probe is incubated with NGF-treated PC12 nuclear extract. (3) In the presence of 100×·molar excess of cold ZNF219 competitor this shift is reduced and (4) the presence of 100× molar excess of non-specific cold competitor has no effect upon the levels of shifted probe. (5) We also observed a shift of the probe in the presence of nuclear extract from naïve PC12 cells. (b) RT-PCR for ZNF219 in PC12 cells. Naïve and neurotrophin-treated PC12 cells express mRNA for the TF ZNF219, with no significant difference in levels between naïve and neurotrophin-treated cells. (1) Naïve (Ctrl), (2) NGF-treated (NGF), and (3) bFGF-treated PC12 cells (bFGF). Treatment of naïve PC12 cells with siRNA against ZNF219 (ZNF siRNA) reduced the levels of ZNF219 mRNA by 50% (± 5%) when compared with scrambled siRNA-treated cells (scr siRNA). (4) Scrambled control siRNA-treated PC12 cells; (5) ZNF219 siRNA-treated PC12 cells, where ZNF, ZNF219; ACT, β-actin loading control. (c) Down-regulation of endogenous SNCA expression in the PC12 cell line. PC12 co-transfected with EGFP and siRNA were cell sorted and then probed for SNCA expression with western immunoblotting. (1) PC12 + NGF + control scrambled siRNA; (2) PC12 + NGF + ZSCAN21 siRNA. There was a small but significant induction of SNCA levels in the presence of NGF and ZNF219 siRNA of 39% (± 6%; lane 2) when compared with NGF-treated cells in the presence of control scrambled siRNA ($p < 0.05$; lane 1); SNCA, α-synuclein; ERK, loading control. (d) Inhibition of NGF induction of the luciferase assay by ZNF219 siRNA in PC12 cells. In the presence of siRNA against ZNF219, there was no significant up-regulation for the 1.9 kb construct. We observed a significant reduction in luciferase activity from both the human 5′-1 kb (H5′-1 kb) and rat 5′-452 bp (R5′-452 bp) constructs when compared with scrambled siRNA-treated cells ($p < 0.01$), where SCR, scrambled siRNA; ZNF219, ZNF219 siRNA; *$p < 0.01$. (e) Down-regulation of SNCA in Primary Cortical Neurons with ZSCAN21 and ZNF219 siRNA. Graph shows the quantification of SNCA levels from ∼100 EGFP-transfected rat cortical neurons. Intensity of staining for SNCA was standardized and the individual scores for cells were grouped into bins of 10 units/bin. We observed a clear down-regulation of the mean intensity of SNCA immunofluorescent staining in neurons transfected with siRNA against ZNF219 and ZSCAN21 when compared with control scrambled siRNA-transfected cells. The majority of transfected cells for these two siRNA are in the two lowest detectable bins (11–20 and 21–30).

further determine the mechanisms that govern the transcriptional regulation of SNCA we examined its promoter to identify transcriptional control elements. In this study, we characterize the role of two TFs, ZSCAN21, and ZNF219 in the expression of SNCA.

Intron 1 is a key regulatory region of SNCA transcription

We have now expanded upon our previous work, in which we demonstrated that the first intron of SNCA was an unappreciated transcriptional regulatory region (Clough and Stefanis 2007). Since our original report, a binding site for the TF GATA binding protein 1 (GATA-1) has been identified, also located in intron 1 (Scherzer *et al.* 2008), further strengthening the importance of this region in the regulation of SNCA. This site is distinct from the two elements we describe here and appears, based on its location, to not be important in regulating the neurotrophic induction of SNCA as determined by the luciferase assay. In this study,

we identified two putative binding sites for TFs in this region. The first is at the 5′-end of intron 1 and is responsive to both NGF and bFGF induction in the luciferase assay. The TF ZSCAN21 that binds to this DNA element is a zinc finger-containing TF. It is a member of a large family of TFs that contain a SCAN domain that mediates protein–protein interactions (Edelstein and Collins 2005). ZSCAN21 is expressed in a wide range of tissues, including the CNS (Su *et al.* 2004). We have confirmed its expression in primary neurons, and, by using an siRNA approach, we conclusively demonstrate its involvement in SNCA regulation in naïve and neurotrophin-treated PC12 cells, as well as in cultured cortical neurons.

As there were no changes in the mRNA levels for ZSCAN21 in PC12 cells in the presence or absence of neurotrophins and no discernible difference in the bandshifts observed for nuclear extracts from naïve or neurotrophin-treated cells, we believe that changes in the protein levels of ZSCAN21 (and ZNF219) are not responsible for the up-regulation of SNCA. It is possible that its phosphorylation or acetylation status, or that of an interacting partner, could be responsible for the observed induction of SNCA expression (Park *et al.* 2007; Siu *et al.* 2008).

These data further demonstrate the importance of the first intron of SNCA in the transcriptional regulation of SNCA, as no other binding sites for ZSCAN21 could be identified within the SNCA promoter. Gamma-synuclein, a member of the synuclein family, has also been shown to contain critical transcriptional regulatory elements within its first intron (Lu *et al.* 2001; Surgucheva and Surguchov 2008).

We were unable to identify the TF that binds to the critical region in the third quadrant of intron 1, which responds solely to NGF-treatment in the luciferase assay. Therefore there is an, as yet, unidentified TF that binds to this DNA sequence and regulates the NGF luciferase induction for this area of intron 1.

Interaction between elements in the 5′-promoter and intron 1

As we observed no luciferase activity for constructs that contained both intron 1 and the 5′-promoter, we examined whether the 5′-promoter could function in isolation from these important intron 1 regulatory regions, and we indeed observed that this was the case. Interestingly, the core promoter is not sufficient on its own to respond to neurotrophins in the luciferase assay. The main kinase signaling pathways utilized for the induction from these rat and human 5′-promoter sequences is the MAP/ERK pathway, as previously seen for intron 1 (Clough and Stefanis 2007).

ZNF219 and SNCA transcriptional regulation

Deletion of 141 bp from the 5′-end of the 1.9 kb construct led to the identification of a binding site for the TF ZNF219, which appears to be responsible for the inhibition of activation in the luciferase assay of constructs containing both this site and intron 1. Constructs containing just the 5′-promoter gave a similar, but inverse, correlation in the luciferase assay; those that contained this critical region were activated in the presence of NGF, but a construct lacking this region lost all activation. This indicates that this element can function as both an activator and a repressor of SNCA transcription depending upon the presence/absence of other genomic elements.

ZNF219 is a member of the Krüppel-like zinc finger gene family and is a 77 kDa protein containing nine sets of C2H2 zinc finger structures (Sakai *et al.* 2003). ZNF219 is widely expressed in many tissues, including the cerebellum, substantia nigra, hippocampus, and cerebral cortex (Sakai *et al.* 2000; Lein *et al.* 2007). ZNF219 functions as a repressor of transcriptional activation in the promoter of the high-mobility group nucleosome binding domain 1 gene and competes for binding to its target sequence with members of the Sp1 family of transcriptional activators (Sakai *et al.* 2003). In support of this view, in the luciferase assay, we observed no activation for constructs that contained either three or one ZNF219 binding sites. For constructs that contained two ZNF219 binding sites we observed an increase in luciferase activity. Therefore, the exact involvement of ZNF219 in the regulation of SNCA is somewhat unclear, and will require further characterization by deleting individual and multiple sites in the context of the full 1.9 kb construct.

In agreement with its proposed function as a transcriptional repressor we observed a small, but significant, increase in the levels of endogenous SNCA protein levels upon inhibition of ZNF219 with siRNA in NGF-treated PC12 cells, when compared with scrambled siRNA-treated cells (Fig. 4c). This effect may be because, in the context of the whole gene, down-regulation of ZNF219 leads to a release of its inhibitory effect on the intron 1 regulatory regions, leading to intron 1-mediated transcriptional activation. In cortical neuron cultures, the intron 1 and 5′-promoter response elements cooperate in the luciferase assay (R.L. Clough, G. Dermentzaki, M. Haritou, A. Petsakou and L. Stefanis, unpublished data). Down-regulation of ZNF219 by siRNA in these cells led to a decrease in SNCA protein expression, indicating that in this setting ZNF219 acts as a transcriptional activator of SNCA expression. These data clearly indicate that ZNF219 functions as both an activator and a repressor of transcription and that this role may depend on the cell type and interactions with other binding proteins and response elements.

We demonstrate here that the SNCA gene has a complicated transcriptional architecture with elements outside of the core promoter having differential effects upon the expression of SNCA. The ability to modulate SNCA expression levels through targeting of specific TFs may provide a therapeutic strategy against the over-expression of SNCA in PD and in

other synucleopathies. Further studies will be needed to characterize the role of these TFs in the regulation of SNCA *in vivo* and to identify other transcriptional targets that they may have in the CNS. It will also be of interest to screen for polymorphisms in the two TFs (ZSCAN21 and ZNF219) and their binding sites in the SNCA promoter in PD patients and to examine if they have a functional effect upon the levels of SNCA expression.

Acknowledgments

References

Abramoff M. D., Magelhaes P. J. and Ram S. J. (2004) Image processing with ImageJ. *Biophotonics Int.* **11**, 36–42.

Baptista M. J., O'Farrell C., Daya S., Ahmad R., Miller D. W., Hardy J., Farrer M. J. and Cookson M. R. (2003) Co-ordinate transcriptional regulation of dopamine synthesis genes by alpha-synuclein in human neuroblastoma cell lines. *J. Neurochem.* **85**, 957–968.

Braak H., Del Tredici K., Rüb U., de Vos R. A., Jansen Steur E. N. and Braak E. (2003) Staging of brain pathology related to sporadic Parkinson's disease. *Neurobiol. Aging* **24**, 197–211.

Cartharius K., Frech K., Grote K., Klocke B., Haltmeier M., Klingenhoff A., Frisch M., Bayerlein M. and Werner T. (2005) MatInspector and beyond: promoter analysis based on transcription factor binding sites. *Bioinformatics* **21**, 2933–2942.

Chartier-Harlin M. C., Kachergus J., Roumier C. *et al.* (2004) Alpha-synuclein locus duplication as a cause of familial Parkinson's disease. *Lancet* **364**, 1167–1169.

Chiba-Falek O. and Nussbaum R. L. (2001) Effect of allelic variation at the NACP-Rep1 repeat upstream of the alpha-synuclein gene (SNCA) on transcription in a cell culture luciferase reporter system. *Hum. Mol. Genet.* **10**, 3101–3109.

Chiba-Falek O., Lopez G. J. and Nussbaum R. L. (2006) Levels of alpha-synuclein mRNA in sporadic Parkinson's disease patients. *Mov. Disord.* **21**, 1703–1708.

Clough R. L. and Stefanis L. (2007) A novel pathway for transcriptional regulation of alpha-synuclein. *FASEB J.* **21**, 596–607.

Clough R. L., Sud R., Davis-Silberman N., Hertzano R., Avraham K. B., Holley M. and Dawson S. J. (2004) Brn-3c (POU4F3) regulates BDNF and NT-3 promoter activity. *Biochem. Biophys. Res. Commun.* **324**, 372–381.

Cookson M. R., Hardy J. and Lewis P. A. (2008) Genetic neuropathology of Parkinson's disease. *Int. J. Clin. Exp. Pathol.* **1**, 217–231.

Dachsel J. C., Lincoln S. J., Gonzalez J., Ross O. A., Dickson D. W. and Farrer M. J. (2007) The ups and downs of alpha-synuclein mRNA expression. *Mov. Disord.* **22**, 293–295.

Dietrich P., Rideout H. J., Wang Q. and Stefanis L. (2003) Lack of p53 delays apoptosis, but increases ubiquitinated inclusions, in proteasomal inhibitor-treated cultured cortical neurons. *Mol. Cell. Neurosci.* **24**, 430–441.

Edelstein L. C. and Collins T. (2005) The SCAN domain family of zinc finger transcription factors. *Gene* **359**, 1–17.

Farrer M., Maraganore D. M., Lockhart P. *et al.* (2001) alpha-Synuclein gene haplotypes are associated with Parkinson's disease. *Hum. Mol. Genet.* **10**, 1847–1851.

Feany M. B. and Bender W. W. (2000) A Drosophila model of Parkinson's disease. *Nature* **404**, 394–398.

Greene L. A. and Tischler A. S. (1976) Establishment of a noradrenergic clonal line of rat adrenal pheochromocytoma cells which respond to nerve growth factor. *Proc. Natl Acad. Sci. USA* **73**, 2424–2428.

Gründemann J., Schlaudraff F., Haeckel O. and Liss B. (2008) Elevated alpha-synuclein mRNA levels in individual UV-laser-microdissected dopaminergic substantia nigra neurons in idiopathic Parkinson's disease. *Nucleic Acids Res.* **36**, e38.

Kingsbury A. E., Daniel S. E., Sangha H., Eisen S., Lees A. J. and Foster O. J. (2004) Alteration in alpha-synuclein mRNA expression in Parkinson's disease. *Mov. Disord.* **19**, 162–170.

Kirik D., Rosenblad C., Burger C., Lundberg C., Johansen T. E., Muzyczka N., Mandel R. J. and Bjorklund A. (2002) Parkinson-like neurodegeneration induced by targeted overexpression of alpha-synuclein in the nigrostriatal system. *J. Neurosci.* **22**, 2780–2791.

Krüger R., Kuhn W., Müller T. *et al.* (1998) Ala30Pro mutation in the gene encoding alpha-synuclein in Parkinson's disease. *Nat. Genet.* **18**, 106–108.

Kyratzi E., Pavlaki M. and Stefanis L. (2008) The S18Y polymorphic variant of UCH-L1 confers an antioxidant function to neuronal cells. *Hum. Mol. Genet.* **17**, 2160–2171.

Larkin M. A., Blackshields G., Brown N. P. *et al.* (2007) Clustal W and Clustal X version 2.0. *Bioinformatics* **23**, 2947–2948.

Lein E. S., Hawrylycz M. J., Ao N. *et al.* (2007) Genome-wide atlas of gene expression in the adult mouse brains. *Nature* **445**, 168–176.

Lu A., Gupta A., Li C., Ahlborn T. E., Ma Y., Shi E. Y. and Liu J. (2001) Molecular mechanisms for aberrant expression of the human breast cancer specific gene 1 in breast cancer cells: control of transcription by DNA methylation and intronic sequences. *Oncogene* **20**, 5173–5185.

Madziar B., Lopez-Coviella I., Zemelko V. and Berse B. (2005) Regulation of cholinergic gene expression by nerve growth factor depends on the phosphatidylinositol-3′-kinase pathway. *J. Neurochem.* **92**, 767–779.

Maraganore D. M., de Andrade M., Elbaz A. *et al.* (2006) Collaborative analysis of alpha-synuclein gene promoter variability and Parkinson's disease. *JAMA* **296**, 661–670.

Masliah E., Rockenstein E., Veinbergs I., Mallory M., Hashimoto M., Takeda A., Sagara Y., Sisk A. and Mucke L. (2000) Dopaminergic loss and inclusion body formation in alpha-synuclein mice: implications for neurodegenerative disorders. *Science* **287**, 1265–1269.

Mueller J. C., Fuchs J., Hofer A. *et al.* (2005) Multiple regions of alpha-synuclein are associated with Parkinson's disease. *Ann. Neurol.* **57**, 535–541.

Nuber S., Petrasch-Parwez E., Winner B. *et al.* (2008) Neurodegeneration and motor dysfunction in a conditional model of Parkinson's disease. *J. Neurosci.* **28**, 2471–2484.

Pals P., Lincoln S., Manning J. *et al.* (2004) alpha-Synuclein promoter confers susceptibility to Parkinson's disease. *Ann. Neurol.* **56**, 591–595.

Papapetropoulos S., Adi N., Mash D. C., Shehadeh L., Bishopric N. and Shehadeh L. (2007) Expression of alpha-synuclein mRNA in Parkinson's disease. *Mov. Disord.* **22**, 1057–1059.

Park M. J., Kwak H. J., Lee H. C., Yoo D. H., Park I. C., Kim M. S., Lee S. H., Rhee C. H. and Hong S. I. (2007) Nerve growth factor induces endothelial cell invasion and cord formation by promoting matrix metalloproteinase-2 expression through the phosphatidylinositol 3-kinase/Akt signaling pathway and AP-2 transcription factor. *J. Biol. Chem.* **282**, 30485–30496.

Polymeropoulos M. H., Lavedan C., Leroy E. *et al.* (1997) Mutation in the alpha-synuclein gene identified in families with Parkinson's disease. *Science* **276**, 2045–2047.

Rideout H. J. and Stefanis L. (2002) Proteasomal inhibition-induced inclusion formation and death in cortical neurons require transcription and ubiquitination. *Mol. Cell. Neurosci.* **21**, 223–238.

Rockenstein E., Hansen L. A., Mallory M., Trojanowski J. Q., Galasko D. and Masliah E. (2001) Altered expression of the synuclein family mRNA in Lewy body and Alzheimer's disease. *Brain Res.* **914**, 48–56.

Sakai T., Toyoda A., Hashimoto K. and Maeda H. (2000) Isolation and characterization of a novel zinc finger gene, ZNF219, and mapping to the human chromosome 14q11 region. *DNA Res.* **7**, 137–141.

Sakai T., Hino K., Wada S. and Maeda H. (2003) Identification of the DNA binding specificity of the human ZNF219 protein and its function as a transcriptional repressor. *DNA Res.* **10**, 155–165.

Scherzer C. R., Grass J. A., Liao Z. *et al.* (2008) GATA transcription factors directly regulate the Parkinson's disease-linked gene alpha-synuclein. *Proc. Natl Acad. Sci. USA* **105**, 10907–10912.

Shastry B. S. (2003) Neurodegenerative disorders of protein aggregation. *Neurochem. Int.* **43**, 1–7.

Singleton A. B., Farrer M., Johnson J. *et al.* (2003) alpha-Synuclein locus triplication causes Parkinson's disease. *Science* **302**, 841.

Siu Y. T., Ching Y. P. and Jin D. Y. (2008) Activation of TORC1 transcriptional coactivator through MEKK1-induced phosphorylation. *Mol. Biol. Cell* **19**, 4750–4761.

Stefanis L., Kholodilov N., Rideout H. J., Burke R. E. and Greene L. A. (2001) Synuclein-1 is selectively up-regulated in response to nerve growth factor treatment in PC12 cells. *J. Neurochem.* **76**, 1165–1176.

Su A. I., Wiltshire T., Batalov S. *et al.* (2004) A gene atlas of the mouse and human protein-encoding transcriptomes. *Proc. Natl Acad. Sci. USA* **101**, 6062–6067.

Surgucheva I. and Surguchov A. (2008) Gamma-synuclein: cell-type-specific promoter activity and binding to transcription factors. *J. Mol. Neurosci.* **35**, 267–271.

Surguchov A. (2008) Molecular and cellular biology of synucleins. *Int. Rev. Cell. Mol. Biol.* **270**, 225–317.

Yamamoto A., Lucas J. J. and Hen R. (2000) Reversal of neuropathology and motor dysfunction in a conditional model of Huntington's disease. *Cell* **101**, 57–66.

Zarranz J. J., Alegre J., Gómez-Esteban J. C. *et al.* (2004) The new mutation, E46K, of alpha-synuclein causes Parkinson's and Lewy body dementia. *Ann. Neurol.* **55**, 164–173.

Zu T., Duvick L. A., Kaytor M. D., Berlinger M. S., Zoghbi H. Y., Clark H. B. and Orr H. T. (2004) Recovery from polyglutamine-induced neurodegeneration in conditional SCA1 transgenic mice. *J. Neurosci.* **24**, 8853–8861.

Regulation of α-synuclein expression in cultured cortical neurons

Richard Lee Clough,* Georgia Dermentzaki,* Maria Haritou,* Afroditi Petsakou* and
Leonidas Stefanis*,†

*Division of Basic Neuroscience, Biomedical Research Foundation of the Academy of Athens, Athens, Greece
†Second Department of Neurology, University of Athens Medical School, Athens, Greece

Abstract

Alpha-synuclein (SNCA) is a predominantly neuronal protein involved in the control of neurotransmitter release. The levels of SNCA expression are closely linked to the pathogenesis of Parkinson's disease; however, the biochemical pathways and transcriptional elements that control SNCA expression are not well understood. We previously used the model system of neurotrophin-mediated PC12 cell neuronal differentiation to examine these phenomena. Although these studies were informative, they were limited to the use of a cell line; therefore, in the current work, we have turned our attention to cultured primary rat cortical neurons. In these cultures, SNCA expression increased with time in culture, as the neurons mature. Luciferase assays based on transient transfections of fusion constructs encoding components of the transcriptional control region of SNCA identified various promoter areas that have a positive or negative effect on SNCA transcription. Intron 1, previously identified by us as an important regulatory

region in the PC12 cell model, cooperates with regions 5′ to exon 1 to mediate gene transcription. Using selective pharmacological tools, we find that tyrosine kinase receptors and the phosphatidyl-inositol 3 kinase signaling pathway are involved in mediating these effects. The exogenous application of the neurotrophin brain-derived neurotrophic factor (BDNF) is sufficient on its own to promote the transcriptional activation of SNCA through this pathway, but a neutralizing antibody against BDNF failed to affect SNCA transcription in maturing cultures, suggesting that BDNF is not the main factor involved in maturation-induced SNCA transcription in this model. Further *in vivo* studies are needed to establish the role of neurotrophin signaling in the control of SNCA transcription.

Keywords: brain-derived neurotrophic factor, intron, neurotrophin, Parkinson's disease, transcription, tyrosine kinase receptor.

J. Neurochem. (2011) 10.1111/j.1471-4159.2011.07199.x

Alpha-synuclein (SNCA) is an abundant neuronal protein of uncertain function with a predominant pre-synaptic localization. It is likely involved in the control of neurotransmission, possibly by modifying the assembly of the soluble NSF attachment protein receptor complex (Chandra *et al.* 2005; Larsen *et al.* 2006; Burré *et al.* 2010). In addition, SNCA has been genetically and pathologically linked to the development of Parkinson's disease (PD). SNCA is thought to comprise the building block of Lewy Bodies (LBs) and Lewy neurites that pathologically characterize PD; furthermore, point mutations or multiplications of the SNCA locus lead to autosomal dominant PD in rare families (Cookson *et al.* 2008). The multiplication cases, in particular, indicate that increased levels of even wild-type (WT) SNCA can lead to PD. Consistent with this notion, the over-expression of WT SNCA also leads to phenotypes resembling PD in various animal models (Feany and Bender 2000; Masliah *et al.* 2000; Kirik *et al.* 2002; Vekrellis *et al.* 2004).

Even sporadic PD is genetically linked to SNCA. A number of polymorphisms in the promoter sequence and 3′ regions of SNCA confer susceptibility to developing PD in case/control studies (Farrer *et al.* 2001; Pals *et al.* 2004, Mueller *et al.* 2005; Hadjigeorgiou *et al.* 2006; Mizuta *et al.* 2006). One of these polymorphisms, the non-amyloid component precursor (NACP) complex dinucleotide repeat

located 10.7 kb upstream of the SNCA gene (Chiba-Falek and Nussbaum 2001) conferred an odds ratio of 1.43 in a large meta-analysis when compared with control subjects (Maraganore *et al.* 2006); however, it is still not known if the NACP–REP polymorphism is responsible for this increased risk or if it is in linkage disequilibrium with the actual causative agent. More recently, unbiased genome-wide association studies established that the SNCA gene represents one of the very few genetic loci conclusively linked to sporadic PD (Satake *et al.* 2009; Simón-Sánchez *et al.* 2009; Edwards *et al.* 2010).

There has been controversy regarding the expression levels of SNCA in the brains of sporadic PD patients, with a number of studies reporting either increased or decreased or unchanged levels of SNCA (Neystat *et al.* 1999; Rockenstein *et al.* 2001; Beyer *et al.* 2004; Kingsbury *et al.* 2004; Chiba-Falek *et al.* 2006; Dachsel *et al.* 2007; Papapetropoulos *et al.* 2007). However, in an elegant study, Gründemann *et al.* (2008) used laser-captured microdissection to clearly demonstrate significantly elevated SNCA mRNA levels in individual, surviving neuromelanin- and tyrosine hydroxylase-positive substantia nigra dopaminergic neurons from idiopathic PD brains when compared with control brains.

Collectively, the above data indicate that the regulation of SNCA expression through elements within or around the SNCA locus may be important for PD pathogenesis. Conversely, although not specifically studied, the regulation of SNCA expression may also be important for the control of synaptic transmission. From a therapeutic standpoint, control of SNCA expression could represent a target for novel PD therapeutics.

Despite the obvious importance of the expression of SNCA, very little is known about the mechanisms, signaling pathways, and transcriptional elements that regulate its expression. SNCA is developmentally induced in the rat brain (Petersen *et al.* 1999; Kholodilov *et al.*, 2001; Vogiatzi *et al.* 2008) and in rat neuronal cell cultures (Rideout *et al.* 2003; Vogiatzi *et al.* 2008). Following an initial surge, the expression levels of SNCA reach a plateau in adult rodent brain (Petersen *et al.* 1999; Adamczyk *et al.* 2005).

In previous studies, to examine the mechanisms involved in the developmental induction of SNCA, we have used the model system of PC12 pheochromocytoma clone cells. In this system, SNCA is up-regulated upon neuronal differentiation with nerve growth factor (Stefanis *et al.* 2001). This up-regulation involves the extracellular receptor kinase (ERK) and phosphatidyl-inositol 3 kinase (PI3-K) pathways, and transcriptional control elements within intron 1 (Clough and Stefanis 2007); the transcription factor Zipro1 was identified as at least one of these factors in a subsequent study (Clough *et al.* 2009).

In this study, we have turned to cultured embryonic rat cortical neurons as another model cell system to examine the mechanisms involved in SNCA transcriptional regulation.

We have used these neurons because they represent a rich, homogeneous source of CNS neurons that mature in culture and that, as we had previously reported, during this process up-regulate SNCA protein levels (Rideout *et al.* 2003). Moreover, these neurons are affected in the later stages of the PD disease process; indeed, the development of SNCA pathology in cortical regions correlates with the impaired cognition observed in PD with dementia (Mattila *et al.*, 2000). Two other related disorders, dementia with LBs and LB variant of Alzheimer's disease also harbor SNCA-positive LBs in cortical neurons (Vekrellis *et al.* 2004; Cookson *et al.* 2008). Therefore, cortical neurons represent an affected population in PD and represent a valuable model to study SNCA transcriptional regulation.

The present studies in cultured cortical neurons underscore similarities and differences to our previous results in the PC12 cell system and reinforce the idea that extracellular signaling via growth factors may potently modulate neuronal SNCA levels.

Materials and methods

Cortical neuronal cultures

Cultures of Wistar rat (embryonic day 18, E18) cortical neurons were prepared as previously described (Rideout and Stefanis 2002; Dietrich *et al.* 2003). Dissociated cells were plated onto poly-D-lysine-coated six-well or 12-well dishes at a density of approximately $1.5–2.0 \times 10^6$ cells/cm^2. Cells were maintained in Neurobasal medium (Gibco, Rockville, MD, USA; Invitrogen, Carlsbad, CA, USA), with B27 serum-free supplements (Gibco; Invitrogen), L-glutamine (0.5 mM), and penicillin/streptomycin (1%). More than 98% of the cells cultured under these conditions represent post-mitotic neurons (Rideout and Stefanis 2002). The time in culture of cells was calculated using days *in vitro* (DIV), with the day of harvesting designated as 0 DIV.

For experiments using the various kinase pathway inhibitors, the cultured cortical neurons were pre-incubated with the inhibitors for 45 min prior to the addition of the growth factors. U0126 (Sigma, St Louis, MO, USA) was added to the complete media at 25 μM, LY294002 (Sigma) at 25 μM; SP600125 (Sigma) at 10 μM; and SB203580 (Sigma) at 30 μM. For western blot analysis, the cells were cultured for a total of 5 days in the presence of the inhibitors and for the luciferase assays, the cells were cultured for 2 days. The Trk inhibitor K252a (Sigma) was added to the culture medium at a concentration of 200 nM.

For experiments using exogenous brain-derived neurotrophic factor (BDNF), BDNF (50 ng/mL; Prospec, Rehovot, Israel) was added to the culture medium and replaced with fresh medium every 2 days.

To neutralize the activity of endogenous BDNF, days 1 and 8 cortical cultures in six-well dishes were cultured in media containing a BDNF-neutralizing antibody (10 μg/mL; Chemicon International, Temecula, CA, USA) or a control antibody matched for species and class (c-myc, 400 ng/mL; Santa Cruz Biotechnology, Santa Cruz, CA, USA) for 5 days. The media were replaced every 2 days. The cells were visualized under phase-microscopy and representative

images were recorded (Leica DFC 350FX; Leica Microsystems, Wetzlar, Germany).

Western immunoblotting

Cortical neurons were washed twice in phosphate-buffered saline and then harvested in lysis buffer (150 mM NaCl, 50 mM Tris pH7.6, 0.1% sodium dodecyl sulfate, 1% NP-40; Sigma, 2 mM EDTA). Protein concentrations were determined using the Bradford method (Bio-Rad Laboratories, Hercules, CA, USA). Ten μg of lysates were mixed with $2 \times$ Laemmli buffer prior to running on 12% sodium dodecyl sulfate–polyacrylamide gels. Following transfer to a nitrocellulose membrane, blots were probed with antibodies directed against: (i) α-synuclein (1 : 1000; BD Biosciences, Sparks, MD, USA) and (ii) ERK (loading control; 1 : 5000; Santa Cruz Biotechnology). Blots were probed with horseradish peroxidase-conjugated secondary antibodies and visualized with Western Lightning (Perkin Elmer, Waltham, MA, USA) and exposed to Super RX film (Fuji Film, P. Phaliro, Greece). Following scanning of the images with Adobe Photoshop, Image J software (NIH, Bethesda, MD, USA) was used to quantify the intensity of the bands. In all cases, the levels of SNCA were normalized to those of ERK for quantification and statistical analysis.

Reverse transcription polymerase chain reaction (RT–PCR)

Total RNA was extracted from cortical neuron cultures using Trizol (Invitrogen) and cDNA was generated with the Reverse Transcription System (Promega, Madison, WI, USA) according to the manufacturer's instructions. We then performed RT-PCR, using the cDNA as a template. In preliminary experiments, all primer pairs were optimized to be in the log-exponential phase of amplification. The following primers were used to perform the PCR: α-synuclein-F – 5′-ttctgcggaagcctagagag-3′, α-synuclein-R – 5′-tcctccaacatttgtcacttgc-3′*; β-actin-F – 5′-tcaccatggatgatgatatc-gcc-3′*, β-actin-R – 5′-ccacacgcagctcattgtagaagg-3′* (all primers marked * from Baptista *et al.* 2003). Products were subsequently resolved on agarose gels stained with ethidium bromide. All RT-PCR results are calculated as the ratio of SNCA to β-actin mRNA, and then compared across conditions.

Transfection and luciferase assay

The 1.46, 3.4, 3.8, 4.1, 6.2, 9.8, and 10.7 kb constructs used in this study were a kind gift from Drs Nussbaum and Chiba-Falek (Chiba-Falek and Nussbaum 2001). The human intron 1 (int1), rat intron 1 (rint1), human 5′ 2-kb promoter (H5′-2 kb), and rat 5′ 452-bp promoter (Rat 5′-452 bp) constructs were generated as previously described (Clough and Stefanis 2007; Clough *et al.* 2009).

All transfections were performed using Lipofectamine 2000 (Invitrogen) according to the manufacturer's instructions and as previously described (Clough and Stefanis 2007). Briefly, for the luciferase assay all transfections were performed in 6 well tissue culture dishes with 6.0×10^5 cells/well with 2.0 μg per well of target vector and 0.5 μg of TK-renilla (internal control) (Promega). A 1 : 3 ratio of transfected DNA to lipofectamine was determined to give the best transfection efficiency in cortical neurons. All transfections were performed overnight and complete medium was added the following day.

In all luciferase assays, the cells were harvested 2 days after the addition of the complete media to the cells. Luciferase assays were detected with the Dual Luciferase Assay (Promega) according the manufacturer's instructions. Graphs show mean value of at least three experiments with error bars depicting the standard error of the mean. All values were first normalized against Renilla activity in the same experiment to control for transfection efficiency and then calculated relative to the screened vector in untreated cortical neurons.

Statistical analysis

Statistical analysis was performed using the Student's *t*-test, for single analyses. Where multiple testing was required, a one-way ANOVA test was utilized, with a *post hoc* Tukey's HSD test. *p*-Values < 0.05 were considered significant. All statistical analyses were performed using the GraphPad Prism 4 suite of software (GraphPad Software, Inc., San Diego, CA, USA).

Results

Developmental regulation of SNCA in cultured cortical neurons

Alpha-synuclein has been shown to be developmentally induced in rat brain (Petersen *et al.* 1999; Vogiatzi *et al.* 2008), and we have shown that this effect can be replicated in cultured CNS neurons, a situation in which neurons mature in culture (Rideout *et al.* 2003; Vogiatzi *et al.* 2008). To begin to study the mechanisms involved in such regulation, we first verified in our cultured cortical neurons this induction of SNCA at the level of protein (Figure S1a). We determined that this developmental induction of SNCA is controlled, at least in part, by transcriptional regulation, as we observed a twofold increase in the levels of mRNA for SNCA after 8 DIV when compared with the levels observed after 1 DIV using RT-PCR (Figure S1b).

Multiple elements in the SNCA promoter are involved in its developmental regulation in cortical neurons

We then used the luciferase assay with a range of different length SNCA promoter constructs (Chiba-Falek and Nussbaum 2001) to identify regions of the promoter involved in the developmental transcriptional regulation of SNCA (Fig. 1a). We observed significant levels of induction for all constructs from 1.9 to 10.7 kb in length when compared with the control empty luciferase construct (Ctrl). We observed no induction from the 1.46 kb construct, which terminated in the first exon of SNCA 3′ of the canonical transcriptional start site (TSS). This observation is of interest as it is the opposite to that which we observed in the rat PC12 cell line in which induction of SNCA by neurotrophins results in an activation for constructs lacking the canonical TSS (Fig. 1b; Clough and Stefanis 2007; Clough *et al.* 2009). In the PC12 cell line, constructs that contain both the canonical TSS (including approximately 500 bp of the 5′ promoter) and intron 1 fail to show activation in the presence of neurotrophins (Clough and Stefanis 2007;
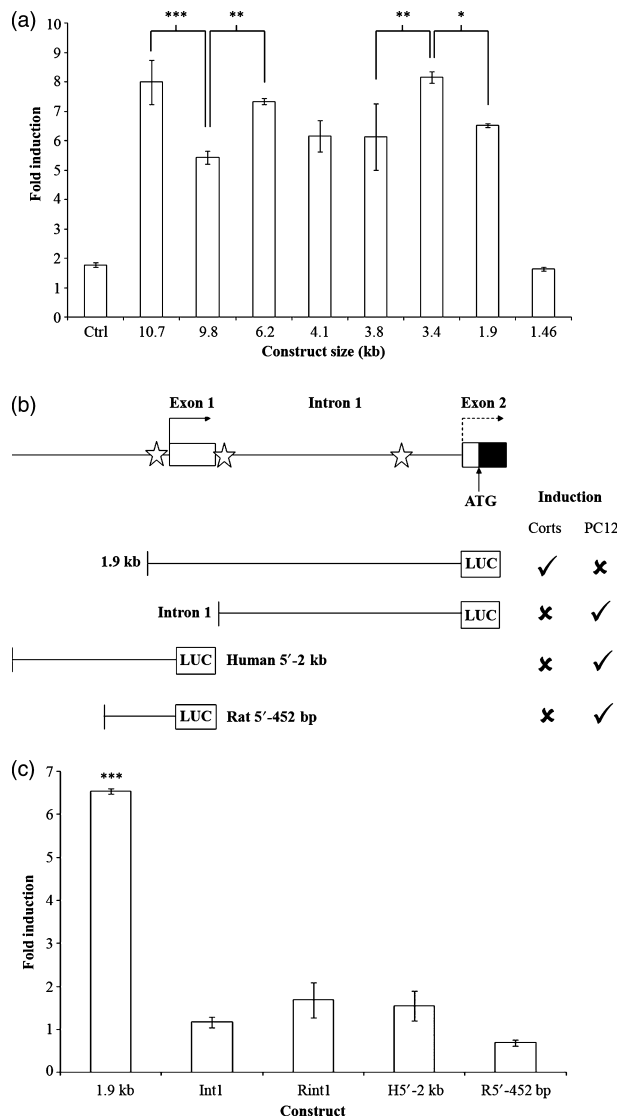
Fig. 1 Developmental regulation by multiple elements in the alpha-synuclein (SNCA) promoter. (a) Induction in the luciferase assay for 5′ promoter constructs longer than 1.9 kb in length. Induction in the luciferase assay was determined by comparing the levels of induction observed in cultures transfected at days *in vitro* (DIV) 1 and those transfected at DIV 8, and then harvested at DIV 3 and 10, respectively. We observe a clear induction for all constructs 1.9 kb and larger. Significant increases in induction were observed between the following constructs: 1.9 versus 3.4 kb and 9.8 versus 10.7 kb. We also observed significant reductions in induction between: 3.4 versus 3.8 kb and 6.2 versus 9.8 kb. $*p < 0.05$; $**p < 0.01$; $***p < 0.001$ for one-way ANOVA with Tukey's *post hoc* test ($n = 3$ per construct). (b) Cartoon depicting the 5′ genomic structure of human SNCA. Exons are depicted as closed boxes, and introns as lines. The two promoter sites are depicted by bent arrows, with the putative intron 1 promoter with a dashed line. Luciferase constructs for this region are depicted as lines connected to a LUC-labeled box. Stars indicate the localization of previously identified transcription factor binding sites in the 5′ promoter and intron 1 sequences (Clough and Stefani 2007; Clough *et al.* 2009). Ticks represent activation in the luciferase assay and crosses represent a lack of induction. Constructs containing the canonical transcriptional start site and intron 1 sequences are induced in the luciferase assay in cultured cortical neurons (cross-mark), as assessed in the present experiments (see results in a). Constructs containing either the 5′ promoter sequence (Human 5′-2kb or Rat 5′-452 bp) or intron 1 (for human and rat sequences) in isolation are not induced in this assay (see results below in c). This is the opposite pattern of induction compared to that observed in PC12 cells in the presence of neurotrophins, based on our previous results (Clough *et al.* 2007; Clough *et al.* 2009). (c) Luciferase assay for the isolated 5′ promoter region and intron 1 sequence of SNCA. There was a significant induction for the 1.9 kb construct for DIV 8 cultures compared with DIV 1 cultures (containing intron 1 and 5′ promoter sequences; $***p < 0.001$, Student's *t*-test); however, we observed no significant developmental induction from constructs containing only the human (Int1) or rat (Rint1) intron 1 sequences for DIV 8 cultures compared with DIV 1 cultures. We also observed no significant induction from the 5′ promoter sequences for either the human (H5′-2kb) or rat (R5′-452 bp) constructs ($n = 3$ per construct).

Clough *et al.* 2009). We observed significant increases in activation between the contiguous constructs 1.9 and 3.4 kb ($p < 0.05$) and 9.8 and 10.7 kb ($p < 0.001$); there were also significant decreases in activation between the 3.4 and 3.8 kb ($p < 0.01$) and 6.2 and 9.8 kb ($p < 0.01$) constructs (one-way ANOVA with Tukey's *post hoc* test). Of particular interest is the significant increase in activation observed between the 9.8 and 10.7 kb constructs as the larger construct contains the complex dinucleotide repeat NACP–REP (Touchman *et al.* 2001); polymorphisms in this region have been linked to an increased risk of developing PD (Maraganore *et al.* 2006).

We then examined if the canonical 5′ promoter or intron 1 would work in isolation in the luciferase assay as we had previously seen in the PC12 cell line (Fig. 1b; Clough and Stefanis 2007; Clough *et al.* 2009). We observed no induction in the luciferase assay when we compare the level

of activation observed in DIV 8 cultures against DIV 1 cultures for the human (Int1) or rat (Rint1) intron 1 sequences, 2 kb of the human 5′ promoter lacking intron 1 (H5′-2kb) or 452 bp of the rat 5′ promoter (R5′-452 bp; Fig. 1c). Therefore, in the cortical neuron system canonical 5′ promoter elements and Intron 1 do not work in isolation, but rather in unison to mediate SNCA transcription.

SNCA developmental induction is regulated through the PI3–K pathway

We then examined if any of the major kinase signaling pathways were involved in the developmental regulation of SNCA. Using pharmacological inhibitors to the mitogen-activated protein kinase/ERK (U0126), PI3-K (LY294002), c-jun N-terminal kinases (SP600125), and p38-MAPK (SB203580) pathways, we first screened the protein levels of SNCA (Fig. 2a). We only observed a significant reduction
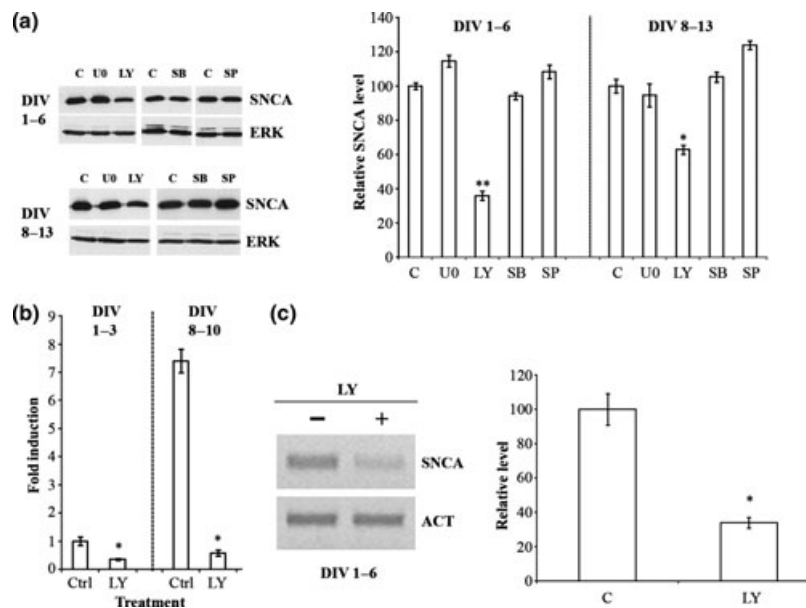
Fig. 2 Developmental induction of SNCA is controlled through the phosphatidyl-inositol 3 kinase (PI3-K) signaling pathway. (a) Western immunoblot of samples harvested from early (DIV 1–6) and late (DIV 8–13) cultures of cultured cortical neurons treated for 5 days with various pharmacological inhibitors of the major kinase signaling pathways. For both sets of cultures, we observe a clear inhibition of the developmental induction of SNCA following treatment with LY, the PI3-K inhibitor. This was confirmed in multiple experiments ($n = 3$), which are depicted on the right panel. LY caused a significant inhibition of SNCA levels at both time points (DIV 1–6, **$p < 0.001$; DIV 8–13, *$p < 0.01$; one-way ANOVA with Tukey's *post hoc* test). C, control; U0, U0126 (MEK/ERK inhibitor); LY, LY294002 (PI3-K inhibitor); SB, SB203580 (p38-MAPK inhibitor); SP, SP6 (JNK inhibitor); SNCA; α-synuclein; ERK, Erk loading control; and DIV, days *in vitro*. (b) Luciferase assay for the 1.9 kb luciferase construct in the presence (LY) or absence of LY2 (Ctrl), a pharmacological inhibitor of the PI3-K pathway. We observed reduced levels of activation in early (DIV 1–3) and late (DIV 8–10) cultures in the presence of LY2 ($n = 3$; both *$p < 0.05$, Student's t-test). Ctrl, control; LY, LY294002 (PI3-K inhibitor); and DIV, days *in vitro*. The levels of induction for the DIV 8–10 cultures in the luciferase assay are measured relative to those observed in the DIV 1–3 cultures. DIV, days *in vitro*; LY, LY294002 (PI3-K inhibitor); and Ctrl, control. (c) Cultured cortical neurons treated with an inhibitor of the PI3-K pathway (LY+) from days 1 to 6 in culture exhibit significantly reduced levels of mRNA for SNCA when compared with untreated control cells (LY−) ($n = 3$; *$p < 0.01$, Student's t-test). The graph represents the quantification of three independent samples. +, treated with the inhibitor of the PI3-K pathway; −, control cells; SNCA, α-synuclein; ACT, β-actin loading control; DIV, days *in vitro*; and LY, LY294002 (PI3-K inhibitor).

in the levels of SNCA for the inhibitor to the PI3-K pathway in cultures incubated from DIV 1–6 and in cultures from DIV 8–13. Using the luciferase assay with the 1.9 kb construct, we observed a reduction in the levels of activation for this construct in cells treated from DIV 1 to 3. For older cultures (DIV 8–10), this reduction in activation was more pronounced (Fig. 2b). SNCA mRNA levels, as measured with RT-PCR, were decreased with LY treatment in cultures treated from DIV 1–6 (Fig 2c).

The PI3-K intracellular signaling pathway is generally activated in response to extracellular factors, and is classically involved in growth factor signaling. The involvement of the PI3-K pathway in SNCA regulation in this model posed the possibility that growth factor signaling, acting in a paracrine or autocrine fashion, may be responsible for the observed phenomenon. To examine this in a general fashion, we applied the general tyrosine kinase receptor (Trk receptor) inhibitor k252a to the cultures. We found that this compound substantially diminished SNCA protein levels both in early (left panels) and in later (right panels) cultures (Fig 3).

We conclude that the PI3-K pathway is the major pathway regulating the induction of SNCA in this cell culture system following extracellular signaling via Trk receptors.

Increased SNCA induction in the presence of the neurotrophin BDNF

Our data with LY2 and k252a suggested to us that the induction of SNCA with maturation in culture may be under the control of exogenous factors secreted by the cultured cortical neurons. Cultured cortical neurons secrete the neurotrophins BDNF, neurotrophin (NT)3, NT4/5 (Sometani *et al.* 2001). We assessed the levels of SNCA in cultures incubated over a 5-day period in the presence of BDNF. As seen in Fig. 4(a), we observed significant increases in SNCA protein in cultures incubated from DIV 1 to 6 or from DIV 8 to 13 in BDNF ($p < 0.05$, Student's t-test), when compared with untreated controls. At the level of mRNA, we also observed a significant increase in the levels of SNCA for both early (DIV 1–6) and late (DIV 8–13) cultures ($p < 0.05$, Student's t-test), when compared with untreated controls,
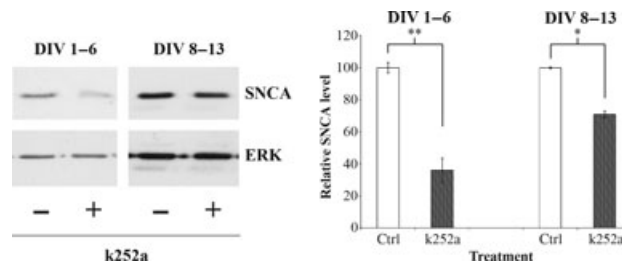
Fig. 3 Developmental induction of alpha-synuclein (SNCA) is inhibited by the Trk inhibitor k252a. Cultured cortical neurons were treated with the general Trk inhibitor k252a (+) or left untreated (−) from days 1 to 6 (left panel) or from days 8 to 13 (right panel). Lysates were then generated and used for western immunoblotting with antibodies against SNCA (top) or ERK (bottom, as loading control). Quantification of the results from multiple experiments ($n = 3$) is presented on the right. With both treatments at the different time points, k252a significantly reduced SNCA levels (**$p < 0.01$ for days 1–6 and *$p < 0.05$ for days 8–13, Student's *t*-test).
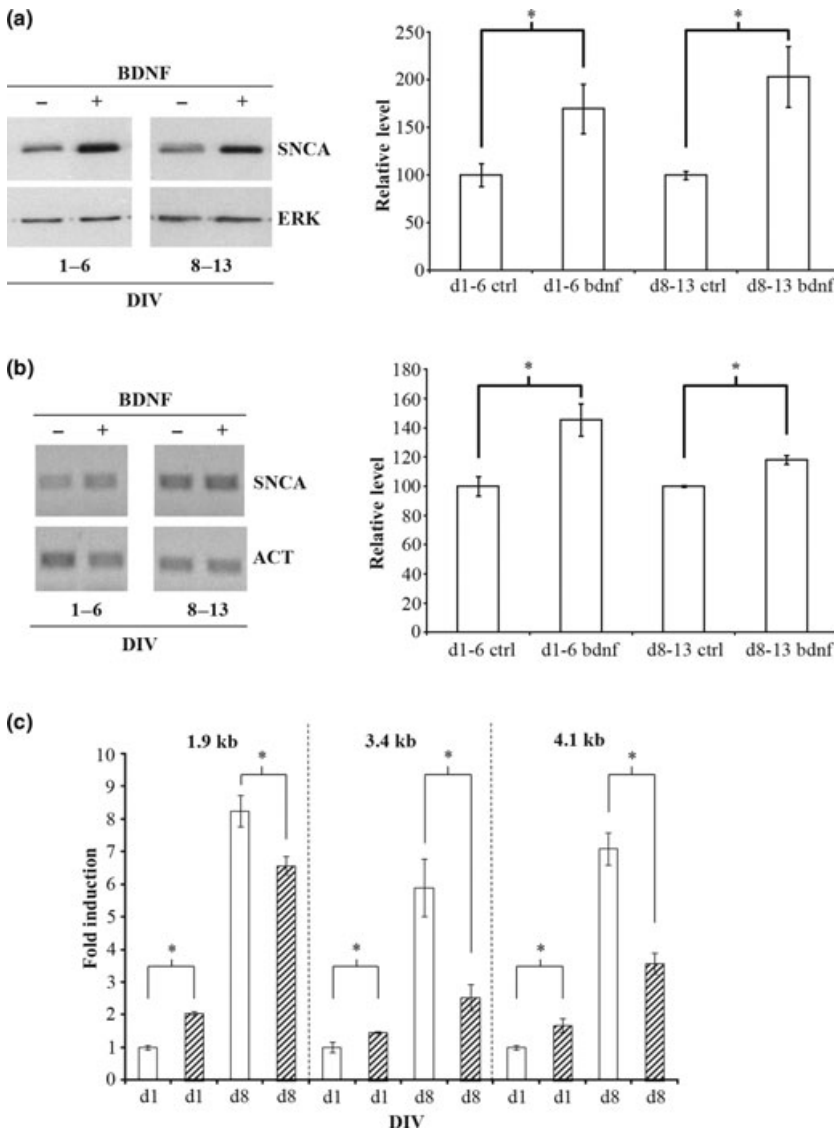

Fig. 4 Increased alpha-synuclein (SNCA) transcriptional induction in the presence of the neurotrophin brain-derived neurotrophic factor (BDNF). (a) Western immunoblot demonstrating that BDNF treatment (+) for 5 days significantly increases the protein levels of SNCA in both early [days *in vitro* (DIV) 1–6] and late (DIV 8–13) cultures of cortical neurons when compared with untreated (−) cultures ($n = 3$; *$p < 0.05$, Student's *t*-test). (b) RT-PCR demonstrates that BDNF treatment (+) for 5 days significantly increases the mRNA levels of SNCA in early (DIV 1–6) and late (DIV 8–13) cultures of cortical neurons when compared with untreated (−) cultures ($n = 3$; $p < 0.05$, Student's *t*-test). (c) The luciferase assay reveals a differential mode of action of BDNF in early and late cultures of cortical neurons. In all three promoter constructs examined (1.9, 3.4, and 4.1 kb), we observed a small, but significant increase in activation of the luciferase assay in early cultures (DIV 1–3) treated with BDNF when compared with control cultures ($n = 3$; *$p < 0.05$, Student's *t*-test). In late cultures (DIV 8–10), we observe a significant reduction in the activation of the luciferase assay for BDNF-treated cultures when compared with control cells ($n = 3$; *$p < 0.05$, Student's *t*-test). Levels of induction for the DIV 8–10 cultures in the luciferase assay are measured relative to DIV 1–3 cultures. DIV, days *in vitro*; −, control untreated cells; +, BDNF-treated cells; SNCA, α-synuclein; ERK, Erk loading control; and ACT, β-actin loading control.

although the difference was marginal in the latter case (Fig. 4b).

In an indicative experiment, we examined the levels of SNCA protein in cultures continuously treated with BDNF from DIV 1 until DIV 13 and compared them with the levels observed in control untreated cells (Figure S2). As we had observed in Figure S1(a), the levels of SNCA in control cultures reach a plateau after 7 DIV, although in the current experiment the level of induction was higher, reaching about sixfold compared with day 1. For cultures treated with BDNF, we observe higher levels of SNCA from day 3 onwards and the levels of SNCA keep increasing until DIV 11 when they too reach a plateau. This increase of SNCA levels over a longer time period that control cells in the presence of BDNF is analogous to the *in vivo* setting where the levels of SNCA keep increasing at least until P21 (Vogiatzi *et al.* 2008).

In the luciferase assay, we observed a consistent pattern of activation in the presence of BDNF in early cultures (DIV 1–3) and a reduction of activation with BDNF treatment in the later cultures (DIV 8–10; Fig. 4c), when compared with untreated control cells. This pattern was observed for a number of different length SNCA promoter constructs (1.9, 3.4, and 4.1 kb) indicating that it was a general feature of the SNCA promoter. It would appear therefore that these transcriptional elements are responsible for the BDNF-induced SNCA induction only in the early cultures.

We then examined if the BDNF molecule signaled through the same PI3-K pathway as the putative secreted factor responsible for the developmental induction of SNCA. As expected (see Fig. 2), the pharmacological inhibitor of the PI3-K pathway LY2 applied over days 1–6 significantly decreased SNCA protein levels in cultures not treated with BDNF. LY2 also reduced the induction observed in the presence of BDNF to background levels (Fig. 5a). We
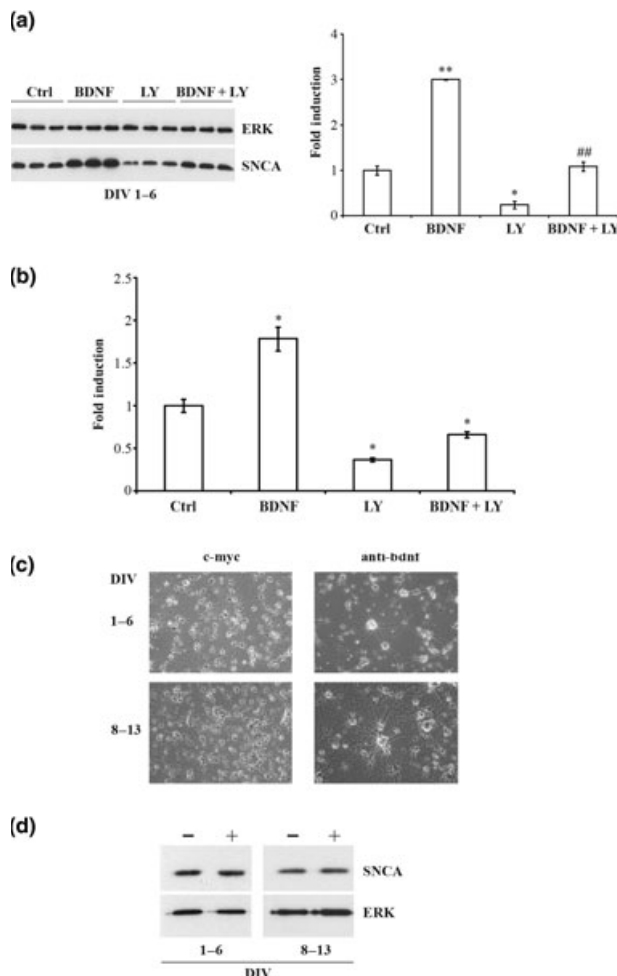

Fig. 5 Brain-derived neurotrophic factor (BDNF) and the developmental induction of SNCA. (a) Developmental induction and BDNF induction signal through the same kinase signaling pathway. Western immunoblot of protein harvested from cultured cortical neurons [days *in vitro* (DIV) 1–6] showing that co-incubation of a phosphatidyl-inositol 3 kinase (PI3-K) inhibitor and BDNF abolishes the induction of SNCA observed in the presence of BDNF on its own, that is, there was no significant difference in the levels of SNCA between conditions Ctrl and BDNF+LY cells. Ctrl, control cells; BDNF, BDNF treatment (**$p < 0.001$ vs. Ctrl; one-way ANOVA with Tukey's *post hoc* test); LY, treatment with a pharmacological inhibitor of the PI3-K pathway (LY294002; *$p < 0.05$ vs. Ctrl; one-way ANOVA with Tukey's *post hoc* test); BDNF + LY, treatment with BDNF and LY294002 (##$p < 0.001$ vs. BDNF; one-way ANOVA with Tukey's *post hoc* test). No other inhibitor of the major kinase signaling pathways (MEK/ERK, JNK, and p38-MAPK) significantly altered the BDNF effect (data not shown). (b) Developmental induction and BDNF induction signal through the same kinase signaling pathway as determined by the luciferase assay. We observed similar inhibition of the luciferase assay for the 1.9 kb construct as to what we observed for SNCA protein levels in Fig. 2(b). Ctrl, control cells; BDNF, BDNF treatment (*$p < 0.01$ vs. Ctrl; one-way ANOVA with Tukey's *post hoc* test); LY, treatment with a pharmacological inhibitor of the PI3-K pathway (LY294002; *$p < 0.01$ vs. Ctrl; one-way ANOVA with Tukey's *post hoc* test); and BDNF + LY, treatment with BDNF and LY294002 (#$p < 0.01$ vs. BDNF; one-way ANOVA with Tukey's *post hoc* test; $n = 3$ per condition). (c) Phenotypic changes associated with treatment of cultured cortical neurons with a neutralizing antibody to BDNF. In cultures from DIV 1 to 6, we observed a loss of cell bodies and fine neuritic network and a thickening and elongation of some cell processes in association with the application of an anti-BDNF antibody when compared with cells treated with a control antibody (c-myc). In these early cultures, we also observed some clustering of the surviving cell bodies. In DIV 8–13 cultures, we again observed a loss of cell bodies and a thickening of the cell processes, when compared with the control-treated cultures ($n = 3$). (d) Neutralizing antibody to BDNF has no effect upon the developmental induction of SNCA. We observed no differences in the levels of SNCA protein in either early (DIV 1–6) or late (DIV 8–13) cultures treated with a neutralizing antibody to BDNF (+) when compared with cultures treated with a control antibody to c-myc (−) ($n = 3$).

observed no effects of inhibition of the other major kinase signaling pathways (mitogen-activated protein kinase–ERK, c-jun N-terminal kinases, and p38-MAPK) on the induction observed upon addition of exogenous BDNF (data not shown). Similar repression of the BDNF effect upon inhibition of the PI3-K pathway were observed for the luciferase assay with the 1.9 kb construct in cultures treated from DIV 1 to 3 (Fig. 5b).

Cultured cortical neurons were then treated with a neutralizing antibody to BDNF to verify if they do indeed use BDNF in the regulation of SNCA (Fig. 5c). We observed no significant differences in the levels of SNCA in early (DIV 1–6) or late (DIV 8–13) cultures upon treatment with this neutralizing antibody. This suggests that BDNF is not a required factor responsible for the maturational induction of SNCA in these neurons. Phenotypically, treatment of cortical cultures with this neutralizing BDNF antibody (anti-bdnf) from DIV 1–6 (upper panel) or DIV 8–13 (lower panel) resulted in a loss of neuronal cell bodies and fine neuritic network, a clustering of neurons, and a thickening and an elongation of some cell processes, when compared to cells treated with a control antibody (c-myc; Fig. 5d), confirming that the antibody had biological effects at the doses utilized.

Discussion

Although SNCA levels play a critical role in familial and sporadic PD, potentially in other neurodegenerative conditions, and in the control of synaptic neurotransmission, the mechanisms that regulate SNCA transcription are not well understood. We have previously used the model system of PC12 cells to examine such mechanisms. This stemmed from our original observation that mRNA and protein levels of SNCA increase following treatment with growth factors in this system, in parallel to the well-known phenomenon of induced neuronal differentiation (Stefanis *et al.* 2001). We expanded these studies by showing that SNCA levels are similarly regulated by basic fibroblast growth factor (bFGF), but not glial cell line-derived neurotrophic factor, in ventral midbrain dopaminergic neurons, although, in this cell culture system, the main determinant of SNCA induction was maturation with time in culture. In this same work, we found that cultured cortical neurons also showed marked SNCA induction with maturation in culture, mimicking a phenomenon observed during development (Rideout *et al.* 2003).

In this work, we have used cultured cortical neurons to examine in more detail the mechanisms regulating the transcription of SNCA in primary CNS neurons, as our previous mechanistic work relied heavily on the use of the PC12 cell line. Our results indicate that there are important similarities and differences between the two model cell culture systems. In our prior work in PC12 cells, we were able to map out the signaling pathways and transcriptional elements involved in nerve growth factor- and bFGF-mediated SNCA induction. Briefly, pharmacological and molecular modulation of the ERK and PI3-K signaling pathways inhibited SNCA induction, indicating the involvement of these pathways in SNCA transcriptional control. Such control was achieved, at least in part, through elements in intron 1 of SNCA and, specifically, within its first and third quadrants (Clough and Stefanis 2007). Subsequent work has shown that the element within the first quadrant represents the binding site for the transcription factor Zipro1 (ZSCAN21), and that the transcriptional control region is quite complex, involving additional transcription factors, such as ZNF219 (Clough *et al.* 2009). Further downstream within Intron 1, another group has mapped out another important element for SNCA transcriptional control, the transcription factor GATA-2 (Scherzer *et al.* 2008).

The complex organization of the SNCA promoter region has been verified in the current work using varying lengths of this region in luciferase reporter assays and assessing luciferase activity over time in culture. It should be noted that these results are based on transient transfections, and may not reflect experiments under stable conditions. There are significant differences in activity between constructs of varying length throughout almost the extent of the promoter region, indicating the existence of multiple transcriptional control regions. A basic difference, however, between the PC12 cells and the primary cortical neurons is that in the former case the intron 1 region was sufficient for the induction of SNCA transcriptional activity, whereas in the latter it is not (Fig. 1). Furthermore, in the PC12 cells, regions 5′ of exon 1 are sufficient to induce SNCA transcriptional activity, whereas in the cortical neurons they are not. In fact, these two regions, the 5′ region to exon 1 and intron 1, appear to act antagonistically in PC12 cells (transcriptional activity can be elicited with each region in isolation, but not when they are present together), whereas they act synergistically in cortical neurons maturing in culture (transcriptional activity can be elicited only when they are present together, but not separately; Fig. 1b). This activity indicates that in both systems these regions contain important regulatory elements, but that they interact in a different fashion in each system.

Our current data, therefore, reinforce the importance of intron 1 regulatory regions in the transcriptional control of SNCA, as in the cortical neuron cultures they are necessary for SNCA transcriptional activation. This is in agreement with our previous data that indicated that Zipro 1, a transcription factor with a binding site at the very 5′-end of intron 1, mediates SNCA transcription, as its down-regulation via RNAi significantly suppressed SNCA protein levels in these cultures (Clough *et al.* 2009).

Differences and similarities are also noted in terms of the biochemical signaling pathways involved. Although in

the PC12 cell model, the ERK pathway is involved in the transcriptional control of SNCA (Clough and Stefanis 2007), this is not the case in cultured cortical neurons (Fig. 2). In contrast, the PI3-K pathway is required in both models for SNCA transcriptional activation. Therefore, modulation of this pathway may provide a more general means through which to limit excessive levels of SNCA. This, however, entails potential toxicity as the Akt/PI3-K pathway is a major regulator of survival (Chong *et al.* 2005).

A recent study suggested that the over-expression of another major genetic cause of PD, leucine-rich repeat kinase 2, activates the ERK pathway and, through this induction, leads to a slight increase of SNCA levels in non-neuronal cells. Of note, only WT leucine-rich repeat kinase 2, but not the PD-associated mutant, had this effect (Carballo-Carbajal *et al.* 2010). Another elegant study in enteric neurons has also identified the Ras/ERK pathway as a regulator of alpha-synuclein transcriptional activation in enteric neurons following elevation of cAMP or depolarization (Paillusson *et al.* 2010). Our present study suggests that a note of caution is required regarding the generalization of these findings in other systems, as even within neuronal populations context-dependent effects are significant, and the ERK pathway may not represent a general mechanism for the transcriptional regulation of SNCA. *In vivo* studies will be required to more conclusively demonstrate involvement of these signaling pathways in SNCA transcription.

Our results with the general inhibitor of Trk receptors indicate that such receptors are involved in the induction of SNCA in cultured cortical neurons. The fact that this induction mimics *ex vivo* the developmental induction observed *in vivo* raises the possibility that similar mechanisms mediated by growth factor signaling may control SNCA induction *in vivo*, at least in the developing rodent CNS. In cortical neuron cultures, TrkB and TrkC receptors are expected to mediate responses to naturally secreted growth factors, such as BDNF, NT3, and NT4–5, which can mediate autocrine or paracrine effects (Maisonpierre *et al.* 1990). BDNF is the best charac-terized of these neurotrophins in terms of its potential relationship to PD, as BDNF promotes the survival of nigral neurons in PD experimental models (Hyman *et al.* 1991), it is required for complete nigrostriatal neuronal development (Baquet *et al.* 2005; Oo *et al.* 2009), and it is down-regulated in PD brains (Howells *et al.* 2000); furthermore, polymor-phisms within the BDNF gene may be linked to PD (Momose *et al.* 2002), although this is controversial (Xiromerisiou *et al.* 2007). We decided, therefore, to focus on this neurotrophin in this study. We have found that BDNF is sufficient to induce SNCA transcriptional activity through the same signaling pathway (i.e., PI3 kinase-dependent) and response elements as the stimulus of time in culture. However, the inhibition of BDNF signaling through the use of neutralizing antibodies had no effect on SNCA levels. This indicates that although BDNF is sufficient for the activation of Trk receptors and the subsequent induction of SNCA transcription, it is not the main neurotrophin responsible for this effect during maturation in culture. The possibility remains that the other secreted neurotrophins, for example, NT3 or NT4/5, could function in a compensatory manner because of the lack of functional BDNF.

Our current and previous (Stefanis *et al.* 2001; Rideout *et al.* 2003; Clough and Stefanis 2007; Clough *et al.* 2009) studies collectively suggest that neurotrophins and growth factors such as bFGF have the potential to regulate the levels of SNCA. Further studies will be required to ascertain whether such neurotrophin-mediated effects actually occur in the *in vivo* setting, especially during development or in situations where SNCA levels change in the setting of plasticity (George *et al.* 1995) or toxic insults (Vila *et al.* 2000). It is tempting to speculate, given the localization of SNCA at the pre-synaptic terminals and its likely function in the regulation of synaptic release that such modulation of SNCA may serve to mediate the effects of neurotrophins, such as BDNF, on neuroplasticity.

In conclusion, we provide here evidence for the complex architecture of the SNCA transcriptional regulatory region in the context of primary cortical neurons that mature in culture. In this setting, the regulatory regions 5′ to exon 1 and in intron 1 cooperate for the induction of SNCA transcription. These effects are mediated through Trk and PI3-K signaling. The application of exogenous BDNF simulates these effects, but inhibition of its effect in maturing cultures does not lead to an appreciable alteration in the levels of SNCA, suggesting that BDNF is not the main factor involved in the induction of SNCA with maturation in culture. These findings highlight the complex regulation and context dependency of SNCA transcriptional control that relies, at least in part, on extracellular signaling via neurotrophins.

Acknowledgements

Supporting information

Additional supporting information may be found in the online version of this article:

Figure S1. (a) Western immunoblot of samples harvested from cultured cortical neurons at days 1, 8, and 15 post-culturing. (b) The developmental induction of SNCA is transcriptionally regulated as mRNA levels for SNCA from DIV 8 cultures are 2-fold higher than those observed in cultures harvested at DIV 1 (*$p < 0.05$ vs. DIV 1; $n = 3$).

Figure S2. Graph showing the relative levels of SNCA protein in control cortical and BDNF treated cultures over 13 DIV in a representative experiment.

As a service to our authors and readers, this journal provides supporting information supplied by the authors. Such materials are peer-reviewed and may be re-organized for online delivery, but are not copy-edited or typeset. Technical support issues arising from supporting information (other than missing files) should be addressed to the authors.

References

Adamczyk A., Solecka J. and Strosznajder J. B. (2005) Expression of alpha-synuclein in different brain parts of adult and aged rats. *J. Physiol. Pharmacol.* **56**, 29–37.

Baptista M. J., O'Farrell C., Daya S., Ahmad R., Miller D. W., Hardy J., Farrer M. J. and Cookson M. R. (2003) Co-ordinate transcriptional regulation of dopamine synthesis genes by alpha-synuclein in human neuroblastoma cell lines. *J. Neurochem.* **85**, 957–968.

Baquet Z. C., Bickford P. C. and Jones K. R. (2005) Brain-derived neurotrophic factor is required for the establishment of the proper number of dopaminergic neurons in the substantia nigra pars compacta. *J. Neurosci.* **25**, 6251–6259.

Beyer K., Lao J. I., Carrato C., Mate J. L., Lopez D., Ferrer I. and Ariza A. (2004) Differential expression of alpha-synuclein isoforms in dementia with Lewy bodies. *Neuropathol. Appl. Neurobiol.* **30**, 601–607.

Burré J., Sharma M., Tsetsenis T., Buchman V., Etherton M. and Südhof T. C. (2010) {alpha}-Synuclein promotes snare-complex assembly *in vivo* and in vitro. *Science* **329**, 1663–1667.

Carballo-Carbajal I., Weber-Endress S., Rovelli G., Chan D., Wolozin B., Klein C. L., Patenge N., Gasser T. and Kahle P. J. (2010) Leucine-rich repeat kinase 2 induces alpha-synuclein expression via the extracellular signal-regulated kinase pathway. *Cell. Signal.* **22**, 821–827.

Chandra S., Gallardo G., Fernández-Chacón R., Schlüter O. M. and Südhof T. C. (2005) Alpha-synuclein cooperates with CSPalpha in preventing neurodegeneration. *Cell* **123**, 383–396.

Chiba-Falek O. and Nussbaum R. L. (2001) Effect of allelic variation at the NACP-Rep1 repeat upstream of the alpha-synuclein gene (SNCA) on transcription in a cell culture luciferase reporter system. *Hum. Mol. Genet.* **10**, 3101–3109.

Chiba-Falek O., Lopez G. J. and Nussbaum R. L. (2006) Levels of alpha-synuclein mRNA in sporadic Parkinson's disease patients. *Mov. Disord.* **21**, 1703–1708.

Chong Z. Z., Li F. and Maiese K. (2005) Activating Akt and the brain's resources to drive cellular survival and prevent inflammatory injury. *Histol. Histopathol.* **20**, 299–315.

Clough R. L. and Stefanis L. (2007) A novel pathway for transcriptional regulation of alpha-synuclein. *FASEB J.* **21**, 596–607.

Clough R. L., Dermentzaki G. and Stefanis L. (2009) Functional dissection of the alpha-synuclein promoter: transcriptional regulation by ZSCAN21 and ZNF219. *J. Neurochem.* **110**, 1479–1490.

Cookson M. R., Hardy J. and Lewis P. A. (2008) Genetic neuropathology of Parkinson's disease. *Int. J. Clin. Exp. Pathol.* **1**, 217–231.

Dachsel J. C., Lincoln S. J., Gonzalez J., Ross O. A., Dickson D. W. and Farrer M. J. (2007) The ups and downs of alpha-synuclein mRNA expression. *Mov. Disord.*, **22**, 293–295.

Dietrich P., Rideout H. J., Wang Q. and Stefanis L. (2003) Lack of p53 delays apoptosis, but increases ubiquitinated inclusions, in proteasomal inhibitor-treated cultured cortical neurons. *Mol. Cell. Neurosci.* **24**, 430–441.

Edwards T. L., Scott W. K., Almonte C. *et al.* (2010) Genome-wide association study confirms SNPs in SNCA and the MAPT region

as common risk factors for Parkinson disease. *Ann. Hum. Genet.* **74**, 97–109.

Farrer M., Maraganore D. M., Lockhart P. *et al.* (2001) alpha-Synuclein gene haplotypes are associated with Parkinson's disease. *Hum. Mol. Genet.* **10**, 1847–1851.

Feany M. B. and Bender W. W. (2000) A Drosophila model of Parkinson's disease. *Nature* **404**, 394–398.

George J. M., Jin H., Woods W. S. and Clayton D. F. (1995) Characterization of a novel protein regulated during the critical period for song learning in the zebra finch. *Neuron* **15**, 361–367.

Gründemann J., Schlaudraff F., Haeckel O. and Liss B. (2008) Elevated alpha-synuclein mRNA levels in individual UV-laser-microdissected dopaminergic substantia nigra neurons in idiopathic Parkinson's disease. *Nucleic Acids Res.* **36**, e38.

Hadjigeorgiou G. M., Xiromerisiou G., Gourbali V. *et al.* (2006) Association of alpha-synuclein Rep1 polymorphism and Parkinson's disease: influence of Rep1 on age at onset. *Mov. Disord.* **21**, 534–539.

Howells D. W., Porritt M. J., Wong J. Y., Batchelor P. E., Kalnins R., Hughes A. J. and Donnan G. A. (2000) Reduced BDNF mRNA expression in the Parkinson's disease substantia nigra. *Exp. Neurol.* **166**, 127–135.

Hyman C., Hofer M., Barde Y. A., Juhasz M., Yancopoulos G. D., Squinto S. P. and Lindsay R. M. (1991) BDNF is a neurotrophic factor for dopaminergic neurons of the substantia nigra. *Nature* **350**, 230–232.

Kingsbury A. E., Daniel S. E., Sangha H., Eisen S., Lees A. J. and Foster O. J. (2004) Alteration in alpha-synuclein mRNA expression in Parkinson's disease. *Mov. Disord.*, **19**, 162–170.

Kirik D., Rosenblad C., Burger C., Lundberg C., Johansen T. E., Muzyczka N., Mandel R. J. and Bjorklund A. (2002) Parkinson-like neurodegeneration induced by targeted overexpression of alpha-synuclein in the nigrostriatal system. *J. Neurosci.* **22**, 2780–2791.

Larsen K. E., Schmitz Y., Troyer M. D. *et al.* (2006) Alpha-synuclein overexpression in PC12 and chromaffin cells impairs catecholamine release by interfering with a late step in exocytosis. *J. Neurosci.* **26**, 11915–11922.

Maisonpierre P. C., Belluscio L., Friedman B., Alderson R. F., Wiegand S. J., Furth M. E., Lindsay R. M. and Yancopoulos G. D. (1990) NT-3, BDNF, and NGF in the developing rat nervous system: parallel as well as reciprocal patterns of expression. *Neuron* **5**, 501–509.

Maraganore D. M., de Andrade M., Elbaz A. *et al.* (2006) Genetic Epidemiology of Parkinson's Disease (GEO-PD) Consortium. Collaborative analysis of alpha-synuclein gene promoter variability and Parkinson disease. *JAMA* **296**, 661–670.

Masliah E., Rockenstein E., Veinbergs I., Mallory M., Hashimoto M., Takeda A., Sagara Y., Sisk A. and Mucke L. (2000) Dopaminergic loss and inclusion body formation in alpha-synuclein mice: implications for neurodegenerative disorders. *Science* **287**, 1265–1269.

Mattila P. M., Rinne J. O., Helenius H., Dickson D. W. and Röyttä M. (2000) Alpha-synuclein-immunoreactive cortical Lewy bodies are associated with cognitive impairment in Parkinson's disease. *Acta Neuropathol.* **98**, 157–169.

Mizuta I., Satake W., Nakabayashi Y. *et al.* (2006) Multiple candidate gene analysis identifies alpha-synuclein as a susceptibility gene for sporadic Parkinson's disease. *Hum. Mol. Genet.* **15**, 1151–1158.

Momose Y., Murata M., Kobayashi K., Tachikawa M., Nakabayashi Y., Kanazawa I. and Toda T. (2002) Association studies of multiple candidate genes for Parkinson's disease using single nucleotide polymorphisms. *Ann. Neurol.* **51**, 133–136.

Mueller J. C., Fuchs J., Hofer A. *et al.* (2005) Multiple regions of alpha-synuclein are associated with Parkinson's disease. *Ann. Neurol.* **57**, 535–541.

Neystat M., Lynch T., Przedborski S., Kholodilov N., Rzhetskaya M. and Burke R. E. (1999) Alpha-synuclein expression in substantia nigra and cortex in Parkinson's disease. *Mov. Disord.* **14**, 417–422.

Oo T. F., Marchionini D. M., Yarygina O., O'Leary P. D., Hughes R. A., Kholodilov N. and Burke R. E. (2009) Brain-derived neurotrophic factor regulates early postnatal developmental cell death of dopamine neurons of the substantia nigra in vivo. *Mol. Cell. Neurosci.* **41**, 440–447.

Paillusson S., Tasselli M., Lebouvier T., Mahé M., Chevalier J., Biraud M., Cario-Toumaniantz C., Neunlist M. and Derkinderen P. (2010) Alpha-synuclein expression is induced by depolarization and cyclic AMP in enteric neurons. *J. Neurochem.* **115**, 694–706.

Pals P., Lincoln S., Manning J. *et al.* (2004) alpha-Synuclein promoter confers susceptibility to Parkinson's disease. *Ann. Neurol.* **56**, 591–595.

Papapetropoulos S., Adi N., Mash D. C., Shehadeh L., Bishopric N. and Shehadeh L. (2007) Expression of alpha-synuclein mRNA in Parkinson's disease. *Mov. Disord.* **22**, 1057–1059.

Petersen K., Olesen O. F. and Mikkelsen J. D. (1999) Developmental expression of alpha-synuclein in rat hippocampus and cerebral cortex. *Neuroscience* **91**, 651–659.

Rideout H. J. and Stefanis L. (2002) Proteasomal inhibition-induced inclusion formation and death in cortical neurons require transcription and ubiquitination. *Mol. Cell. Neurosci.* **21**, 223–238.

Rideout H. J., Dietrich P., Savalle M., Dauer W. T. and Stefanis L. (2003) Regulation of alpha-synuclein by bFGF in cultured ventral midbrain dopaminergic neurons. *J. Neurochem.* **84**, 803–813.

Rockenstein E., Hansen L. A., Mallory M., Trojanowski J. Q., Galasko D. and Masliah E. (2001) Altered expression of the synuclein family mRNA in Lewy body and Alzheimer's disease. *Brain Res.* **914**, 48–56.

Satake W., Nakabayashi Y., Mizuta I. *et al.* (2009) Genome-wide association study identifies common variants at four loci as genetic risk factors for Parkinson's disease. *Nat. Genet.* **41**, 1303–1307.

Scherzer C. R., Grass J. A., Liao Z. *et al.* (2008) GATA transcription factors directly regulate the Parkinson's disease-linked gene alpha-synuclein. *Proc. Natl Acad. Sci. USA* **105**, 10907–10912.

Simón-Sánchez J., Schulte C., Bras J. M. *et al.* (2009) Genome-wide association study reveals genetic risk underlying Parkinson's disease. *Nat. Genet.* **41**, 1308–1312.

Sometani A., Kataoka H., Nitta A., Fukumitsu H., Nomoto H. and Furukawa S. (2001) Transforming growth factor-beta1 enhances expression of brain-derived neurotrophic factor and its receptor, TrkB, in neurons cultured from rat cerebral cortex. *J. Neurosci. Res.* **66**, 369–376.

Stefanis L., Kholodilov N., Rideout H. J., Burke R. E. and Greene L. A. (2001) Synuclein-1 is selectively up-regulated in response to nerve growth factor treatment in PC12 cells. *J. Neurochem.* **76**, 1165–1176.

Touchman J. W., Dehejia A., Chiba-Falek O., Cabin D. E., Schwartz J. R., Orrison B. M., Polymeropoulos M. H. and Nussbaum R. L. (2001) Human and mouse alpha-synuclein genes: comparative genomic sequence analysis and identification of a novel gene regulatory element. *Genome Res.* **11**, 78–86.

Vekrellis K., Rideout H. J. and Stefanis L. (2004) Neurobiology of alpha-synuclein. *Mol. Neurobiol.* **30**, 1–21.

Vila M., Vukosavic S., Jackson-Lewis V., Neystat M., Jakowec M. and Przedborski S. (2000) Alpha-synuclein up-regulation in substantia nigra dopaminergic neurons following administration of the parkinsonian toxin MPTP. *J. Neurochem.* **74**, 721–729.

Vogiatzi T., Xilouri M., Vekrellis K. and Stefanis L. (2008) Wild type alpha-synuclein is degraded by chaperone-mediated autophagy and macroautophagy in neuronal cells. *J. Biol. Chem.* **283**, 23542–23556.

Xiromerisiou G., Hadjigeorgiou G. M., Eerola J. *et al.* (2007) BDNF tagging polymorphisms and haplotype analysis in sporadic Parkinson's disease in diverse ethnic groups. *Neurosci. Lett.* **415**, 59–63.
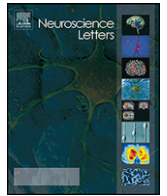
Increased dimerization of alpha-synuclein in erythrocytes in Gaucher disease and aging

Assimina Argyriou [a,1], Georgia Dermentzaki [a,1], Themistoklis Papasilekas [a,b,1], Marina Moraitou [c], Eleftherios Stamboulis [d], Kostas Vekrellis [a], Helen Michelakakis [c], Leonidas Stefanis [a,d,∗]

[a] Division of Basic Neurosciences, Biomedical Research Foundation of the Academy of Athens, Athens, Greece
[b] Department of Neurosurgery, National and Kapodistrian University of Athens Medical School, Athens, Greece
[c] Department of Enzymology and Cellular Function, Institute of Child Health, Athens, Greece
[d] Second Department of Neurology, National and Kapodistrian University of Athens Medical School, Athens, Greece

HIGHLIGHTS

- ► Alpha-synuclein (AS) dimers can be detected in human erythrocytes.
- ► No difference in AS monomer between Gaucher disease (GD) patients and controls.
- ► Increase of dimer to monomer ratio of AS in GD patients vs. controls.
- ► No change of AS monomer with aging.
- ► Increase of AS dimer to monomer ratio with aging.

ARTICLE INFO

ABSTRACT

Gaucher disease (GD) patients and carriers of glucocerebrosidase mutations are at an increased risk for Parkinson's disease (PD). The presynaptic protein alpha-synuclein (AS) is linked to PD. In the current work we examined biochemical properties of AS in GD patients. We generated membrane-enriched lysates from erythrocytes of 27 patients with GD and 32 age- and sex-matched controls and performed Western immunoblotting with antibodies against AS. Levels of monomeric AS did not differ between GD patients and controls and did not change as a function of age. However, the ratio of dimeric to monomeric AS was significantly increased in GD patients, and showed a significant positive correlation with age. Therefore, two major risk factors for PD, aging and GD status, are associated with an increased AS dimer to monomer ratio in erythrocytes. This ratio needs to be validated in further studies as a potential biomarker for PD risk.

1. Introduction

Gaucher disease (GD) is a rare autosomal recessive disorder characterized by a deficiency of the lysosomal enzyme gluco-cerebrosidase (GBA), leading to accumulation of its substrate glucocerebroside [11]. A body of work has emerged demonstrating an association between GD and Parkinson's disease (PD). In particular, GD patients [3] and heterozygote carriers of GBA mutations [17,21,8] have an increased risk of developing PD, and subjects with GBA mutations who develop Parkinsonism demonstrate on autopsy the typical neuropathological hallmarks of PD [17,8]. The mechanism through which GBA mutations predispose to PD is unknown.

Based on genetic, neuropathological and experimental data, alpha-synuclein (AS) has emerged as a major player in PD pathogenesis. It is widely believed that the pathway of AS misfolding, oligomerization and fibrillization, collectively termed aggregation, participates in neurodegeneration in PD and other synucleinopathies [6]. Although AS aggregates in PD cases associated with GBA mutations [17,8,10], it is unknown whether AS levels are actually elevated in GD patients, and whether AS provides the link that connects GD with PD. To address this issue, we have examined material derived from GD red blood cells (RBCs), an abundant source of AS, and compared levels of AS monomeric and dimeric species with those present in RBCs of an age- and gender-matched control group. In the process, we have also assessed whether AS in RBCs manifests age-dependent alterations.

∗ Corresponding author at: Laboratory of Neurodegenerative Diseases, Biomedical Research Foundation of the Academy of Athens, Soranou tou Efesiou 4, Athens 11527, Greece. Tel.: +30 210 6597214; fax: +30 210 6597545.
E-mail address: lstefanis@bioacademy.gr (L. Stefanis).
[1] These authors contributed equally to this work.

2. Materials and methods

2.1. Standard protocol approvals, registrations and patient consents

The protocol of the study was approved by the Institutional Boards and Ethics Committees of each institution involved in the study (Institute of Child Health, Athens, Greece; Evaggelsimos Hospital, Athens, Greece; Attikon Hospital, Athens, Greece). Most samples were available from stored material at the Department of Enzymology and Cellular Function, Institute of Child Health. For new samples obtained during the course of the study, written informed consent was obtained from all patients (or guardians of patients) participating in the study.

2.2. Population of patients and controls

Blood samples from 27 Gaucher patients, both male (11 patients) and female (16 patients) were studied. Their age ranged from 7 days to 77 years (mean age 39.8 years). The control group comprised 32 age and sex-matched normal subjects (13 male subjects; 19 female subjects; age ranging from 12 days to 78 years; mean age 35.2 years). The Department of Enzymology and Cellular Function, Institute of Child Health, provided GD, as well as most control samples. GD was diagnosed through assaying of glucocerebrosidase in leucocytes and/or skin fibroblast culture. Control samples were derived from children who tested negative for peroxisome diseases (plasmalogens and long chain fatty acid levels were estimated in erythrocytes and in plasma serum samples respectively) or healthy adult hospital/laboratory personnel. Additional controls were obtained from the Second Department of Neurology, Attikon Hospital, and the Department of Neurosurgery, Evaggelismos Hospital, Athens, Greece. These included patients with degenerative disease of the spine or healthy volunteers.

2.3. Obtaining of samples and protein extraction

Red blood cell (RBC) pellets were prepared from heparinized blood samples through spinning at $2200 \times g$ for 10 min at 4 °C and 3 consecutive washing steps with 1 volume of 0.9% NaCl. The RBC pellets were stored at −80 °C in 0.9% NaCl (1:1, v/v) and were thawed (cell lysis) upon use. Membrane pellets were purified from lysed RBCs through repeated washings in cold PBS and centrifugation at 13,000 rpm for 10 min at 4 °C. Supernatants containing cytosolic proteins, mainly hemoglobin, were discarded. The membrane pellets were then solubilized with 50 μl STET lysis buffer (50 mM Tris (pH 7.6), 150 mM NaCl, 2 mM EDTA, 1% Triton-X) on ice for 30 min. Solubilized membrane extracts were finally centrifuged (13,000 rpm; 10 min; 4 °C) and the supernatant was transferred to a new tube and used for Western immunoblotting.

2.4. Western Immunoblotting

Protein concentrations from membrane-enriched erythrocyte extracts were determined using the Bradford method (Bio-Rad, Hercules, CA, USA). Forty micrograms of protein was run on 12% sodium dodecyl sulfate-polyacrylamide gels. Following transfer to a nitrocellulose membrane, blots were probed with antibodies directed against AS: Syn 1 (BD Biosciences, San Jose, CA, USA), C-20 (Santa Cruz Biotechnology), and Syn 2.11 (Santa Cruz Biotechnology), and ERK (BD Biosciences, San Jose, CA, USA). Blots were probed with horseradish peroxidase-conjugated secondary antibodies and visualized with enhanced chemiluminescence substrate (ECL) following exposure to Super RX film (FUJI FILM, Europe GmbH, Germany).

2.5. Band quantification

The Gel analyzer software 1.0 (Biosure, Greece) was used to quantify the intensity of the bands, following scanning of the images with Adobe Photoshop 7.0. The ratio of monomeric AS to ERK, used as loading control, was first assessed. In order to perform the comparison across different Western blots, an internal control was always included on each blot as the reference point regarding the monomeric AS/ERK ratio.

Ratios of dimer to monomer of AS were assessed in a similar fashion. Values were normalized using the same blood sample as an internal control, the ratio of which was set as 1. Of note, the absolute AS dimer to monomer ratio of the internal control sample was similar across all blots (range from 0.19 to 0.36, mean = 0.29, SEM = 0.02, $n = 7$), attesting to the reproducibility of this ratio across blots.

2.6. Peptide competition

To test whether the Syn 1 monoclonal antibody and the C-20 polyclonal antibody react specifically with AS species, antibodies diluted in PBS were incubated for 1 h at room temperature in the presence of 10-fold molar excess of recombinant AS or 187-fold molar excess of the blocking peptide sc-7011 P (Santa Cruz Biotechnology) respectively. Following a 10-fold dilution in the case of the C-20 polyclonal antibody, the Syn 1-recombinant AS or the C-20–peptide sc-7011 mixture were used at a 1:1000 dilution to detect AS following SDS PAGE and immunoblotting.

2.7. Statistical analysis

Statistical analysis was performed either via Student's *t*-test or with linear regression with the GraphPad Prism 4 program with statistical significance set at $P < 0.05$. Data were parametrically distributed, and similar results with linear regression analysis were achieved using correlation analysis.

3. Results

3.1. AS species are readily detected in human erythrocytes

Initial attempts to detect AS by Western immunoblotting in biological material other than RBCs were unsuccessful, as AS was not detected in cell lysates derived from cultured skin fibroblasts, and only a small amount was detected in an isolated white blood cell (WBC) preparation. However, since it was not clear to what extent it was derived from contaminating erythrocytes and/or platelets [1], it was not pursued any further. Thus, and despite the fact that other investigators have used ELISA to measure AS in peripheral blood mononuclear cells (PBMCs) [2], our investigation focused only on RBCs. The first step involved the detection of AS in RBCs using Western immunoblotting as previously reported [1]. Typical results of such experiments are shown in Fig. 1. A band migrating at the level of monomeric AS, at around 17 kDa could invariably be detected. In some samples, high molecular species (HMS), and in particular a band migrating at the expected size for a dimer, around 35 kDa, were also detected. This band migrated at the same level on the blot using either one of the antibodies, and was also detected using the human-specific 211 antibody (data not shown). Such species were competed out when the antibodies were previously incubated either with an excess of the immunizing peptide (the case for C-20), or human recombinant AS (in the case of Syn-1) (Fig. 1).
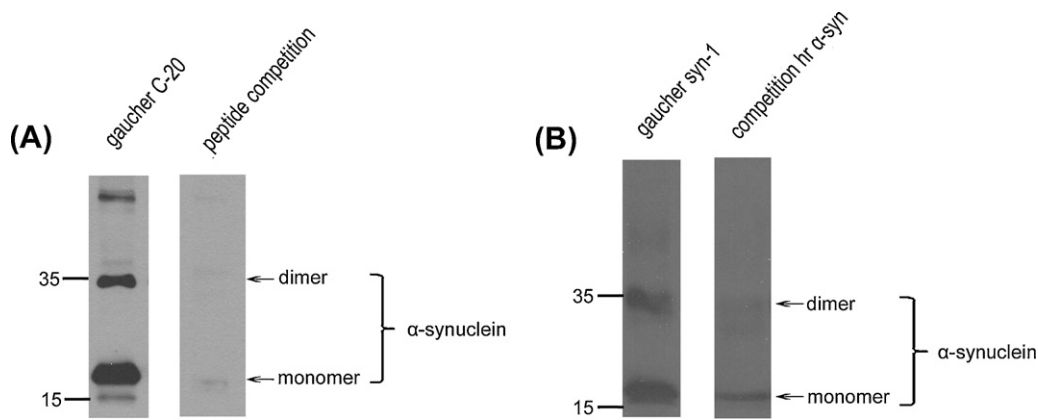
Fig. 1. Specificity of Syn-1 and C-20 antibodies to α-synuclein species. Lysates from Gaucher erythrocytes were separated by SDS PAGE and immunoblotted with the C-20 polyclonal (A) or Syn 1 monoclonal (B) antibodies to α-synuclein (AS). AS immunoreactivity was diminished when antibodies were preincubated with molar excess of either the peptide to C-20 (A) or human recombinant AS (B).

3.2. Monomeric AS levels are not significantly different between GD and control RBCs

Since the C-20 antibody appeared to be more sensitive toward the detection of AS (Fig. 1), and especially the presumed oligomeric species, this antibody was used in all subsequent experiments. The levels of monomeric AS across the two groups, GD and control subjects, were initially investigated, using ERK as the loading control. As shown in Fig. 2A, there was considerable variability in AS levels across samples, even within the same group, i.e. GD or controls. Overall, statistical analysis showed no significant difference between monomeric AS levels in our two study groups (Fig. 2B), i.e. no significant correlation between monomeric AS levels and GD status was found. Similar results were obtained when we used beta-actin as a loading control (data not shown).

3.3. AS dimer to monomer ratio is higher in GD patients compared to controls

Even from our initial experiments (see Figs. 1 and 2), it appeared that AS oligomeric species might be more prominent in GD patients. To assess this in a systematic fashion, we went on to compare the dimer/monomer AS ratio in the two groups. Longer exposure times were used in such Western immunoblotting experiments, so that the dimer would be readily visible. As shown in Fig. 3, the initial impression was confirmed, as statistical analysis showed that the dimer/monomer ratio was significantly higher in the GD compared to the control group.

3.4. AS monomer levels show no correlation to age

We also examined possible changes of monomeric AS levels as a correlation of age. We assessed each group separately; linear regression analysis of normalized protein loading data showed no significant age-related association in the levels of AS monomer in either of the two groups (Fig. 4A). Assessment of all samples together also failed to show any correlation of monomeric AS levels with age (data not shown).

3.5. AS dimer to monomer ratio increases with age in the control, but not in the GD group

We performed a similar linear regression analysis to assess whether the dimer/monomer AS ratio changed with aging. We observed a statistically significant positive correlation of this ratio with aging in the control, but not in the GD group (Fig. 4B). Interestingly, the AS dimer/monomer ratio in the GD group differed markedly from the control group in early and middle ages, but was similar to that of the older control subjects (>70 years of age). There was no correlation of the dimer/monomer ratio with age when all samples were assessed together (data not shown).

4. Discussion

The genetic link of GD to PD is now widely accepted, yet the molecular and biochemical underpinnings of this effect remain unknown. Given the pivotal role of AS oligomerization and aggregation in PD pathogenesis, we hypothesized that AS homeostasis could somehow be affected in GD. Support for this idea is provided
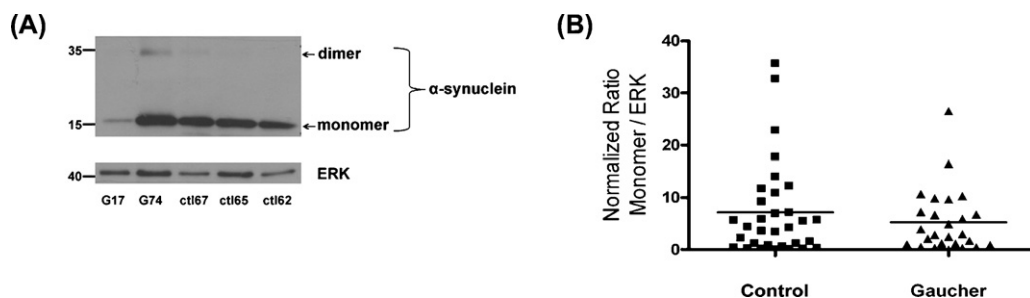

Fig. 2. Monomeric AS levels in Gaucher and control samples. (A) Lysates from Gaucher (G), (G17 55 years old and G74 7 days old subjects) and control (ctl) (ctl67 4, ctl65 10 and ctl62 38 years old subjects) erythrocytes were separated with SDS-PAGE, and immunoblotted with the C-20 polyclonal antibody to AS and the loading control ERK. Note the wide variability in monomeric AS levels and the faint, in this exposure, presence of the dimeric form. (B) The graph shows the normalized AS monomer to ERK ratio in control (black solid squares) and Gaucher (black solid triangles) samples respectively. Statistical analysis made via t test showed no significant difference of AS monomer to ERK ratio between control ($n = 32$) and Gaucher samples ($n = 27$). P value $= 0.3698$.
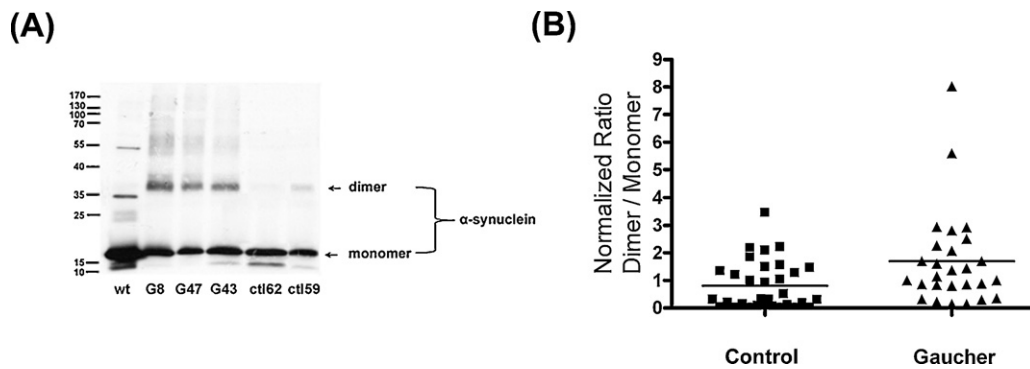
Fig. 3. (A) AS dimer to monomer ratio in Gaucher and control samples. Lysates from Gaucher (G8 32, G47 71, and G43 4.5 years old subjects) and control (ctl62 38 and ctl59 27 years old subjects) erythrocytes were separated with SDS-PAGE and immunoblotted with the C-20 polyclonal antibody to AS. There is an apparent increase of the AS dimer, but also of higher molecular weight species, in Gaucher compared to control samples. In the first lane, a lysate derived from human neuroblastoma SH-SY5Y cells inducibly expressing WT AS (wt) [24] is depicted for comparison. Note that both the monomer and the dimer in these samples migrate lower than the corresponding bands in the human erythrocytes. (B) The graph shows the normalized AS dimer to monomer ratio in control (black solid squares) and Gaucher (black solid triangles) samples respectively. Statistical analysis made via *t* test showed a significant increase for this ratio in Gaucher samples ($n = 27$), with a *P* value = 0.0135 compared to controls ($n = 32$).

by the presence of AS pathology in the brains of GD patients who develop Parkinsonism [17,8,10], and by the increase of monomeric and/or oligomeric AS in pharmacological or genetic cell culture and in vivo models of GD [13,25,7,15]. To further explore this hypothesis in human tissue material, we embarked on a study to systematically assess AS in various accessible tissues using Western immunoblot. The lack of significant expression in other accessible tissues however has forced us to restrict our study to RBCs.

The main finding from our study is the significantly increased ratio of dimer/monomer of AS in RBCs in patients with GD compared to age- and gender-matched controls. As this was not accompanied by an increase of monomeric alpha-synuclein, it suggests an increased tendency of conversion of the monomeric to the dimeric form. There was the impression that higher molecular weight forms were also increased in the group of GD patients (see for example Fig. 3), however because such bands were rather broad and fuzzy they were not formally quantified. The AS dimer is thought to be the limiting step toward oligomer formation [12]. Such findings suggest increased tendency of oligomerization of AS in GD patients, which may act as a risk factor for PD development. Consistent with this idea, the major risk factor for PD development, aging, was also associated with an increase of the dimer/monomer ratio, but only in the group of controls. The lack of an association of aging with this ratio in GD patients may be due to the fact that in this group blood was obtained for diagnostic purposes; therefore in all cases it represents the subjects' state at the time of diagnosis,

which may be rather homogeneous regarding AS oligomerization potential. Alternatively, this may represent a state marker, which cannot be increased above a certain threshold.

The fact that two risk factors for PD development, GD and aging, are associated with increased tendency of AS to oligomerize in RBCs provides important biological insights into PD pathogenesis, placing AS oligomerization, detectable in peripheral tissues, at an early stage of the pathogenetic process. How can we explain the increased tendency of AS to oligomerize in GD RBCs and with aging? Given the fact that we are assessing AS in membrane-rich fractions, it is tempting to speculate that alterations in membrane composition, and in particular the lipid bilayer, may occur in these two conditions, and may lead to enhanced AS oligomerization. Accumulation of glycosphingolipids, and in particular glucocerebroside, as occurs in GD, may lead to alterations in membrane lipid trafficking [9]. Erythrocytes, despite their lack of lysosomes, also have increased levels of glucocerebroside [18], probably through internalization of plasma lipoprotein-derived glucocerebroside [5]. Aging has also been associated with alterations of membrane-associated cholesterol [14]. It is known that change of membrane and lipid composition can profoundly influence AS oligomerization behavior [20,23]. Another possibility is that in these two conditions, aging and GD, there is increased oxidative stress that drives conversion of monomeric AS to the dimeric and other oligomeric forms. Indeed, both conditions have been associated with erythrocyte oxidative stress [4,16], and in turn oxidative stress is known
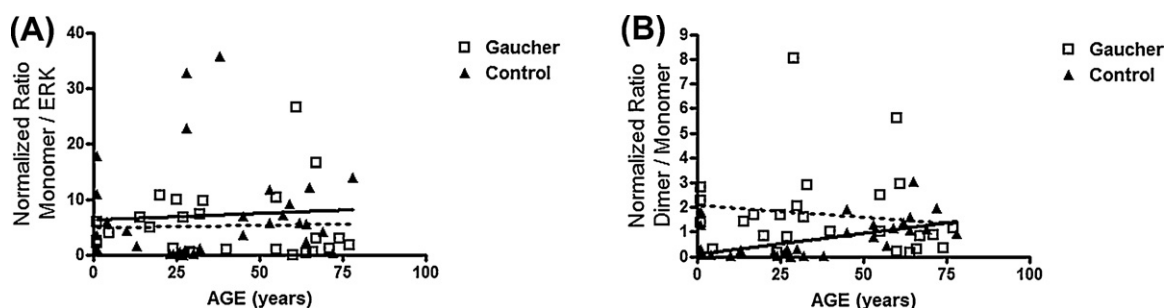

Fig. 4. Correlation of AS monomer and AS dimer/monomer ratio with age. (A) The graph shows the AS monomer to ERK ratio with the corresponding age in Gaucher (open white squares, dotted line) and control (black solid triangles, black line) samples. We observed no significant age-related difference in the AS monomer to ERK ratio neither in the Gaucher nor in the control group. Statistical analysis made through the GraphPad Prism Linear Regression program showed $r^2 = 0.004158$ and *P* value = 0.7259 for control group ($n = 32$) and $r^2 = 0.001624$ and *P* value = 0.8450 for Gaucher group ($n = 27$) respectively. (B) The graph shows the correlation of the AS dimer to monomer ratio with the corresponding age in Gaucher (white open squares, dotted line) and control (black solid triangles, black line) samples. We observed an age-related significant increase in the AS dimer to monomer ratio for the control group, whereas there was no significant age-dependent correlation in the Gaucher group. Statistical analysis through the GraphPad Prism Linear Regression program showed $r^2 = 0.2907$ and *P* value = 0.0015 for control group ($n = 32$) and $r^2 = 0.01983$ and *P* value = 0.4836 for Gaucher group ($n = 27$) respectively.

to enhance AS dimerization and oligomerization [12]. Of potential relevance is a study providing evidence of increased nitrosylation of AS in PBMCs of PD patients [19].

Our findings are based on a modest sample size and the study had a retrospective design, analyzing for the most part material that had already been obtained and preserved for other purposes. Our work therefore needs replication in a larger prospective and longitudinal study, where RBCs can also be obtained prior- and post-enzymatic replacement therapy. It will also be very important to include in such a study heterozygotes, carriers of GBA mutations. The aging effect will also need to be validated in such a future study.

The AS oligomer/monomer ratio was recently reported to be elevated in PD patients compared to controls in a study performed in CSF [22]. It will be very important to examine whether the dimer/monomer ratio in RBCs used here also differentiates PD patients from controls, as would be expected if this ratio reflects relative PD risk. Further work along these lines will be needed to test the possibility that this ratio may be a useful biomarker for disease risk, disease onset and/or progression. An advantage of such a biomarker would be the ease of accessibility of the tissue and the relative simplicity of the method employed.

References

[1] R. Barbour, K. King, J.P. Anderson, K. Banducci, T. Cole, L. Diep, M. Fox, J.M. Goldstein, F. Soriano, P. Seubert, T.J. Chilcote, Red blood cells are the major source of alpha-synuclein in blood, Neurodegenerative Diseases 5 (2008) 55–59.
[2] L. Brighina, A. Prigione, B. Begni, A. Galbussera, S. Andreoni, R. Piolti, C. Ferrarese, Lymphomonocyte alpha-synuclein levels in aging and in Parkinson disease, Neurobiology of Aging 31 (2010) 884–885.
[3] G. Bultron, K. Kacena, D. Pearson, M. Boxer, R. Yang, S. Sathe, G. Pastores, P.K. Mistry, The risk of Parkinson's disease in type 1 Gaucher disease, Journal of Inherited Metabolic Disease 33 (2010) 167–173.
[4] M.Y. Cimen, Free radical metabolism in human erythrocytes, Clinica Chimica Acta 390 (2008) 1–11.
[5] J.T. Clarke, The glycosphingolipids of human plasma lipoproteins, Canadian Journal of Biochemistry 59 (1981) 412–417.
[6] M.R. Cookson, M. Van der Brug, Cell systems and the toxic mechanism(s) of alpha-synuclein, Experimental Neurology 209 (2008) 5–11.
[7] V. Cullen, S.P. Sardi, J. Ng, Y.H. Xu, Y. Sun, J.J. Tomlinson, P. Kolodziej, I. Kahn, P. Saftig, J. Woulfe, J.C. Rochet, M.A. Glicksman, S.H. Cheng, G.A. Grabowski, L.S. Shihabuddin, M.G. Schlossmacher, Acid beta-glucosidase mutants linked to Gaucher disease, Parkinson disease, and Lewy body dementia alter alpha synuclein processing, Annals of Neurology 69 (2011) 940–953.
[8] J. DePaolo, O. Goker-Alpan, T. Samaddar, G. Lopez, E. Sidransky, The association between mutations in the lysosomal protein glucocerebrosidase and parkinsonism, Movement Disorders 24 (2009) 1571–1578.
[9] E.N. Glaros, W.S. Kim, C.M. Quinn, J. Won, I. Gelissen, W. Jessup, B. Garner, Glycosphingolipid accumulation inhibits cholesterol efflux via the ABCA1/apolipoprotein A-I pathway: 1-phenyl-2-decanoylamino-3-morpholino-1-propanol is a novel cholesterol efflux accelerator, Journal of Biological Chemistry 280 (2005) 24515–24523.
[10] O. Goker-Alpan, B.I. Giasson, M.J. Eblan, J. Nguyen, H.I. Hurtig, V.M. Lee, J.Q. Trojanowski, E. Sidransky, Glucocerebrosidase mutations are an important risk factor for Lewy body disorders, Neurology 67 (2006) 908–910.
[11] P. Guggenbuhl, B. Grosbois, G. Chalès, Gaucher disease, Joint, Bone, Spine 75 (2008) 116–124.
[12] S. Krishnan, E.Y. Chi, S.J. Wood, B.S. Kendrick, C. Li, W. Garzon-Rodriguez, J. Wypych, T.W. Randolph, L.O. Narhi, A.L. Biere, M. Citron, J.F. Carpenter, Oxidative dimer formation is the critical rate-limiting step for Parkinson's disease alpha-synuclein fibrillogenesis, Biochemistry 42 (2003) 829–837.
[13] A.B. Manning-Boğ, B. Schüle, J.W. Langston, Alpha-synuclein glucocerebrosidase interactions in pharmacological Gaucher models: a biological link between Gaucher disease and parkinsonism, Neurotoxicology 30 (2009) 1127–1132.
[14] M. Martin, C.G. Dotti, M.D. Ledesma, Brain cholesterol in normal and pathological aging, Biochimica et Biophysica Acta 1801 (2010) 934–944.
[15] J.R. Mazzulli, Y.H. Xu, Y. Sun, A.L. Knight, P.J. McLean, G.A. Caldwell, E. Sidransky, G.A. Grabowski, D. Krainc, Gaucher disease glucocerebrosidase and alpha-synuclein form a bidirectional pathogenic loop in synucleinopathies, Cell 146 (2011) 37–52.
[16] M. Moraitou, E. Dimitriou, D. Zafeiriou, C. Reppa, T. Marinakis, J. Sarafidou, H. Michelakakis, Plasmalogen levels in Gaucher disease, Blood Cells, Molecules, and Diseases 41 (2008) 196–199.
[17] J. Neumann, J. Bras, E. Deas, S.S. O'Sullivan, L. Parkkinen, R.H. Lachmann, A. Li, J. Holton, R. Guerreiro, R. Paudel, B. Segarane, A. Singleton, A. Hardy, H. Houlden, T. Revesz, N.W. Wood, Glucocerebrosidase mutations in clinical and pathologically proven Parkinson's disease, Brain 132 (2009) 1783–1794.
[18] O. Nilsson, G. Håkansson, S. Dreborg, C.G. Groth, L. Svennerholm, Increased cerebroside concentration in plasma and erythrocytes in Gaucher disease: significant differences between type I and type III, Clinical Genetics 22 (1982) 274–279.
[19] A.A. Prigione, F. Piazza, L. Brighina, B. Begni, A. Galbussera, J.C. Difrancesco, S. Andreoni, R. Piolti, C. Ferrarese, Alpha-synuclein nitration and autophagy response are induced in peripheral blood cells from patients with Parkinson disease, Neuroscience Letters 477 (2010) 6–10.
[20] R. Sharon, I. Bar-Joseph, M.P. Frosch, D.M. Walsh, J.A. Hamilton, D.J. Selkoe, The formation of highly soluble oligomers of alpha-synuclein is regulated by fatty acids and enhanced in Parkinson's disease, Neuron 37 (2003) 583–595.
[21] E. Sidransky, M.A. Nalls, J.O. Aasly, J. Aharon-Peretz, G. Annesi, E.R. Barbosa, A. Bar-Shira, D. Berg, J. Bras, A. Brice, C.M. Chen, L.N. Clark, C. Condroyer, E.V. De Marco, A. Dürr, M.J. Eblan, S. Fahn, M.J. Farrer, H.C. Fung, Z. Gan-Or, T. Gasser, R. Gershoni-Baruch, N. Giladi, A. Griffith, T. Gurevich, C. Januario, P. Kropp, A.E. Lang, G.J. Lee-Chen, S. Lesage, K. Marder, I.F. Mata, A. Mirelman, J. Mitsui, I. Mizuta, G. Nicoletti, C. Oliveira, R. Ottman, A. Orr-Urtreger, L.V. Pereira, A. Quattrone, E. Rogaeva, A. Rolfs, H. Rosenbaum, R. Rozenberg, A. Samii, T. Samaddar, C. Schulte, M. Sharma, A. Singleton, M. Spitz, E.K. Tan, N. Tayebi, T. Toda, A.R. Troiano, S. Tsuji, M. Wittstock, T.G. Wolfsberg, Y.R. Wu, P.C. Zabetian, Y. Zhao, S.G. Ziegler, Multicenter analysis of glucocerebrosidase mutations in Parkinson's disease, New England Journal of Medicine 361 (2009) 1651–1661.
[22] T. Tokuda, M.M. Qureshi, M.T. Ardah, S. Varghese, S.A. Shehab, T. Kasai, N. Ishigami, A. Tamaoka, M. Nakagawa, O.M. El-Agnaf, Detection of elevated levels of α-synuclein oligomers in CSF from patients with Parkinson disease, Neurology 65 (2010) 1766–1772.
[23] K. Vekrellis, H.J. Rideout, L. Stefanis, Neurobiology of alpha-synuclein, Molecular Neurobiology 30 (2004) 1–21.
[24] K. Vekrellis, M. Xilouri, E. Emmanouilidou, L. Stefanis, Inducible overexpression of wild type alpha-synuclein in human neuronal cells leads to caspase-dependent nonapoptotic death, Journal of Neurochemistry 109 (2009) 1348–1362.
[25] Y.H. Xu, Y. Sun, H. Ran, B. Quinn, D. Witte, G.A. Grabowski, Accumulation and distribution of alpha-synuclein and ubiquitin in the CNS of Gaucher disease mouse models, Molecular Genetics and Metabolism 102 (2011) 436–447.

PLOS ONE

Loss of β-Glucocerebrosidase Activity Does Not Affect Alpha-Synuclein Levels or Lysosomal Function in Neuronal Cells

Georgia Dermentzaki[1], Evangelia Dimitriou[2], Maria Xilouri[1], Helen Michelakakis[2], Leonidas Stefanis[1,3]*

1 Division of Basic Neurosciences, Biomedical Research Foundation of the Academy of Athens, Athens, Greece, 2 Department of Enzymology and Cellular Function, Institute of Child Health, Athens, Greece, 3 Second Department of Neurology, National and Kapodistrian University of Athens Medical School, Athens, Greece

Abstract

To date, a plethora of studies have provided evidence favoring an association between Gaucher disease (GD) and Parkinson's disease (PD). GD, the most common lysosomal storage disorder, results from the diminished activity of the lysosomal enzyme β-glucocerebrosidase (GCase), caused by mutations in the β-glucocerebrosidase gene (GBA). Alpha-synuclein (ASYN), a presynaptic protein, has been strongly implicated in PD pathogenesis. ASYN may in part be degraded by the lysosomes and may itself aberrantly impact lysosomal function. Therefore, a putative link between deficient GCase and ASYN, involving lysosomal dysfunction, has been proposed to be responsible for the risk for PD conferred by GBA mutations. In this current work, we aimed to investigate the effects of pharmacological inhibition of GCase on ASYN accumulation/aggregation, as well as on lysosomal function, in differentiated SH-SY5Y cells and in primary neuronal cultures. Following profound inhibition of the enzyme activity, we did not find significant alterations in ASYN levels, or any changes in the clearance or formation of its oligomeric species. We further observed no significant impairment of the lysosomal degradation machinery. These findings suggest that additional interaction pathways together with aberrant GCase and ASYN must govern this complex relation between GD and PD.

Introduction

Gaucher Disease (GD), is the most prevalent lysosomal storage disorder (estimated incidence 1 in 40.000–60.000) that follows an autosomal recessive trait. It is due to the diminished activity of the enzyme β-glucocerebrosidase (GCase). As a consequence glucosylceramide (GluCer) and, its deacylated form, glucosylsphingosine (GlcSph), accumulate in practically every tissue examined, including the brain. This accumulation is believed to lead to cellular pathology, through a mechanism that is not completely understood. The disease exhibits a remarkable heterogeneity that has been observed in its clinical symptoms, even among twins carrying identical mutations, suggesting the involvement of additional modifiers [1,2]. Classically, GD is divided into three clinical types, GD type 1, GD type 2 and GD type 3 depending on the presence, degree and rate of progression of neurologic involvement. GD 1, the most common type, is distinguished as the non-neuronopathic type, a classification that has been challenged due to its association with Parkinson's Disease (PD) and parkinsonism [3]. More specifically, genetic studies have identified GBA mutations as one of the most common reported risk factors for PD [4–12]. Many studies have attempted to shed light on the complex relation between GD and PD. One candidate culprit for this relation is alpha-synuclein (ASYN). Firstly, ASYN is an abundant neuronal protein that has been linked to PD pathogenesis. Intraneuronal inclusions, mainly consisting of ASYN

(Lewy bodies, Lewy neurites), are pathological hallmarks of PD and other synucleinopathies. Secondly, ASYN degradation has been proposed to take place in lysosomes, in part via chaperone-mediated autophagy (CMA) [13–16]; therefore, potential lysosomal dysfunction in neuronal cells due to diminished GCase activity could in time lead to ASYN accumulation and PD pathology.

In support to the presence of an interaction (direct or indirect) between ASYN and aberrant GCase, gain and/or loss-of-function models have been proposed. Immunofluorescence studies in brain samples from PD and/or Lewy body dementia individuals, along with GD or GBA mutation carriers, have shown the presence of GCase in LBs and LNs in most cases [17,18], suggesting a gain-of-function mechanism via a direct interaction. In accordance with the above, a recent study has demonstrated aggregation of ASYN in brain samples from individuals with GBA mutations [19]. Another study revealed that the direct interaction between WT GCase and ASYN under acidic conditions was stronger compared to the interaction with mutant GCase [20]. Likewise, GBA mutants were reported to promote ASYN accumulation whereas pharmacological inhibition of GCase activity did not affect ASYN levels *in vitro* [21]. On the other hand, other groups favor a positive correlation between loss of GCase activity and ASYN accumulation. Manning Bog et al [22] showed elevated ASYN levels following pharmacological inhibition of GCase. In support of the
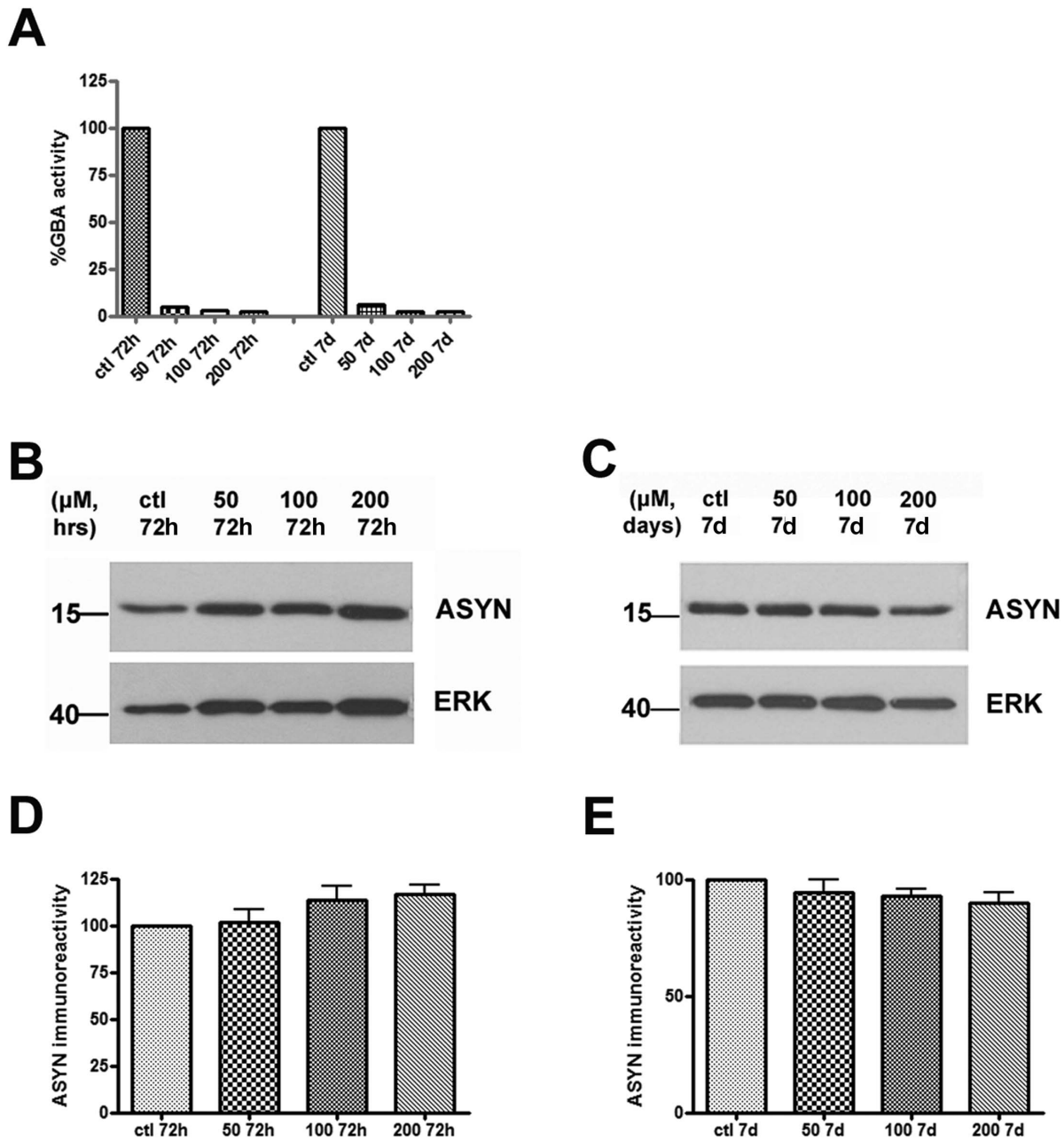
Figure 1. ASYN levels remain unchanged following GCase inhibition in differentiated SH-SY5Y cells. (A) Differentiated SH-SY5Y cells were exposed to increasing doses of CBE (50, 100, 200 μM) for 72 h and 7 days respectively. Untreated cells served as control (ctl). Cell pellets were assessed for GCase enzymatic activity at the aforementioned doses and time points. (B–C) Cell lysates were separated with SDS-PAGE and immunoblotted with the C-20 polyclonal antibody to ASYN. ERK = loading control. (D–E) Graphs show quantification of ASYN immunoreactivity (vs ERK) via densitometric analysis at 72 h and 7 day time point respectively. Statistical analysis made via One Way Anova showed no significant difference in ASYN levels at the given doses and time points (n = 8).
doi:10.1371/journal.pone.0060674.g001

notion of loss of function, in an extended study, Mazzulli et al [23] demonstrated accumulation of toxic, soluble oligomeric intermediates of ASYN and impaired lysosomal function, both in primary neuronal cultures, in which GBA had been lowered via RNAi, and in human iPS neurons derived from a GBA mutation carrier. Under the scope of this evidence, we undertook the present study to further investigate the contribution of deficient GCase activity to ASYN levels and lysosomal function in differentiated SH-SY5Y cells, in a doxycycline-inducible Tet-Off system for ASYN, and in primary neuronal cultures. We found that GCase deficiency was

not sufficient to either up-regulate ASYN or compromise the lysosomal degradation machinery, suggesting the presence of additional molecular mechanisms which, synergistically with aberrant GCase activity, contribute to the pathogenesis of PD and related synucleinopathies.
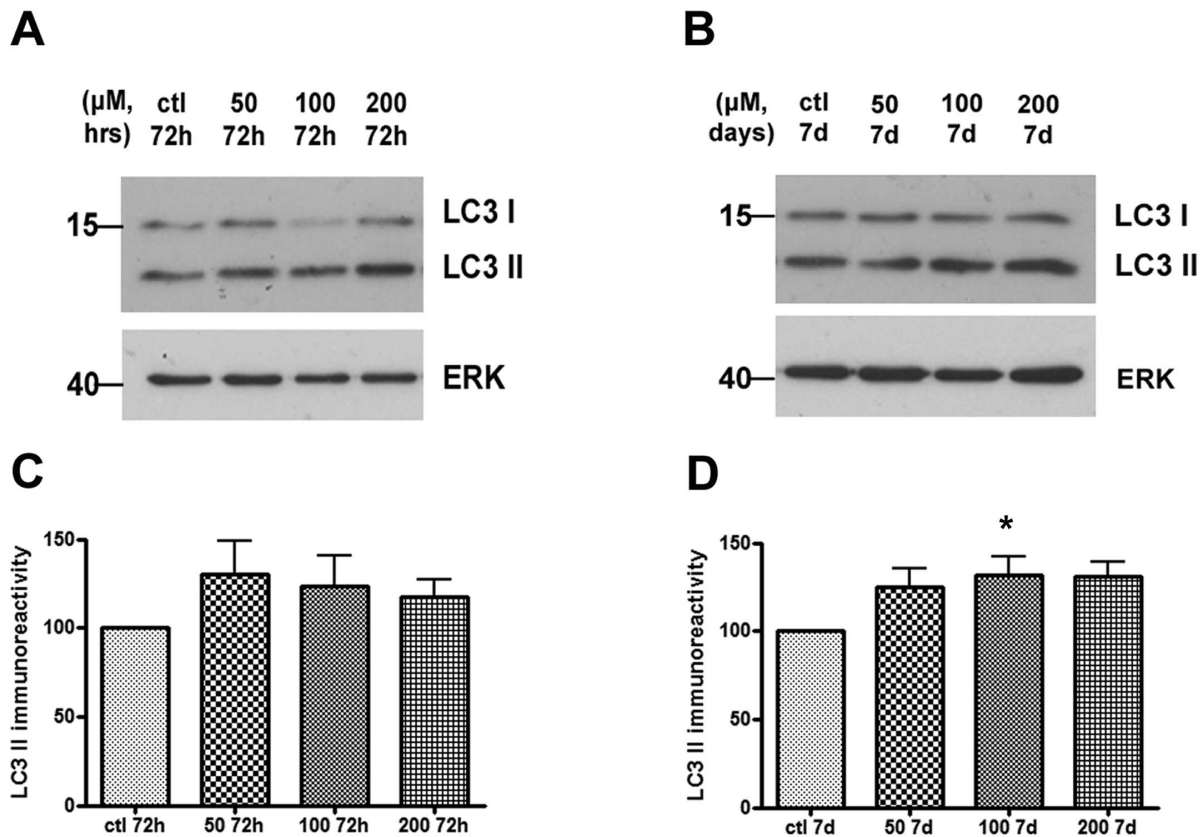
Figure 2. LC3 II levels slightly increase following GCase inhibition in differentiated SH-SY5Y cells. (A–B) Differentiated SH-SY5Y cells were exposed to increasing doses of CBE (50, 100, 200 μM) for 72 h and 7 days respectively. Untreated cells served as control (ctl). Cells were lysed, separated with SDS-PAGE and immunoblotted with the LC3 polyclonal antibody. ERK = loading control. (C–D) Graphs show quantification of LC3 II immunoreactivity (vs. ERK) via densitometric analysis at 72 h and 7 day time point respectively. Statistical analysis made via One Way Anova showed a significant increase in LC3 II levels for the 100 μM dose at the 7 day time point only, compared to ctl cultures ($P<0,05$; n = 8).
doi:10.1371/journal.pone.0060674.g002

Materials and Methods

Cell Culture

Neuroblastoma SH-SY5Y cells were cultured in RPMI 1640 plus L-glutamine (Sigma, St. Louis, MO, USA) supplemented with 10% heat-inactivated FBS and 1% penicillin/streptomycin (complete medium). The stable inducible Tet-Off SH-SY5Y neuroblastoma cell line overexpressing WT ASYN described in [14,24] was also cultured in the above complete medium in the presence (WT+dox) or in the absence (WT – dox) of doxycycline (2 μg/mL) (dox, Clontech). Differentiation of SH-SY5Y cells was with all-trans Retinoic Acid (RA, 20 mM, Sigma). With the particular SH-SY5Y line we are working with, there is full neuronal differentiation, as assessed by neuronal markers, 5 days after RA application [24]. For pharmacological studies Conduritol B-Epoxide (CBE, Sigma), 3-Methyladenine (3MA, Sigma-Aldrich), Bafilomycin (Baf, Sigma-Aldrich), NH$_4$Cl (Sigma-Aldrich) and rapamycin (rap, Sigma-Aldrich) were added at indicated time points and concentrations. In particular, the CBE inhibitor was replenished every other day together with the change of the medium.

Primary Culture

Cultures of Wistar rat (embryonic day 18) cortical neurons were prepared as previously described [25,26]. 1.5×10^6 cells were plated onto poly-D-lysine-coated six-well dishes. Cells were maintained in Neurobasal medium (Gibco, Rockville, MD, USA; Invitrogen, Carlsbad, CA, USA), with B27 serum-free supplement (Gibco; Invitrogen), L-glutamine (0,5 mM), and penicillin/streptomycin (1%). More than 98% of the cells cultured under these conditions represent post-mitotic neurons [27]. All efforts were made to minimize animal suffering and to reduce the number of the animals used, according to the European Communities Council Directive (86/609/EEC) guidelines for the care and use of laboratory animals. All animal experiments were approved by the Institutional Animal Care and Use Committee of Biomedical Research Foundation of the Academy of Athens.

Assay of GCase Activity

Cell pellets from differentiated SH-SY5Y cells or rat embryonic cortical cultures treated with or without CBE were homogenized in water by sonication. GCase activity was determined in whole cell homogenates using the artificial fluorogenic substrate 4-methylumbelliferyl β-D-glucopyranoside in the absence of taurocholate. The reaction mixture contained 5 mmol/L substrate in citrate phosphate buffer pH:4,5. The reaction was stopped after 30 min incubation at 37°C by the addition of 0,25 mol/L glycine-NaOH, pH:10,4 [28].
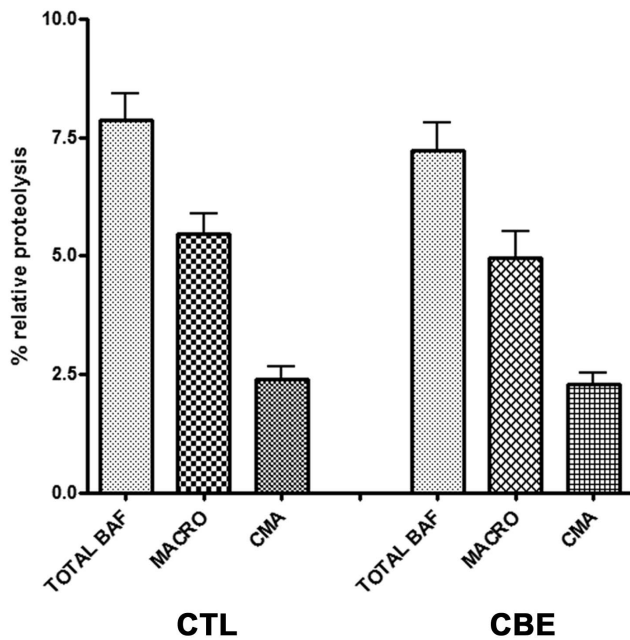
Figure 3. Lysosomal activity is not compromised following GCase inhibition in differentiated SH-SY5Y cells. Differentiated SH-SY5Y cells were treated or not (control cells) with CBE (200 μm) for 5 days. Following this, cells were radiolabelled with [³H] leucine supplemented with either 3MA (10 mM) or Baf (500 nM) and then assayed for long-lived protein degradation as described analytically in "Materials and Methods". Untreated cells were also used as control (ctl). Values are the mean ±SE of two independent experiments that were represented in triplicate per condition. Statistical analysis made via One Way Anova revealed no difference in the activity of the different lysosomal pathways between CBE-treated and control cells.
doi:10.1371/journal.pone.0060674.g003

Fractionation Assay

Stable inducible Tet-Off SH-SY5Y neuroblastoma cell lines overexpressing WT ASYN [14,29] were cultured in the presence (+) or absence (−) of dox (2 μg/mL) for 7 days. Subsequently, cells were differentiated for 5 days and then were exposed for various periods of time to CBE (200 μM), a pharmacological GCase inhibitor, either in the presence or absence of dox. Untreated cells were also used (ctl). Following this, cells were lysed in mild lysis buffer (50 mM Tris, pH 7,6, 1 mM EDTA, PH 8,0) and protease inhibitors. Lysates were passed through an insulin syringe and centrifuged at 600×g for 5 min at 4°C. Supernatant was transferred to a new tube and centrifuged at 100.000×g for 2 h at 4°C. The resultant supernatant represents the cytosolic fraction. The pellet was washed ×5 with solution: 50 mM Tris, pH 7,6, 1 M NaCl, 1 mM EDTA, PH 8,0 and centrifuged at 10.000 X g for 5 min at 4°C. Finally the pellet was resuspended in STET lysis buffer (50 mM Tris, pH 7,6, 150 mM NaCl, 1% Triton X-100, 2 mM EDTA) with protease inhibitors. This fraction represents the membrane-associated, Triton X-100 soluble fraction [30].

Intracellular Protein Degradation

Total protein degradation in differentiated SH-SY5Y cultured cells was measured by pulse-chase experiments [13,14,29,31] with modifications. Briefly, differentiated SH-SY5Y cells were exposed to CBE (200 μM) at day 5 of differentiation for 5 days. Untreated cells were used as well as controls. Following this treatment, cells were labeled with [³H] leucine (2 μCi/ml) (leucine, L-3,4,5; PerkinElmer Life Sciences) at 37°C for 48 h, in the presence or

absence of CBE. The cultures were then extensively washed with medium and returned in starvation medium (0,5% FBS) containing 2,8 mM of unlabeled excess leucine for 6 h. This medium containing mainly short lived proteins was removed and replaced with complete fresh medium containing the general lysosomal inhibitor Baf (500 nM)/NH₄Cl (20 mM) or the inhibitor of macroautophagy 3MA (10 mM) in the presence or absence of CBE (200 μM), as above. At this concentration 3MA is known to completely inhibit macroautophagy [32,33] and in our hands it abolishes the rapamycin-induced induction of LC3 II (Figure S1). Aliquots of the medium were taken at 14 h and proteins in the medium were precipitated with 20% trichloroacetic acid for 20 min on ice and centrifuged (10,000×g, 10 min, 4°C). Radioactivity in the supernatant (representing degraded proteins) and pellet (representing undegraded proteins) was measured in a liquid scintillation counter (Wallac T414, PerkinElmer Life Sciences). At the same time point, cells were also harvested and lysed with 0.1% NaOH. Proteolysis was expressed as the percentage of the initial total acid precipitable radioactivity (protein) in the cell lysates transformed to acid-soluble radioactivity (amino acids and small peptides) in the medium during the incubation. Baf or NH₄Cl-inhibited degradation represented total lysosomal degradation, whereas 3MA-inhibited proteolysis represented macroautophagic degradation. Relative CMA-dependent degradation was calculated as total lysosomal minus macroautophagic-dependent degradation [14], as microautophagy is not thought to play a significant role in bulk lysosomal protein degradation. In addition CMA activity is routinely measured in this fashion in our laboratory and others [13,14;29]. Such activity is drastically and commensurately altered with molecular manipulation of LAMP-2A expression [14; Xilouri et al., manuscript submitted], confirming that it reflects CMA-related activity. We cannot exclude the possibility that this measurement includes a small component of microautophagy.

Western Immunoblotting

Cultured cells (differentiated neuroblastoma SH-SY5Y cells or differentiated WT ASYN ± dox cells or embryonic rat cortical neurons), were washed twice in cold PBS and then harvested in STET lysis buffer (50 mM Tris, pH 7,6, 150 mM NaCl, 1% Triton X-100, 2 mM EDTA) with protease inhibitors. Lysates were centrifuged at 10.000×g for 10 min at 4°C. Protein concentrations were determined using the Bradford method (Bio-Rad, Hercules, CA, USA). Twenty to thirty micrograms of lysates were mixed with 4x Laemmli buffer prior to running on 10% (for LAMP-2A, Hsc70), 12% (for ASYN) or 15% (for LC3) SDS–polyacrylamide gels. Following transfer to a nitrocellulose membrane, blots were probed with the following antibodies: polyclonal ASYN C-20 (Santa Cruz Biotechnology), polyclonal LC3 (Molecular Probes), polyclonal p62 (Molecular and Biological Laboratories), polyclonal rat LAMP-2A (Zymed, Invitrogen), polyclonal human LAMP-2A (Abcam), polyclonal Hsc70 (Abcam), polyclonal ERK (BD Biosciences, San Jose, CA, USA), and monoclonal β-actin (Santa Cruz Biotechnology). Blots were probed with horseradish peroxidase-conjugated secondary antibodies and visualized with enhanced chemiluminescence substrate (ECL) following exposure to Super RX film (FUJI FILM, Europe GmbH, Germany). After scanning the images with Adobe Photoshop 7,0, Gel analyzer software 1,0 (Biosure, Greece) was used to quantify the intensity of the bands.

Statistical Analysis

Statistical analysis was performed using One-way ANOVA with a post hoc Tukey's. Values of $p < 0,05$ were considered significant.

A

B

C
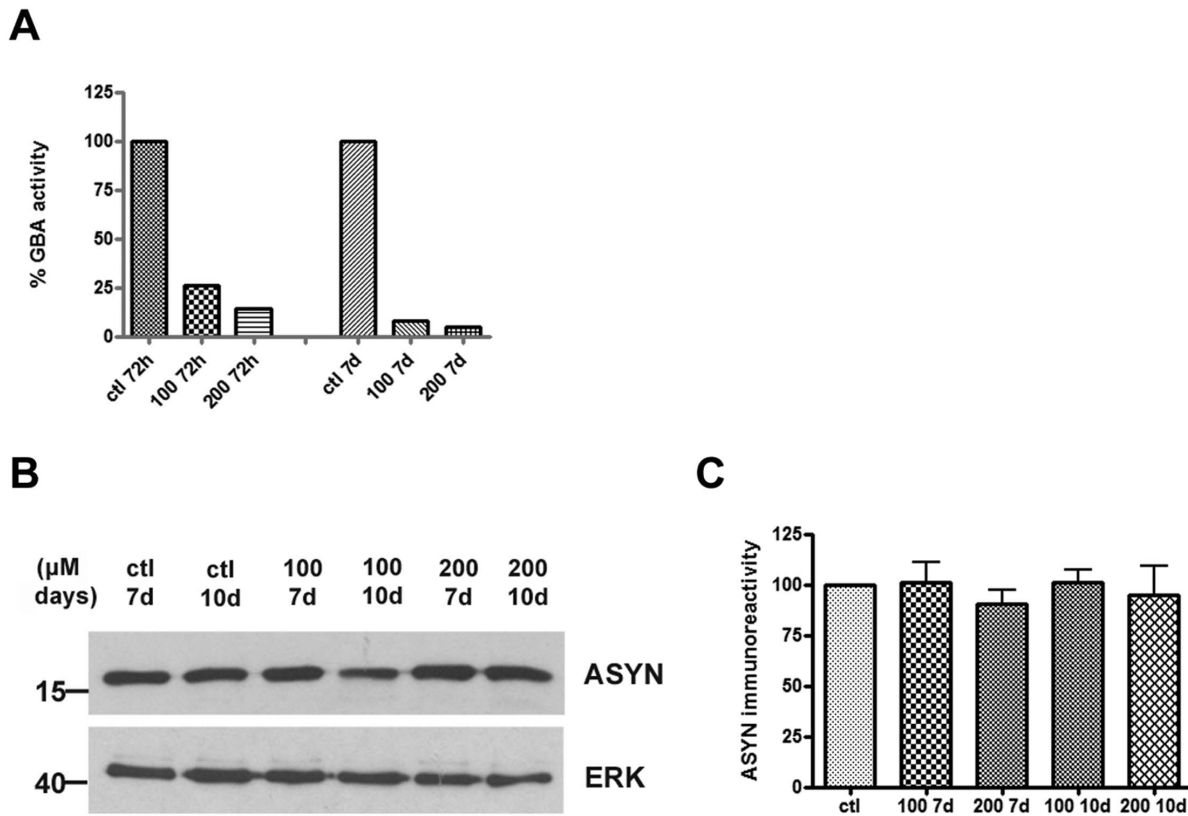
Figure 4. ASYN levels remain unchanged following GCase inhibition in rat embryonic cortical cultures. (A) Rat cortical neuron cultures were prepared from embryonic day 18 (E18) rat foetuses and were exposed at the 6th day of culture to increasing doses of CBE (100, 200 μM) for 72 h and 7 days respectively. Untreated cells served as control (ctl). Cell pellets were assessed for GCase enzymatic activity at the aforementioned doses and time points. (B) Cell lysates were separated with SDS-PAGE and immunoblotted with the C-20 polyclonal antibody to ASYN. ERK = loading control. (C) Graph shows quantification of ASYN immunoreactivity (vs ERK) via densitometric analysis at the 7 and 10 day time points respectively. Statistical analysis made via One Way Anova showed no significant difference in ASYN levels at the given doses and time points (n = 6 samples/2 different culture preparations with 3 independent biological samples per condition).
doi:10.1371/journal.pone.0060674.g004

All statistical analyses were performed using the GRAPHPAD PRISM 4 suite of software (GraphPad Software, Inc., San Diego, CA, USA).

A

B
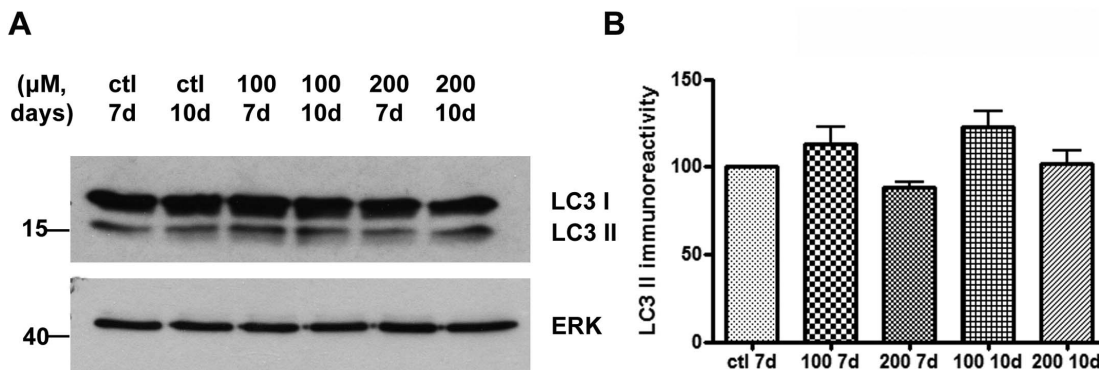
Figure 5. LC3 II shows no change following GCase inhibition in rat embryonic cortical cultures. (A) Cultured cortical neurons (E18) were exposed to increasing doses of CBE (100, 200 μM) for 7 and 10 days respectively. Untreated cells served as control (ctl). Cells were lysed, separated with SDS-PAGE and immunoblotted with the LC3 polyclonal antibody. ERK = loading control. (B) Graphs show quantification of LC3 II immunoreactivity (vs. ERK) via densitometric analysis at the 7 and 10 day time points respectively. Statistical analysis made via One Way Anova showed no difference in the LC3 II levels for the corresponding doses and time points of CBE in comparison to the control samples (n = 6 samples/2 different culture preparations with 3 independent biological samples per condition).
doi:10.1371/journal.pone.0060674.g005
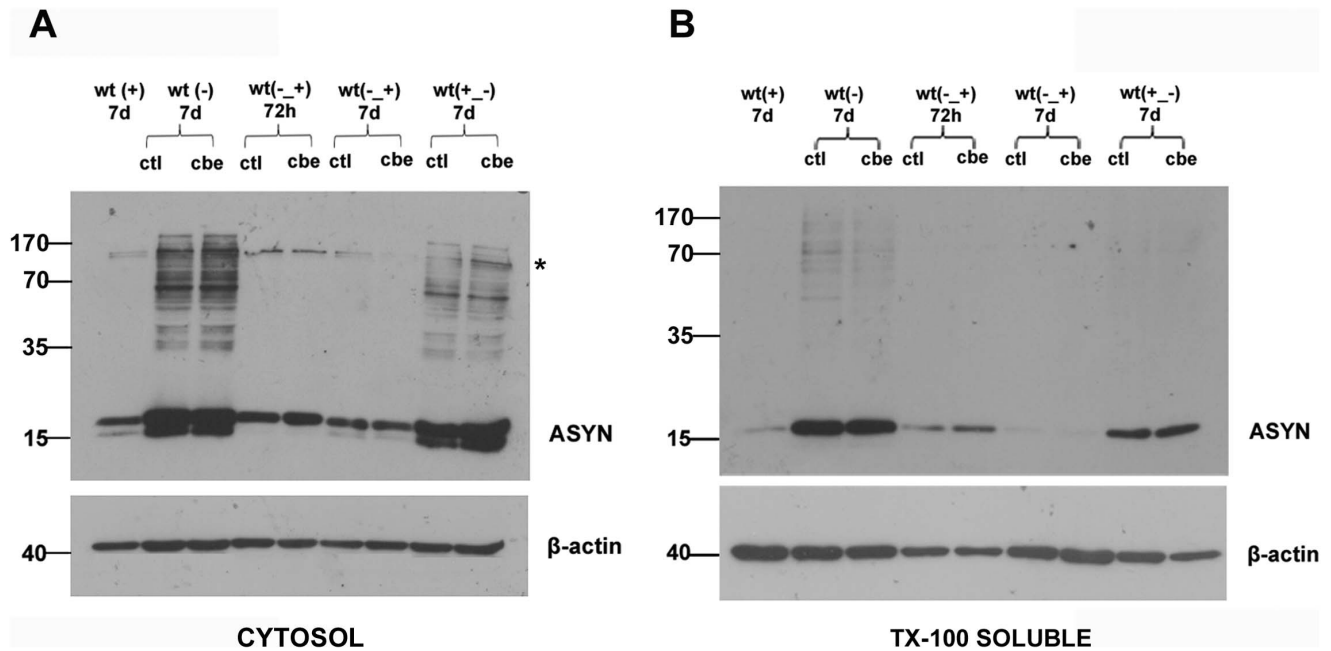
Figure 6. GCase inhibition does not affect ASYN-specific HMW species in differentiated WT ASYN cells. A stable inducible Tet-Off SH-SY5Y neuroblastoma cell line overexpressing WT ASYN was used in this assay. Initially cells were cultured in the presence (+) or absence (−) of dox (2 μg/mL) for 7 days. Subsequently cells were differentiated for 5 days and then were exposed to CBE (200 μM) at different conditions. Untreated cells were also used (ctl). WT (+) 7 d: differentiated WT ASYN cells expressing basal levels of ASYN in the presence of dox for 7 days, WT (−) 7 d: differentiated WT ASYN overexpressing cells in the absence of dox, treated with CBE, or not (ctl) for 7 days. WT (−_+) 72 h: differentiated WT ASYN overexpressing cells were switched to +dox conditions for 72 h along with the presence or not of CBE, WT (−_+) 7 d: differentiated WT ASYN overexpressing cells were switched to +dox conditions for 7 days, along with the presence or not of CBE. WT (+_−) 7 d: differentiated WT ASYN cells expressing basal levels of ASYN were switched to -dox conditions for 7 days, along with the presence or not of CBE. Cell lysates were separated with SDS-PAGE and immunoblotted with the C-20 polyclonal antibody to ASYN. β-actin = loading control. At no condition was there any difference in the presence or relative amount of ASYN monomers or ASYN-specific High Molecular Weight (HMW) species between the CBE and control-treated cells in the cytosol (A) and the membrane-associated, Triton X-100 soluble fraction (B) respectively. A doublet that is also present in the+dox conditions represents no specific immunolabeling (designated with an asterisk).
doi:10.1371/journal.pone.0060674.g006

Results

ASYN Levels Show No Change after CBE Treatment in Differentiated SH-SY5Y Cells

Previous data have shown that both pharmacological and molecular inhibition of GCase activity can lead to increased ASYN levels in *in vitro* systems [22,23]. To analyze the effect of GCase inhibition upon ASYN levels we inhibited GCase activity by the use of the specific inhibitor CBE. We used a well-established cell line available in our laboratory, the neuroblastoma SH-SY5Y cells. These cells assume a neuron-like phenotype upon differentiation and express both ASYN and GCase. The first step was to assay GCase activity in these cells cultured in the presence of the CBE inhibitor for various periods of time (72 h, 7 days) and at various doses of the inhibitor (50, 100, 200 μM). We observed a dramatic inhibition of GCase enzymatic activity, even at the lower dose of 50 μM, following a 72 h exposure to CBE (∼ 95%) (Figure 1A). We then evaluated ASYN levels by Western immunoblot analysis under these conditions. No changes in ASYN levels were observed even at the higher dose and exposure time of CBE (200 μM, 7 days) (Figure 1B–E). Similar results were obtained in non-differentiated SH-SY5Y cells (data not shown). These data demonstrate that inhibition of the GCase is not sufficient to alter ASYN levels at the given time points in neuronal SH-SY5Y cells.

Inhibition of GCase Activity does not Compromise Lysosomal Function in Differentiated SH-SY5Y Cells

As inhibition of GCase activity appeared to not affect ASYN levels in differentiated SH-SY5Y cells at the given doses and time points, we next examined whether GCase inhibition could affect lysosomal function.

Lysosomal function has been found to be compromised upon partial depletion of the lysosomal form of GCase and in GD iPS neurons *in vitro* [23]. In a first level, we aimed to assess changes in LC3 II levels (an autophagosome marker per se) in differentiated SH-SY5Y cells. Increases in the conversion of LC3 I to LC3 II are a strong indication of accumulation of autophagosomes, which could occur either due to induction of macroautophagy or to inhibition of lysosomal function downstream of autophagosome formation [34]. To test this, we used the well-established general lysosomal inhibitor bafilomycin (Baf) which inhibits lysosomal acidification and prevents fusion of autophagosomes with lysosomes, thus leading to accumulation of autophagosomes and LC3 II (Figure S2). LC3 II levels were evaluated by Western blot analysis in differentiated SH-SY5Y cells upon treatment with CBE at different time points (72 h, 7 days) and doses (50, 100, 200 μM). We observed a trend for a slight increase of the LC3 II protein at all time-points and doses tested; however, this reached statistical significance only for the dose of 100 μM at 7 days (Figure 2). We also examined the levels of CMA markers, the lysosome-associated membrane protein type 2A (LAMP-2A) and the lysosomal Heat shock cognate protein of 70 kDa (Hsc70) [35–37] in the presence

of the CBE inhibitor. We detected no alterations in the levels of the aforementioned proteins (Figure S3A).

Next, in order to examine lysosomal function per se, we measured the proteolysis of long-lived proteins in these cells with or without CBE treatment. This is a well-established method to monitor deviations in the lysosomal degradation capacity. Cells were radiolabelled with [^{3}H] leucine in a pulse-chase experiment and then treated with the general lysosomal inhibitor bafilomycin (Baf) or the macroautophagy inhibitor 3 methyladenine (3MA) respectively. Untreated cells served as controls. These experiments revealed no alterations in the lysosomal degradation pathways, including macroautophagy (Figure 3). To further assess the possibility of subtle dysfunction of lysosomes, we examined the levels of p62, a sensitive indicator of macroautophagic failure [38]; levels of p62 were unaltered in these experiments with CBE application (Figure S4), further reinforcing the idea that profound GCase inhibition fails to lead to significant lysosomal/autophagic dysfunction.

ASYN Levels Show No Change after CBE Treatment in Embryonic Rat Cortical Cultures

Given the lack of change of ASYN levels with CBE treatment in differentiated SH-SY5Y cells, we wished to investigate whether we could detect any changes in primary neuron cell cultures. We used embryonic (E18) rat cortical cultures as they represent a homogenous source of near-pure post-mitotic neurons. Again, we measured GCase activity in these cultures upon treatment with CBE at different time points (72 h, 7 days) and doses (100, 200 μM). We observed strong inhibition of GCase activity in this cell culture system as well, even at the lower dose of 100 μM, at 72 h following exposure to CBE; this inhibition was more dramatic at the highest dose of 200 μM at 7 days (95%) (Figure 4A). ASYN levels showed no change upon treatment with the CBE inhibitor (100, 200 μM) at 7 and 10 days respectively (Figure 4B–C), similarly to differentiated SH-SY5Y cells. These results suggest that GCase inhibition does not affect ASYN levels, at least in cultured neuronal cells, and over the relatively short time frames utilized in this study.

Macroautophagy and CMA Markers Show No Alteration after CBE Treatment in Embryonic Rat Cortical Cultures

Following the same strategy as for SH-SY5Y neuroblastoma cells, we next assessed the effect of GCase inhibition on LC3 II levels in embryonic rat cortical cultures. The ability to detect accumulation of autophagosomes in this primary neuron culture system was verified by the use of the general lysosomal inhibitor ammonium chloride (NH$_4$Cl) (Figure S2). LC3 II levels were then analyzed by Western blot upon application of the CBE inhibitor (100, 200 μM) at 7 and 10 days respectively. No alteration in LC3 II levels was observed in any of the given time points (Figure 5). CMA markers were also assessed revealing once again no alterations (Figure S3B). Given these results and the fact that no significant lysosomal impairment was evident in the differentiated SH-SY5Y cells upon CBE exposure, we did not further assess proteolysis of long-lived proteins in these cultures.

GCase Inhibition does not Affect The Formation or Clearance of ASYN Oligomers

As GCase inhibition did not appear to increase the monomeric levels of ASYN, we next assessed the effects of such inhibition on ASYN oligomers. Others have presented data suggesting that GCase deficiency can influence the aggregation of ASYN *in vitro* by stabilizing oligomeric intermediates [23]. For this, we used a doxycycline inducible Tet- Off system for ASYN. In the absence of doxycycline ASYN is overexpressed and creates oligomeric species (Off system), whereas in the presence of doxycycline ASYN is expressed at basal levels. ASYN monomeric and oligomeric levels were assessed in the presence or absence of CBE in this inducible system via Western blot analysis at different stages of the formation or clearance of these species. We were not able to detect alterations in ASYN oligomeric or monomeric species upon treatment with CBE (Figure 6). Of note, ASYN was not detectable in the SDS or urea-soluble fraction in these cells (data not shown) and this is consistent with the fact that we do not detect aggregated ASYN by immunostaining in these cultures. These results support the notion that profound GCase inhibition is not sufficient to influence ASYN in neuronal cell cultures, at least within the time frame employed in the current experiments.

Discussion

A variety of genetic, pathological and clinical studies have suggested a potential biological link between Type 1 Gaucher (GD) and Parkinson's disease (PD). Interestingly, this link has been proposed to be attributed, at least to an extent, to the interplay between GCase and ASYN [17–20,23]. Gain-of-function, loss-of-function and prion theories have been proposed to date, describing either a direct or an indirect interaction between GCase and ASYN, but all with significant limitations [18–23,39–43]. In the present study, we demonstrate that profound deficiency of GCase activity via pharmacological inhibition was not sufficient, within the time frame examined, to alter ASYN levels, neither in neuronally differentiated SH-SY5Y cells, nor in primary cortical neuronal cultures. In support of the above results, fractionation studies in a doxycycline inducible Tet-Off system for ASYN revealed again no changes in the clearance or formation of oligomeric forms of ASYN following GCase inhibition. Further, GCase inhibition did not appear to significantly compromise lysosomal function in the above cell culture models. We observed only a slight increase of the LC3 II protein levels at one specific time-point and no distortion in any of the lysosomal degradation pathways, including macroautophagy.

Taken together, our results demonstrate that GCase deficiency is not sufficient to alter ASYN levels (monomeric or oligomeric) in differentiated SH-SY5Y cells and rat cortical neuronal cultures. Our findings thus contrast with a study showing that loss of GCase activity through a similar pharmacological approach led to enhanced ASYN levels in neuroblastoma cells [22]. Mazzulli et al. [23] showed that significant, but partial, reduction of the levels of the GCase protein was sufficient to induce protein levels of ASYN, but this study is not directly comparable to ours, as in our experiments GCase protein is still present, but dysfunctional due to the pharmacological inhibition. There are certainly limitations inherent to the approach we have used, and in particular the use of cell systems (cell lines or primary cultures) and the short time frames of monitoring for an effect, which could potentially mask the outcome of an interaction between loss-of-function of GCase and ASYN, which otherwise might have been obvious in longer-term *in vivo* settings. Our findings are more in accord with those of Cullen et al. [21], who did not find alterations in ASYN levels following profound chemical inhibition of GCase activity by CBE in cell lines. In the current work, we have extended these findings by assessing lysosomal function in the face of GCase inhibition. Our results indicate no significant impairment of the lysosomal degradation machinery. Mazzulli et al. [23] in contrast, found that loss of GCase protein levels and resultant loss of activity was associated with lysosomal dysfunction, and

posited that such lysosomal dysfunction led to secondary ASYN accumulation. Methodological differences, in particular in the cell types tested, may account for the observed discrepancies. Alternatively, loss of GCase protein levels may have other effects on lysosomal function, independent of the known GCase enzymatic activity.

Our results suggest that the scenario of a direct sequence of events of GCase inhibition leading to lysosomal dysfunction, and this in turn leading to ASYN accumulation, is unlikely. It could be instead that the link of GBA mutations to ASYN accumulation in PD involves gain-of-function mechanisms, rather than loss-of-function, whereby GBA mutations could potentially result in an unstable or misfolded protein, which in turn could contribute to the enhanced accumulation and aggregation of ASYN. In addition, subsequent substrate accumulation could synergistically add to the pathology of ASYN. This would be in accord with the data of Cullen et al. [21], who found enhanced levels of ASYN in situations where mutant GBA was overexpressed, without loss of the enzymatic activity. Alternatively, more prolonged GCase inhibition may be needed to lead to ASYN accumulation and/or aggregation. This could occur secondary to the accumulation of GCase substrates, as suggested by our finding that ASYN has an increased tendency to oligomerize in erythrocyte membranes of GD patients, compared to controls [44]; it has been demonstrated that glucosylceramide (GluCer), a GCase substrate, accumulates in GD erythrocyte membranes [45], and we have suggested that such accumulation may underlie the increased oligomerization of ASYN [44]. Another explanation could be that the interaction between aberrant GCase and ASYN is in fact indirect and that contribution of other gene modifiers is pivotal for the development of the disease. This would account for the discrepancies observed across studies, and also explain why only a fraction of carriers and GD patients develop PD.

Concluding, to date, the contribution of an association between GCase deficiency and ASYN to PD and related disorders remains elusive. Our study questions a simplistic model in which GCase inhibition leads to ASYN accumulation/aggregation via lysosomal dysfunction, as neither of these phenomena occur in neuronal cells exposed to profound GCase inhibition. A future challenge will be to unmask other risk factors that, together with aberrant GCase, synergistically add to the pathology of the disease, thus providing new insights for therapeutic intervention.

Supporting Information

Figure S1 Complete inhibition of the rapamycin-induced induction of LC3 II with 3MA in cortical neuron cultures. Rat embryonic cortical cultures (E18) on their 7th day of culture were exposed either to the macroautophagy inhibitor 3MA (10 mM) or the mTOR inhibitor rapamycin (activator of macroautophagy) (500 nM) (rap) or in 3MA together with rapamycin (rap+3MA). Untreated cells served as control (ctl). 24 h later the cells were harvested for SDS-PAGE analysis against

the polyclonal LC3 antibody. ERK = loading control. (A) Increased levels of the LC3 II protein were found in the presence of rapamycin, whereas in the presence of the rapamycin together with 3MA the LC3 II levels decreased, reaching the levels of the 3MA-alone treated cells. (B) Statistical analysis made via One Way Anova showed significant difference between 3MA vs ctl (*$P<0,05$), 3MA vs rap ($^{\#\#}p<0,001$) and rap+3MA vs rap (*$P<0,01$).
(TIF)

Figure S2 Induction of autophagic vacuoles in differentiated SH-SY5Y cells and cortical neuron cultures. Differentiated SH-SY5Y cells or rat embryonic cortical cultures (E18) on their 6th day of culture were exposed to the general lysosomal inhibitor bafilomycin (Baf) (500 nM) or ammonium chloride (NH_4Cl) (20 mM) respectively overnight. Untreated cells served as control (ctl). Cells were lysed, separated with SDS-PAGE and immunoblotted with an LC3 polyclonal antibody. ERK = loading control. Increase in the conversion of the LC3 I to LC3 II was evident in both differentiated SH-SY5Y cells and cultured cortical neuron cultures.
(TIF)

Figure S3 No alteration in LAMP-2A and Hsc70 levels in differentiated SH-SY5Y cells and cortical neuron cultures. Differentiated SH-SY5Y cells or rat cultured cortical neurons (E18) on their 6th day of culture, were exposed to increasing doses of CBE (50, 100, 200 μM) for 7 days. Untreated cells served as control (ctl). Cells were lysed, separated with SDS-PAGE and immunoblotted with a LAMP-2A (human or rat) and Hsc70 polyclonal antibody. ERK = loading control. No significant alterations in the LAMP-2A and Hsc70 levels were evident either in the differentiated SH-SY5Y cells (A) or primary cortical neurons (B). The band corresponding to LAMP-2A protein is indicated by an arrow. Similar results were achieved in one or two other independent experiments in the differentiated SH-SY5Y cells and primary cortical cultures respectively.
(TIF)

Figure S4 No alteration in p62 levels in differentiated SH-SY5Y cells. Differentiated SH-SY5Y cells were exposed to increasing doses of CBE (50, 100, 200 μM) for 72 h and 7 days respectively. Untreated cells served as control (ctl). Cells were lysed, separated with SDS-PAGE and immunoblotted with a p62 polyclonal antibody ERK = loading control. No significant differences in p62 levels were detected at the given doses and time points (representative of 4 experiments).
(TIF)

Author Contributions

References

1. Goker-Alpan O, Hruska KS, Orvisky E, Kishnani PS, Stubblefield BK, et al. (2005) Divergent phenotypes in Gaucher disease implicate the role of modifiers. J Med Genet 42: e37.
2. Sidransky E (2004) Gaucher disease: complexity in a "simple" disorder. Mol Genet Metab 83: 6–15.
3. Neudorfer O, Giladi N, Elstein D, Abrahamov A, Turezkite T, et al. (1996) Occurrence of Parkinson's syndrome in type I Gaucher disease. QJM 89: 691–694.
4. Sidransky E, Nalls MA, Aasly JO, Aharon-Peretz J, Annesi G, et al. (2009) Multicenter analysis of glucocerebrosidase mutations in Parkinson's disease. N Engl J Med 361: 1651–1661.
5. Mitsui J, Mizuta I, Toyoda A, Ashida R, Takahashi Y, et al. (2009) Mutations for Gaucher disease confer high susceptibility to Parkinson disease. Arch Neurol 66: 571–576.
6. Kalinderi K, Bostantjopoulou S, Paisan-Ruiz C, Katsarou Z, Hardy J, et al. (2009) Complete screening for glucocerebrosidase mutations in Parkinson disease patients from Greece. Neurosci Lett 452: 87–89.
7. Mata IF, Samii A, Schneer SH, Roberts JW, Griffith A, et al. (2008) Glucocerebrosidase gene mutations: a risk factor for Lewy body disorders. Arch Neurol 65: 379–382.

8. Bras J, Paisan-Ruiz C, Guerreiro R, Ribeiro MH, Morgadinho A, et al. (2009) Complete screening for glucocerebrosidase mutations in Parkinson disease patients from Portugal. Neurobiol Aging 30: 1515–1517.

9. Neumann J, Bras J, Deas E, O'Sullivan SS, Parkkinen L, et al. (2009) Glucocerebrosidase mutations in clinical and pathologically proven Parkinson's disease. Brain 132: 1783–1794.

10. Nichols WC, Pankratz N, Marek DK, Pauciulo MW, Elsaesser VE, et al. (2009) Mutations in GBA are associated with familial Parkinson disease susceptibility and age at onset. Neurology 72: 310–316.

11. Lesage S, Anheim M, Condroyer C, Pollak P, Durif F, et al. (2011) Large-scale screening of the Gaucher's disease-related glucocerebrosidase gene in Europeans with Parkinson's disease. Hum Mol Genet 20: 202–210.

12. Moraitou M, Hadjigeorgiou G, Monopolis I, Dardiotis E, Bozi M, et al. (2011) beta-Glucocerebrosidase gene mutations in two cohorts of Greek patients with sporadic Parkinson's disease. Mol Genet Metab 104: 149–152.

13. Cuervo AM, Stefanis L, Fredenburg R, Lansbury PT, Sulzer D (2004) Impaired degradation of mutant alpha-synuclein by chaperone-mediated autophagy. Science 305: 1292–1295.

14. Vogiatzi T, Xilouri M, Vekrellis K, Stefanis L (2008) Wild type alpha-synuclein is degraded by chaperone-mediated autophagy and macroautophagy in neuronal cells. J Biol Chem 283: 23542–23556.

15. Pan T, Kondo S, Le W, Jankovic J (2008) The role of autophagy-lysosome pathway in neurodegeneration associated with Parkinson's disease. Brain 131: 1969–1978.

16. Mak SK, McCormack AL, Manning-Bog AB, Cuervo AM, Di Monte DA (2010) Lysosomal degradation of alpha-synuclein in vivo. J Biol Chem 285: 13621–13629.

17. Wong K, Sidransky E, Verma A, Mixon T, Sandberg GD, et al. (2004) Neuropathology provides clues to the pathophysiology of Gaucher disease. Mol Genet Metab 82: 192–207.

18. Goker-Alpan O, Stubblefield BK, Giasson BI, Sidransky E (2010) Glucocerebrosidase is present in alpha-synuclein inclusions in Lewy body disorders. Acta Neuropathol 120: 641–649.

19. Choi JH, Stubblefield B, Cookson MR, Goldin E, Velayati A, et al. (2011) Aggregation of alpha-synuclein in brain samples from subjects with glucocerebrosidase mutations. Mol Genet Metab 104: 185–188.

20. Yap TL, Gruschus JM, Velayati A, Westbroek W, Goldin E, et al. (2011) Alpha-synuclein interacts with Glucocerebrosidase providing a molecular link between Parkinson and Gaucher diseases. J Biol Chem 286: 28080–28088.

21. Cullen V, Sardi SP, Ng J, Xu YH, Sun Y, et al. (2011) Acid beta-glucosidase mutants linked to Gaucher disease, Parkinson disease, and Lewy body dementia alter alpha-synuclein processing. Ann Neurol 69: 940–953.

22. Manning-Bog AB, Schule B, Langston JW (2009) Alpha-synuclein-glucocerebrosidase interactions in pharmacological Gaucher models: a biological link between Gaucher disease and parkinsonism. Neurotoxicology 30: 1127–1132.

23. Mazzulli JR, Xu YH, Sun Y, Knight AL, McLean PJ, et al. (2011) Gaucher disease glucocerebrosidase and alpha-synuclein form a bidirectional pathogenic loop in synucleinopathies. Cell 146: 37–52.

24. Vekrellis K, Xilouri M, Emmanouilidou E, Stefanis L (2009) Inducible over-expression of wild type alpha-synuclein in human neuronal cells leads to caspase-dependent non-apoptotic death. J Neurochem 109: 1348–1362.

25. Stefanis L, Park DS, Friedman WJ, Greene LA (1999) Caspase-dependent and -independent death of camptothecin-treated embryonic cortical neurons. J Neurosci 19: 6235–6247.

26. Dietrich P, Rideout HJ, Wang Q, Stefanis L (2003) Lack of p53 delays apoptosis, but increases ubiquitinated inclusions, in proteasomal inhibitor-treated cultured cortical neurons. Mol Cell Neurosci 24: 430–441.

27. Rideout HJ, Stefanis L (2002) Proteasomal inhibition-induced inclusion formation and death in cortical neurons require transcription and ubiquitination. Mol Cell Neurosci 21: 223–238.

28. Michelakakis H, Dimitriou E, Van Weely S, Boot RG, Mavridou I, et al. (1995) Characterization of glucocerebrosidase in Greek Gaucher disease patients: mutation analysis and biochemical studies. J Inherit Metab Dis 18: 609–615.

29. Xilouri M, Vogiatzi T, Vekrellis K, Park D, Stefanis L (2009) Abberant alpha-synuclein confers toxicity to neurons in part through inhibition of chaperone-mediated autophagy. PLoS One 4: e5515.

30. Liu Z, Meray RK, Grammatopoulos TN, Fredenburg RA, Cookson MR, et al. (2009) Membrane-associated farnesylated UCH-L1 promotes alpha-synuclein neurotoxicity and is a therapeutic target for Parkinson's disease. Proc Natl Acad Sci U S A 106: 4635–4640.

31. Franklin JL, Johnson EM (1998) Control of neuronal size homeostasis by trophic factor-mediated coupling of protein degradation to protein synthesis. J Cell Biol 142: 1313–1324.

32. Kaushik S, Cuervo AM (2009) Methods to monitor chaperone-mediated autophagy. Methods Enzymol 452: 297–324.

33. Klionsky DJ, Abdalla FC, Abeliovich H, Abraham RT, Acevedo-Arozena A, et al. (2012) Guidelines for the use and interpretation of assays for monitoring autophagy. Autophagy 8: 445–544.

34. Xilouri M, Stefanis L (2010) Autophagy in the central nervous system: implications for neurodegenerative disorders. CNS Neurol Disord Drug Targets 9: 701–719.

35. Agarraberes FA, Terlecky SR, Dice JF (1997) An intralysosomal hsp70 is required for a selective pathway of lysosomal protein degradation. J Cell Biol 137: 825–834.

36. Cuervo AM, Knecht E, Terlecky SR, Dice JF (1995) Activation of a selective pathway of lysosomal proteolysis in rat liver by prolonged starvation. Am J Physiol 269: C1200–1208.

37. Cuervo AM, Dice JF (2000) Regulation of lamp2a levels in the lysosomal membrane. Traffic 1: 570–583.

38. Bjorkoy G, Lamark T, Johansen T (2006) p62/SQSTM1: a missing link between protein aggregates and the autophagy machinery. Autophagy 2: 138–139.

39. Sardi SP, Clarke J, Kinnecom C, Tamsett TJ, Li L, et al. (2011) CNS expression of glucocerebrosidase corrects alpha-synuclein pathology and memory in a mouse model of Gaucher-related synucleinopathy. Proc Natl Acad Sci U S A 108: 12101–12106.

40. Kordower JH, Chu Y, Hauser RA, Freeman TB, Olanow CW (2008) Lewy body-like pathology in long-term embryonic nigral transplants in Parkinson's disease. Nat Med 14: 504–506.

41. Desplats P, Lee HJ, Bae EJ, Patrick C, Rockenstein E, et al. (2009) Inclusion formation and neuronal cell death through neuron-to-neuron transmission of alpha-synuclein. Proc Natl Acad Sci U S A 106: 13010–13015.

42. Olanow CW, Prusiner SB (2009) Is Parkinson's disease a prion disorder? Proc Natl Acad Sci U S A 106: 12571–12572.

43. Goldin E (2010) Gaucher disease and parkinsonism, a molecular link theory. Mol Genet Metab 101: 307–310.

44. Argyriou A, Dermentzaki G, Papasilekas T, Moraitou M, Stamboulis E, et al. (2012) Increased dimerization of alpha-synuclein in erythrocytes in Gaucher disease and aging. Neurosci Lett. 528: 205–9.

45. Moraitou M, Dimitriou E, Zafeiriou D, Reppa C, Marinakis T, et al. (2008) Plasmalogen levels in Gaucher disease. Blood Cells Mol Dis 41: 196–199.